Appendix XI

Doctoral Thesis – Alan Chester

Petroleum source rocks, maturation and thermal history, onshore Tasmania.

Alan D. Chester. B.Ed., B.Sc. (Hons.)

Submitted in fulfilment of the requirements for the degree of Doctor of Philosophy.
University of Tasmania.

March, 2006.

Declaration of originality and statement of authority of access.

This thesis contains no material which has been accepted for a degree or diploma by the University or any other institution, except by way of background information and duly acknowledged in the thesis. To the best of my knowledge and belief the thesis contains no material previously published or written by another person except where due acknowledgement is made in the text of the thesis.

This thesis may be made available for loan and limited copying in accordance with the *Copyright Act 1968.*

Alan D. Chester.

March 2006

ABSTRACT.

Discoveries of bitumen, oil and gas have been made in onshore Tasmania associated with rocks ranging in age from Neoproterozoic to Permian, suggesting that three stacked petroleum systems may occur. The three petroleum systems identified are named Centralian, Larapintine 2 and Gondwanan. As yet no commercial discoveries of oil or gas have been made in these systems. A basin wide reconnaissance level investigation was undertaken, using outcrop samples, to determine petroleum source potential and thermal maturity of available source rocks. The findings add to the basic geoscientific knowledge of these systems and provide a basis for realistic planning of petroleum exploration.

The Kubler Indices of potential Neoproterozoic source rocks were measured to try and overcome the unreliability of maturity results found when using Rock-Eval pyrolysis on outcrop samples. Kubler Indices of potential Neoproterozoic source rocks shows they have very high thermal maturity, up to greenschist facies, so there is no possibility of a viable Centralian petroleum system. Results of Kubler Indices analysis were used to map regional variations in metamorphic grade of northwest Tasmania.

Within the potential Ordovician source rocks the high organic content beds are thin (<200 mm thick) and rare with discontinuous distributions. Even these thin beds have low source potential as measured by Rock-Eval pyrolysis (Hydrogen Index 3-106, average 40, $S_1 + S_2$ average 0.3), probably due to the high maturity (T_{max} 465-496°C). No evidence for petroleum migration pathways were found during field investigations however hydrocarbon gases were extracted from outcrop samples and identified by gas chromatographic analysis. Biomarker analysis of extracts from Gordon Group samples indicates the hydrocarbons were locally derived from an algal/bacterial source deposited in an anoxic environment. Sterane distribution indicates marine oil derived from carbonates consistent with source rocks within the Gordon Group. Examination of cross cutting relationships of mineralised and bituminous veins from possible Mississippi Valley-type Pb-Zn deposits, hosted by Gordon Group, indicates oil generation occurred in the Early Devonian before Tabberabberan trap

development. Maximum palaeotemperatures were developed due to tectonic thickening during the mid-Devonian Tabberabberan folding and thrusting. This study found that there is no exploration potential within the Larapintine 2 petroleum system of onshore Tasmania.

Previous studies identified potential source rocks within the Parmeener Supergroup and this study found further potential coal and associated siltstone source rocks with high total organic content and high hydrogen index values (TOC up to 75%, HI 442) indicating excellent potential. Maturity within the oil window was determined by Rock-Eval pyrolysis T_{max} and vitrinite reflectance. Vitrinite reflectance data from coal exploration was collated with data obtained from Rock-Eval pyrolysis and vitrinite reflectance on samples obtained during this study to confirm previous basin maturity assessments.

Near Zeehan, a breached reservoir, in Upper Permian sandstone contains relict bitumen sourced from Permian siltstone and coal. This is positive evidence that the Gondwanan petroleum system has generated petroleum. A potential complication is that depositional conditions for source rocks and higher heat flows during the Cretaceous may have provided conditions suitable for petroleum generation in western Tasmania that did not apply in the Tasmania Basin.

Only the Gondwanan petroleum system is a potential exploration target for onshore Tasmania as source rocks, within the oil and gas maturity range, are widespread across the southern Tasmania Basin. However, the search for suitable trap structures in the complexly faulted sequence will be difficult. Both the Larapintine 2 and Centralian petroleum systems are over mature throughout Tasmania making them poor exploration targets.

ACKNOWLEGEMENTS.

An Australian Postgraduate Award Industry (APAI), the University of Tasmania and Great South Land Minerals supported this research.

The project was initiated by Malcolm Bendall (Chairman of Great South Land Minerals), who has been the driving force behind the current investigations into the possibility of oil or gas being found onshore Tasmania. I would like to thank my supervisors Dr. Clive Burrett, Dr. Peter Haines, Dr. Ron Berry and Dr. Pat Quilty for their help and guidance.

Dr. Catherine Reid gave me valuable help in the day-to-day processes of research and was always ready to discuss ideas. Dr. Garry Davidson offered suggestions, which led to an investigation of the Centralian petroleum system. Dr. Alan Cook performed the vitrinite and bitumen reflection measurements and during discussions offered ideas that led to the discovery of the source for the bitumen found at Comstock mine. Dr. Ralph Bottrill arranged for the Mineral Resources Tasmania Laboratory to analyse samples for Kubler Index. Dr. Noel Davies from Central Science Laboratories, University of Tasmania, extracted and analysed gases from samples of Gordon Limestone. Carmelina Valente from AMDEL, Adelaide, gave me some useful advice about selection of appropriate geochemical procedures and sampling techniques.

Simon Stephens prepared the thin sections used in this study. Paul Heath gave assistance in locating samples of bitumen at the Comstock mine.

Katie McGoldrick gave advice and assistance in relation to the preparation of samples for geochemical analysis. Michael Pemberton arranged for permits so that I could sample sites within National Parks. Direct help and valuable informal discussions were also forthcoming from my office companions Kate Bull, Robin Cantrill, Mawson Croaker, Lee Evans, Russell Fulton, Jubo Liu, Nicky Pollington, and Andrew Stacey.

I would also like to thank my wife Helena for encouraging me during the project and for putting up with me living away from home.

TABLE OF CONTENTS.

LIST OF FIGURES.

LIST OF TABLES.

LIST OF APPENDICES.

CHAPTER ONE.

PETROLEUM EXPLORATION ONSHORE TASMANIA.

1.1. Introduction.

No oil or gas fields have ever been discovered onshore Tasmania and this project was initiated to determine if there is potential for petroleum systems to operate either below or within the Tasmania Basin. Great South Land Minerals (GSLM), a company currently holding an exploration lease for oil and gas over much of the Tasmania Basin, has sponsored the project. Obtaining basic geoscientific knowledge is important to attract international investment for exploration and this study is intended to augment geologic and geochemical data relevant to the search for petroleum onshore Tasmania.

Australian oil production is forecast to decline by approximately 40% over the next ten years (Anon, 2005). However Australia is gas-rich and is well able to maintain supplies for local demand and export into the foreseeable future but eastern Australian gas basins are estimated to be depleted by 2023 (Fainstein et al., 2002), unless further resources can be found. A gas pipeline has been built to supply gas to Tasmania from Victoria and initially gas will be supplied for industrial purposes and then as reticulation services are installed domestic use will follow. Gas consumption in Tasmania is expected to be 15 PJ by 2009-10 and 28 PJ by 2019-20 (Fainstein et al., 2002). A client base and distribution network would thus be established should any local resources be discovered.

1.2. Outline of historical search for oil and gas onshore Tasmania.

Oil shale deposits were discovered in the Mersey Valley near Latrobe in 1851 and these deposits were worked between 1910-15 (Rudd, 1951). Refer to Figure 1.1 for a map showing the locations of places mentioned in this chapter and also Appendix J. The Tasmanite Shale Oil Company operated from the early 1920's until 1935 selling fuel oil derived from the Latrobe deposits to the Tasmanian Government Railways and Mount Lyell Company (Wilkinson, 1991). Production costs eventually made the shale oil more expensive than imported oil and its higher sulphur content made it a

less desirable product. During its 25 year history the company produced 1 623 443 L of crude oil from 42 237 tonnes of shale (Wilkinson, 1991).

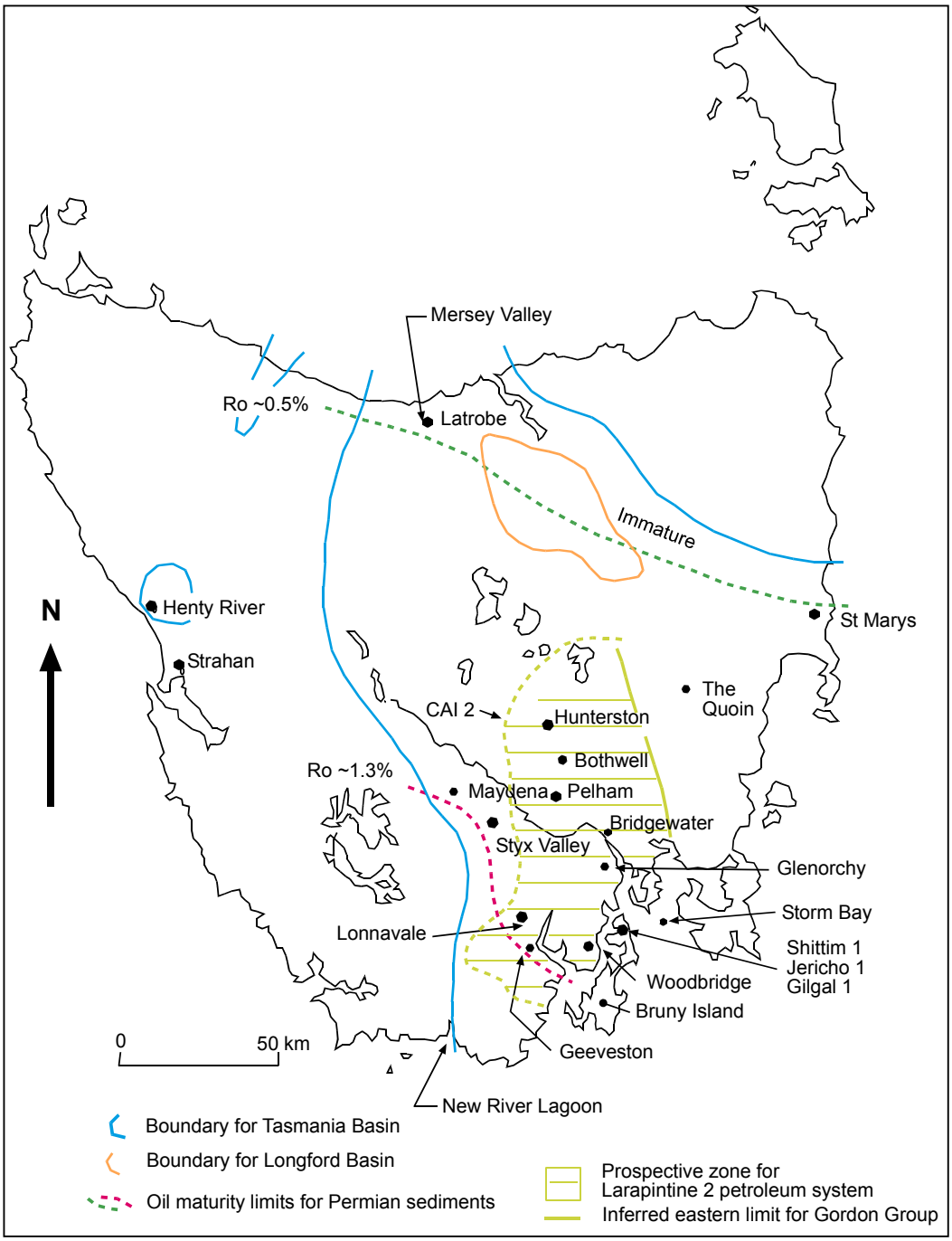

Figure 1.1. Map showing places mentioned in Chapter 1 and effective outline for the Tasmania and Longford Basins. Red and green dashed lines indicate oil maturity limits for Permian sediments within the central parts of the Tasmania Basin. The region shown by horizontal hatching is determined to be within the gas window of maturity for the Gordon Group below the Tasmania Basin.

Reports of oil and gas seeps have been made since 1871 from sites throughout Tasmania with government geologists Charles Gould and Alexander McIntosh Reid confirming some reports (Reid, 1923; Twelvetrees, 1917). Shallow exploratory drilling has taken place near some of these sites without any commercial discoveries being made (Bacon et al., 2000). Many reports seem to have been made of bitumen stranded on beaches and some of these have been mistaken for seeps. The most frequent reporting of seeps, or presumed seeps, occurred towards the end of the nineteenth century and again in the 1930's and these periods coincide with recordings of many earthquakes (Leaman, 1988a). Carey (1960) catalogued 2540 seismic events in the period 1883-86 and it is possible that reservoirs may have leaked through tight migration pathways due to pumping effects induced by these seismic events (Leaman, 1988a).

A prospecting syndicate, The Asphaltam Glance and Oil Syndicate, was formed in 1915 to follow up on reports of oozing tars in New River Lagoon and oil scums onshore. The government geologist, W.H. Twelvetrees, (1915) inspected the site and identified the Ordovician limestone outcropping on the eastern shores of New River Lagoon as a possible source for hydrocarbons. He correlated these outcrops with the Trenton Limestone in the Texas Panhandle, which was famous for oil gushes at the time, and is still a major source rock and reservoir in the Appalachian Plateau oil and gas region in the United States of America (Laughrey and Baldassare, 1998).

Oil exploration in Tasmania seems to have been influenced by the attitudes of the government geologists currently in office. Hills (1922) in a lecture to the Royal Society of Tasmania stated that it was a waste of time to search for liquid oil in Tasmania. Hills was removed from office in 1923 and his successor Alexander McIntosh Reid encouraged companies to explore for oil in areas where he considered the conditions were favourable (Bacon et al., 2000). During Reid's time in office a number of companies drilled wells in the central north of Tasmania. The Mersey Oil Company also pegged leases north of Strahan up to the Henty River (Bendall, 1990). Reid was sacked in 1930 and interest in oil exploration subsequently declined (Wilkinson, 1991).

H.G. Raggatt, a leader in the scientific search for oil in Australia, delineated some areas he considered prospective for oil in 1954 and these included an area in the

central north of Tasmania based on the presence of the Permian *Tasmanites* in the Mersey Valley. He also included an area in the southwest of Tasmania based on the presence of Ordovician limestone to the east of New River Lagoon (Raggatt, 1954). However, by 1960, the Bureau of Mineral Resources had dismissed Tasmania as a potential site for oil and gas exploration (Wilkinson, 1991).

A further wave of exploration took place from 1965-1974 when Sulzberger drilled eight wells in central northern Tasmania (Bendall, 1990). All these wells bottomed in dolerite and were unsuccessful. Nudec and the Electrolytic Zinc Company also explored for oil in 1965 without success (Lucarelli, 1965). Broken Hill Propriety Company drilled two holes in the Styx Valley and intersected siltstones, which yielded a maximum of 7L/tonne from Fischer analysis (Anon, 1981). Exploration was abandoned due to low yields and thin tasmanite beds. Esso carried out aeromagnetic surveys offshore Tasmania, including Storm Bay, in an attempt to locate suitable structures for oil exploration wells (Steenland, 1967).

The current phase of exploration for oil and gas in Tasmania commenced in 1984 with the establishment of Conga Oil to follow up on reports of oil seeps on Bruny Island. This company held a number of exploration licences in southern Tasmania and conducted exploration on the basis that hydrocarbon sources could be Ordovician and/or Permian. Conga Oil eventually became Great South Land Minerals, which currently holds a petroleum exploration licence over most of the Tasmania Basin.

1.3. Aims of this project.

There are five main aims to this project:

1. To determine if there is a potential petroleum system hosted within the Wurawina Supergroup.

2. Investigate the possibility of hydrocarbon source rocks hosted by Precambrian sediments onshore Tasmania.

3. Consider the potential of Permian coals and associated siltstones as possible hydrocarbon source rocks.

4. Identify maturity zones onshore Tasmania.

5. Investigate occurrences of reported hydrocarbon seeps onshore Tasmania.

1.4. Previous work.

Onshore Tasmania can be regarded as a frontier for petroleum exploration as there has been very little specific geoscientific study of its petroleum potential. The geology of Tasmania has been mapped in detail over most areas and the stratigraphy is well understood but no petroleum reservoirs have been discovered.

Some specific investigations have been made for petroleum potential onshore Tasmania but many observations recorded are incidental to mineral or coal exploration. Bitumen has been noted in association with Gordon Group and bituminous odours have been noted emanating from fresh samples when struck with a hammer (Calver, 1977; Morris and Taylor, 1995; Reid, 1964; Weldon, 1974). These occurrences have been taken to indicate potential of the Gordon Group as source rocks for hydrocarbons. Burrett (1992) investigated the maturity of the Gordon Group using the Colour Alteration Index (CAI) and found that an area in southern Tasmania is within the gas window of maturity. This study has established areal constraints on the potential exploration zone for hydrocarbons from Ordovician source rocks.

Denwer (1981) investigated Tasmanite Oil Shale as a possible source rock for hydrocarbons and found that outcrops in northern Tasmania were too immature to be viable source rocks. Valuable geochemical data was collected in this study, which could be used in the future to help correlate oils with source rocks (Revill et al., 1994).

Randall (1997) found that the Thermal Alteration Indexes of the palynomorphs of the Upper Carboniferous to Lower Permian shales of the Tasmania Basin all lie within the oil and gas windows. Kerogen types and maturation indicators show that these rocks are prone mainly to gas production. Woods (1995) found, using theoretical modelling, that potential source rocks within the Tasmania Basin were within the oil window. Maynard (1996) found potential reservoir units with good porosity within the Liffey/Faulkner Groups.

Lane (2002) undertook an analysis of seismic data GSLM had obtained over the Longford Basin to determine the structural architecture of this basin, which has

relevance for consideration of structural traps. Bedi (2003) considered the potential of Triassic sandstones as possible reservoir rocks and found that these have some potential.

Bendall et al., (1991) used results from organic geochemistry, geophysics, structural geology and palaeontology to outline a case for the hydrocarbon prospectivity of lower Palaeozoic rocks onshore Tasmania. These ideas were expanded and further developed to form the philosophical basis for GSLM's exploration onshore Tasmania (Bendall et al., 2000).

GSLM have also completed some stratigraphic drilling into the Tasmania Basin with wells at Jericho-1 on Bruny Island, Lonnavale-1, Bridgewater-1, Pelham-1and Hunterston-1. The predecessor company Condor Oil Pty. Ltd. drilled three stratigraphic wells on Bruny Island, Shittim-1, Jericho-1 and Gilgal-1. Minor gas was recorded in the Shittim-1, Jericho-1, Lonnavale-1 and Pelham-1 wells with the Shittim-1and Jericho-1 gas shown to be of high thermal maturity containing methane, carbon dioxide, nitrogen, hydrogen and helium. Carbon isotopes show the thermogenic origin of the gas from Jericho-1 (Burrett and Tanner, 1997). The Hunterston diamond drill hole, completed by GSLM for stratigraphic purposes (Reid et al., 2003), penetrated to basement, which was found to be Precambrian dolomite with no potential as a hydrocarbon source rock (AMDEL data, 2002).

Geophysical interpretation of the area below the Tasmania Basin has been made (Gunn et al., 1997; Leaman, 1990), however this requires confirmation by drilling. Most of the area below the Tasmania Basin has unknown stratigraphy at this stage and only inferences can be made about possible source rocks being present. Source rocks are inferred to occur beneath the Tasmania Basin because exposed sequences on basin margins, which contain possible source rocks, are assumed to continue beneath the basin.

Some organic geochemical analyses have been made of bitumens located within Tasmania and in some cases these have identified bitumen as being flotsam from offshore sources (Volkman, 1999). Analysis of bitumens has also established fingerprints for locally derived bitumens such as those from Permian sources including *Tasmanites* and Ordovician sources with possible *Gloeocapsomorpha*

prisca input (Volkman, 1988). These data should be useful for correlation of any oil discovered with the appropriate source rocks.

One genuine seep has been identified using modern geochemical analysis and this was discovered in 1995 at Lonnavale (Bottrill, 1996). The bitumen and oil from this seep has been linked with Permian *Tasmanites* and demonstrates potential for the Gondwanan Petroleum System onshore Tasmania (Volkman, 1999; Wythe and Watson, 1996).

Reid (2004; Reid and Burrett, 2004) has completed a study of the potential of the Gondwanan Petroleum System within the Tasmania Basin that showed potential source rocks exist at a number of horizons throughout the Permian sequence. Maturity measurements from this study show that source rocks are mature for oil in the Tasmania Basin south of an east-west line drawn at the latitude of St Marys through to another line drawn from Geeveston to Maydena. South of the oil maturity zone is a zone mature for gas. Potential reservoir rocks occur in freshwater sequences within the Permian sediments and also in Triassic sandstones (Reid, 2004). Dolerite intrusions within the Parmeener sediments tend to reduce the potential of possible reservoir rocks by reduction in porosity and permeability due to the introduction of secondary minerals (Reid, 2004). However porosity and permeability are sometimes dramatically increased by hydrothermal activity related to dolerite (Reid et al., 2003).

Seismic surveys have been undertaken by GSLM to try and identify structural traps and these have shown some domal structures within the Parmeener Supergroup and major thrusts in the pre-Carboniferous rocks below the Tasmania Basin. In locations where reliable drill or outcrop data is available links have been made between structures and stratigraphy. A parallel study by Andrew Stacey is considering the structural aspects of the Tasmania Basin related to potential hydrocarbon exploration.

1.5. Assumptions on which this study is based.

This study has been initiated and supported by GSLM and they have an exploration philosophy upon which this study has been based. Two potential petroleum systems are assumed to operate, one within and one below the Tasmania Basin (Bendall et al., 2000). The system below the Tasmania Basin, with potential Ordovician source rocks within the Gordon Group, is known as the Larapintine 2 petroleum system in

accordance with the nomenclature of Bradshaw (1993). Reservoir rocks for this system may occur within Gordon Group palaeokarst and/or overlying sandstones within the Eldon Group and sealed by mudstones. Trap structures are assumed to have formed during the Tabberabberan Orogeny and thus have been in place before hydrocarbon generation and migration occurred. A diagram illustrating the concepts of the Larapintine 2 petroleum system onshore Tasmania upon which the GSLM exploration philosophy is based in shown in Figure 1.2.

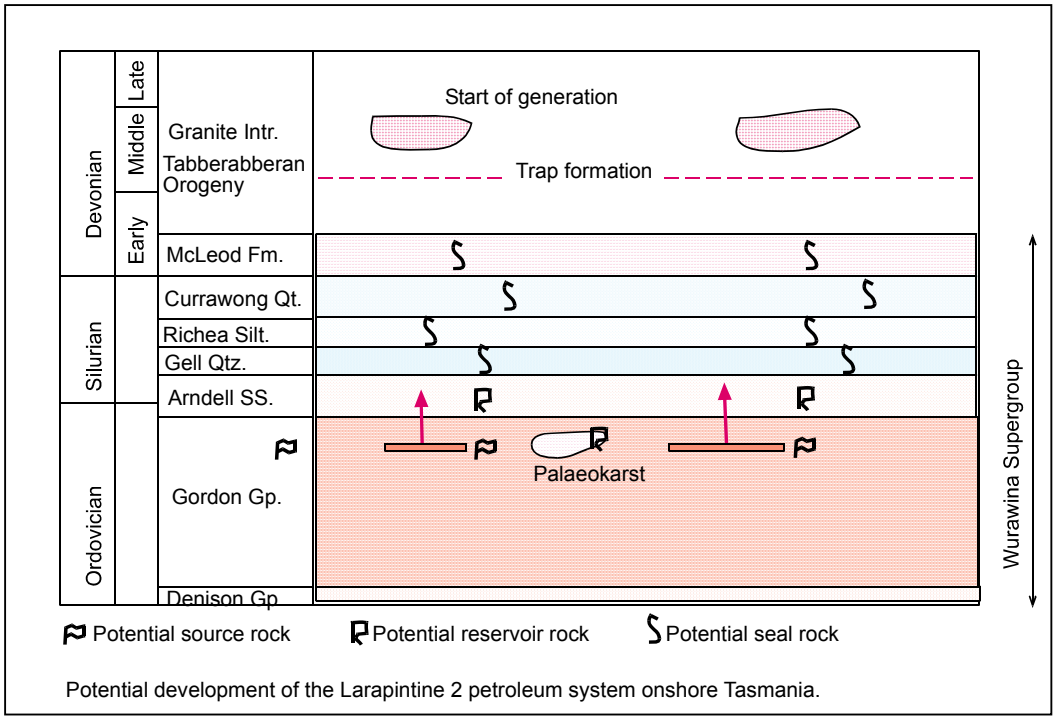

Figure 1.2. Diagram illustrating the assumptions made about the Larapintine 2 petroleum system components onshore Tasmania on which the Great South Land Minerals exploration philosophy for petroleum exploration below the Tasmania Basin is based. Source rocks potentially within the Gordon Group expel hydrocarbons into Eldon Group sandstone reservoirs sealed by Eldon Group mudstones. Traps have potentially been formed due to folding and faulting during the Tabberabberan Orogeny. Hydrocarbon generation is assumed to occur after trap formation.

The second potential petroleum system, known as the Gondwanan petroleum system, is assumed to have formed within the Permo-Triassic Parmeener Supergroup. A number of potential source rocks are found within the Permian sequence and overlying sandstones could provide potential reservoirs. Adequate seal rocks appear to be available and dolerite may provide a regional seal.

A third potential system known as the Centralian petroleum system may also operate below the Tasmania Basin and this system may have source rocks formed from Mesoproterozoic?-Neoproterozoic sediments. At this early stage of investigation the Centralian system is considered to be of marginal prospectivity. However in a frontier investigation all possibilities must be considered.

Figure 1.3 is a map showing the distributions of outcrops of potential source rocks of the three petroleum systems investigated during this study. Continuation or correlates of the exposed potential source rocks are assumed to occur within or beneath the Tasmania Basin. To illustrate the time and stratigraphic relationships between the three petroleum systems investigated, Figure 1.4 shows simplified stratigraphic columns for regions across Tasmania along with tectonic events of significance to possible petroleum systems.

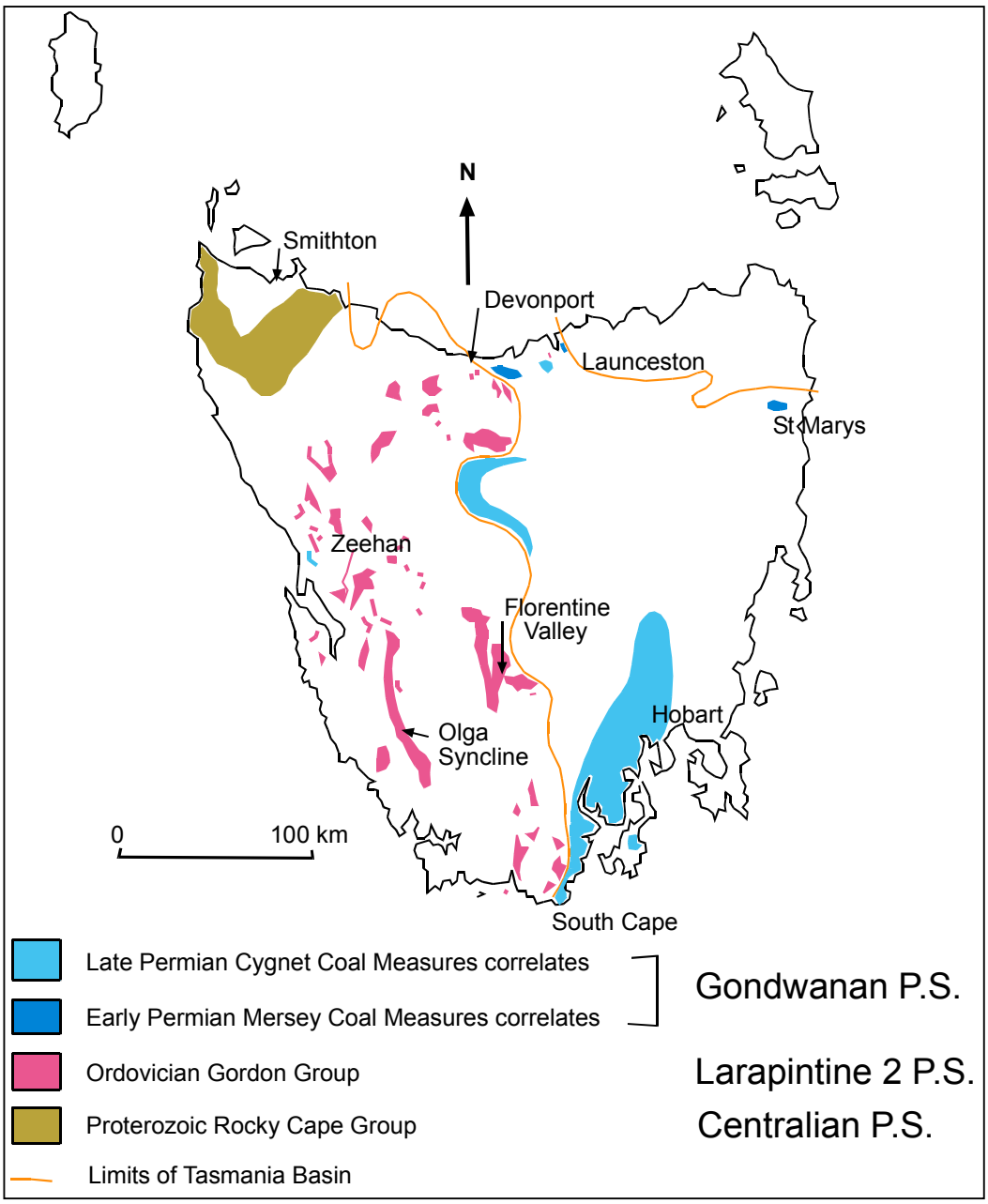

Figure 1.3. Extent of known outcrop of potential source rocks for the three petroleum systems investigated during this study. All of these sediments or correlates are inferred to occur within or beneath the Tasmania Basin, the outline of which is also shown on the map.

Figure 1.4. Time-space diagram for the parts of Tasmania and time intervals significant to the petroleum systems on-shore Tasmania considered in this thesis. Significant events in relation to petroleum systems are shown in the right hand column. The diagram is shown as a series of columns each representing a region within Tasmania, termed elements, and these are shown on a map of Tasmania. The Tasmania Basin covered most of the previous elements and dashed lines show the possible extent of the Tyennan Element beneath the Tasmania Basin. The diagram has been simplified from Seymour and Calver (1995b).

1.6. Methods used.

1. Field surveys to try and locate potential source rocks from the:

    (a) Gordon Group

    (b) Permian coals and associated siltstones

    (c) Neoproterozoic siltstones in northwestern Tasmania

2. Field investigation of reports of oil and gas seeps and bitumen sightings.

3. Organic geochemical testing of rock samples.

4. Physical measurement of maturity, vitrinite reflection (R_0), bitumen reflection.

5. Thin section examination of selected samples.

6. Estimation of the timing for hydrocarbon generation events based on burial history, mineral textures and geological history.

7. Collation of extant data related to source rock maturity.

8. Kubler Index (KI) regional survey of northwestern Tasmania.

1.7. Lithostratigraphic overview.

Due to the wide scope of this study reference is made to many group, member and formation names, some of which have correlates with differing names in various parts of Tasmania. The following paragraphs provide a brief overview of the stratigraphy referred to later in the thesis and reference should also be made to Figure 1.4 to help in an understanding of the time and spatial relationships.

The oldest rocks investigated belong to the Rocky Cape Group, which outcrop in northwestern Tasmania and consist of:

Cowrie Siltstone (base), black pyritic shale and interbedded siltstone.
Detention Subgroup, supermature cross-bedded sandstone with interbedded siltstone.
Irby Siltstone, siltstone with black shale.
Jacob Quartzite, supermature quartzarenite with silica cement.

Gee (1971) considered the initial depositional basin to have been a stable shelf with generally increasing clastic input. In southwestern Tasmania the Clark Group consists of shallow-marine orthoquartzite with minor siltstone and carbonates, some of which contain stromatolites (Seymour and Calver, 1995). This succession may be of similar age to the Rocky Cape Group.

Stratigraphically above the Rocky Cape Group and separated from it by a northeasterly trending metamorphic belt, known as the Arthur Lineament, is the

Burnie Formation, a sandy, turbidite-facies, quartzose wacke. The coeval Oonah Formation is of similar character but contains dolomite, chert and conglomerate facies in addition to quartzose wacke (Turner, 1989).

Directly overlying the Rocky Cape Group with an unconformable contact is the Togari Group, a sequence of clastic sedimentary rocks commencing with the Forest Conglomerate, overlain by the Black River Dolomite containing dolomite and chert. The Forest Conglomerate contains clasts derived dominantly from the Rocky Cape Group. Overlying the Black River Dolomite is the Kanunnah Subgroup consisting of interbedded mudstone, siltstone and turbidite wacke with several phases of mafic lava. The top unit in the group is the Smithton Dolomite. In southwestern Tasmania two sequences of dolomite, the Jane River Dolomite and Weld River Group, may be broadly coeval with the Upper Togari Group (Brown, 1989).

A significant period of folding and faulting followed the deposition of these groups and this can be recognised right across Tasmania. This deformation is related to a possible major continent/island arc collision event at approximately 500 Ma. This event is shown on Figure 1.4 as thrusting and polyphase folding.

Erosion of the Tyennan region followed the Cambrian tectonic events resulting in the deposition of the Dundas Group, Roland Conglomerate and Denison Group. These sequences all commence with conglomerate and pass upwards through shallow-water sandstone to siltstone and include chert sequences in the upper formations. The Wurawina Supergroup is a conformable sequence deposited from late Cambrian to Devonian times and includes the Denison, Gordon and Tiger Range Groups and the lateral equivalent to the Tiger Range Group, the Eldon Group. The Gordon Group is a limestone dominated, richly fossiliferous, shallow-water, platform sequence with the greatest development in the Florentine Valley. The Gordon Group covered much of western Tasmania, apart from the Rocky Cape Region, by Late Ordovician times. The tops of the Tiger Range and Eldon Groups have been removed by erosion (Baillie, 1989).

Following the deposition of the Wurawina Supergroup another major tectonic event, the Tabberaberan Orogeny, caused major folding, faulting and thrusting across

Tasmania. Granitoid intrusions occurred across Tasmania soon after this tectonic episode.

A period of erosion followed the granitoid intrusions before deposition once more commenced. The Parmeener Supergroup was deposited within the Tasmania Basin and although this is shown on Figure 1.4 in four different regions the deposition was continuous across these regions and probably a much greater area with the margins of the basin unknown. Deposition began with diamictite and tillite known as the Wynyard Tillite in the north of Tasmania and Truro Tillite in the south. Above the tillite sequences siltstone sequences were deposited, known as Woody Island Siltstone in the south, Quamby Mudstone in the north and Inglis Formation in the northwest. These siltstones contain beds of oil shale (Tasmanite) near the base, which was once worked near Latrobe to extract oil. Oil shale also occurs in the northwest at Hellyer Gorge, on the east coast at Douglas River and in the south within the Styx Valley.

Overlying the siltstones, thin fluvial units known as the Lower Freshwater Sequence have been deposited. These units include the Faulkner Group and its lateral equivalents, the Liffey Group and Mersey Coal Measures. These units are inferred to have been deposited on a coastal plain with carbonaceous units deposited near the seaward margin.

In southern Tasmania the Berriedale Limestone, a shallow-marine unit, overlies the Lower Freshwater Sequence. Most of northern and western Tasmania was probably emergent at this time. Gentle uplift and erosion occurred before renewed marine deposition of the Malbina and Deep Bay Formations of fossiliferous siltstone and poorly-sorted sandstone in which ice-rafted dropstones are common. Overlying these formations are the sandstones and calcareous siltstones of the Bogan Gap Group and Ferntree correlates.

The Upper Parmeener Supergroup has been divided into four units (Forsyth, 1989). Unit 1 corresponds to the Late Permian Cygnet Coal Measures and correlates, consisting of well-bedded sandstone in southern Tasmania and carbonaceous siltstone and mudstone in the north. Thin coal seams are present in the far southeast and also in the central highlands. The coal seams wedge out to the northeast, partly due to erosion, which occurred prior to the deposition of Unit 2.

Unit 2 consists of well-sorted quartzarenite, with intervals of lutite found near Hobart. This sequence was probably deposited from low-sinuosity rivers flowing east or south east. Unit 3 has quartz granule sandstone overlain by interbedded quartz sandstone, lithic sandstone and lutite with thin coal seams present in places. Unit 4 is predominantly lithic sandstone with minor lutite and coal, all of Tasmania's economic coal reserves (Bacon, 1991). Rare felsic tuff horizons occur near the top of Unit 4 indicating a volcanic source probably to the east of Tasmania during the time of deposition of Unit 4 (Bacon and Everard, 1981).

During the Jurassic, dolerite was intruded into the Tasmania Basin. This intrusion was related to tensional stresses building up prior to the rifting of Australia and Antarctica (Veevers and Eittreim,1988). The dolerite sills provide a cap over the Tasmania Basin and, throughout much of Tasmania, sequences above the dolerite have now largely been eroded.

CHAPTER TWO.

GEOLOGICAL HISTORY OF TASMANIA.

2.1. Introduction.

Hydrocarbon accumulations require special geological conditions in order to form and be preserved and for this reason it is important to understand the geological history of an area before deciding to proceed with any petroleum exploration project. In order to establish a context for interpretation of the following geological history the basic components of a petroleum system will first be described. The primary component of any petroleum systems is a source rock (a high organic content sediment usually deposited under anoxic conditions). In order to generate hydrocarbons, source rocks must, after deposition, be subjected to suitable conditions of time, temperature and pressure to allow chemical reactions to transform organic matter into hydrocarbons by a process known as maturation. The reactions involved are complex and not fully understood but the process requires temperatures in the range 50-120° C over a suitable time, generally requiring burial to a depth of 2 km or more (Hunt, 1995). Maturation is actually incipient metamorphism and the chemical and physical changes in the sediments allow measurements of the level of maturity to be determined.

Hydrocarbon generation liberates the oil and/or gas from source rocks, which is then able, to migrate if expulsion pressure is great enough and suitable migration pathways exist. Hydrocarbon accumulations occur when migrating oil and/or gas becomes trapped in suitable structures and the flow of hydrocarbons is arrested. Seals such as fine-grained sediments prevent the escape of hydrocarbons from trap structures so accumulations can be contained. Traps must be in place before migration of hydrocarbons occurs and trap formation often requires tectonic activity involving folding or faulting.

Major tectonic activity after the filling of hydrocarbon reservoirs is likely to breach reservoir seals and allow oil/gas to be lost. Thermal events such as igneous activity may destroy reservoired hydrocarbons, and hydrothermal fluids can also turn hydrocarbons into pyrobitumens. Consequently after hydrocarbons are trapped subsequent geological conditions must be quiescent to ensure preservation.

The following brief geological history of Tasmania will commence in the Mesoproterozoic when the earliest known sedimentation relevant to petroleum systems occurred. Events of importance to the development of petroleum systems and the preservation of hydrocarbon accumulations occurring in later times will then be considered. It is not intended to be an overall discourse on Tasmanian geological history and thus will concentrate on areas, which at particular times were, important to the deposition of suitable sediments or development of structures likely to be important to petroleum systems. The locations of places mentioned in this chapter are shown in Figure 2.1.

2.2. Mesoproterozoic- Neoproterozoic.

In northwestern Tasmania Mesoproterozoic? to Neoproterozoic sediments known as the Rocky Cape Group crop out and, although the depositional age of these sediments is unknown, detrital zircons have been dated (SHRIMP ages) from this sequence to give a maximum age of 1450 Ma for the Detention Quartzite and 1250 Ma for the Jacob Quartzite (Black et al., 2004). Minimum age is constrained by a low-angle unconformity between the Rocky Cape Group and the overlying Ahrberg and Togari Groups which is attributed to the Wickham Orogeny dated at 760 $\pm$ 12 Ma by ion-probe dating of zircons from the Cape Wickham Granite (Turner et al., 1998). The age of the unconformity is not accurately dated however it is older than 650 Ma (Calver, 1998). Another constraint on the age of these sediments is that the Bowry Granite intrudes these sediments and has been dated at 777 $\pm$ 7 Ma (Turner et al., 1998) and this event is also correlated with the Willouran flood basalts of South Australia which together record the ca 780 Ma break-up of Rodinia (Holm et al., 2003). This break-up has been linked to extreme environmental and biogeochemical fluctuations and explosive evolution of metazoan life (Hoffmann et al., 1998). Thus the Rocky Cape Group was deposited between 1200 Ma and 650 Ma.

The Rocky Cape Group is a relatively unmetamorphosed shallow-marine association of quartz arenite, siltstone and mudstone which occurs in a synclinal structure with the hinge plunging gently to the north (Spry, 1964). The stratigraphy, as shown in Figure 2.2, was originally determined by Gee, (1968) from coastal exposures along the north coast and the sediments have since been mapped across the Smithton Synclinorium

and stratigraphy refined (Everard et al., 2004). The 2450 m thick Cowrie Siltstone within this sequence is of interest as a potential hydrocarbon source rock due to its high organic carbon content (up to 4% TOC, AMDEL, 2004) and low metamorphic grade (Calc. R_o 0.6%, AMDEL, 2004).

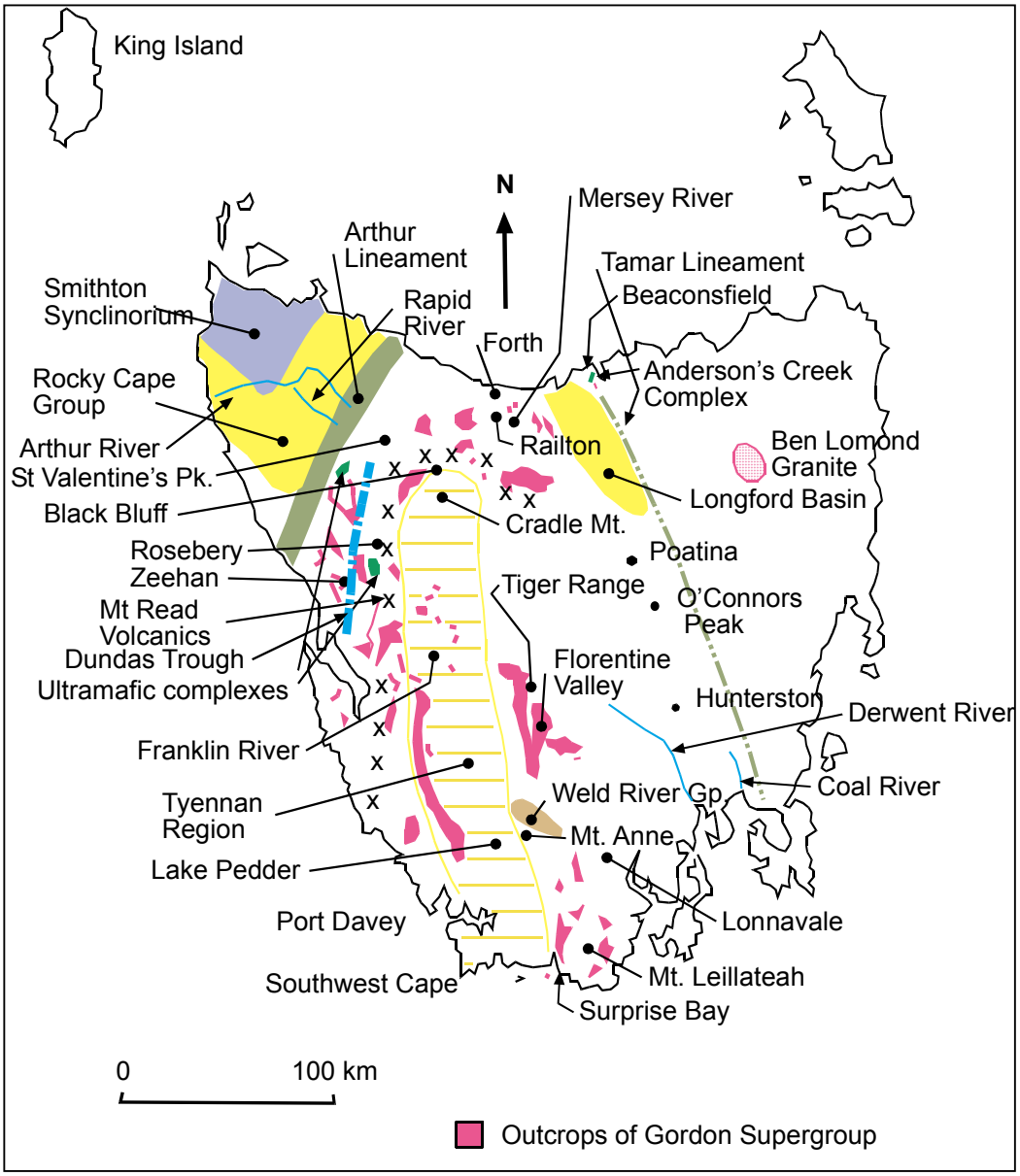

Figure 2.1. Map of Tasmania showing places and generalised shapes of lithostratigraphic units mentioned in Chapter 2.

Evidence of open folding in this sequence was noted in the Arthur River area (McNeil, 1960) and also in the Rapid River area (Matthews, 1960). Gentle folding in this area has been confirmed by fieldwork during the course of this investigation,

however the folding becomes more intense on the eastern side, close to the Arthur Lineament.

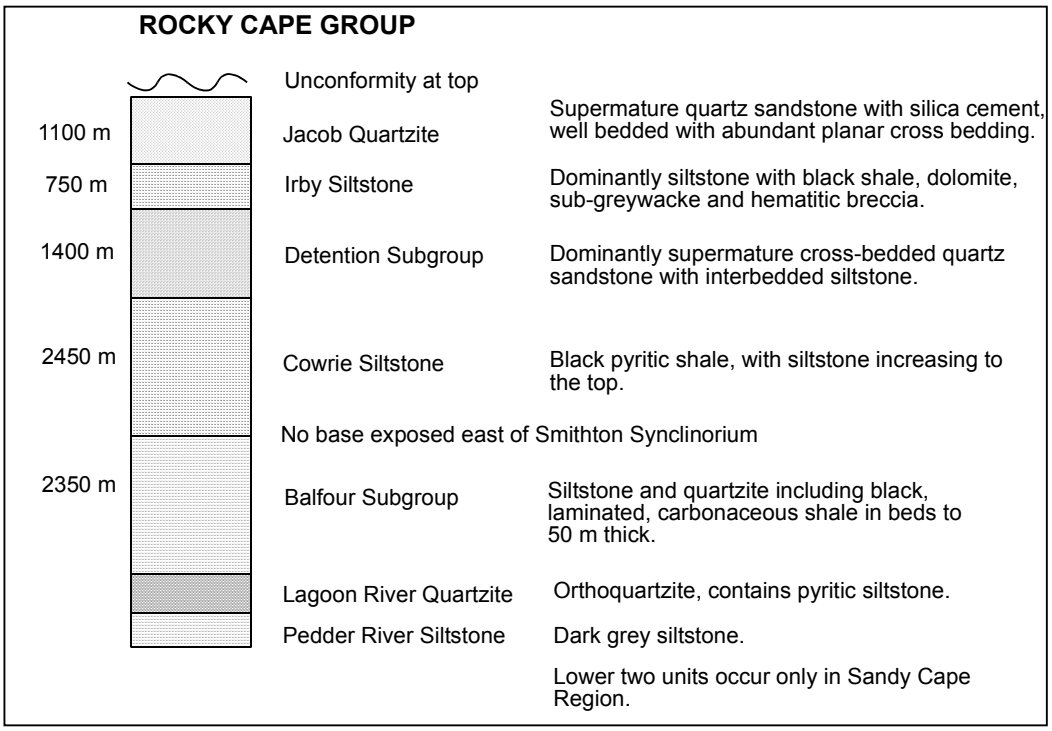

Figure 2.2. Stratigraphic column for the Rocky Cape Group in northwestern Tasmania. After Everard et al., (2004).

The eastern half of King Island consists of a thick 6-7 km succession of relatively unmetamorphosed shale, siltstone and fine-grained, muscovitic, quartz, sandstone of presumed Proterozoic age which lithologically resembles the Cowrie Siltstone (Calver and Walter, 2000). As shown in Figure 2.2, the shelfal siliclastics of the Rocky Cape Group also have a total thickness of approximately 6 km (Gee, 1968). Calver and Walter (2000) have shown that there is a strong lithostratigraphic and chemostratigraphic resemblance between the succession on King Island and the lowermost Wilpena Group of the Adelaide Rift Complex together with the rest of Centralian petroleum basins. Calver and Walter (2000) show that northwestern Tasmania probably rifted away from the mainland before King Island and this accounts for differences in the stratigraphy between the two areas.

The high organic content within the sediments of northwestern Tasmania was probably derived from microbial mats, which at the time of deposition would not have

been grazed and so efficient burial of organic matter occurred. Lack of bioturbation confirms that benthic organisms did not re-work sediments. The depositional environment is inferred to be a shallow shelf and coupled with the warm environment inferred from palaeomagnetic measurements, indicating low latitudes (Pisarevsky et al., 2001), conditions for high organic productivity would have ensued. Anoxic bottom conditions can be inferred from the presence of abundant sedimentary pyrite, particularly along certain bedding planes in the Cowrie Siltstone (Berner, 1970). Shallow water can also be inferred from ripple casts found on bedding planes of Cowrie Siltstone as shown by photograph Figure 2.3.

Figure 2.3. Photograph of ripple casts on a pyrite covered bedding plane of Cowrie Siltstone, indicating shallow-water, anoxic conditions. Photograph taken at Holder Spur 1 Quarry, Holder Plains.

Possible evaporitic conditions may also have occurred as fossil mud cracks were found in a siltstone 2 m above black, pyritic, carbonaceous Cowrie Siltstone at Holder Road Quarry (349936 mE 5449899 mN). Evaporitic casts were also found in Cassiterite Creek (322264 mE 5430798 mN) suggesting local emergence (Everard et al., 2004).

Stratigraphically above the Rocky Cape Group and with a low-angle, unconformable contact marked by the Forest Conglomerate, the Ahrberg and Togari Groups have

been deposited. These consist of silicified dolomite overlain by tholeiitic volcanics and associated volcaniclastics. The basal Black River Dolomite often has a breccia texture in which fragments comprise pieces of algal mat with silicified stromatolites. Stromatolites are also present in the uppermost parts of the formation. Parts of the Julius River Member of the Black River Dolomite also have potential as source rocks with TOC 2.08% and T_{max} 439°C (AMDEL, 2004). These sediments are black, carbonaceous, siltstones and mudstones, which are weakly fissile. In thin section they are almost opaque due to the presence of carbonaceous material. Chitinozoan-like microfossils, ovoid or flask-shaped, 60-120 μm long, have been found in these sediments (Everard et al., 2004; Saito et al., 1988). The stratigraphy of the Togari Group is shown in Figure 2.4.

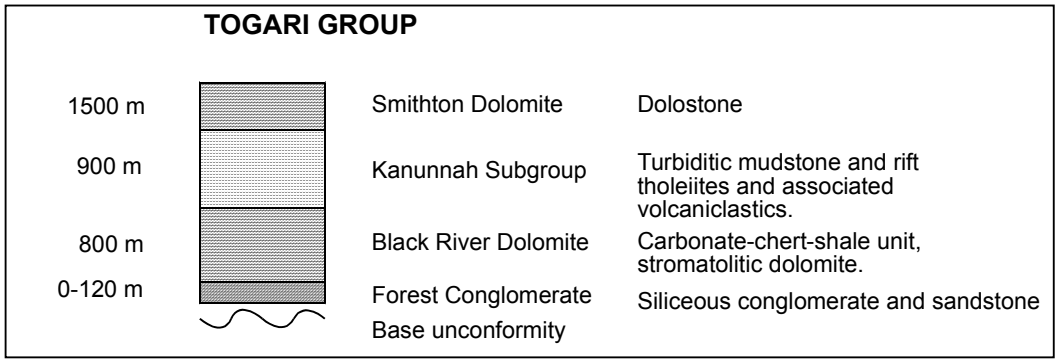

Figure 2.4. Stratigraphic column for the Togari Group in northwestern Tasmania. After Calver (1998).

Calver (1998) has dated the Black River Dolomite using isotope stratigraphy as ca 750-650 Ma. The Kanunnah Subgroup is inferred to be 650-580 Ma and the Smithton Dolomite 580-545 Ma. The Black River Dolomite contains a stromatolite *Baicalia cf. burra* also known from the Adelaide Geosyncline suggesting that northwestern Tasmania was part of the Centralian Basin depositional system at the time (Hill et al., 2000). Other indications of a link with the Centralian Superbasin are suggested by similar lithologies on King Island to those in the Adelaide Rift Complex, particularly the cap dolostones, overlying shale and benthic microbial mats (Calver and Walter, 2000).

Dolerite dykes, which occur within the Rocky Cape Group, have yielded K-Ar whole rock ages of 600 $\pm$ 8 Ma and 588 $\pm$ 8 Ma (Brown, 1989) and these may be genetically

related to the Kanunnah Subgroup. These dolerite dykes have been intruded along strike of the Rocky Cape Group and are magmatic expressions of rifting which occurred 650-580 Ma (Holm et al., 2003).

Suggested correlates of the Togari Group are widespread in Tasmania including the Success Creek Group-Crimson Creek Group of western Tasmania and Weld River Group of central-south Tasmania (Calver, 1998). Possible correlates have been found in the Bass 3 (Bass Strait petroleum drill hole) (Anon, 1967) and diamond drill hole at Poatina (Hassell, 1996) and also Precambrian dolomite found in the Hunterston DDH (Reid et al., 2003). The Clark Group in southwest Tasmania has outcrops of black micaceous shale and the Weld River Group has thick (300 m), black, pyritic mudstone implying high organic content (Calver et al., 1985). Outcrops of possible correlates of the Crimson Creek Formation occur near O'Connors Peak, on the western edge of the Longford Basin, and these are directly overlain by Permian tillite.

The distribution of possible correlates of Mesoproterozoic?-Neoproterozoic sediments could imply that significant portions of western Tasmania may have once been part of the Centralian Superbasin however care needs to be exercised before a conclusion is reached. As will be shown in section 2.3 an apparent subduction boundary crossed Tasmania from north to south during the Cambrian so it is unlikely that the same depositional basin was continuous across Tasmania during the Mesoproterozoic?-Neoproterozoic. Similar sediments may have been deposited in two different depositional basins or similar sediments may have been deposited upon shelves surrounding islands to those deposited upon a continental shelf. If this was the case, it could account for the apparent discontinuous distribution of shallow-water Mesoproterozoic?-Neoproterozoic sediments present in western Tasmania outside the Rocky Cape Group. Another explanation is that shallow-water sediment blocks have been dismembered and transported by tectonic processes to separate locations.

Evidence presented by Foster et al., 2005, suggests that the western Tasmania terrane may have been either a promontory along the Gondwanan margin or else a continental ribbon rifted during the break-up of Rodinia. Because the western Tasmania terrane does not have a direct counterpart exposed on mainland Australia it records important clues to the possible inversions of the Neoproterozoic-Early Cambrian margin of Gondwana. Structural data from the Forth Metamorphic Complex suggests that there

was a change from accretionary deformation to back arc extension along the Australian margin of Gondwana and that Tasmania was involved in both the Delamerian-Ross orogeny and the Lachlan orogeny (Foster et al., 2005).

2.3. Cambrian.

Cambrian tectonic activity was important from the perspective of petroleum exploration onshore Tasmania because it established the framework upon which later sedimentation and folding/thrusting events were focussed. Sedimentary basins developed in structural sags initiated along lineaments dating from the Cambrian and further discussion of these will be made in following sections. Thrusting, faulting and folding events at later dates, creating possible hydrocarbon traps, were also directed by trends established during the Cambrian.

A collision between continental crust in the west, and oceanic crustal rocks, including island-arc type rocks, in the east occurred during the Cambrian (Holm and Berry, 2002). This led to the final suturing of Gondwana, known as the Ross-Delamerian Orogeny, beginning at 515 $\pm$ 5 Ma (Boger and Miller, 2004; Reed et al., 2002). Cambrian aged metamorphic complexes mark the positions of these convergent margins in Tasmania trending from near Beaconsfield in northern Tasmania through the Mersey River Metamorphic Complex near Cradle Mountain then southwards via the Franklin River to Port Davey (Meffre et al., 2000). The actual collisional events seem to have been rather passive, but post-collisional events involving extension with graben formation and explosive magmatism were more dramatic.

Mafic-ultramafic complexes were emplaced in western and northern Tasmania at this time during west-directed subduction with possibly multiple east-dipping subduction zones (Holm and Berry, 2002). Reed et al. (2002) have suggested that two subduction zones operated within Tasmania and these intersected at a triple junction located somewhere to the north of Tasmania. In western Tasmania six mafic-ultramafic complexes occur, Port Davey, Franklin River, Mersey River, Forth, Settler's Schist and Arthur Lineament and these mark the position of a possible subduction zone (Meffre et al., 2000). Further evidence of a subduction boundary in northern Tasmania is derived from seismic images of east dipping reflectors at the site of the Tamar Lineament, indicating this may be a Cambrian suture (Reed et al., 2002). East

dipping reflectors were also noted at the site of the Arthur Lineament on a deep seismic transect (Barton, 1999).

Mesoproterozoic? to Neoproterozoic rocks on opposite sides of the Arthur Lineament in northwestern Tasmania have contrasting lithologies; the western side Rocky Cape Group are shelfal siliclastics (Everard et al., 2004) while the eastern side Burnie Group are deep-water turbidites (Turner, 1990). The Arthur Lineament is a Cambrian structure (Holm and Berry, 2002) and marks the convergence of continental rocks to the west and oceanic rocks to the east. Metamorphic effects are minimal beyond the lineament itself indicating a relatively passive event. Convergence of continental and oceanic type crust is also indicated across the Tamar Lineament, another Cambrian suture, with continental crust to the west and oceanic crust to the east (Elliott et al., 1993).

Convergence of eastern and western Tasmania would have depressed the Tyennan crust, and post-compressional buoyancy-driven uplift of this region led to rapid erosion and the deposition of Upper Cambrian-Ordovician coarse-grained clastics (Reed et al., 2002). Thinning and extension of crust followed the collision events in western Tasmania with the collapse of the continental margin forming the Dundas, Smithton and King Island Troughs, and these were rapidly filled with volcaniclastic sediments from post-collisional volcanism of the Mount Read Volcanics (Haines and Flottman, 1998).

Significant economic mineral deposits were formed as a result of Cambrian volcanism and associated granite emplacement particularly along the margins of the Tyennan Nucleus. Some of these mineral deposits possibly formed at reduction boundaries due to the presence of thick, organic-rich sediments such as the 85 m thick black slates just below the hanging wall to the Rosebery Mine (Graves et al., 1998). Redox reactions between very immature organic matter and brine sulphate produce reduced sulphide, which results in the precipitation of base metal sulphides (Eldridge et al., 1993; Hinman, 1996).

2.4. Late Cambrian - Ordovician.

During the Late Cambrian-Early Ordovician, erosion of the Tyennan region resulted in the deposition of the siliciclastic Denison Group into adjacent topographically

lower areas (Corbett, 1970). The deposition began with slope or basinal deposits and passes up through shallow marine into alluvial-fan associations, above which are shallow marine mudstones. The sequence represents a regression (Late Cambrian) and then transgression (Early to Middle Ordovician). This process built a basement of conglomerates and shallow-marine shelf deposits (Black et al., 2005) upon which later shallow-water, shelf-carbonates were established during the Ordovician as shown diagrammatically in Figure 2.5.

Western Tasmania was established in its current position relative to mainland Australia during the Late Cambrian and it has remained in this same relative position until the present (Cayley et al., 2002). No Late Cambrian conglomerates are found west of the Arthur Lineament and this suggests that northwestern Tasmania may have been uplifted at the time and probably remained so during the Ordovician period as no sediments of this age occur west of the Arthur Lineament.

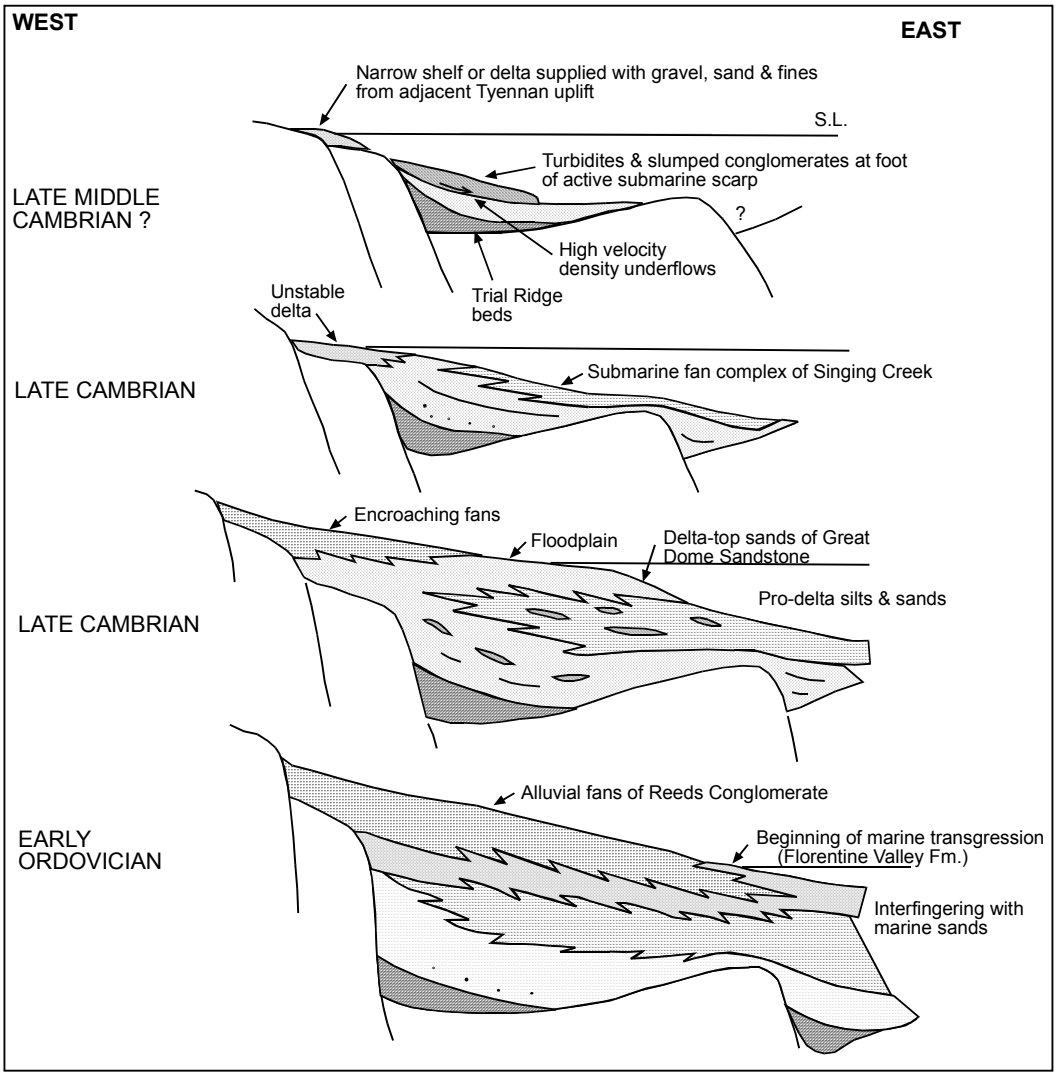

Figure 2.5. Evolution of the Denison Range (After Corbett, 1970); n.b. the nature of the faults shown as normal has not been established; they may have been thrusts at the time of their formation and may have had some lateral movement; however the palaeogeographic and sedimentary environments and their relationships are regarded as valid.

2.5. Ordovician.

During the Ordovician a seaway separated the two separate terranes, which make up Tasmania. The basement of the eastern Tasmania terrane is composed of a suite of turbidites, the Mathinna Group, deposited in a basin elongated NNW-SSE along strike from the Melbourne Trough (Baillie and Powell, 1989). This terrane was deposited in deeper water offshore from the western terrane, possibly from sediments eroded from

the Delamerian mountain chain (Jones et al., 1993), and was folded during the 460-435 Ma Benambran Orogeny (Reed et al., 2002).

The western terrane was a shallow shelf environment on which mainly carbonate deposition occurred, but with some minor intervals of siliciclastics. Deeper water limestone has been recognised at Surprise Bay in southern Tasmania and near Beaconsfield in northern Tasmania and these areas were probably at the edges of the shallow shelf (Burrett et al., 1981). The Gordon Group, deposited on this shallow shelf, has been well studied in the Florentine Valley, having been divided into a number of mappable units as shown in Figure 2.6 (Corbett and Banks, 1974).

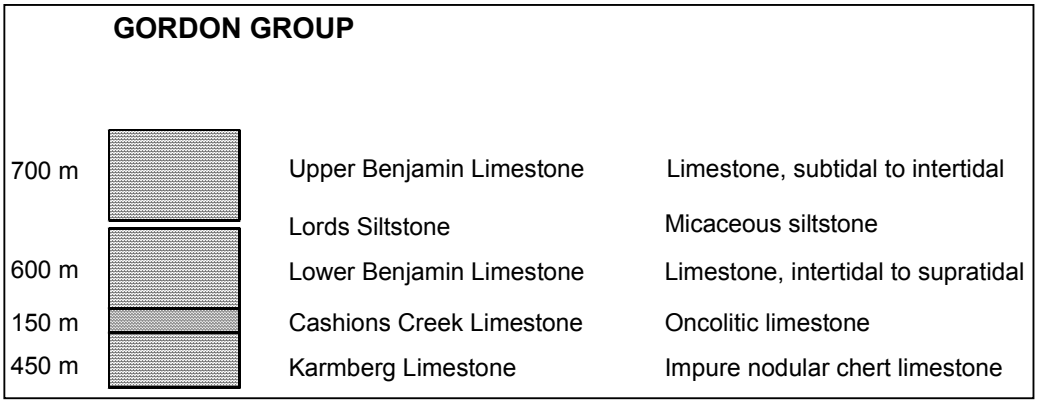

Figure 2.6. Stratigraphic column for the Gordon Supergroup in the Florentine Valley, Tasmania. After Corbett and Banks (1974).

The Gordon Group has been preserved in large (5-7 km wide) Devonian synclines right across western Tasmania except for the Rocky Cape Region, indicating that shelf conditions occurred across most of western Tasmania throughout the Ordovician. Burrett (1978) has shown that deposition commenced during the Arenig in the east at Beaconsfield and encroached westwards in northern Tasmania, reaching Railton in the Llanvirn. Islands probably remained in parts of the Tyennan Region and a shoreline existed somewhere near the present Arthur Lineament in northwestern Tasmania. The probable palaeogeography of Tasmania during the Late Ordovician is shown in Figures 2.7 and 2.8.

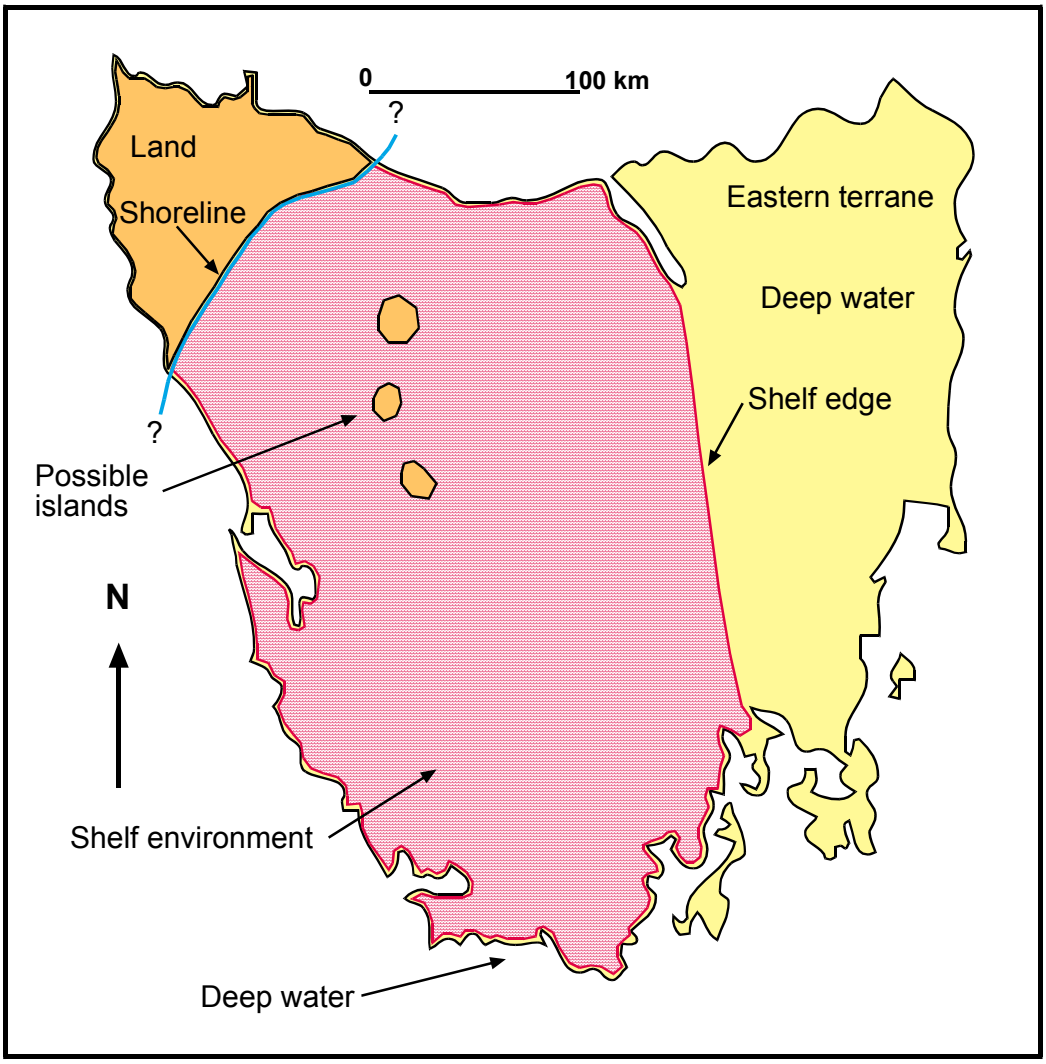

Figure 2.7. Possible palaeogeography of Tasmania during the Late Ordovician. No attempt has been made to account for effects of folding or thrusting. Land was emergent in the northwestern part of the state with the rest, apart from possible islands, submerged below sea level. The major portion of Tasmania was a shallow shelf environment based on continental crust and the eastern regions were covered by deeper water over oceanic crust. The shelf edge was probably close to the line of the Tamar Lineament.

Maximum extent of the carbonate platform was reached during the Caradoc and the gradual increase in size of this platform is shown in a series of maps as Figure 2.9 A-D, showing probable palaeogeography from Tremadoc to Ashgillian. These maps were drawn using information from the following sources (Cook and Totterdell, 1991; Li and Powell, 2001; Seymour and Calver, 1995).

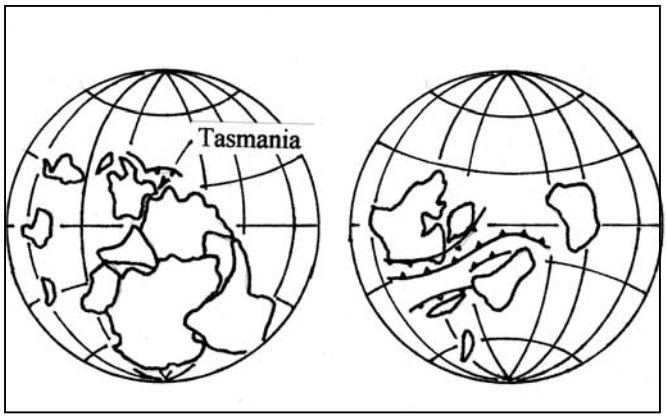

Figure 2.8a. Late Ordovician world reconstruction (ca. 450 Ma), showing the probable position of Tasmania on the margin of Gondwana. After Li and Powell (2001).

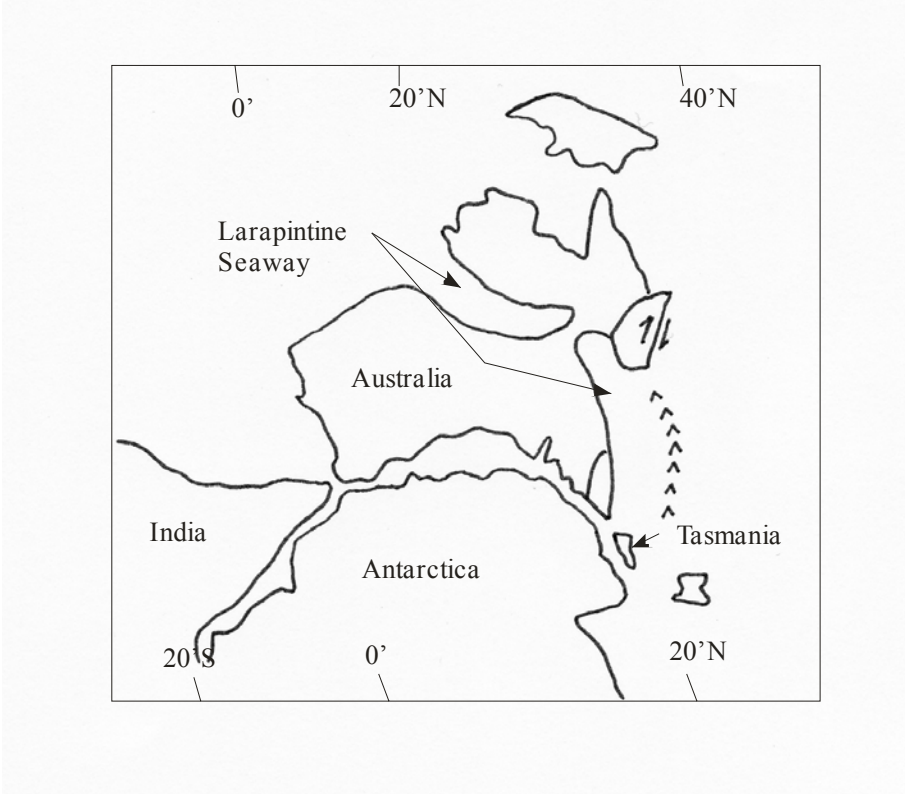

Figure 2.8b. Late Ordovician palaeogeography of Australia showing the probable position of Tasmania and the closure of the Larapintine Seaway. Modified from Li and Powell (2001).

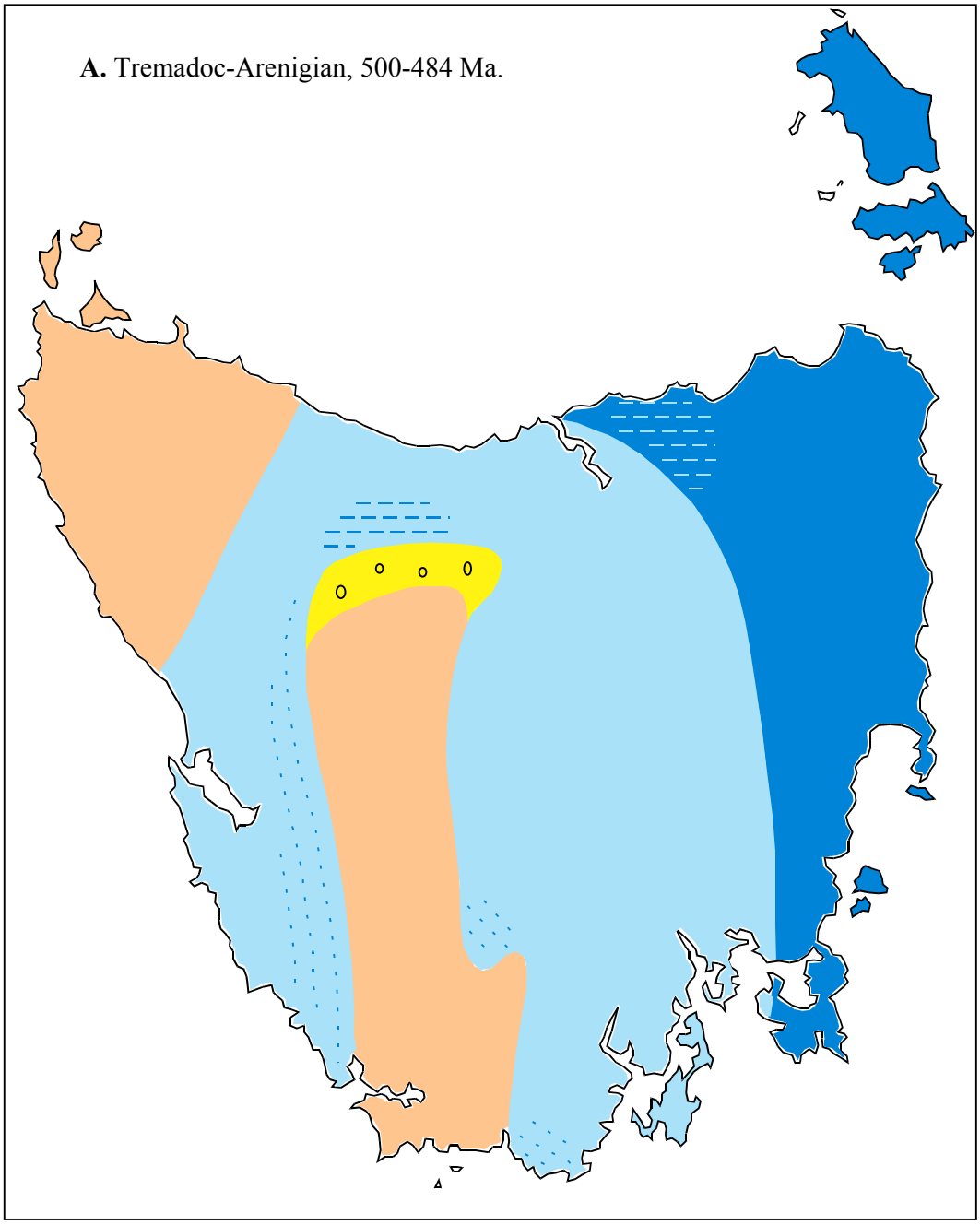

Figure 2.9. A-D. Probable palaeogeography of Tasmania is shown for some intervals within the Ordovician illustrating progressive growth of a carbonate platform. During Early Arenig the carbonate platform began forming at the seaward margins of siliclastic sediments derived from eroding highlands. See common key for interpretation of colours and symbols on Figures A-D.

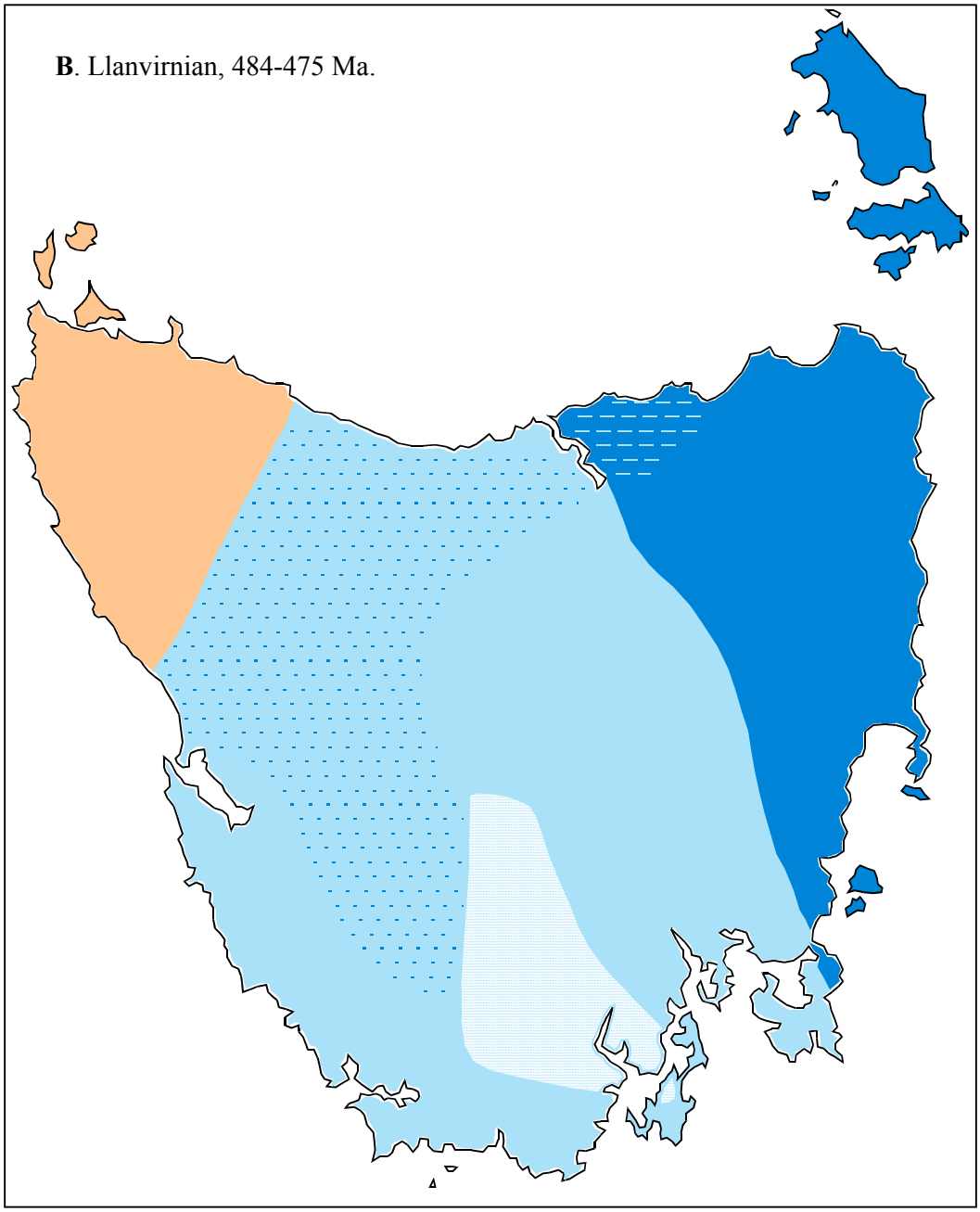

Figure 2.9B. Growth of the carbonate platform occurred during the Llanvirn due to basinal subsidence.

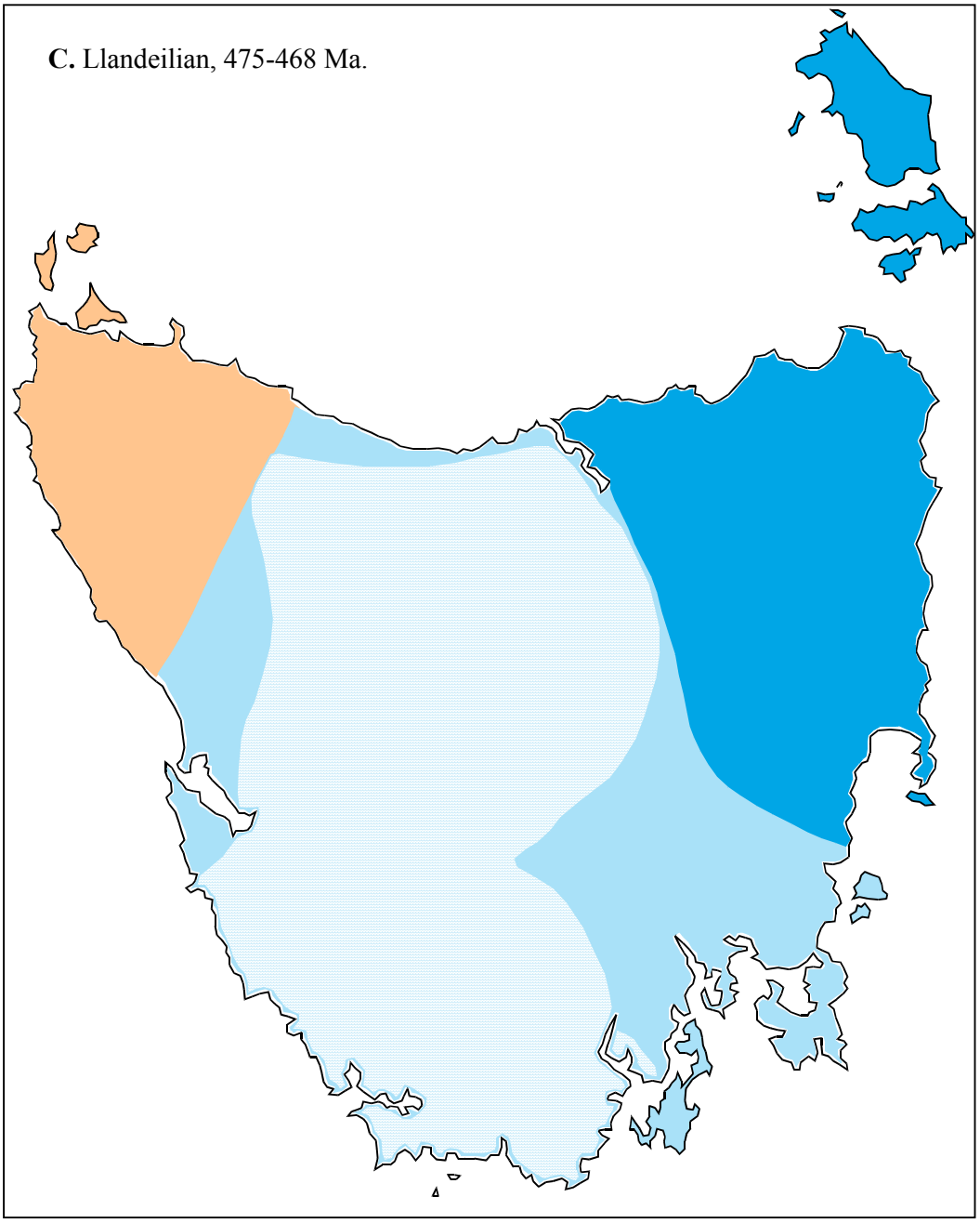

Figure 2.9C. Westward growth of carbonate platform continued during Llandeilian due to basin subsidence.

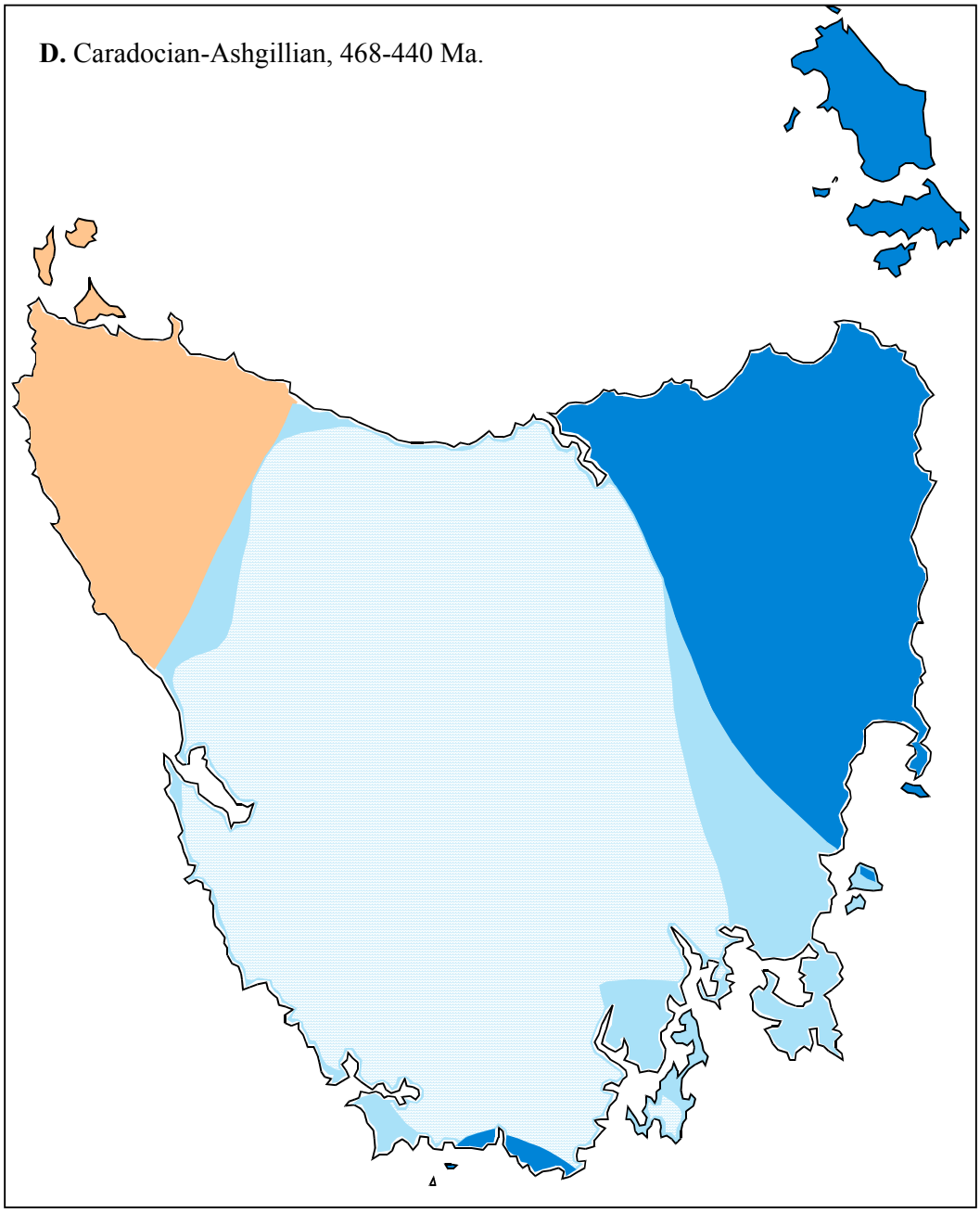

Figure 2.9D. Probable palaeogeography of Tasmania when carbonate platform had reached maximum extent. Maps were compiled from data derived from Cook and Totterdell (1991), Li and Powell (2001), Seymour and Calver (1995).

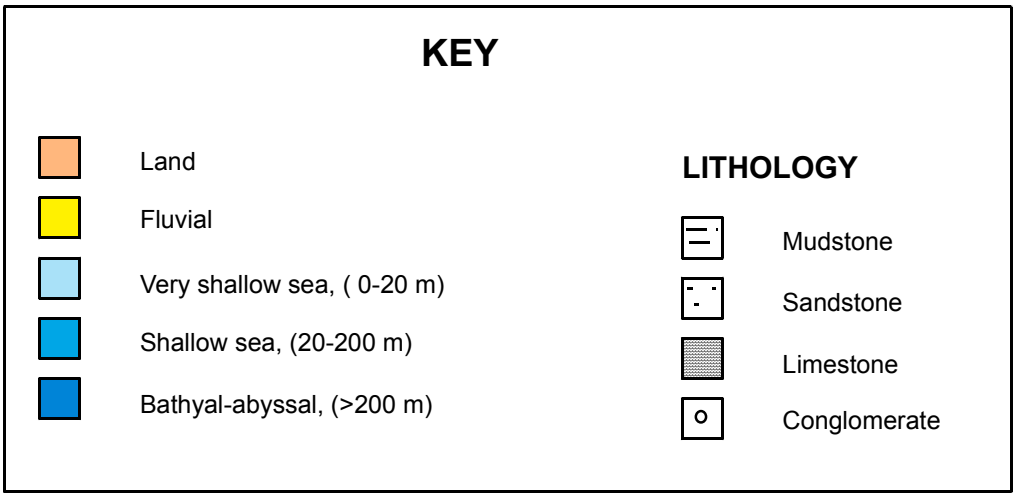

Figure 2.9E. Key for use with Figures 2.9A-D. Colour coding is used to represent inferred land and sea environments. Where lithology can be determined symbols are used to represent major types.

Fine-scale progradation-transgression cycles have been noted in the Gordon Group and these are most likely to be related to episodic local subsidences or with an autocyclic mechanism (Banks and Calver, 1989). Thin organic-rich shale layers mark these cycle boundaries, which have potential as hydrocarbon source rocks with TOC up to 1.83%. Thick, organic-rich, black shales were deposited further north in the Tabberabbera Zone of the Lachlan Fold Belt during the Late Ordovician, recognised as a worldwide oceanic anoxic event (Jones et al., 1993). No similar deposits have been noted in Tasmania. During the Ordovician total subsidence on the Tasmanian Shelf was in the order of 2.5 km (Banks and Burrett, 1989).

2.6. Silurian-Devonian.

The Tiger Range Group lies stratigraphically above the Florentine Valley Ordovician sediments and these are Silurian-Devonian shallow-marine, quartz-sandstone and mudstone sequences. This group is conformable with the Gordon Group and the stratigraphic column for the Tiger Range Group is shown in Figure 2.10.

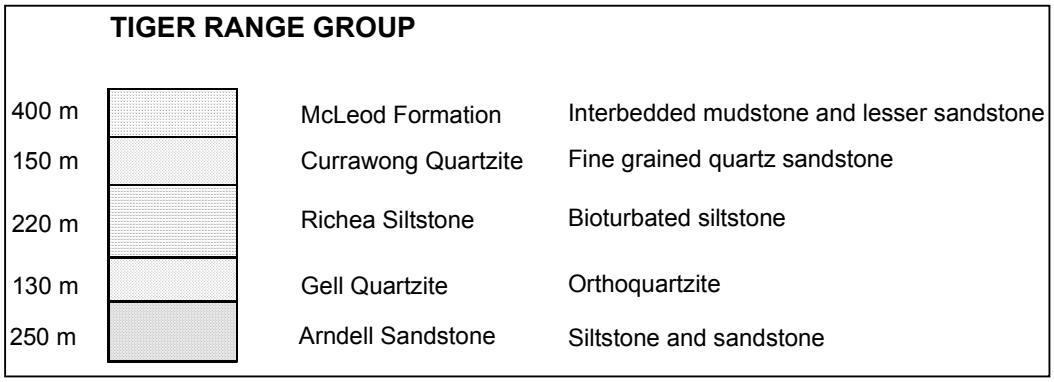

Figure 2.10. Stratigraphic column for the Tiger Range Group, which outcrop on the western side of the Florentine Valley, Tasmania. After Corbett and Banks, (1974).

In the Zeehan area, correlates of the Tiger Range Group are known as the Eldon Group (Baillie, 1989b). The stratigraphy for the Eldon Group is shown in Figure 2.11. In places there is an unconformity between the Gordon Group and Eldon Group probably related to the Benambran Orogeny (Reed et al., 2002).

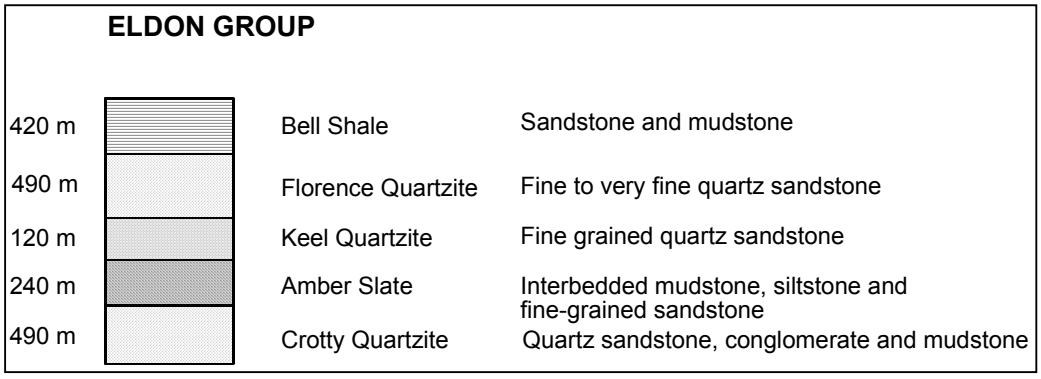

Figure 2.11. Stratigraphic column for the Eldon Group in western Tasmania. After Baillie, (1989b).

The deposition of clastic material over the Ordovician carbonates indicates that the commencement of a significant uplift in the source area occurred combined with regression of the sea. The sequence of sandstone to later mudstone/siltstone sequences is consistent with a reduction in uplift with time, and consequent lowering in the rate of erosion. Significant for hydrocarbon exploration, these sediments mark a burial phase of possible source rocks and the sequence also contains possible sandstone reservoir rocks and suitable fine-grained mudstones as seals.

2.7. Devonian deformation.

The Lower Devonian and earlier rocks of Tasmania are extensively deformed and this is partly due to two phases of deformation associated with the Tabberabberan Orogeny (Seymour, 1980). The earlier folds developed between converging blocks with the Tyennan Region behaving as a competent block. Later folding was in a more northerly and northwesterly direction and where these later folds intersect the earlier folds near Black Bluff-St Valentine's Peak dome and basin structures have developed (Seymour, 1989). The trends of Devonian folding are shown in Figure 2.12. Extensive thrusting can be observed in northern Tasmania resulting from the eastern Tasmanian terrane being thrust over the western Tasmanian terrane due to failure of a Cambrian suture (Woodward et al., 1993). Thrusts are also inferred to be present below cover in the Tasmania Basin based on the interpretation of gravity and magnetic data (Leaman, 2001). Similar interpretations of large scale thrusting have been made from examination of seismic data collected by Great South Land Minerals (Blackburn, 2004; Stacey, 2004).

Thrusting and folding during the Tabberabberan Orogeny is significant for hydrocarbon exploration because trap structures could have formed at this time, and according to GSLM exploration philosophy, in a sequence favourable for hydrocarbon accumulation from Ordovician source rocks. Suitable reservoir rocks and seals had also been deposited. The folding and faulting may also have initiated fractures within the Gordon Group so as to provide migration routes through otherwise tight limestone.

2.8. Mid-Devonian granitoid emplacement.

Following the folding and thrusting of the Tabberabberan Orogeny granitoids were intruded commencing in eastern Tasmania from 400.5 $\pm$ 4.0 Ma to 376.5 $\pm$ 2.7 Ma and in western Tasmania 373.6 $\pm$ 1.8 Ma to 350.8 $\pm$ 1.7 Ma (Black et al., 2005). Many of these granitoid intrusions resulted in associated mineral deposits such as scheelite-bearing skarns, cassiterite-stannite-pyrrhotite carbonate replacement, argentiferous lead-zinc veins and gold veins. The granitoids generally have narrow contact thermal aureoles, but it could be assumed that lower grade thermal effects of importance to source rock maturation were widely distributed and Tasmania's current high geothermal gradient may in part be due to heat generated by radioactive decay

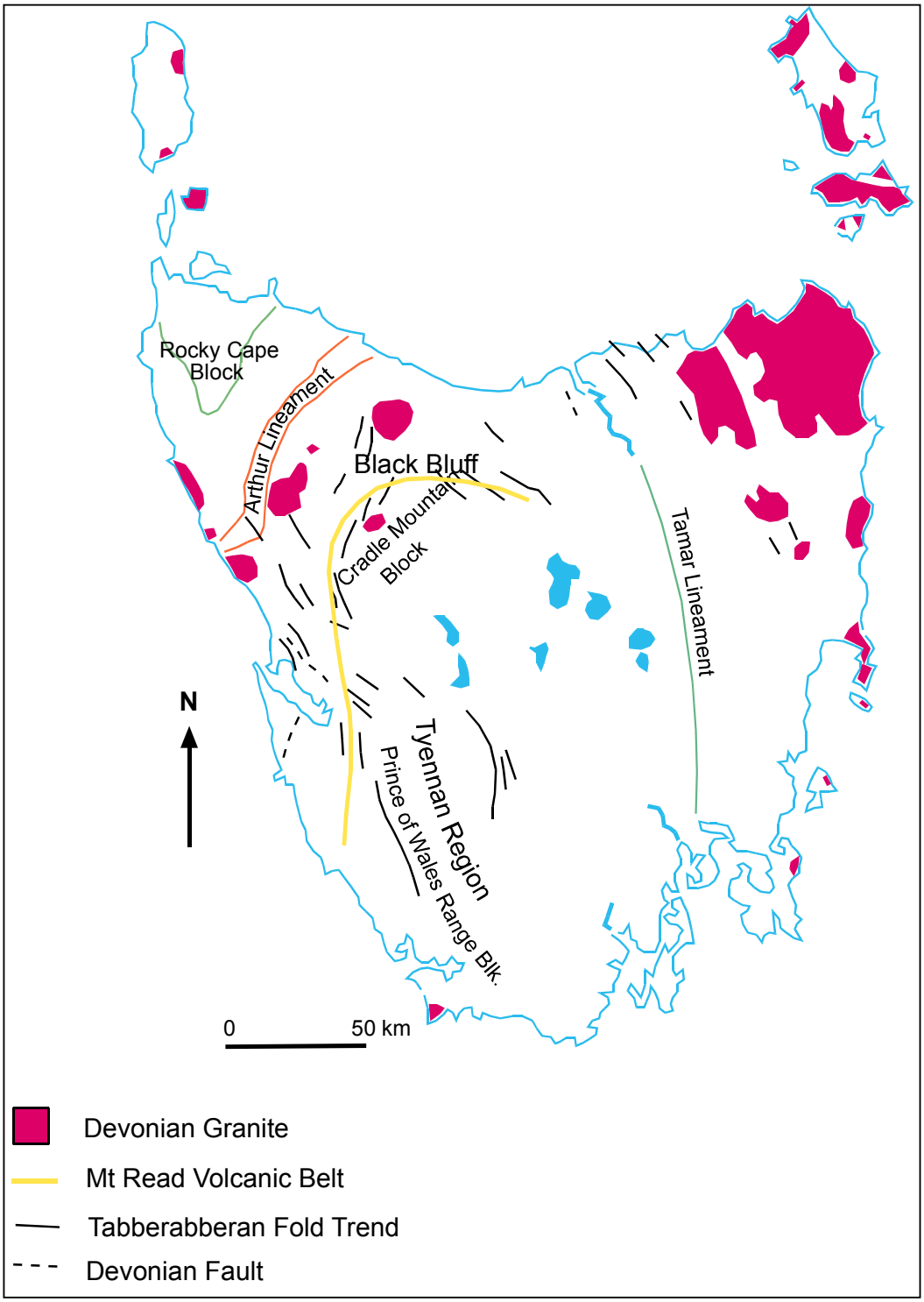

Figure 2.12. Major structures and intrusions formed during Devonian tectonic events in Tasmania. Outcrops of granites shown but buried extents, inferred by geophysical means, are much greater. The Mt. Read Volcanic Belt follows the western and northern edges of the Tyennan Nucleus as defined by Prince of Wales and Cradle Mountain Blocks. The shape of the Tyennan Nucleus also controls Tabberabberan Fold trends and faults. Compiled from Seymour (1989) and Minerals Resources Tasmania mapping.

within these granites. Uranium prospects have been investigated related to granites in northeastern Tasmania and central Tasmania (Hughes, 1961). Anomalously high levels of uranium (23 ppm) have been found in the Ben Lomond Granite (De Graaf, 1983). High levels of radioactivity related to both uranium and thorium (0.025% U and 0.95% Th) have also been related to Cambrian granites near Cradle Mountain in north central Tasmania (Collins, 1975).

2.9. Carboniferous.

This was a time when much of Gondwana was covered by continental ice, and fjord glaciers reached sea level (Martini and Banks, 1989). As a consequence, widespread and deep erosion occurred. Highly metamorphosed rocks of the Tyennan Region and folded Devonian sediments and granites were resistant to erosion but older structural zones such as the Arthur Lineament and the Tamar Fracture system were preferentially eroded (Banks, 1989). This erosion produced a landscape with a relief of about 1000 m and the Tyennan Region and the northeastern granites stood out as positive features (Banks, 1989). Anticlines formed in Gordon Group and Eldon Group sediments must have been eroded at this time as only major synclines of these groups are now exposed in western Tasmania and presumably similar erosion occurred beneath the Tasmania Basin cover rocks.

Deposition commenced again in the late Carboniferous with the deposition of the basal tillites of the Parmeener Supergroup within the Tasmania Basin. The climate gradually changed from being polar to cool temperate and the ice sheets retreated (McLoughlin, 1993).

2.10. Permian.

As the ice sheets retreated Permian sediments began deposition over the basal tillites and a sequence of dark, massive-bedded, pyritic and carbonaceous siltstones with abundant glendonites known as the Quamby Mudstone in northern Tasmania and Woody Island Siltstone in southern Tasmania was deposited (Clarke, 1989). Note that glendonites are calcite pseudomorphs of ikaite, a mineral that forms in water at less than 5° C and within sediments containing abundant organic matter (De Lurio and Frakes, 1999). An oil shale about 2 m thick formed near the base of this sequence, which contains the alga *Tasmanites punctatus* (Cane, 1968). The oil shale formed in

shallow water along shorelines and around islands in northern Tasmania and has also been noted in places in southern Tasmania and may occur in the highlands (Reid, 2003). Northern deposits of Tasmanite Oil Shale are too immature to act as petroleum source rocks (Denwer, 1981). However, in southern Tasmania, *Tasmanites* has been linked to an oil seep at Lonnavale indicating maturity within the oil window in this region (Revill, 1996; Wythe and Watson, 1996). The great thickness (100-250 m) of the Woody Island Siltstone increases its potential as a source rock, even discounting the oil shale within it (Reid and Burrett, 2004).

Marine conditions continued as the Tasmania Basin was gradually filled until a regression of the shoreline southwards resulted in the deposition of freshwater sandstones and carbonaceous siltstones (Clarke, 1989). Coal measures, with potential as oil source rocks, were deposited in northern Tasmania at this time and the associated freshwater sandstones have potential as reservoir rocks. However the main importance for this phase of sedimentation for hydrocarbon development was the burial of earlier deposited potential source rocks.

Following the widespread freshwater deposition, marine transgression deposited shallow shelf fossiliferous siltstone, limestone and minor sandstone (Clarke, 1989). Dropstones are present within this sequence indicating a cold-water environment. Continued deposition almost filled the Tasmania Basin by the Late Permian leading to quiet water mudstone and siltstone deposition, which have formed a regional hydrocarbon seal in the Tasmania Basin (Reid, 2003).

Near the top of the Permian sedimentation, another fresh-water sequence, Cygnet Coal Measures, was deposited in peat swamps (Forsyth, 1989b). These, as will be shown later, have generated oil and gas in western Tasmania. Coarse-grained sandstones within the sequence have acted as reservoirs, which were sealed by the fine matrix of conglomerate beds and overlying dolerite. A simplified stratigraphic column for the Permian is shown as Figure 2.13.

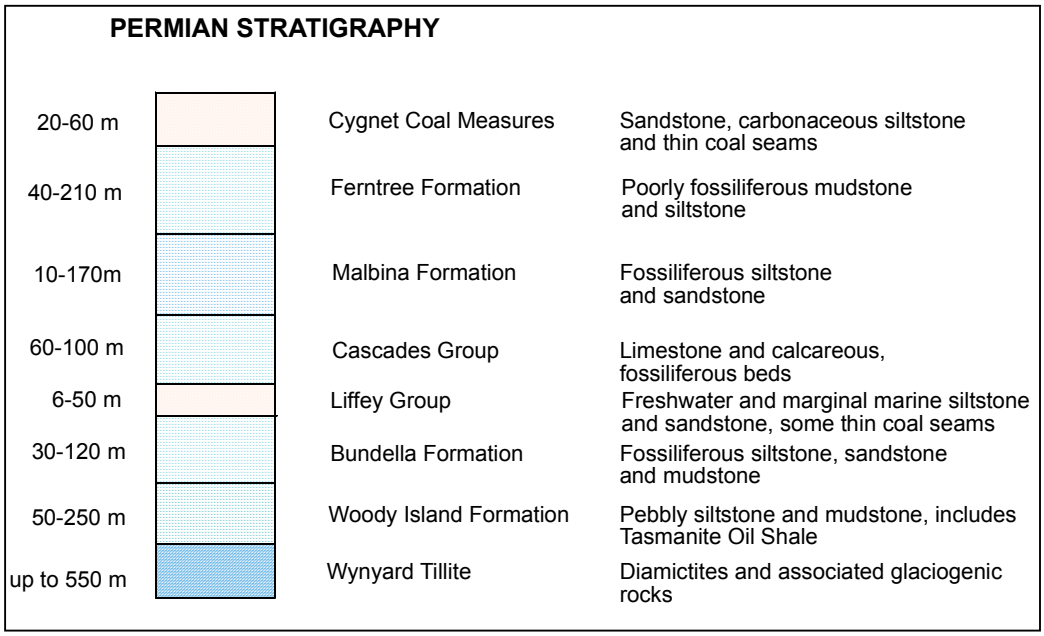

Figure 2.13. Generalised stratigraphic column for the Permian system in Tasmania to reflect broad units recognisable basin wide. Range in thicknesses is due to differences in the depositional conditions across the Tasmania Basin. After Reid and Burrett (2004).

2.11. Triassic.

The boundary between the Permian and Triassic is generally taken to be the top of the carbonaceous beds and the base of overlying non-carbonaceous quartzose beds (Banks and Naqvi, 1967). The Triassic sandstone beds exist as cycles grading from medium to coarse up into finer beds, and were probably deposited from low sinuosity rivers with palaeocurrents predominantly from southeast to east (Forsyth, 1989b). Uppermost in the sequence are volcanic lithic sandstone and lutite beds with coal seams of economic grade. The coals may have organic carbon contents high enough to make them potential source beds but the burial depth is unlikely to be deep enough to make them mature source rocks (Reid, 2003). Maturity estimation of Triassic coals based on calorific values indicates marginal maturity with an equivalent vitrinite reflectance of ~0.5% (Bacon, 1991). Maturity assessment of underlying Permian coal is marginally mature for oil with R_v = 0.4% based on T_{max} from Rock-Eval (AMDEL, 2004). These maturity assessments confirm Reid's assessment. The Triassic coals in Tasmania also appear to have high inertinite content (60-70%) which has poor hydrocarbon source potential (Anon, 1984a).

Investigations have shown Triassic sandstones have potential as reservoir rocks with lutites forming seals (Bedi, 2003). However, shallow burial depths may not provide enough confining pressure, so these intervals may have marginal potential as reservoir sequences.

2.12. Jurassic-Cretaceous.

The intrusion of large volumes of dolerite into the Parmeener sediments over much of Tasmania during the mid-Jurassic was a precursor to Gondwana continental break-up (Baillie, 1989a). Jurassic sandstones and conglomerates may have been deposited over parts of southern Tasmania as indicated by remnants near Lune River (Bromfield, 2004). Maturity measurements, as shown in Chapter 4, suggest that burial of Permian coals and siltstones has been at least two kilometres deeper than can be accounted for by presently known stratigraphy in southern Tasmania. Rifting occurred during the Cretaceous and the rift-basins surrounding Tasmania rapidly filled with alluvial fan, fluviatile, volcanic and pyroclastic sediments (Moore et al., 1992). These basins have now become important offshore petroleum provinces. The high heat flows generated by rifting zones also had implications for onshore petroleum exploration, allowing shallowly buried organic-rich sediments to reach oil and gas maturity levels on the west coast of Tasmania.

Intrusions of dolerite may also have had deleterious effects on any reservoired petroleum preserved prior to this event because the associated faulting and deformation may have ruptured seals and allowed the escape of petroleum. Widespread thermal effects could also have destroyed petroleum reservoirs.

2.13. Tertiary.

Faulting occurred during the Tertiary and formed a series of grabens such as those occupied by the Derwent and Coal Rivers and the Longford Basin (Leaman, 2001). The grabens probably formed due to two ocean spreading systems operating on opposite sides of Tasmania with New Zealand rifting away on the east and Antarctica rifting away on the west (Leaman, 2001). Uplift continued so that grabens formed at this time were filled with Tertiary sediments. The Longford Basin has been investigated as a possible site for petroleum accumulations including 21 drill holes (Bacon et al., 2000). Major Tertiary fault trends in some cases follow basement fracture zones such as the Tamar Lineament. Alkali basalts have formed short valley

flows in these grabens, and large lava flows to the north of Cradle Mountain filled Cretaceous valleys (Sutherland, 1989). The continuing high heat flow under Tasmania at the time may have been significant in allowing shallowly buried source rocks such as Permian Cygnet Coal Measures to reach maturity.

Tertiary faulting and igneous activity could have had similar deleterious effects on petroleum reservoirs as previously mentioned for the Jurassic events. The Tertiary events have largely formed the current Tasmanian landscape. Major faults discernible within the Tasmania Basin follow four intersecting trends, north-south, east-west, northwest-southeast, and northeast-southwest and probably follow basement structures. Complex faulting patterns suggest the most likely trap structures present would be fault traps, where blocks containing reservoir sequences have been moved so that porous and permeable units are sealed against impermeable units.

2.14. Summary.

In terms of petroleum geology three main periods were important for the deposition of possible hydrocarbon source rocks. These were Mesoproterozoic? to Neoproterozoic, Ordovician and Permian-Triassic. Potential source beds have been noted within these stratigraphic intervals across Tasmania suggesting that stacked petroleum systems may operate onshore Tasmania. Intervening time periods have allowed deposition of overburden to ensure maturation of these probable source beds and also to provide possible reservoir and seal units.

Significant tectonic activity has occurred throughout Tasmania's geological history and this has developed structures such as folds, thrusts and domes, all of which could be potential hydrocarbon traps. The most significant events occurred during the Cambrian and Devonian, but major tectonic disturbances during Jurassic, Cretaceous and Tertiary times have also been important in developing structures suitable for hydrocarbon traps. The same events could also have ruptured seals of earlier developed reservoirs. Some of these tectonic events have also been accompanied by thermal disturbances, which could have been significant factors in determining the maturity of possible source beds. As a consequence, probable hydrocarbon source beds onshore Tasmania have not only been subjected to burial heating but thermal effects of intrusions and rifting and any maturity modelling must consider all these

effects. Thermal disturbances may also have destroyed previously reservoired hydrocarbons.

The complex geological history of Tasmania has fragmented many sedimentary sequences, particularly those deposited prior to the Carboniferous. This may mean that some possible hydrocarbon accumulations are small and dispersed, making exploitation difficult and uneconomic. Large-scale intrusion of dolerite during the Jurassic has also posed difficulties for seismic imaging used to determine hidden structures during hydrocarbon exploration.

Tasmania's geological history indicates three potential hydrocarbon systems may have operated onshore Tasmania and the following chapters will consider some aspects of these three systems. Based on the age of deposition of the source rocks petroleum systems of Mesoproterozoic? to Neoproterozoic, Ordovician and Permian-Triassic may operate onshore Tasmania. These three systems have been named Centralian, Larapintine 2 and Gondwanan (Bradshaw, 1993) and will be considered in turn in later chapters. Figure 2.14 depicts a geological timescale with events of significance to the deposition of petroleum source rocks and shows the time relationships of the three potential petroleum systems that may operate onshore Tasmania. Data for this diagram has been drawn from (Bradshaw, 1993; Calver and Walter, 2000; Johnson, 2004; Longley et al., 2000).

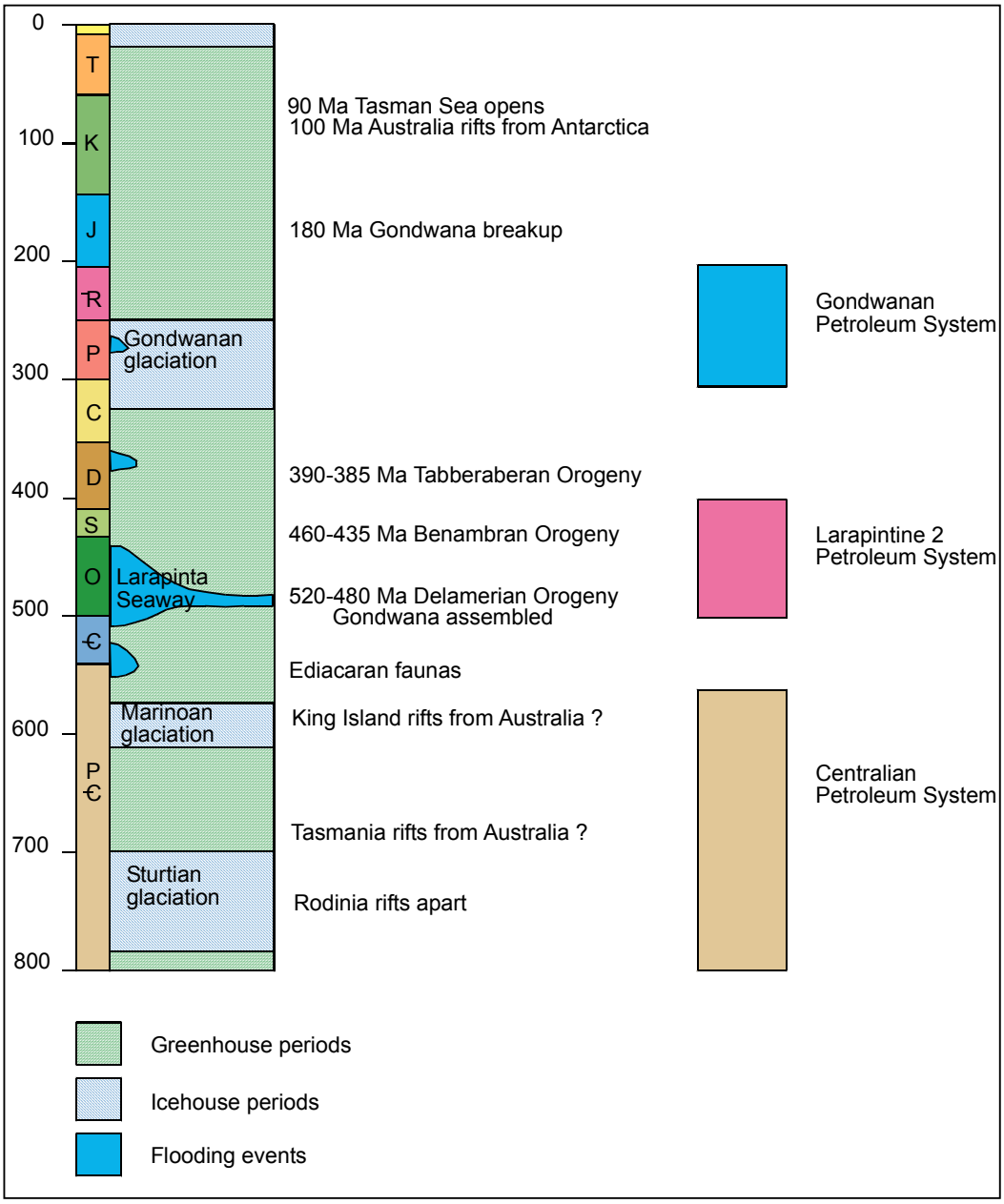

Figure 2.14. Geological timescale showing major events of significance to petroleum systems onshore Tasmania. Major greenhouse and icehouse events were significant for the deposition of source rocks with warm conditions depositing marine source rocks and cold conditions primarily coals. Flooding events provided ideal conditions for deposition of source rocks on shallow shelves. Major tectonic events produced folds, thrusts and faults to form hydrocarbon traps. Data has been drawn from (Bradshaw, 1993; Calver and Walter, 2000; Johnson, 2004; Longley et al., 2000).

CHAPTER THREE.

PETROLEUM SOURCE ROCK POTENTIAL ONSHORE TASMANIA.

3.1. The importance of source rocks.

Petroleum systems consist of two major subsystems, the first being a generative system and the second a migration-entrapment system (Demaison and Huizinga, 1991). The most critical subsystem is the generative because without hydrocarbons in the subsurface then migration-entrapment subsystems are irrelevant so the first critical step in any potential hydrocarbon exploration must be to assess the viability of potential source rocks.

A petroleum source rock is one that has the capability to generate and expel enough hydrocarbons to form an accumulation of oil and/or gas. Chemical reactions occur within source rocks to break down biologically produced macromolecules into the simpler molecules found in petroleum. The full nature of the chemical reactions involved in maturation is at present unknown but the reaction temperatures and reaction rates are known. Organic matter deposited within sediments is termed protokerogen and during diagenesis this is converted into kerogen. Kerogen is insoluble organic matter, which remains after treatment with common organic solvents (benzene, methanol, toluene, methylene chloride) followed by dissolution of the rock matrix by hydrochloric and hydrofluoric acids (Tissot and Welte, 1978). Kerogen typing classifies the organic matter according to the source of the biological material from which it was derived and is useful for determining whether oil or gas is likely to be generated.

3.2. Characteristics of an ideal source rock.

An ideal source rock must contain 2+% lipid-rich organic matter and would generally be deposited within an anoxic basin in a marine or lacustrine setting (Demaison and Moore, 1980). Rich source rocks are invariably laminated, fine-grained sediments with laminae 0.5-2.0 mm in thickness and fissility usually highly developed along laminae (Hunt, 1995). The fine laminae prove that burrowing fauna were absent and therefore dissolved oxygen levels were below 0.2 mL/L (Waples, 1985). Burrowing fauna consume organic matter and thus reduce the effectiveness of the source rock

(Demaison and Moore, 1980). Anaerobic bacterial decomposition can however be beneficial because the bacteria contain lipids, which improve the properties of organic matter for the generation of petroleum (Powell and Boreham, 1991, 1994). Total organic content increases as particle size of the sediment decreases and this is probably due to the quiet depositional conditions required for organic matter to settle into the sediment (Hunt, 1995).

Dark laminae are visually opaque and immensely rich in organic matter with common colours ranging from dark brown to black but colour is an unreliable indicator as many black rocks are not rich in organic matter. The richest sections are closely packed remains of pelagic organisms, commonly a single type or even a single species for example *Gloeocapsomorpha prisca* in kukersite (Diessel, 1992). Some source rocks are phosphatic and sulphides are common, especially pyrite, an indicator of anoxic conditions (Berner, 1970).

High organic productivity is required to provide input of organic matter and this is largely controlled by nutrient availability. High productivity occurs in warm seas and two thirds of the world's known source rocks were deposited between the palaeoequator and palaeolatitude 45° (Klemme and Ulmishek, 1991). The Tethyan realm, a latitudinal seaway between Gondwana and the northern group of continents, contains 69% of the world's oil and gas reserves (Bois et al., 1982). These areas cover less than one fifth of the world's land areas (Klemme and Ulmishek, 1991).

Marine transgressions, especially early deposits, are highly favourable to the formation of source rocks as the area of shallow seas are increased accompanied by a significant increase in primary productivity of phytoplankton (Bois et al., 1982). The depositional model would appear to be global warming and eustatic sea level rise with weak ventilation of oceans by oxygen-rich polar water impinging on to continents and so favouring the development of anoxic conditions (Klemme and Ulmishek, 1991). The Tethys region provides a good example of this as the latitudinal ocean provided a circulation system devoid of polar currents with increased sea level on shelves favouring the stratification of water so that below thermoclines, anoxic conditions prevailed.

Major source rock intervals were deposited during the Cambrian, Ordovician, Devonian, Jurassic and Quaternary and these can all be correlated with second order transgressions as illustrated in the chart Figure 3.1.

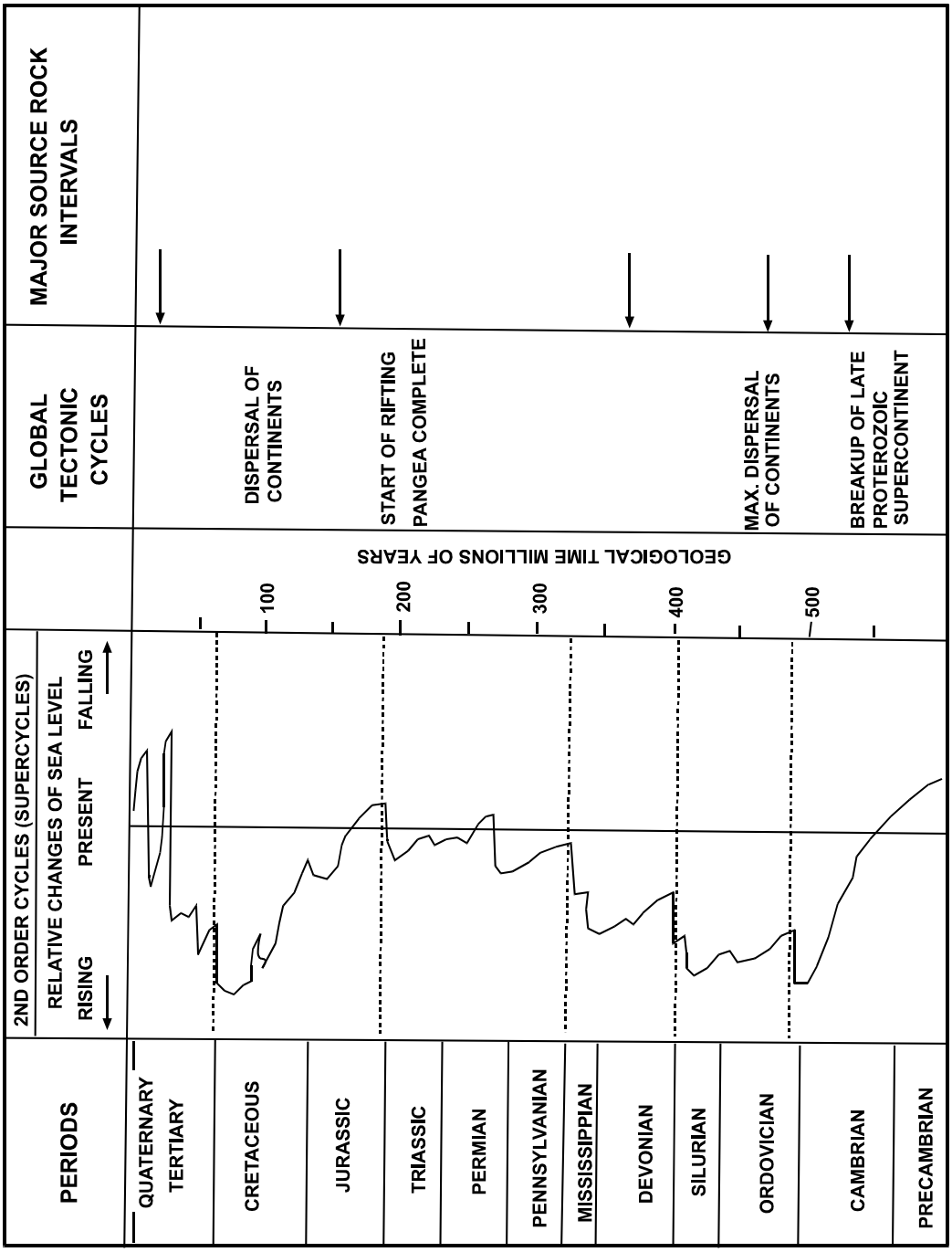

Figure 3.1. Major source rock intervals correlated with major second order transgression cycles. Modified from Plint et al., (1992).

3.3. Results of investigations into the source rock potential of Proterozoic sequences in northwest Tasmania.

Evidence for a potential petroleum system present within the Mesoproterozoic? - Neoproterozoic sediments of the Rocky Cape Block of northwestern Tasmania came from the finding of bitumen within the Forest 1 DDH (Brown, 1985) and also within amygdales in basalt at Kanannuh Bridge (Legge, 2001). A photomicrograph of bitumen found at Kanannuh Bridge is shown in Figure 3.2. The finding of bitumen implies that a source rock must be present either within or below the Black River Dolomite because it occurs close to both sites where bitumen was located. As correlates of this sequence are widely distributed across western Tasmania similar source rocks may also be present below the Tasmania Basin.

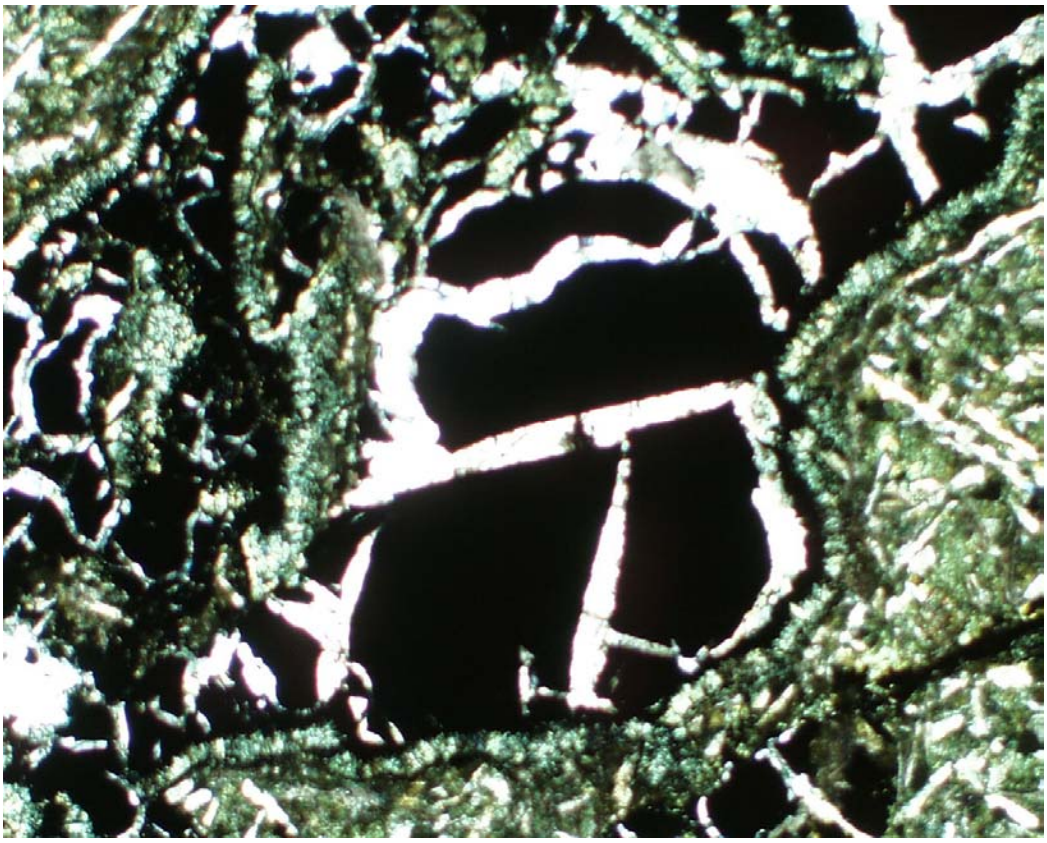

Figure 3.2. Photomicrograph of bitumen enclosed within amygdale of tholeiitic basalt from the Spinks Creek Volcanics, part of the Kanunnah Subgroup of the Togari Group. Sample was collected from exposure on the south bank of the Arthur River at Kanunnah Bridge, 35 km south of Smithton. Photographed using plane polarised light with 1 mm field of view. Thin section prepared by J. Legge (2001).

Sections of the Black River Dolomite have the classic source rock characteristics of being fine-grained, black, pyritic and fissile with no evidence of bioturbation. The underlying Cowrie Siltstone has beds up to 300 m thick of similar potential source rocks so samples of these units were analysed initially by Rock-Eval pyrolysis for source rock potential. Samples were collected along a north-south traverse parallel to the eastern edge of the Smithton Trough in a zone of apparently low metamorphic grade. Table 3.1 shows the results of these analyses.

Table 3.1.

Table of Rock-Eval pyrolysis data from Cowrie Siltstone samples and one Black River Dolomite sample.

Test	Units	CP2	CP3	CP4	AR1	JR1	TB1
Tmax	°C	489	402	497	475	439	458
S_1	mg/g	0.02	0.28	0.03	0.04	0.02	0.02
S_2	mg/g	0.49	0.77	0.16	0.13	0.03	0.06
S_3	mg/g	0.21	0.14	0.50	0.57	0.32	0.25
$S_1 + S_2$	mg/g	0.51	1.05	0.19	0.17	0.05	0.08
PI		0.04	0.27	0.17	0.25	0.50	0.25
S_2/S_3		2.33	5.50	0.32	0.22	0.09	0.24
PC	mg/g	0.04	0.08	0.01	0.01	0.00	0.00
HI		76	56	22	3	1	3
OI		32	10	71	2	14	15
TOC	Wt%	0.64	1.37	0.70	4.02	2.08	1.85

Analyses by AMDEL (2004).

Sample JR1 is from Black River Dolomite.

All samples have TOC values above 0.5%, the minimum value generally accepted for potential source rocks. Hydrogen Index (HI) values are generally very low and do not indicate any potential as source rocks and only two samples gave HI values that might be considered possible gas source rocks. Generative potential as indicated by S_1 and S_2 is poor overall.

Possible correlates for the Black River Dolomite were encountered in the Hunterston DDH and three samples were tested for TOC and all had <0.02% TOC indicating no potential as source rocks.

As will be detailed in Chapter Four the maturity levels as indicated by the T_{max} figures in Table 3.1 are inaccurate and the real maturity levels are much higher thus further

reducing the source potential of these sediments. The low generative potential for these sedimentary rocks may be due to the maturity levels approaching sub-greenschist conditions.

3.4. Results of investigations into Ordovician Gordon Group source potential.

3.4.1. Depositional environments within the Gordon Group and the potential for source rocks.

Gordon Group limestones were deposited from Arenig to Ashgill a time span of approximately 45 myr. so it is expected that significant differences would have occurred in the depositional conditions over this time period and thus have implications for source rock potential. Mappable units demonstrate that changing depositional conditions occurred related to stages in the gradual build-up of a carbonate shelf and each of these units will be briefly considered in an attempt to predict the likely locations of source rocks within the Gordon Group.

A number of studies (Burrett, 1978; Burrett et al., 1981; Calver, 1977; Page, 1978; Scanlon, 1976; Sharples, 1979; Stait and Laurie, 1980; Stait, 1976; Weldon, 1974) have considered the palaeogeography and palaeoecology of the Gordon Group at sites around Tasmania and these studies were used to predict the most likely stratigraphic positions for potential source rocks.

As explained in Chapter Two the Gordon Group was deposited on a substrate of siliciclastic rocks deposited as platform siliciclastics due to rapid erosion of high ground. The consensus opinion is that Gordon Group was deposited on a shallow shelf environment that may have been 260+ kilometres wide similar to modern environments such as the Bahamas and the Persian Gulf. These are low-energy environments on gently subsiding shelves some distance from rivers or littoral conditions and the resulting tidal effects often have more to do with winds and storms than astronomical phenomena.

Current Gordon Group outcrop is poor even though, at the time of deposition, it formed a widespread platform, as described in Chapter Two. During the Tabberabberan Orogeny the pre-Carboniferous rocks of Tasmania were folded and thrusted and this was followed by a period of intense erosion during the Carboniferous. Outcrop or sub-outcrop of Gordon Group now mainly occurs within

synclinal structures. Carbonate rocks subjected to folding tend to fracture and exposed fractures allow ready access by fluids, which quickly dissolve the limestone, leading to rapid erosion. Deposition of younger sequences also covers parts of Tasmania assumed to contain Gordon Group at depth, such as east of the Florentine Valley, and this further reduces exposures.

Due to the tendency of Gordon Group to be rapidly eroded it is often found in valleys where it is covered by scree, fluvial and glacial deposits making outcrop difficult to find. Compounding this, heavy forest cover generally occurs in valleys and this can easily hide outcrops. In areas of regrowth forest the cover can be almost impenetrable.

The thickest and most complete sections of the Gordon Group occur in the Florentine Valley and the stratigraphy in this locality has been used for correlation purposes with other outcrops around Tasmania. Biostratigraphy using conodonts (Burrett, 1978) and brachiopods (Laurie, 1982) established the framework for dating the Gordon Group and the mappable units within the Florentine Valley are shown in Figure 2.6.

Each of these members will now be considered in sequence to evaluate source rock potential from the point of view of depositional environment.

The Florentine Valley Formation has a diverse fauna and represents waning siliciclastic deposition in quiet water below wave base. It has little potential as a source rock due to low organic content probably due to an oxic environment as evidenced by fossil assemblage of trilobites, brachiopods and gastropods (Stait and Laurie, 1980).

The base of the carbonate deposition is formed by the Karmberg Limestone, which outcrops on the slopes of Wherret's Lookout at the southern end of the Florentine Valley. Deposition of the Karmberg Limestone occurred during the Arenig in quiet water conditions and built up carbonate sediments to near wave base (Weldon, 1974). Periodically thin layers of clastic material accumulated on the sea floor and during compaction these were forced into the carbonate layers to form the nodular appearance characteristic of the Karmberg Limestone. The Wherret's Chert Member, at the top of the Karmberg Limestone, probably formed on tidal flats around the edge of the basin and may have been subaerially exposed for long periods allowing

evaporite minerals to form. Evaporite minerals were subsequently replaced by silica-rich diagenetic fluids and became chert nodules.

Potentially the depositional environment could have preserved organic matter due to the quiet water conditions, however, very little organic matter has been preserved. It is likely that bottom conditions were too oxic to allow preservation of organic matter and as a result this member has no potential as a source rock.

Cashions Creek Limestone was deposited in shallow water in which agitation was sufficient to roll algally coated grains about on the substrate and during diagenesis these became oncolites (Weldon, 1974). Similar oncolitic limestone formations occur at Ida Bay, Precipitous Bluff, Zeehan and Mole Creek and these have been assigned to a moderately energetic environment above wave base (Sharples, 1979). Energetic environments are unlikely to provide suitable depositional conditions for potential source rocks and the low organic content confirms this assessment.

The Benjamin Limestone has been subdivided into three members each with characteristic depositional environments. The Lower Limestone Member of the Benjamin Limestone was deposited on tidal flats within predominantly shallow water with periodically desiccating conditions (Calver, 1977). The tidal flats may have been many kilometres wide and in such an environment it is not surprising that a complex series of facies changes occurred both laterally and vertically. Storms and tidal fluctuations caused channel changes in the short term and over longer time periods there were small changes in sea-level, climatic variations, changes in rates of subsidence and changes in rates of deposition. Calver (1977) noted shaly horizons ranging in thickness from 20-300 mm where dark carbonaceous material accumulated in low-energy environments under reducing conditions. These thin shales are the only likely candidates for source rocks within the Lower Limestone Member of the Benjamin Limestone. In general the TOC values of the limestone are low with maximum measured value 0.16%. A table with sample values is contained in Appendix H.

Transgression of the sea ended this phase of carbonate deposition and an influx of terrigenous siliciclastics resulted in the deposition of the Lords Siltstone Member in quiet water conditions below wave base. This siltstone has a discontinuous

distribution in the Florentine Valley but similar siltstone at the same stratigraphic level occurs near Zeehan (Burrett, 1995) and also at Mole Creek (Banks and Burrett, 1979) and Precipitous Bluff (Burrett et al., 1981). The event, which initiated the deposition of the Lords Siltstone, did not last long and carbonate deposition soon recommenced. This member has no potential as a source rock due to low organic content.

The Upper Limestone Member of the Benjamin Limestone has a complex mosaic of facies but in general deeper water facies dominate. Page (1978) states that the subtidal-intertidal carbonates form the major components of the Upper Limestone Member of the Benjamin Limestone. Corals are present within this member and, at the top, large rolled corals indicate rather turbulent conditions. Only the subtidal parts of this member could be considered potential source rocks and only thin (<200 mm) shaly beds have characteristics expected of petroleum source rocks. A survey made of TOC levels throughout the full Upper Limestone Member of the Benjamin Limestone indicated an average background TOC level of 0.15%. The results of this survey are contained in Appendix H. TOC values were plotted against a stratigraphic column with the inferred transgressive-regressive record plotted from sections in the Westfield Quarry Area and Eleven Road Area of the Florentine Valley by Calver (1990 Figure 3.3). On this plot the highest TOC recorded occurs at a stratigraphic level inferred to have been sub-tidal however other samples taken from similar sub-tidal positions have very low organic content implying that to deposit potential source rocks a set of complex conditions must be satisfied.

The depth of water above the depositing Upper Limestone Member of the Benjamin Limestone combined with low palaeolatitude may have produced conditions where no thermocline existed with warm water continuing to the substrate. Under such conditions it is likely that organic matter would have been recycled rather than preserved in the sediment.

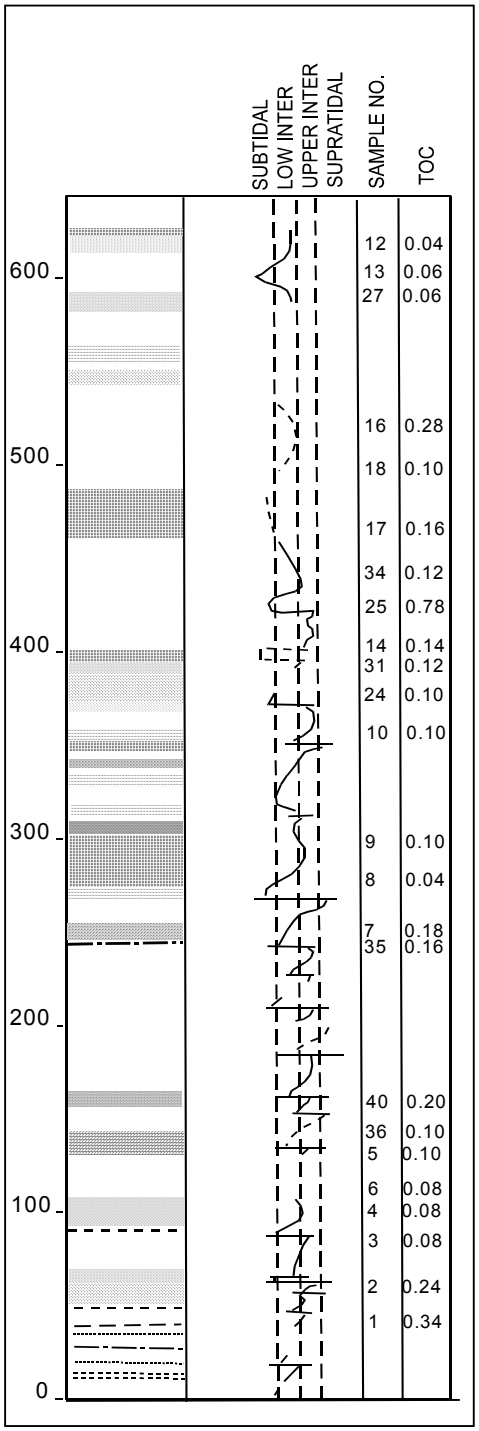

Figure 3.3. Stratigraphic column for the Upper Limestone Member of the Benjamin Limestone with inferred transgressive-regressive record from sections in the Westfield Quarry and Eleven Road Areas of the Florentine Valley. TOC values from samples collected in the Westfield Quarry Area are shown in their relative stratigraphic positions. Note that the highest TOC value corresponds to a sub tidal depositional environment but that other samples in similar positions have much lower TOC values. The transgressive-regressive record was compiled from Calver (1990). Due to the confines of space not all samples are shown. Blanks in the stratigraphic column occur due to lack of outcrop.

On the basis of this assessment of depositional environments for the Gordon Group only the Upper Limestone Member of the Benjamin Limestone has any possibility of containing intervals of potential source rock. The only beds with source rock potential are thin discontinuous shaly beds and due to the complex mosaic of facies changes in this member and lack of outcrop it is difficult to determine their extent. From a petroleum exploration perspective it is perhaps fortuitous the Upper Limestone Member of the Benjamin Limestone is the most widely distributed member of the Gordon Group.

3.4.2. Rock-Eval pyrolysis results from Upper Limestone Member of the Benjamin Limestone.

To establish source potential of the Upper Limestone Member of the Benjamin Limestone a series of samples were collected at intervals through its full extent and these samples were tested for TOC. Any samples above 0.5% TOC were then tested by Rock-Eval pyrolysis. Forty samples from the initial survey were submitted for evaluation of TOC and only one had enough organic content to be considered for Rock-Eval pyrolysis. The sample tested by Rock-Eval pyrolysis has poor generative potential and is in the gas range due to low HI and high T_{max} temperature. Full Rock-Eval pyrolysis results are contained in Appendix B.

Further selective sampling was conducted from intervals with the physical characteristics of potential source rocks from outcrops within the zone previously identified by CAI to be mature for gas generation and these were tested by Rock Eval pyrolysis. Selected items from these results are shown in Table 3.2.

Table 3.2.

Selected items from results of Rock-Eval pyrolysis of Gordon Group samples.

Sample	T_{max}	$S_1 + S_2$	TOC	HI	OI
LR2	496	0.38	0.70	34	22
SM1	461	0.11	0.40	22	57
11R1	518	0.06	1.37	10	18
WQR1	544	0.29	1.83	14	20
UL13	446	0.11	0.46	22	37
UL14	467	0.05	1.16	3	16
17/2	522	0.32	0.57	54	49
17/16	439	0.43	0.80	51	66
MC1	467	0.30	0.02	28	17
175	465	0.63	0.48	106	89
CB16	545	0.46	0.58	74	87
CB26	508	0.29	0.70	34	34
CB30	488	0.22	0.43	44	76
CB32	520	0.55	0.64	76	117

Analyses by AMDEL.

See plot Figure B.1 in Appendix B.

3.4.3. Analysis of biomarkers from Upper Limestone Member of the Benjamin Limestone.

To further refine the source rock potential of Gordon Group extraction of organic matter (EOM) from one sample of the Upper Limestone Member of the Benjamin Limestone was undertaken to allow analysis of biomarkers. This extraction involves crushing a sample to fine particle size and extracting hydrocarbons with a solvent such as dichloromethane, evaporating the solvent, then separating the hydrocarbon extracts by means of column chromatography. Final analysis of the extracts can then be achieved using gas chromatography mass spectrometry (Hunt, 1995).

Sample 175 had 28 ppm EOM and the C_{12+} bulk composition was 38% saturated hydrocarbons, 19% aromatics and 43% nitrogen, sulphur and oxygen compounds. Alkane ratios were determined as 0.48 Norpristane/Pristane, 1.39 Pristane/Phytane, 0.58 Pristane/n-heptadecane, 0.53 Phytane/n-octadecane.

3.4.3.1. Calculated vitrinite reflectance from aromatic maturity indicators.

The following results were determined from analysis of biomarkers from sample 175 of the Gordon Group.

Table 3.3. Aromatic maturity results for Gordon group sample.

A	B	C	D	E
0.87	1.83	1.17	0.77	1.14

A $VR_{calc.} = 0.6\ MPI + 0.4$ (for VR < 1.35%)

B $VR_{calc.} = -0.6\ MPI + 2.3$ (for VR > 1.35%)

C $VR_{calc.} = 0.99\ \log_{10}MPR + 0.94$ (for VR = 0.5-1.7%)

D $VR_{calc.} = 0.7\ MPI + 0.22$ (for VR < 1.7%)

E $VR_{calc.} = -0.166 + 2.242\ MPDF$

The maturity values for each of the methods reported are quite different and the variations can be explained due to the fact that aromatic maturity parameters are specific for particular maturity ranges and so must be used carefully. The methylphenanthrene index indicates two maturity values for each methylphenanthrene ratio because the rates of generation and destruction of the α- and β-isomers of the methlyphenanthrenes increase and then decrease with increasing maturity (Peters et al., 2005). Thus to interpret results the approximate range of expected maturity must be known by use of another method for determining maturity. In this instance Rock-Eval pyrolysis T_{max} and CAI values can be used for approximating maturity range. The CAI 3 determined for the region where the sample was obtained does not discriminate A or B but Rock-Eval T_{max} suggests a maturity ~1.35% so it is likely that value B is too high. Method C covers the range of expected maturity and method E tends to correspond so it is likely the true value is close to these values. Methods A and D appear to indicate a maturity value lower than expected. Aromatic maturity indexes must be calibrated to each petroleum system and due to the frontier nature of this study no such calibration can be attempted so the results are only indicative.

3.4.3.2. Genetic affinity.

Genetic affinity was determined from a plot of pristane/n-heptadecane versus phytane/n-octadecane. Figure 3.4 shows this plot and indicates that the organic matter was derived from an algal/bacterial source.

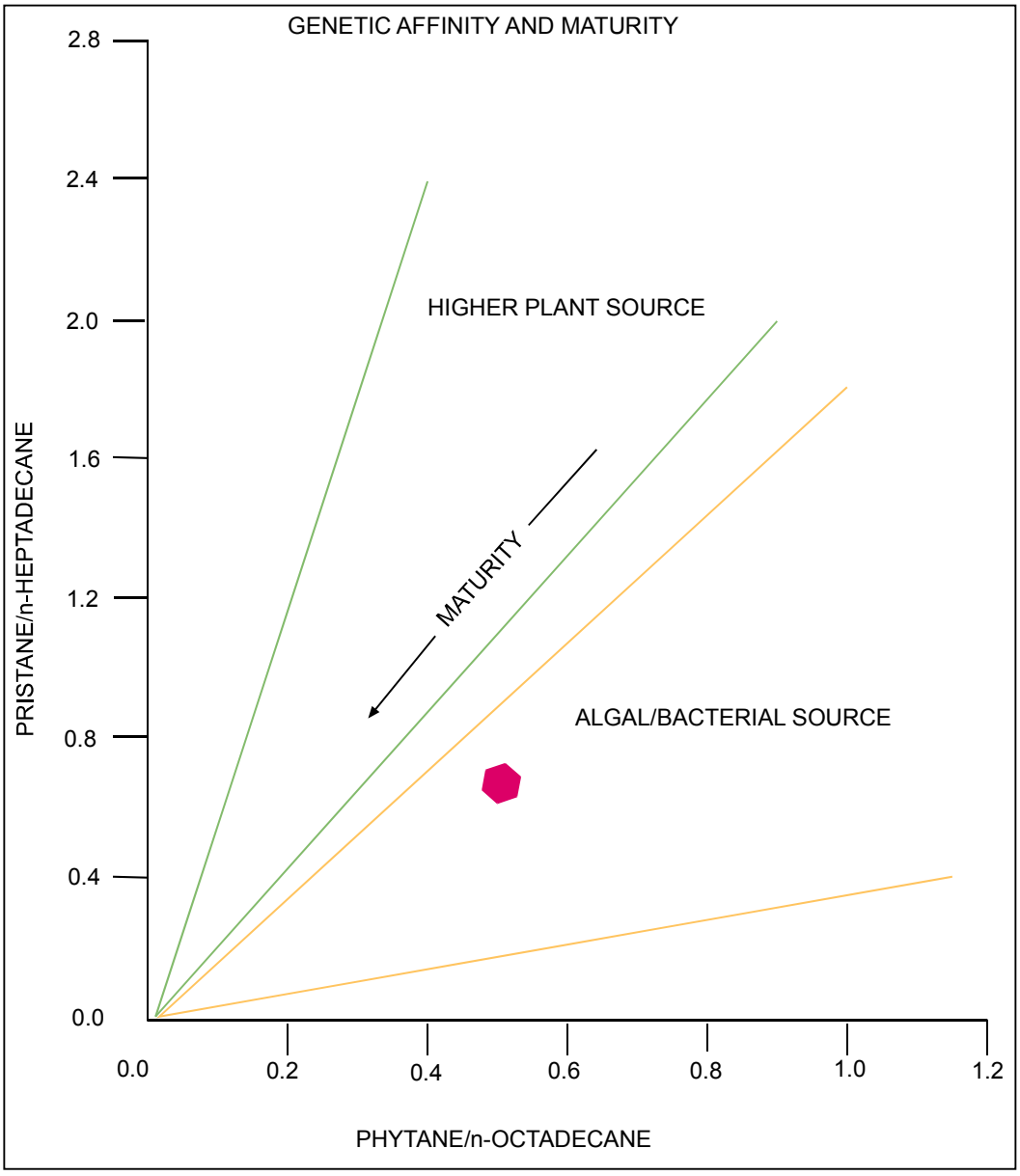

Figure 3.4. Genetic affinity and maturity plot for Gordon Group sample 175 showing affinity with algal/bacterial source and gas maturity. Analysis by AMDEL.

3.4.3.3. Source affinity.

Source affinity was derived from a plot of pristane/phytane versus C_{29}/C_{27} diasterane shown in Figure 3.5 indicating an algal source deposited in anoxic conditions.

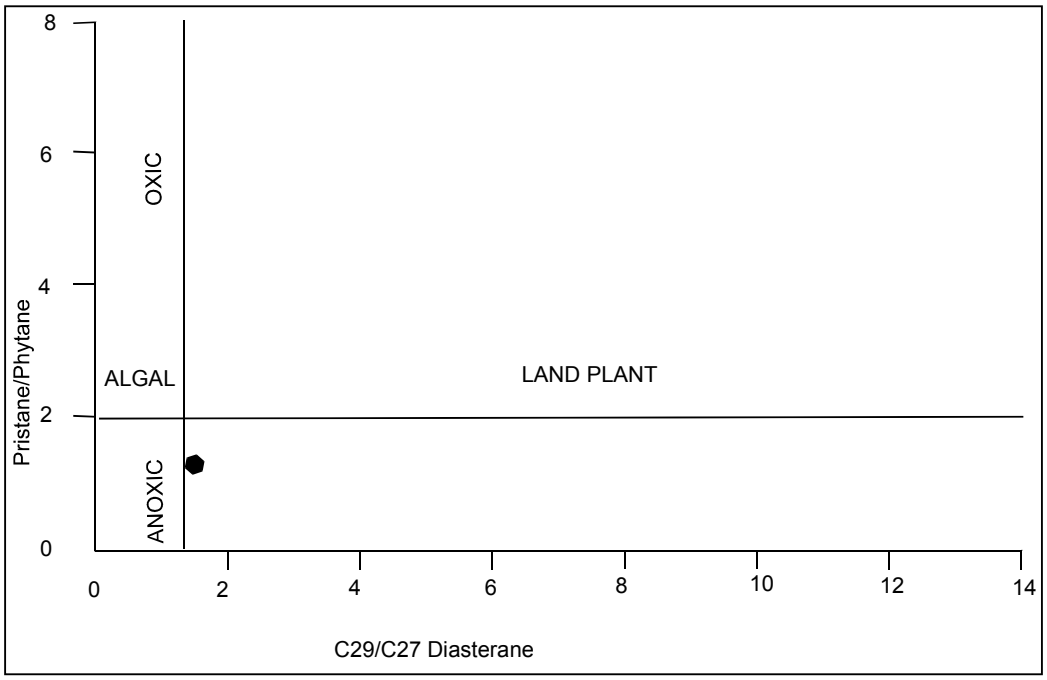

Figure 3.5. Oil source affinity plot for Gordon Group sample 175 showing affinity with algal source and anoxic depositional conditions. Analysis by AMDEL.

3.4.3.4. Maturity.

The sterane maturity-migration plot Figure 3.6 shows that the sample tested has plotted along the modal source-rock maturation curve to a position indicating post-oil maturity.

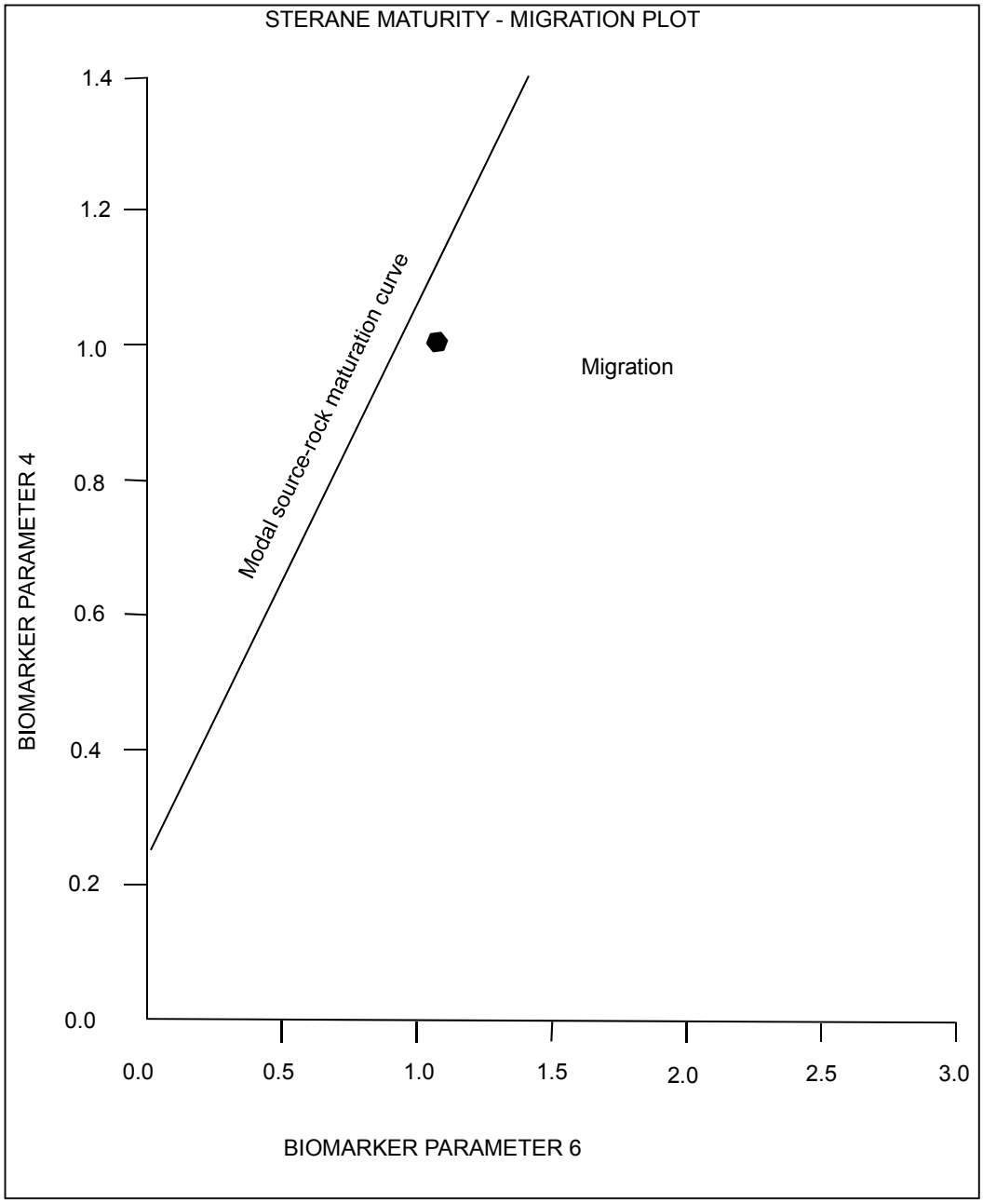

Figure 3.6. Sterane maturity – migration plot for sample 175 of Upper Benjamin Limestone, sampled from Eleven Road in the Florentine Valley. This plot shows that the hydrocarbons contained in this sample have been generated by the host rock and have not migrated as the sample lies along the modal source-rock maturation curve.
Biomarker parameter 4 is,
$C_{29}5\alpha(H)14\alpha(H)17\alpha(H)$ 20S sterane/$C_{29}5\alpha(H)14\alpha(H)17\alpha(H)$ 20R sterane
Biomarker parameter 6 is,
$C_{29}5\alpha(H)14\beta(H)17\beta(H)$ 20R sterane/$C_{29}5\alpha(H)14\alpha(H)17\alpha(H)$ 20R sterane
Analysis by AMDEL.

3.4.3.5. Source rock type.

The ternary diagram Figure 3.7 shows the distribution of C_{27}, C_{28} and C_{29} regular steranes with zones colour coded to show typical distributions for particular hydrocarbon types, marine oils from shales, marine oils from carbonates and lacustrine shale oils (Hunt, 1995). The peaks C_{27}, C_{28} and C_{29} represent zones where the steranes are derived from red algae and zooplankton, green algae and diatoms, higher plants and red and green algae respectively. Sample 175 plots in the field of marine oil from carbonates.

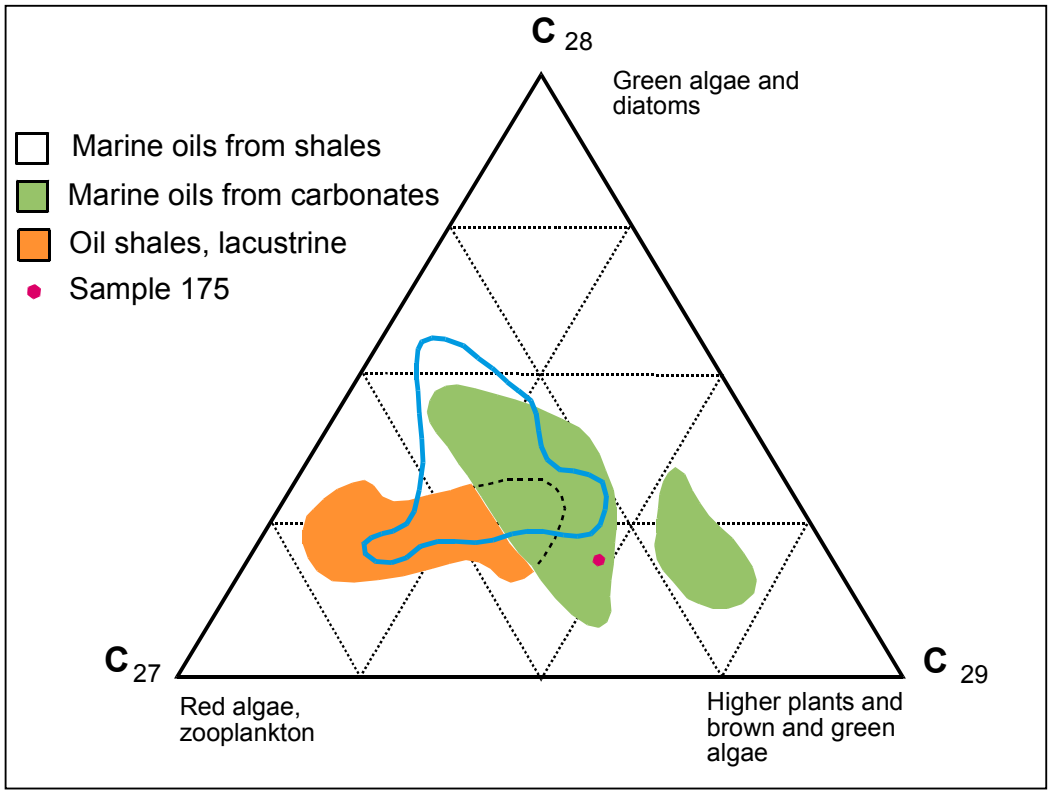

Figure 3.7. Distribution of C_{27}, C_{28}, C_{29} regular steranes for Gordon Group sample 175. Colour coded zones indicate typical distributions for particular hydrocarbon types after Hunt (1995). Sample 175 plots in the field of marine oil from carbonate as would be expected.

Results of biomarker analysis are shown in Appendix E.

3.4.4. Gas chromatograms of alkanes extracted from Gordon Group limestone samples.

The gas chromatogram from a Gordon Group limestone sample from Queenstown, Figure 3.8, shows a loss of light n-alkanes typical for near surface weathering and/or biodegradation as n-alkanes in the range ~C_8-C_{12} are preferentially removed in the early stages of biodegradation (Peters et al., 2005). The gas chromatogram also shows the typical odd over even preference particularly C_{17}>C_{18} and C_{19}>C_{20} shown by Ordovician oils worldwide and is believed to be due to the contribution of *Gloeocapsomorpha prisca* to the organic matter within the sediment. The unique geochemical fingerprint for Ordovician oils is characterised by;

1. Odd over even preference in the C_{15}-C_{19} n-alkanes.
2. Low abundance of C_{20+} n-alkanes.
3. Absence of pristane and phytane.

(Reed et al., 1986).

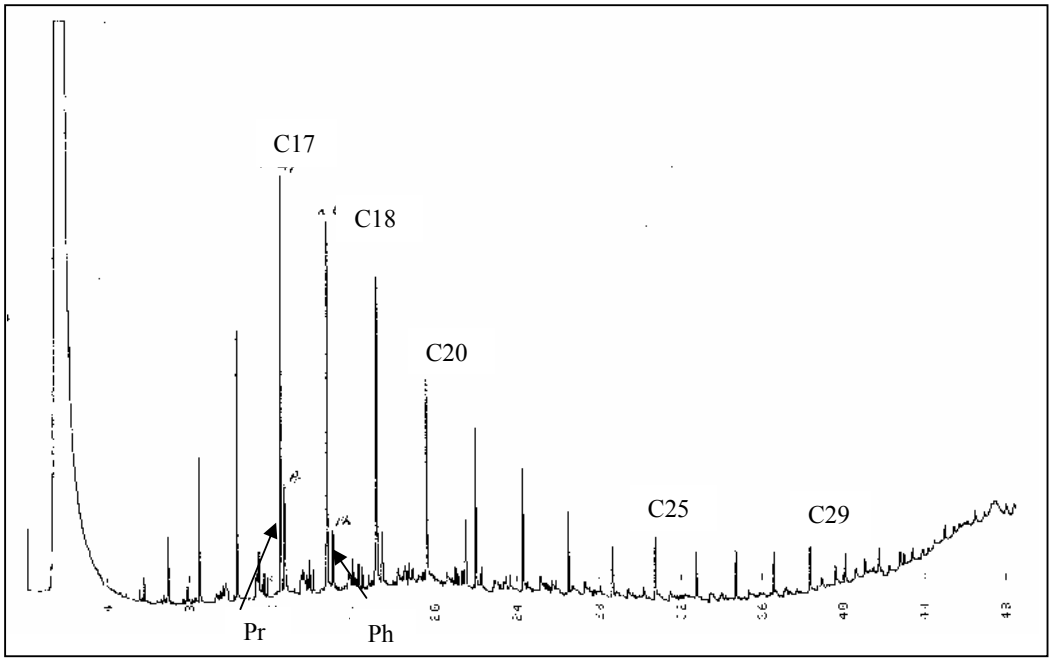

Figure 3.8. Gas chromatogram of n-alkane distribution extracted from a sample of Gordon Group limestone from Queenstown. (Volkman, 1999).

The gas chromatogram has a low abundance of C_{20+} n-alkanes and although it contains both pristane and phytane they are both in low abundance indicating that this sample has typical characteristics for Ordovician oil.

Guthrie and Pratt (1995) compared a series of gas chromatograms derived from Ordovician sediments containing mixtures of *G. prisca* and amorphous matter and found that the C_{20+} n-alkane abundance increased along with pristane and phytane as the concentration of amorphous matter increased. The volume of C_{20+} n-alkanes present in the gas chromatogram from Queenstown shows that amorphous organic matter has formed approximately 80% of the organic matter in the source rock, according to the results obtained by Guthrie and Pratt (1995). The observations made on palynological slides also indicate a major contribution of amorphous matter to the organic matter.

3.4.5. Evidence of gas generated by Gordon Group.

A number of reports have been made of petroliferous odours emanating from Gordon Group limestone when freshly cracked open and so an attempt was made to analyse some of this gas. A sample of the Upper Benjamin Limestone Member (UL29) that exhibited a petroliferous odour was collected from the Westfield Quarry area of the Florentine Valley (459100 mE, 5277900 mN). This sample was crushed inside a chamber and the gas liberated was analysed by Dr. Noel Davies at the Central Science Laboratories, University of Tasmania. The major gas liberated is methane with gases up to C_9 identified thus clearly indicating a thermogenic origin for the gases. This is an indication that gas/condensate has been generated by Gordon Group and possibly migrated a short distance through the limestone. Figures 3.9 and 3.10 are chromatograms showing the analysis of gases liberated from Gordon Group samples. The chromatogram shown in Figure 3.9 was plotted by direct analysis of liberated gas. To plot the chromatogram in Figure 3.10, gases were collected by absorption onto a probe before analysis.

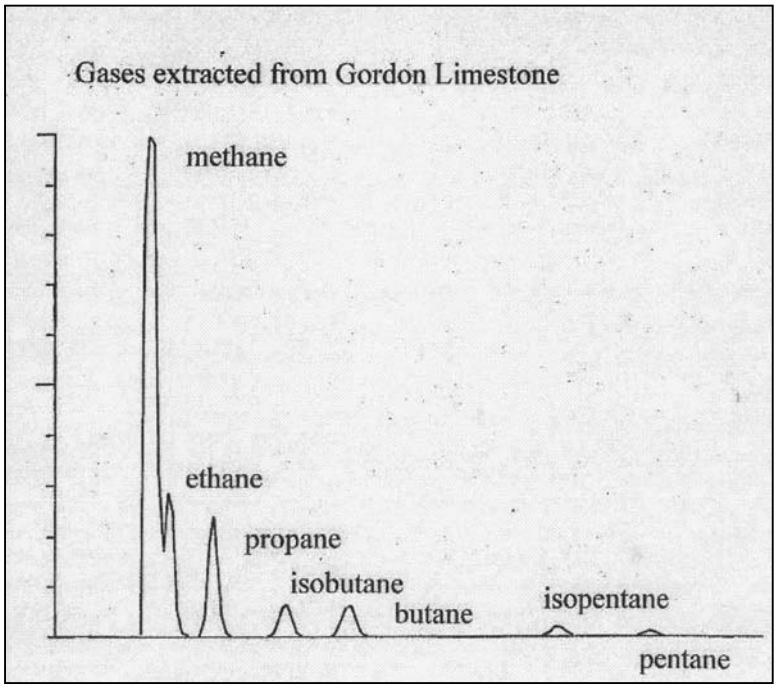

Figure 3.9. Gas chromatogram of the major gases analysed from a crushed sample of Gordon Group limestone. Analysed by Dr. Noel Davies of Central Science Laboratories, University of Tasmania.

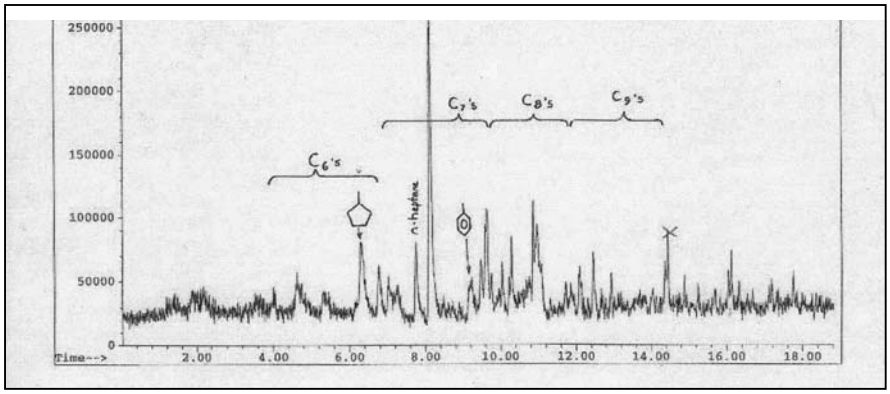

Figure 3.10. Gas chromatogram of minor gases, collected by use of probe. Note that gases up to C_9 have been identified. Analysis by Dr. Noel Davies of the Central Science Laboratories, University of Tasmania.

3.4.6. Discussion of results.

Geochemical analysis of outcrop samples from Gordon Group samples has shown that the only horizons with any potential as source rocks are thin (generally <200 mm) black shales found near the top of the Upper Limestone Member of the Benjamin Limestone. TOC values indicate good potential with values ranging up to 1.83% however the generative potential is very low. Hydrogen Index values, an indicator of

the source rock potential, are generally low. Oxygen Index values are generally high but this may be due to the fact that surface samples were tested. These results indicate low potential as source rocks and combined with the thin and discontinuous nature of the beds suggests that no commercially viable source rocks are contained within the Gordon Group in exposures close to the Tasmania Basin.

The C_{12+} bulk composition of sample 175 suggests that the hydrocarbons have been generated by the rock in which it was found and has not migrated because typically migrated hydrocarbons are enriched in saturated and aromatic hydrocarbons and depleted in NSO compounds (Peters et al., 2005). Further evidence for the hydrocarbons present being generated by the host rock is shown by the sterane maturity migration plot where the sample 175 plots along the modal source-rock maturation curve rather than out into the migration field as shown in Figure 3.6. Gordon Group has potential to generate hydrocarbons but not in sufficient quantity to build up the pressures required to ensure that migration results.

The maturity of Gordon Group samples tested using Rock-Eval pyrolysis correlate well with previous maturity estimates made using the colour alteration index where a range of CAI 2-6 was determined (Burrett, 1992). Maturity determined by Rock-Eval pyrolysis and aromatic maturity indicators are also in agreement and indicate maturity within the gas window. This range of maturity has been verified by analysis of gas extracted from an outcrop sample. Maturity will be considered in greater detail in Chapter Four.

Genetic affinity as determined by pristane/n-heptadecane versus phytane/n-octadecane is in accordance with the expected result of an algal source deposited within anoxic sediment. Ordovician source rocks world-wide have characteristic signatures determined to be from the organism *Gloeocapsomorpha prisca* and this signature can also be detected from the analysis undertaken from potential Gordon Group source rocks. The characteristic geochemical fingerprint of Ordovician oils has:

1. Odd over even preference in the C_{15}-C_{19} n-alkanes.

2. Low abundance of C_{20+} n-alkanes.

3. Absence of pristane and phytane.

(Reed et al., 1986).

The fossil alga *G. prisca* has been shown to give this signature within Larapintine 2 sediments of the southern Canning Basin in Australia (Hoffman et al., 1987). *G. prisca* is not the only organism responsible for contributing to the organic matter within Ordovician sediments and the petroleum generative capacity of other organic matter is usually less than that of *G. prisca.* Guthrie and Pratt (1995) compared the n-alkane distributions from source rocks containing a mixture of organic matter derived from *G. prisca* and amorphous matter. The n-alkane distribution from rocks containing a mixture of organic matter including amorphous matter still showed the characteristic odd over even n-alkane distribution but also included greater abundances of C_{20+} n-alkanes. The characteristic Ordovician fingerprint shows through even though the organic matter may not derive solely from *G. prisca*. Greater amounts of amorphous matter changes the composition of generated hydrocarbons to a more ordinary signature with greater abundances of C_{20+} n-alkanes and also contain pristane and phytane. The amorphous matter is derived from acritarchs, chitinous scolecodonts, chitinozoa, siculae of graptolites and has less than one quarter of the generative potential for hydrocarbons than the organic matter derived from *G. prisca* (Guthrie and Pratt, 1995).

Kerogen derived from *G. prisca* has HI values greater than 750 mg HC/g TOC indicating Type I kerogen. Kerogen from amorphous organic matter is gas-prone Type II or Type III. Rock-Eval pyrolysis results from the Gordon Group samples indicate low HI values indicating Type III, gas-prone kerogen most likely derived from amorphous kerogen. Palynological extracts confirm this assessment with amorphous matter being the only organic matter visible.

Rock-Eval pyrolysis indicates that Gordon Group has very low potential as source rock with generative potential, as indicated by S_1 and S_2, falling within the poor range. Poor generative potential combined with very thin and discontinuous beds does not offer the potential for commercial quantities of hydrocarbons to be generated. No commercially viable potential source beds have been identified during this study.

3.5. Results of investigations into Permian freshwater coal source potential.

Coal is recognised as a potential source rock for gas but is not generally considered as a source rock for oil however Permian Gondwanan coals are an exception as is demonstrated within the Cooper Basin where coal is a source for oil (Curry et al., 1994; Powell and Boreham, 1991; Vincent et al., 1985). If Permian coals in the Cooper Basin generate oil it may also be that Permian freshwater coals onshore Tasmania could also generate oil and/or gas.

The palaeoenvironment of deposition for the Cygnet Coal Measures in Tasmania was essentially the same as that for Permian coals within the Cooper Basin with both regions being alluvial and delta plain environments at high latitudes (Lang et al., 2000; Martini and Banks, 1989; McLoughlin, 1993). The Cygnet Coal Measures were deposited on wide sandy plains formed by braided streams flowing generally from the west towards south eastern Tasmania. The coal was mainly deposited within channels eroded into the underlying Ferntree Mudstone with very few overbank deposits and as a result the seams are thin and discontinuous. The coal has been formed in part from *Glossopteris* and *Vertebraria* (Bacon, 1991).

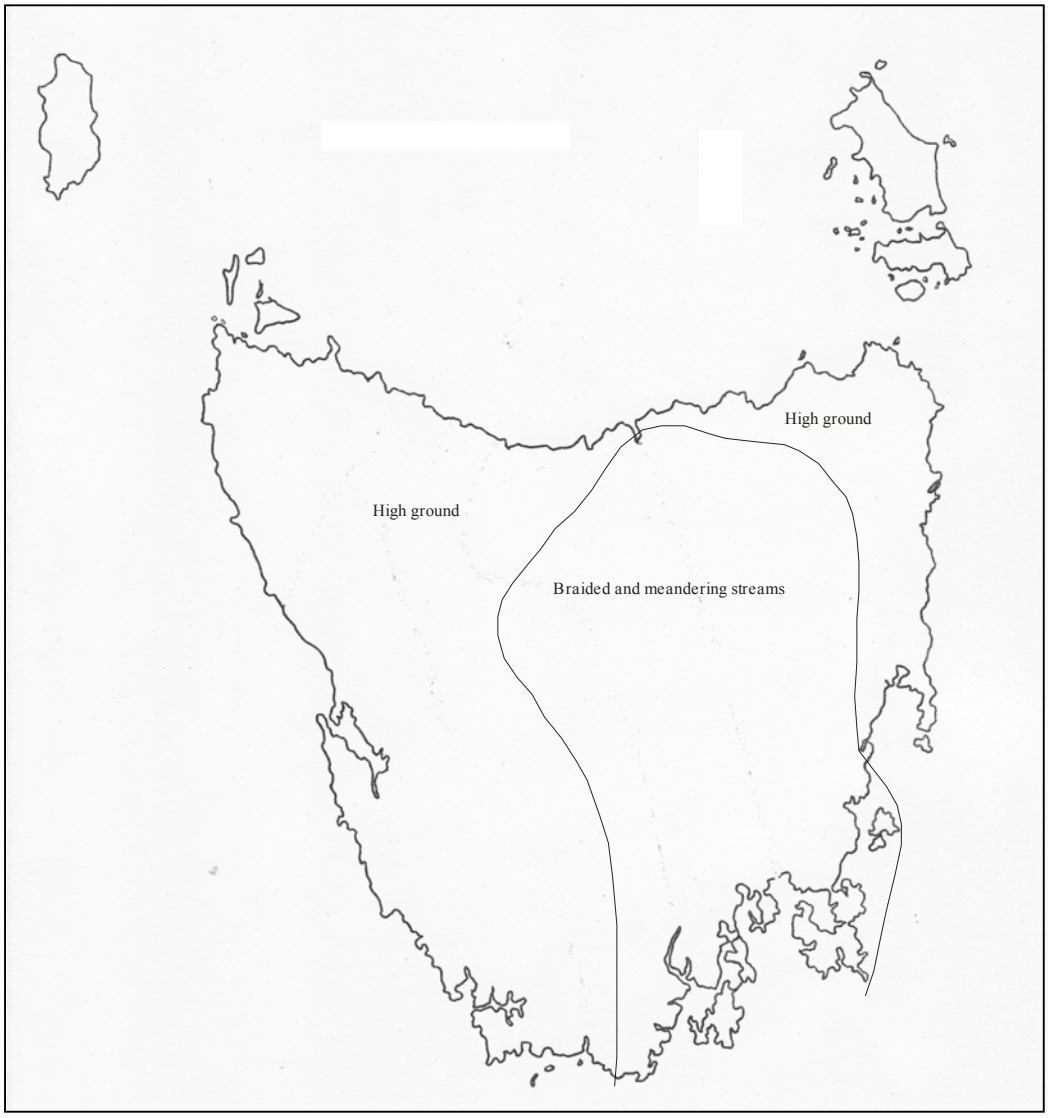

Figure 3.11. Palaeogeography of Tasmania during the deposition of the Cygnet Coal Measures, Late Permian. Coal forming sequences were probably deposited throughout the whole basin depicted prior to some being eroded before cover sequences were deposited. Cygnet Coal Measures are now only found in a distribution as shown in Figure 5.9. After Reid (2002).

Samples from Cygnet Coal Measures or correlates were collected from a number of sites within the Tasmania Basin and tested for source potential by Rock-Eval pyrolysis. Selected components of the results of these tests are shown in Table 3.4. Full results are contained in Appendix B.

Table 3.4. Selected components of Rock-Eval pyrolysis results from Cygnet Coal Measures and correlates.

Sample	T_{max}	$S_1 + S_2$	TOC	HI	OI
BR7	437	22.51	47.8	45	30
MQ2	456	3.30	3.4	85	17
MQ3	457	3.68	3.25	102	10
5949	450	1.05	2.65	34	67
LC1	497	2.49	32.9	6	17
CCM2	539	0.86	14.3	4	0
MQC1	456	2.93	4.75	55	37
MQC2	496	1.68	6.15	23	21
BP1	431	0.09	3.24	1	2

Analyses by AMDEL.

3.5.1. Discussion of results.

Cygnet Coal Measures have generated and expelled a significant quantity of both oil and gas as evidenced by bitumen-saturated rocks in the Badger River to Comstock region near Zeehan on the west coast of Tasmania. This visible evidence of source rock capacity is supported by Rock-Eval pyrolysis results, which show that Cygnet Coal Measures correlates on the west coast have the capacity to generate both oil and gas. In Table 3.4 the first four samples are siltstones and the next four samples are gas and from the results it is likely that the siltstones were the major source rocks due to the generally higher $S_1 + S_2$ values and much higher HI values. Two samples with very high T_{max} values LC1 and CCM2 are from coals collected in the far south east of Tasmania at Leprana and South Cape. BP1 is a marginally mature sample from the Piper's River area in northeastern Tasmania. Further details of maturity zoning will be covered in Chapter Four but the T_{max} temperatures indicate that maturity of Cygnet Coal Measures in far southern Tasmania is above the level considered viable for commercial quantities of gas and northern Tasmanian samples are immature for oil.

3.6. Results of investigations into the source potential of Lower Freshwater Mersey Coal Measures correlates.

Table 3.5 shows the results of samples with the highest source potential of any sequence found during this investigation. These coals are immature to marginally mature but generative potential is high and indicates that the possibility exists for excellent source rocks within the Tasmania Basin.

Table 3.5. Selected components of Rock-Eval pyrolysis results from samples of torbanite from the Lower Freshwater sequence of the Permian Parmeener Supergroup.

Sample	T_{max}	$S_1 + S_2$	TOC	HI	OI
Cat1	424	336.11	70.40	442	0
Cat2	432	273.12	74.80	354	8

Analyses by AMDEL.

3.6.1. Discussion of results of analysis of torbanite.

The results shown in Table 3.5 were from samples collected from Cotas Creek just north of St Marys in northeastern Tasmania. Another occurrence of torbanite from the same stratigraphic position occurs in the upper reaches of Relapse Creek near West Takone in northwestern Tasmania. At Preolenna, torbanite was mined for a short while and a seam in this area dips steeply in the upper reaches of the Flowerdale River (Bacon, 1991).

Permian torbanite was used as an oil shale at Joadja and Glen Davis, in central New South Wales, where the maximum seam thickness was 2 m but mostly 1 m (Hutton, 1987). In Tasmania the maximum seam thickness actually found was 700 mm in Cotas Creek north of St Marys. The Tasmanian outcrops all occur on the northern flanks of the Tasmania Basin and this is probably due to the palaeogeography where upland areas rimmed the margins of the Tasmania Basin creating the depositional environment required for the formation of these deposits.

In 1944, J.A. Dulhunty, as quoted by Hutton (1987), outlined a number of geological conditions necessary for the deposition of torbanite.

1. Upland areas rimming the margins of the basin.
2. Rivers sourced by runoff waters from upland areas that distributed the sediment along the margins of the basin.
3. The floodplain contained meandering streams, which were frequently flooded.
4. Temporary lakes formed and these received water by infiltration through swamps, peat bogs, sand dunes and silt beds.
5. Alternative filling and emptying of the lakes prevented permanent establishment of swamps or terrestrial vegetation.
6. The waters were well aerated and contained suspended sediment, dissolved mineral matter and only small quantities of humic matter.
7. The lakes were characterised by the abundant seasonal growth of *Botryococcus.*

These conditions also seem to apply to the Tasmanian situation where the early Permian (Mersey Coal Measures) were deposited in a wet environment with virtually no woody tissue being deposited as determined by the use of TGI (measure of moisture available in swamp) and TPI (wood ratio) (Bacon, 1986). The environment was likely a treeless moor and the presence of alginite and sporinite supports this interpretation (Bacon and Calver, 1986). The sediments in Huntsmans Creek (close to Cotas Creek) represent paralic deposition and may represent marginal conditions at the conclusion of the Lower Marine Sequence (Turner and Calver, 1984).

Palaeocurrents are from the north or northwest and inferred Permian basement topography suggests high ground to the north and the basin rapidly thickens to the south (Martini and Banks, 1989; Turner and Calver, 1984). The coals in Catos and Huntsmans Creeks are correlates of the Mersey Coal Measures and were deposited in a wet, relatively treeless environment, probably a lagoonal environment behind a barrier beach (Bacon and Calver, 1986). Other inferences made were that the

sequence was deposited in low sinuosity fluvial systems and probably brackish water. An environment such as this could not be expected to allow widespread deposition and so these coals have a confined and laterally discontinuous distribution.

Cane and Albion (1973) state that torbanite is derived from prodigious blooms of Permian fresh water alga virtually identical with extant *Botryococcus brauni* and originally this was based on the observation of fossilised outer walls of the algal colonies. Analysis of pyrolysis products from torbanite has now been able to show genetic links between *Botryococcus brauni* and biomarkers (Derenne et al., 1994; Landais et al., 1993).

Coal seams from the Mersey Coal Measures were formed on narrow coastal plains by rivers carrying run-off from higher ground. Organic matter was buried in bogs by the alternate filling of lakes and lagoons by seasonal floods in a cold wet environment. From the distribution of coal seams at Barn Bluff, Preolenna, Relapse Creek, Mersey Valley and torbanite in the Cotas Creek area all deposited on coastal plains and with Mersey Coal Measures correlates in south eastern Tasmania being marine deposits it can be implied that the coastline had an embayment extending into north. Marine conditions covered much of the Tasmania Basin at the time.

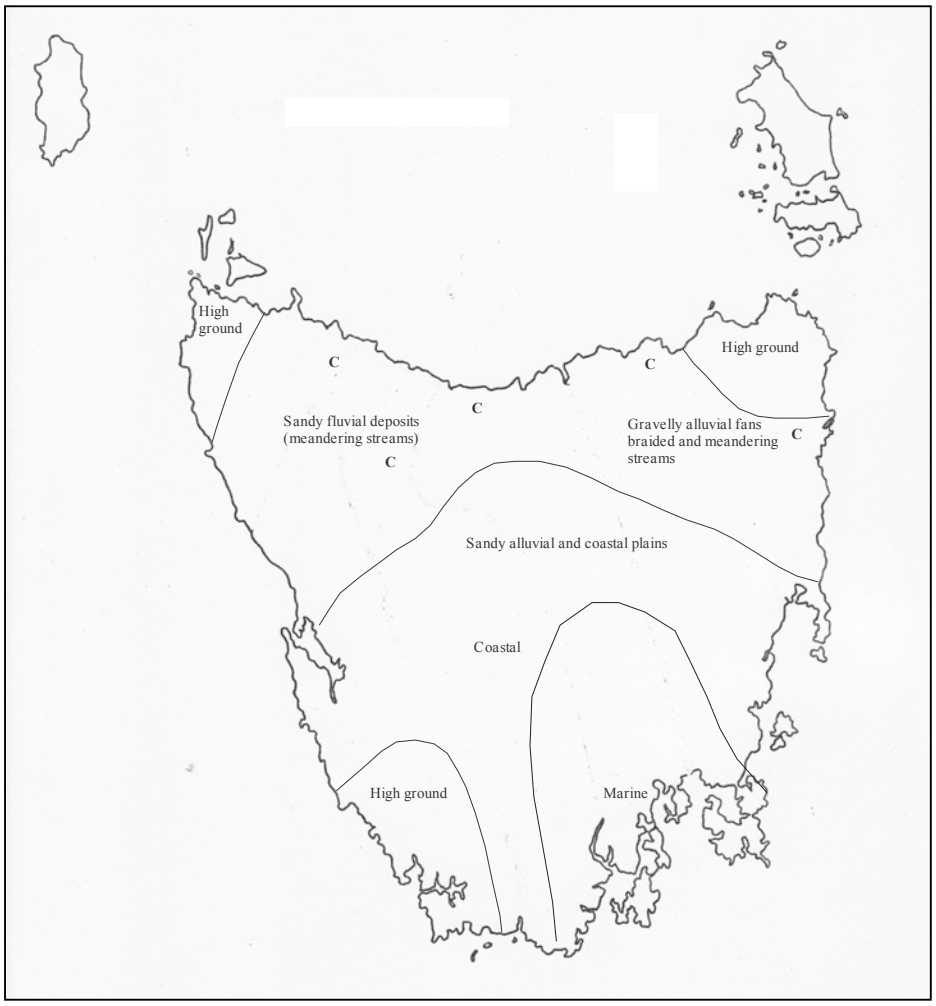

Figure 3.12. Palaeogeography for Tasmania during the deposition of the Mersey Coal Measures, Early Permian. After Reid (2002).

3.7. Summary of the potential source rocks identified and their distributions onshore Tasmania.

Sequences investigated for source rock potential in this study range in age from Mesoproterozoic?-Neoproterozoic to Upper Permian covering the most likely intervals for the deposition of petroleum source sediments. The depositional environments range from marine shelves to brackish littoral swamp deposits as well as fluvial and freshwater swamp deposits. As this is a frontier study and no commercial reservoirs of oil or gas have yet been discovered onshore Tasmania it was important to cover all possibilities. Major potential sequences within the Parmeener

Supergroup were not considered in this study because they were investigated in a parallel study (Reid, 2004).

3.7.1. Source potential of the Mesoproterozoic?-Neoproterozoic sequences.

Mesoproterozoic?-Neoproterozoic sequences were found to have negligible potential as source rocks mainly due to the high maturity as indicated by measurements of Kubler Index. More details of the maturity of these sequences will be considered in Chapter Four.

3.7.2. Source potential of the Ordovician Gordon Group.

The Ordovician Gordon Group was found to have very little potential as source rock due to a number of factors. Primarily the potential source beds within the Gordon Group are thin (generally <200 mm thickness) and discontinuous so that even if they had high generative potential only low quantities of hydrocarbons could be generated. The generative potential of these beds is low and this is due to two major factors, the type of organic matter from which the kerogen was derived and the high level of maturity. Another major problem is that the Gordon Group limestone has very low porosity and unless it was fractured very high generation pressures would be required to allow any hydrocarbons to migrate out of source beds. Although faulting and fracturing does occur within the Gordon Group the limited zones over which it occurs would not provide sufficient migration pathways for commercial petroleum systems.

The organic matter within the Gordon Group potential source beds is primarily amorphous matter and plots as Type III or Type IV with very low generative potential. The depositional environment was probably in general too oxic to allow preservation of organic matter and instead was probably reworked and recycled by burrowing organisms. Only thin beds were deposited under anoxic conditions and these are the only potential source beds.

The maturity of Gordon Group sediments is within the gas range and at this level most of the generative potential has been expended so that only small quantities of gas could be generated and most likely not have enough pressure to escape from source beds. This is why gas has been found trapped within the Gordon Group and can be detected when samples of the Upper Limestone Member of the Benjamin Limestone are cracked open.

3.7.3. Source potential of Upper Permian coals.

The evidence of significant generation and migration of bitumen and presence of oil and gas inclusions in Permian sandstones near the Badger River in western Tasmania shows that coals and carbonaceous siltstones in this region have obvious source potential. Geochemical analysis of coals and carbonaceous siltstones has shown that they have potential as source rocks. The area where the bitumen was found is an outlier of the Tasmania Basin and has been subjected to a somewhat different thermal history to the main basin. When considering the potential of similar sediments within the main Tasmania Basin, in respect to source potential, two major factors need to be considered, extent and thickness of potential source rocks and secondly the maturity of these sediments.

Cygnet Coal Measures correlates were the identified source rocks for the bitumens found on the west coast of Tasmania and these are also found within the main Tasmania Basin however coal seams are generally thin and discontinuous and have a limited distribution throughout the basin. The distribution of the Cygnet Coal Measures is such that some parts could only be considered marginally mature for gas generation and others are too mature for consideration. The generally thin and discontinuous distribution coupled with marginal maturity does not offer great potential as a source rock in the Tasmania Basin. In places the coal seams are close to dolerite intrusions and in these situations the maturity is too high for potential source rocks.

3.7.4. Source potential of Mersey Coal Measures correlates.

The Mersey Coal Measures correlates appear to have the greatest potential as source rocks of any of the sequences considered in this study. However there are a number of problems associated with these sediments in terms of source rocks and primarily this relates to marginal maturity and thin and discontinuous distribution. The Mersey Coal Measures correlates have only been identified in the northern sections of the Tasmania Basin, which has been found to be immature for oil generation. The palaeogeography of the time implies that deposition outside the known extent of the Mersey Coal measures in northern Tasmania was unlikely and thus there is little possibility of finding source rocks from this sequence with higher maturity and thus more potential for petroleum generation.

These sediments could provide potential as oil shale deposits, however outcrop is restricted and seams are thin (generally <500 mm). Due to the locations of the known seams extraction costs would be too high to make an oil shale operation viable.

The Mersey Coal Measures cannot be considered as potential oil source rocks.

3.7.5. Summary.

No commercially viable petroleum source rocks have been identified in any of the sequences investigated during this study. This would suggest that no stacked petroleum systems are likely to be found within the Tasmania Basin.

CHAPTER FOUR.

METAMORPHISM IN TASMANIA AND MATURITY OF POTENTIAL SOURCE ROCKS.

4.1. Concept of maturity.

As was explained in Chapter Three petroleum is generated from source rocks due to a process known as maturation and this occurs largely because of increasing temperature. Coal petrologists were the first to recognise relationships between increasing depth of burial and physical changes in coal properties that were caused by increasing temperatures at greater depths. The changes in coal are referred to as ranks ranging from lignite, where diagenesis is still occurring, through subbituminous, high, medium and low-volatile bituminous, semianthracite and anthracite. The organic matter within petroleum source rocks also undergoes progressive changes in properties and these can be used to define the level of maturity or in other words determine the maximum palaeotemperature to which the sediment has been subjected.

Organic maturity is usually divided into three stages known as diagenesis, catagenesis and metamorphism. During diagenesis the sediment is compacted and pore fluids are expelled often leading to migration of ions and organic molecules within the sediments. Cementing of the sediment may occur leading to lithification. Diagenesis operates until a temperature of ~50°C is reached, which with a normal geothermal gradient of 30°C/km is equivalent to a depth of approximately 1.7 km. Minor methane may be generated during diagenesis but essentially sediments at this maturity level would be considered immature in terms of petroleum generation.

Catagenesis is the stage of organic maturity where the main phase of petroleum is generated and is usually divided into the oil and gas windows. Oil generation starts at ~50°C and increases to a maximum at ~100°C and finishes by ~130°C. Wet gas, C_2H_6 to C_6H_{14}, may start generating at the same time as oil but the volume generated increases much more slowly attaining a maximum of ~140°C and finishing at ~180°C. Dry gas, CH_4, may be generated to some extent during diagenesis but the maximum generation occurs between ~180°C and ~200°C. No exact figures can be given for these cut-off points as the type of organic matter, sediment matrix and rate

of burial all have a bearing on the temperatures at which the generation of various components occur.

Metamorphism occurs above ~200°C and can be recognised by changes in the mineralogy of the sediments. Maturation can be considered as incipient metamorphism and the level of maturity can be recognised by physical changes in the organic matter enclosed within the sediment. As was shown in Chapter Three it is important to understand the state of maturity of any source rock as petroleum can only be generated from mature source rocks and dry gas only is generated from late mature samples.

4.2. Common methods for measuring organic maturity of source rocks.

The increasing temperature due to deeper burial causes physical and chemical changes to occur to organic matter trapped within sediments and methods of measuring maturity depend on measurements of these changes. A range of different methods has been developed to measure the physical and chemical changes in organic matter during maturation and it is useful to use a variety of methods to determine the maturity of any particular sediment so as to avoid any bias that may be introduced by using just one particular method. Most methods also have only a limited range over which they are effective and so each must be used appropriately.

The accepted standard measurement for maturity is vitrinite reflectance (R_0), because it extends over a wider maturity range than any other indicator (Hunt, 1995). Vitrinite reflectance is a method developed by coal petrologists for assessing the rank of coal by measuring the light reflected from the polished surface of vitrinite usually with the microscope objective immersed in oil. Vitrinite is a maceral of coal derived from the cell-walls of land plants and it also occurs in many carbonates and shales (Tissot and Welte, 1978). Vitrinite is formed from clusters of condensed aromatic rings and as maturity increases these rings fuse into larger rings and eventually form flat sheets of condensed rings that assume an orderly structure (Hunt, 1995). The increased size of the condensed rings and flat surfaces formed allows greater reflectivity so that maturity can be determined by the amount of light reflected. Due to the fact that vitrinite is derived from land plant materials, the method of vitrinite reflection can only be used for sediments deposited post-Silurian.

Colour changes of palynomorphs are commonly used to determine maturity with spores and pollen changing from light to dark as maturity increases. Samples are observed under transmitted light and the microscopes are fitted with meters to measure light absorption so as to semi-quantitatively measure maturity. Staplin (1969) developed a scale known as the Thermal Alteration Index (TAI) and it is widely used as a rough and inexpensive maturation indicator (Hunt, 1995).

Conodonts change colour due to what appears to be a carbon-fixing process that parallels systematic changes in other forms of organic matter. Thermal cut-offs for oil, condensate and dry gas generation can be determined from the colour changes of conodonts (Epstein et al., 1977). Irreversible colour changes occur to conodonts, ranging from yellow to black, due to increases in maturity and these changes were correlated with other maturity scales by Epstein et al., (1977) to establish a scale known as the Colour Alteration Index (CAI). CAI was used by Burrett (1992) to determine the maturity of Ordovician carbonates in Tasmania.

Rock-Eval pyrolysis is commonly used as a rapid method of assessing source rock potential and the T_{max} and PI parameters from this process can be used to establish maturity at the same time. T_{max} is the temperature at which the maximum volume of hydrocarbons is generated during pyrolysis and can be correlated with other maturity parameters. This method is most useful over the range from the beginning of oil generation (0.4 % R_o) to near maximum condensate generation (1.5 % R_o) (Snowdon, 1989). As with other maturity parameters the type of organic matter will change the temperatures indicated for various stages of maturity and this is a reason for using a range of maturity assessment methods. For Type II organic matter, ~435°C marks the beginning of oil generation and ~470°C the beginning of condensate generation during experiments (Peters, 1986).

Fluorescence microscopy is used to estimate the level of maturity by observation of the colour of light emitted from source rocks under excitation. A blue (477 nm) exciting light is generally used and colours change from blue/green to green/yellow then golden yellow, dull yellow, orange, red and then fluorescence ends. Changes in colours occur at coalification jumps which occur at 0.5 % R_o, 0.8-0.9 % R_o and 1.2-1.6 % R_o, corresponding to the beginning of oil generation, the maximum oil

generation and end of oil generation (Hunt, 1995). Fluorescence is thus only useful over the range of oil generation.

Biomarkers can be used to determine maturity primarily by changes in the shapes of complex macromolecules due to thermal stress on the ring systems and side chains. These changes are generally expressed as ratios such as 20S/(20S + 20R) determined during gas chromatograph mass spectrometer (GCMS) analysis. It is usual to use several biomarker parameters in parallel to establish maturity (Hunt, 1995). Biomarker separation, analysis and interpretation require a skilled operator with considerable experience and so the process is relatively expensive.

The various methods of maturity assessment can be approximately correlated but because they all measure different physical and chemical changes in different materials the rates of change in each case are different. The ranges of maturity at which they operate are also different and thus the methods used in any given situation must be determined according to the type of sediment being investigated, its age, depositional environment, accuracy required and estimated maturity. A chart compiled by Hunt (1979) showing approximate correlations between maturity methods appears as Figure 4.1.

4.3. Previous maturity investigations onshore Tasmania.

4.3.1. Maturity of Permian and Triassic coals.

Maturity studies have been made on aspects of organic maturity onshore Tasmania with the first of these applied to coal exploration. Coal exploration has taken place over the southern and eastern Tasmania Basin within the Parmeener Supergroup sediments. As these sedimentary rocks are probable hosts to the Gondwanan petroleum system maturity measurements made on coal are directly applicable to petroleum exploration.

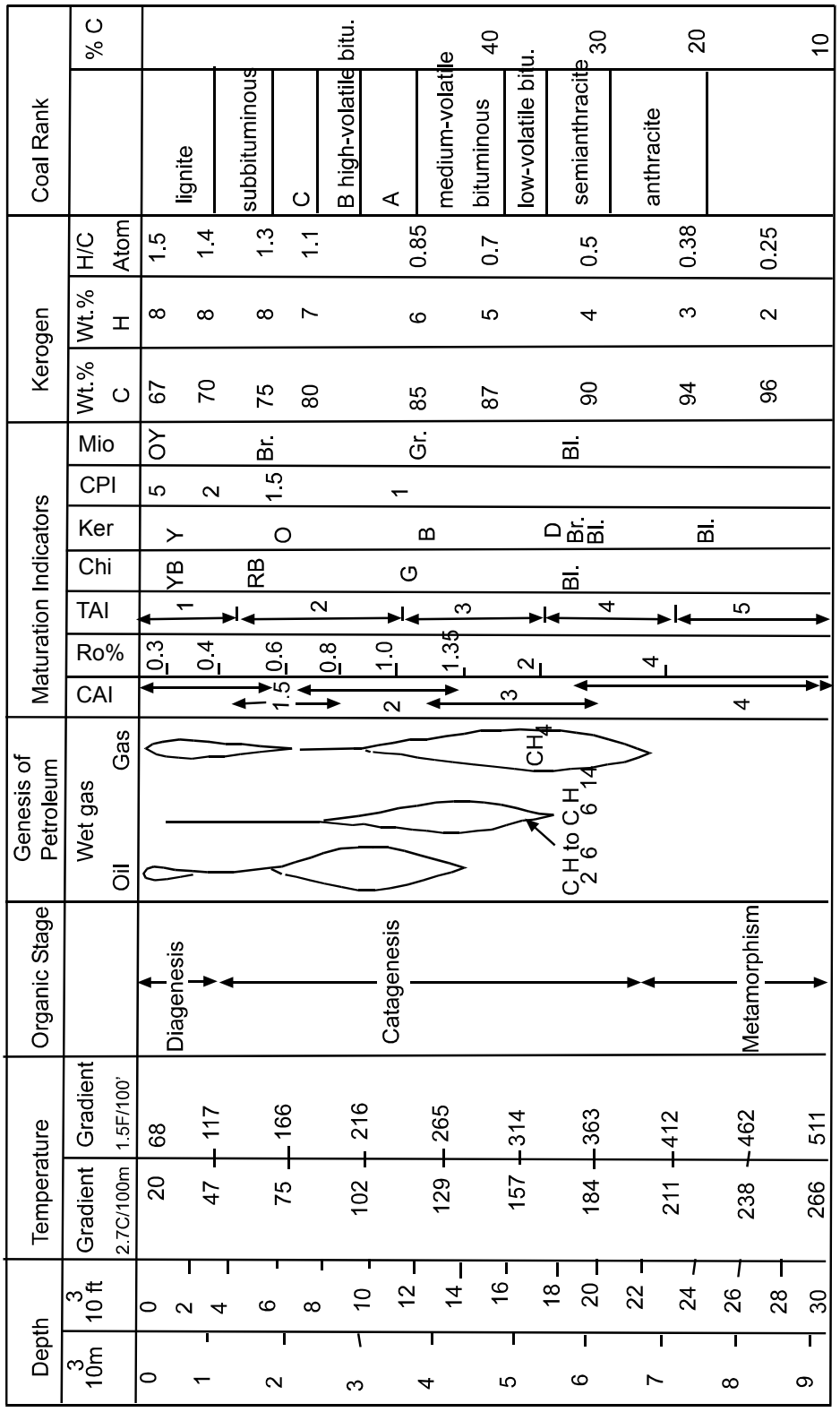

Figure 4.1. Correlation chart for common maturity indexes and their relationships to maturity stages, temperature and depths of burial. After Hunt (1979).

Vitrinite reflectance data has been extracted from company reports of coal mining and exploration activities on Triassic and Permian coal measures within the Tasmania Basin. In some cases calorific values have been used to determine maturity of coal and so a conversion of this data is necessary so that comparisons with vitrinite reflection measurements may be made. Table 4.1 shows a compilation of data derived mainly from coal investigations but also includes some results from stratigraphic drilling.

Table 4.1. Compilation of maturity measurements made on coal and limestone samples from stratigraphic drilling within the Tasmania Basin.

Site	Original Data	Vitrinite Reflect.	Reference
Ross	Tmax 440	0.8%	(Forsyth, 1989)
Tunbridge	Tmax 450	0.9%	(Forsyth, 1989)
Woodbury	22.4 MJ/kg	0.48%	(Bacon, 1991)
Stonehenge	VR 1.18%	1.18%	(Anon, 1984a)
Hunterston	VR 1.19%	1.19%	(Reid et al., 2003)
York Plains	26.02 MJ/kg	0.62%	(Bacon, 1991)
Wetheron Tier	VR 0.85%	0.85%	(Anon, 1984a)
Elderslie	VR 1.07%	1.07%	(Anon, 1984a)
Styx Valley	VR 1.3%	1.3%	(Bacon et al., 2000)
Mt Lloyd	25.5 MJ/kg	0.6%	(Bacon, 1991)
Kaoota	25.3 MJ/kg	0.59%	(Bacon, 1991)
Strathblane	26 MJ/kg	0.61%	(Bacon, 1991)
Lune River	Tmax 496	1.57%	(AMDEL, 2002b)
Adventure Bay	22.7 MJ/kg	0.49%	(Bacon, 1991)
Florentine Valley	Tmax 490	1.55%	(AMDEL, 2002a)
Catagunya	VR 0.8%	0.8%	(Anon, 1984a)
Mt Vernon	28.16 MJ/kg	0.74%	(Anon, 1984a)
Colebrook	26.9 MJ/kg	0.64%	(Bacon, 1991)
Pelham	Tmax 450	0.9%	(Reid, 2003)
Lonnavale	Calc. VR 1.0%	1.0%	(Reid, 2004)

The maturity measurements derived from coals have never been combined to show the trends of maturity within the Tasmania Basin. To give a more complete picture further maturity measurements were made on Permian coals of particular interest as

potential petroleum source rocks. Using the combined data from coal exploration and investigations made during the course of the present investigations, Tables 3.4, 3.5 and 4.2, a maturity map of the Tasmania Basin was constructed (Figure 4.2).

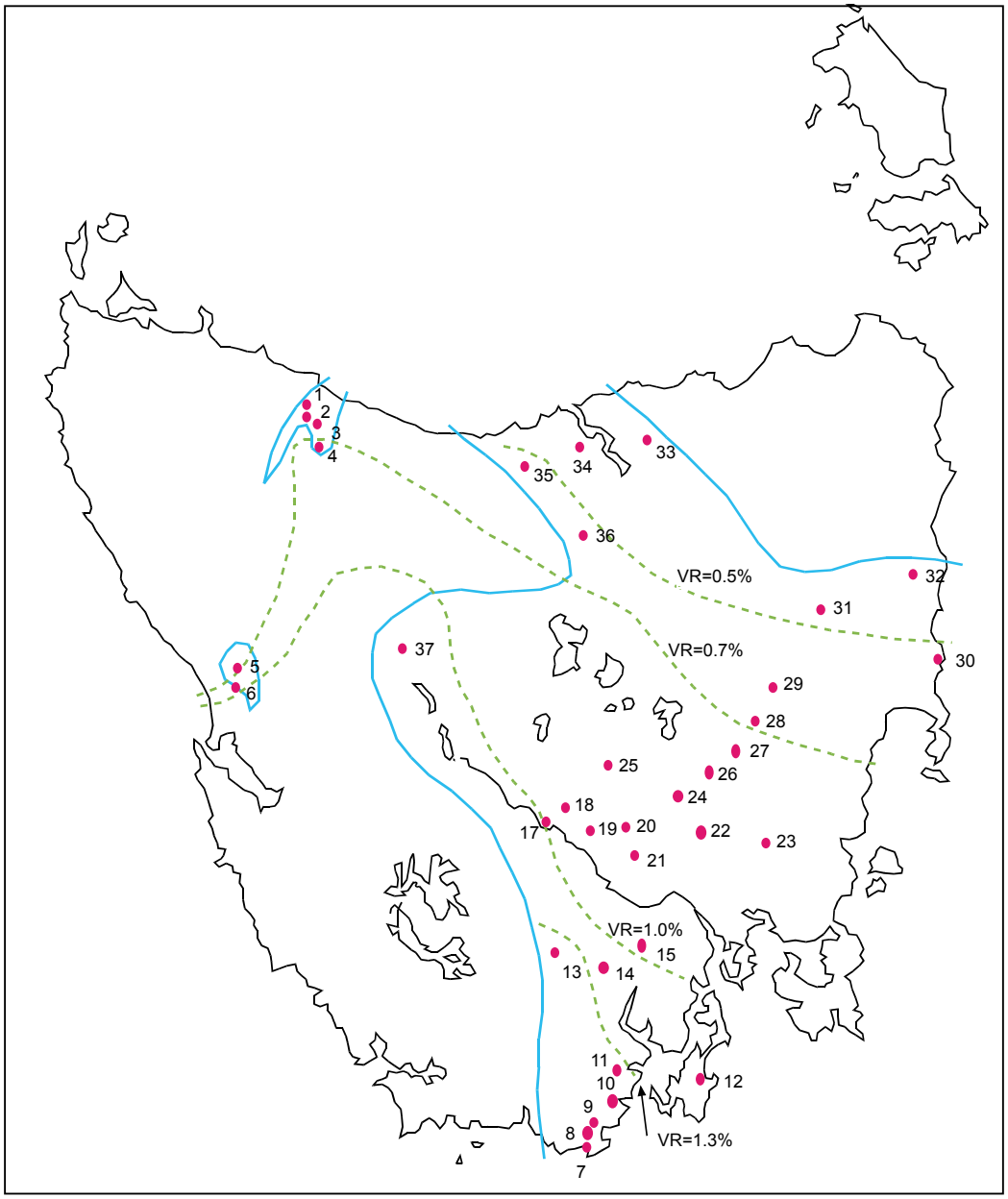

Figure 4.2. Maturity determined for Parmeener Supergroup sequences within the Tasmania Basin from vitrinite reflectance and calorific values of coal, vitrinite reflectance from potential source rocks and Rock-Eval pyrolysis of potential source rocks. Blue lines show the boundaries of the Tasmania Basin and note that there are outliers of this basin in the northwest and west of the state. Green dashed lines are vitrinite reflectance contours showing an increase in maturity from north to south. Contours have been selected to show approximate position for beginning of oil generation (VR = 0.5%), peak oil generation (VR = 0.7%), peak wet gas generation

(VR = 1.0%) and end of oil generation (VR = 1.3%). Locations for data points are numbered and details are given in Table 4.2.

Table 4.2. Locations and data for numbered points on Figure 4.2.

Number	Location	Lithology	T_{max}	Equiv. VR%	Source
1	Preolenna	Liffey Group	438	0.5	(Reid, 2004)
2	Relapse Creek	Liffey Group	443	0.6	(Reid, 2004)
3	Oonah	Oil shale	442	0.6	(Reid, 2004)
4	Hellyer Gorge	Oil shale	449	0.7	(Reid, 2004)
5	Badger River	Cygnet C.M.	437	0.65	(AMDEL, 2004b)
6	Mallana	Cygnet C.M.	457	1.0	(AMDEL, 2004d)
7	South Cape	Cygnet C.M.	539	2.3	(AMDEL, 2004a)
8	Kaoota	Cygnet C.M.		0.59	(Bacon, 1991)
9	Leprena	Cygnet C.M.	497	1.7	(AMDEL, 2004b)
10	Lune River	Gordon Lst.		1.57	(AMDEL, 2002b)
11	Strathblane	Triassic coal		0.61	(Bacon, 1991)
12	Adventure Bay	L.Permian coal		0.49	(Bacon, 1991)
13	Styx Valley	Woody Is. Silt.	453	1.0	(Reid, 2004)
14	Lonnavale	Permian U.M.		1.0	(Reid, 2004)
15	Mt Lloyd	Cygnet C.M.		0.6	(Bacon, 1991)
16	Florentine Val.	Gordon Lst.		1.55	(AMDEL, 2002a)
17	Catagunyah	Cygnet C.M.		0.8	(Anon, 1984a)
18	Langloh	Cygnet C.M.		0.6	(Hofto and Morrison, 1989)
19	Pelham	Ferntree Mudst.	454	1.0	(Reid, 2004)
20	Wetheron Tier	Cygnet C.M.		1.5-1.7	(Anon, 1984a)
21	Elderslie	Cygnet C.M.		1.07	(Anon, 1984a)
22	Colebrook	Triassic coal		0.64	(Bacon, 1991)
23	Stonehenge	Cygnet C.M.		1.18	(Anon, 1984a)
24	Mt. Vernon	Cygnet C.M.		0.74	(Anon, 1984a)
25	Hunterston	Liffey Group	455	1.1	(Reid, 2004)
26	York Plains	Triassic coal		0.62	(Bacon, 1991)
27	Woodbury	Triassic coal		0.48	(Forsyth, 1989)
28	Tunbridge	Woody Is. Silt.	445	0.6	(Reid, 2004)
29	Ross	Woody Is. Silt.	441	0.6	(Reid, 2004)
30	Bicheno	Woody Is. Silt.	437	0.65	(Reid, 2004)
31	Fingal	Triassic coal		0.55	(Hofto and Morrison, 1989)
32	Cotas Creek	Mersey C.M.	432	0.5	(AMDEL, 2004e)
33	Bangor	Cygnet C.M.	431	0.4	(AMDEL, 2004c)
34	Anderson's Ck.	Woody Is. Silt.	435	0.5	(Reid, 2004)
35	Mersey Gt. B.	Oil shale	444	0.6	(Reid, 2004)
36	Golden Valley	Macrae Mudst.	444	0.6	(Reid, 2004)
37	Mt. Pelion	Pelionite	473	1.2	(Reid, 2004)

The general trend of increasing maturity from northeast to south across the Tasmania Basin is not as simple as it appears because at various places samples have been measured with maturity values higher than predicted from the contours shown in Figure 4.2. Samples with higher than predicted maturity are particularly noticeable in the northeastern parts of the Tasmania Basin where background maturity as measured by vitrinite reflectance is below 0.5%. Bacon et al., (2000) record vitrinite reflectance values for Upper Triassic coals from Fingal up to 0.67% and from Mt. Nicholas 0.59%. A coal sample from Langloh, mentioned as being collected 100 m from dolerite, has a vitrinite reflectance value of 0.6%. A table of vitrinite reflectance values presented by Bacon et al., (2000) shows a bimodal distribution, and they state that the upper mode is related to local contact metamorphism with dolerite. Due to the widespread intrusion of dolerite within the Tasmania Basin the effects of local heating from dykes and sills of dolerite has to be considered when determining the maturity of any particular part of the basin. Heating effects from dolerite intrusions are not simply due to their size but also depend upon the water content of the country rocks at the time of intrusion. Wet rocks conduct and convect heat more rapidly than dry rocks thus a larger zone can have a higher maturity around a dolerite intrusion that penetrated wet country rocks.

4.3.2. Maturity of Gordon Group based on Colour Alteration Index.

Colour alteration index (CAI) values from Early to Middle Palaeozoic marine carbonate rocks of the west Tasmania terrane were used by Burrett (1992) to determine areas where Gordon Group carbonate rocks may have been or still may be in the oil and gas windows of maturity. Burrett's (1992) study showed that much of western and northwestern Tasmania has been subjected to metamorphic temperatures above 300°C (CAI 5) and that metamorphic temperatures decrease towards the southeast with lowest temperatures 50-90°C (CAI 1.5) in southern Tasmania. This low value seems to be an isolated occurrence as the general lowest values for southern Tasmania are in the range 110-200°C (CAI 3).

Epstein et al., (1977) did their original conodont studies in the Appalachian region where depth of burial and attendant increase in temperature were considered responsible for the colour changes in conodonts. In Tasmania the required depth of burial to achieve temperatures necessary for CAI 5 is unlikely to have occurred if only

the known stratigraphic thicknesses are considered. Siluro-Devonian sequences are of the order of two kilometres in thickness as shown in Chapter Two. Consideration of reasons for high CAI values will be given in section 4.7.

4.3.3. Lopatin method for establishing maturity in the Tasmania Basin.

Woods (1995) investigated thermal maturity of the Gordon Limestone and Woody Island Formation using the theoretical Lopatin method, known burial history and postulated geothermal gradients. In Tasmania burial history is not fully understood due to extensive erosion having removed unknown thicknesses of rocks and geothermal gradients can only be estimated. To overcome these major impediments to his study Woods (1995) used maximum and minimum burial scenarios and average geothermal gradients. Models developed during this study found that the Woody Island Formation is placed near the base of the oil window. Maximum burial scenarios shows the Gordon Limestone enters the oil and gas windows rapidly and currently would be over mature for petroleum generation. Lower burial rates for the Gordon Limestone show that it could still be presently in the upper limits of the oil window or within the gas window. Due to the theoretical basis of this study it can only be used as a guide to possibilities.

4.4. Results of maturity investigations of Proterozoic sequences in northwest Tasmania.

Potential petroleum source rocks have been identified at three different stratigraphic levels onshore Tasmania and the maturity of each of these will be considered in turn. Precambrian potential source rocks outcrop in northwestern Tasmania and correlates also outcrop in the upper Weld Valley (Calver, 1989). Possible correlates have been identified during stratigraphic drilling (Hassell, 1996; Reid et al., 2003) and also by geophysical interpretation (Leaman, 1991) to underlie parts of the Tasmania Basin. Source potential and maturity of exposed sequences in northwestern Tasmania was assessed in order to gauge the possibility for Precambrian sequences below the Tasmania Basin to be prospective source rocks. Rock-Eval pyrolysis results from samples in the Rocky Cape Block are shown in Table 4.3.

Rock-Eval pyrolysis results from Black River Dolomite and Cowrie Siltstone within the Rocky Cape Block suggest that the Cowrie Siltstone has some potential as a

petroleum source rock. These results have low T_{max} values indicating maturity values much lower than expected from previously determined metamorphic grades for the Rocky Cape Block. To resolve the disparity between Rock-Eval pyrolysis maturity determinations and previously determined metamorphic grades a survey of Kubler Index values was undertaken to independently assess maturity.

Table 4.3. Rocky Cape Block Rock-Eval pyrolysis results.

Sample	Location	T_{max}	S_1	S_2	S_3	$S_1 + S_2$	PI	S_2/S_3	PC	HI	OI	TOC
SRSS	Salmon River	501	0.07	0.47	2.55	0.54	0.13	0.18	0.04	55	303	0.85
CS1	Cowrie Point	470	0.06	0.32	0.33	0.38	0.16	0.96	0.03	22	22	1.45
CP2	" "	489	0.02	0.49	0.21	0.51	0.04	2.33	0.04	76	32	0.64
CP3	" "	402	0.28	0.77	0.14	1.05	0.27	5.50	0.08	56	10	1.37
CP4	" "	497	0.03	0.16	0.50	0.19	0.17	0.32	0.01	22	71	0.70
AR1	Apiary River	475	0.04	0.13	0.57	0.17	0.25	0.22	0.01	3	14	4.02
JR1	Julius River	439	0.02	0.03	0.32	0.05	0.50	0.09	0.00	1	15	2.08
TB	Tayatea Bridge	458	0.02	0.06	0.25	0.08	0.25	0.24	0.00	3	13	1.85

Analyses by AMDEL

4.4.1. Kubler Index and its relationship to petroleum source rock maturity.

The universally accepted maturation indicator is vitrinite reflectance; however in sequences deposited prior to the Silurian no woody plant material is available so alternative maturity measurements must be made. In the case of the fine-grained siltstones within the Rocky Cape Group an appearance of low metamorphic grade may also be due to the lack of generally recognised index minerals used for conventional metamorphic conditions. Rock-Eval pyrolysis T_{max} values seemed to indicate a low maturity yet the generative potential in relation to TOC levels implied a higher maturation state. Further indications of problems with the Rock-Eval pyrolysis results were displayed by disagreement between T_{max} and Production Index.

Kubler Index, which specifically measures increases in the thickness of illite-muscovite crystallites due to an increase in burial/rise in temperature, was selected as an alternative method to measure maturity. The standard method of measuring illite changes was developed by Kubler (1967) and is now termed the Kubler Index. Kubler Index corresponds to the width of the (001) peak of illite at half-height and was originally measured in millimetres but is now expressed in terms of an angular value $°\Delta 2\theta$ so as to minimise effects such as goniometer scanning rate and chart speed on

the measurement (Kisch, 1990). Older measurements in millimetres can be converted to °Δ2θ by multiplying millimetres by 0.079 (Guthrie et al., 1986).

Clays undergo changes due to increasing temperature analogous to those in vitrinite where the atomic structure becomes more ordered as temperatures increase and this can be detected by X-ray diffraction patterns. During diagenesis and incipient metamorphism there is an increase in the crystallinity of authigenic illite as a result of dehydration, K-fixation and rearrangement of ions and this can be detected by the narrowing of the width of the (001) peak on X-ray diffractograms (Brill, 1988). Progressive changes in the smectite group of clays occur during diagenesis until, at approximately 100°C, they start to lose their interlayer water and incorporate K^+ in place of cations such as Ca^{2+} with the result that these layers are converted to illite. As the diagenesis advances, the transformation is accompanied by a gradual ordering of the mixed layer phase. This ordering continues in a single layer phase until the ultimate conversion of the illite to muscovite (Duba and Williams-Jones, 1983). The narrowing of the basal (001) peak, which accompanies this ordering, reflects the decreasing variability of the d-spacings as the illite layers become more alike i.e. the structure becomes more homogenous or crystalline. The Kubler Index can be used as a semi-quantitative geothermometer (Akande and Erdtmann, 1998).

The log of the Kubler Index decreases with increasing mean vitrinite reflectance and this relationship suggests that the same geologic agents that control vitrinite reflectance, namely temperature and time, control the Kubler Index (Guthrie et al., 1986). A number of studies have been made to statistically correlate vitrinite reflectance and Kubler Index so as to provide a useful means of estimating thermal maturity of strata that do not contain vitrinite either because of age or low organic content (Guthrie et al., 1986). There are major difficulties with these correlations because the two methods are measuring the effects of totally different processes although both are due to increases in temperature. Kubler Index and vitrinite reflectance may not equilibrate to temperature changes at the same rate (Guthrie et al., 1986). Dalla Torre et al., (1996) showed this clearly by comparing vitrinite reflectance and Kubler Index measurements from a number of basins. A further difficulty in the present study is the age of the sediments involved and as Heroux et al., (1979) point out it is hazardous to extrapolate temperatures to Mesozoic and

Palaeozoic sediments due to the temperature and time relationships involved in organic maturation.

Transition from diagenesis to anchizone occurs at ~0.42 °Δ2θ and can be correlated with a temperature of 235° ± 10°C (Mullis et al., 1995). The onset of anchizone conditions corresponds to vitrinite reflectance of 2.0% (Merriman and Frey, 1999). Commencement of anchizone is the upper limit of liquid hydrocarbon preservation (Blenkinsop, 1988). Transition from oil to gas occurs at 1.0°Δ2θ at approximately 120°C (Mullis et al., 1995). In conventional metamorphic grade terminology the diagenetic zone is equivalent to the zone containing zeolite facies assemblages in meta-basaltic rocks, anchizone is equivalent to the zone containing prehnite-pumpellyite facies in meta-basaltic rocks and epizone is equivalent to lower greenschist facies.

Keeping these problems in mind, a correlation between vitrinite reflectance and Kubler Index and palaeotemperature is shown in Figure 4.3. This correlation must only be regarded as approximate due to the large number of variables involved in comparing two methodologies based on quite different mechanisms. Vitrinite reflectance itself can only be approximately related to palaeotemperatures as relationships vary due to rates of heating, type of organic matter and matrix sediment and so scales have to be developed for each individual basin in order to determine direct conversions. The Kubler Index operates from a completely different mechanism and changes relative to temperature probably are slower than those occurring on organic matter. For the purposes of this study the range of Kubler Index measurements are well outside the uncertainties of correlations between vitrinite reflectance and Kubler Index so that definitive conclusions can be made on the maturity of the Rocky Cape Group.

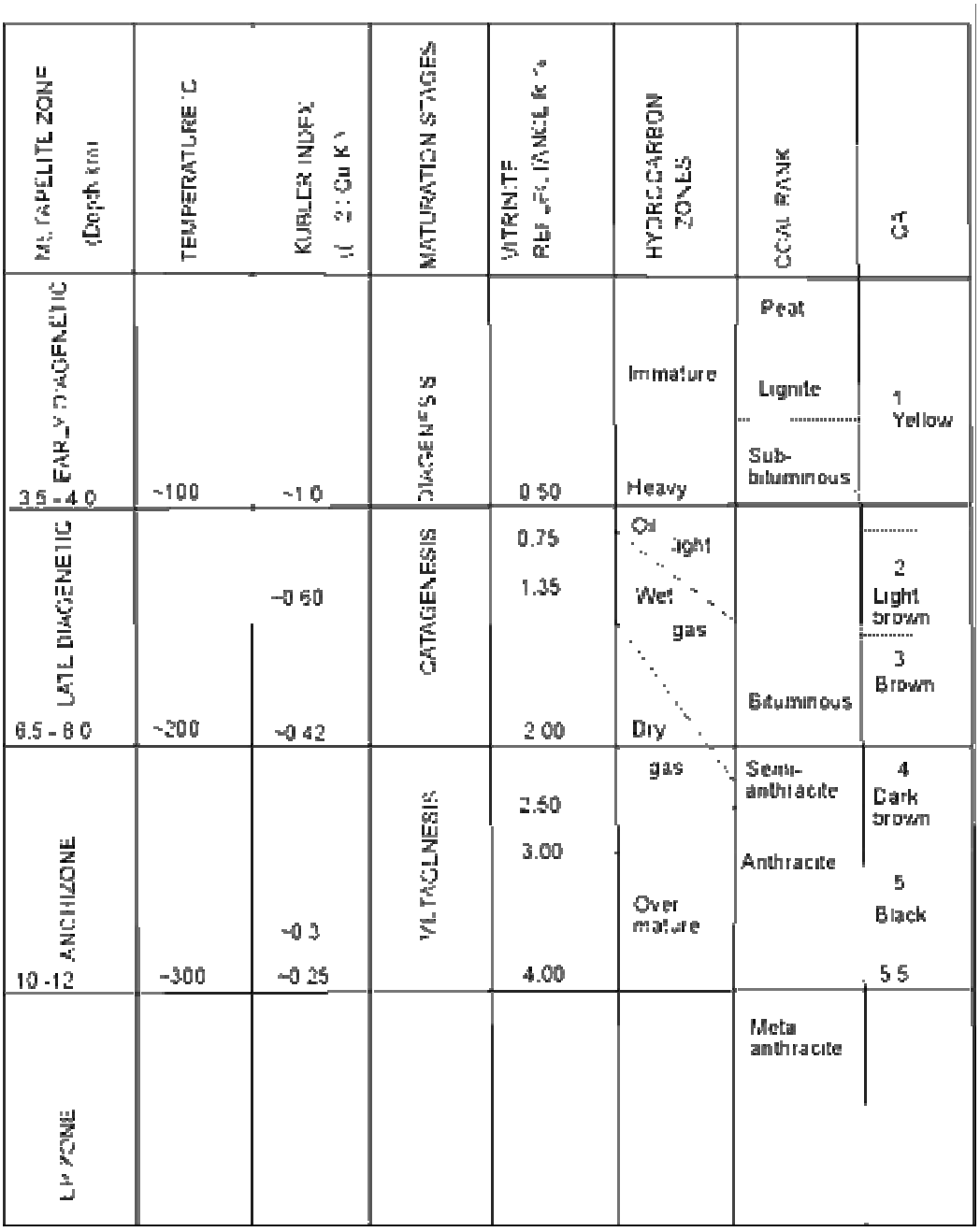

Figure 4.3. Correlation chart showing relationships between some commonly used maturation indices, metapelitic zones, maximum palaeotemperatures, hydrocarbon zones and coal rank. Note that these correlations are only approximate as each scale is based on different processes that proceed at different rates. Figure has been modified from Merriman and Frey, (1999).

4.4.2. Methods used to determine maturity of Proterozoic sequences in northwest Tasmania.

Samples of pelite were collected at approximately 10 km spacings across the Rocky Cape Block where outcrop permitted. Five samples of pelite were collected from within a 100 square metre quadrant at each site taking care to make sure each sample came from a different bed. Hunziker (1986) found that five samples were the minimum number required to produce a reliable average result for the maturity of a particular location. The samples were cleaned and broken into small pieces and then crushed in a chrome steel swing mill for 60 seconds. Kubler Index measurements were performed at Mineral Resources Tasmania, Rosny, on an automated Philips X-ray diffractometer system: PW 1729 generator, PW 1050 goniometer, PW 1710 microprocessor, with nickel-filtered copper radiation at 40 kV/30mA, a graphite monochrometer (PW 1752), sample spinner and proportional detector (sealed gas-filled, PW 1711). The analytical procedure used was based on the Warr and Rice (1994) method. A sedimented mount is prepared for each sample. The (001) illite peak is scanned five times (speed 0.01°/second). An average width at half peak height is calculated. Each sample was analysed air-dried and then ethylene glycol treated and both results reported and the raw widths were corrected by calibration against Warr and Rice (1994) standards.

4.4.3. Results of maturity investigations of Proterozoic sequences in northwest Tasmania.

Mean values for the Kubler Index results from each site within the Rocky Cape Block are shown in Table 4.4. Full Kubler Index results are shown in Appendix D.

Table 4.4. Mean Kubler Index values for sites across the Rocky Cape Block.

Site	ID	Easting mE	Northing mN	Mean KI	Est. max. Palaeotemp.
Peggs Beach	PB 1-5	361000	5476300	0.26	320 °C
Sisters Beach	SB 1-5	377350	5470400	0.25	330 °C
Bluff Hill Rd	BHR 1-5	303800	5457550	0.28	290 °C
Alert Creek	ACQ 1-5	306425	5450250	0.27	300 °C
Couta Rocks	CRQ 1-5	306990	5439400	0.24	370 °C
Waratah Ck	WarQ 1-5	327100	5424700	0.25	330 °C
Dollie Creek	DP 1-5	350250	5455300	0.28	290 °C
Wedge Plains	WPQ 1-5	356200	5453600	0.27	300 °C
Tipunah Rd	TipR 1-5	351000	5467700	0.36	240 °C
South Sumac	SS 1-5	336800	5426650	0.28	290 °C
Holder Quarry	HQ 1-5	349850	5449800	0.32	255 °C
Salmon River	SRSS 3	319250	5453155	0.43 *	190 °C

* Note: Single sample of uncertain reliability from higher stratigraphic level (Cambrian) than other samples in table.

The sample sites are shown on Figure 4.6 along with inferred palaeotemperature contours determined from the Kubler Index results. Maximum palaeotemperatures were determined using the correlation chart shown as Figure 4.7 based on the work of Arkai (1991) but it must be kept in mind that this correlation is approximate due to factors discussed earlier.

4.4.4. Orientation of white micas in samples used for KI determinations.

The orientation of neocrystalline white micas within the Rocky Cape Group samples used for KI determinations should give a good indication as to whether burial metamorphism or tectonic metamorphism was responsible for the metamorphic peak. If burial metamorphism was the dominant factor for the metamorphic peak then the neocrystalline white micas should largely be parallel to bedding whereas if tectonic

metamorphism was the major factor then the neocrystalline white micas would largely parallel the cleavage.

To determine the orientation of the neocrystalline white micas within the samples used to determine KI values some thin sections were cut from samples on both the eastern and western limbs of the Rocky Cape Block. Photomicrographs of these samples are shown in Figures 4.4 and 4.5. Sample 157374 from Bluff Hill (BHR on Figure 4.4) on the western side of the Rocky Cape Block has approximately 90% of the micas aligned parallel to bedding. The orientation of the micas in this sample is consistent with burial metamorphism being responsible for the metamorphic peak. It is also consistent with the results of the KI survey where peak metamorphism correlates directly with the thickness of overlying stratigraphy.

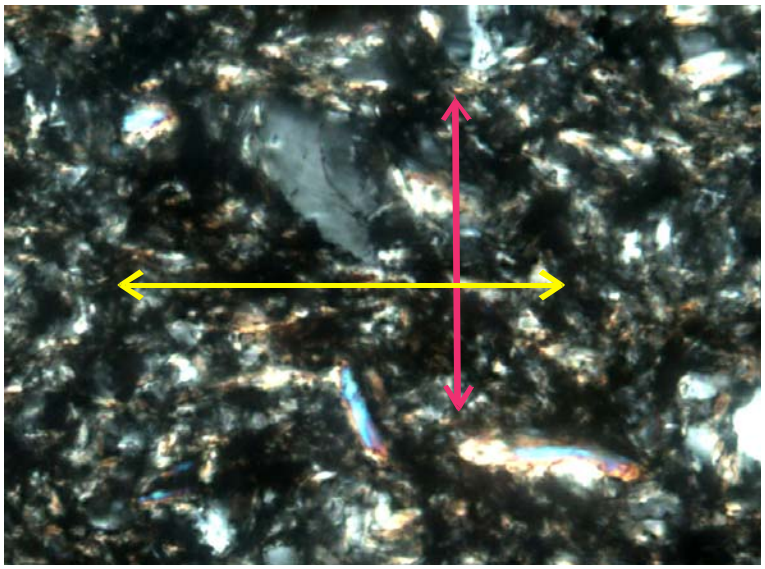

Figure 4.4. Photomicrograph of sample 157374, the location is shown as BHR on Figure 4.6. Most of the visible white micas are aligned parallel with bedding, (direction shown with red arrow) with approximately 10% aligned parallel with cleavage (direction shown with yellow arrow). The alignment of the majority of the white micas parallel with bedding is consistent with peak metamorphism being due to burial metamorphism and this is also suggested by the Kubler Index results showing a close correlation between stratigraphic depth and metamorphic peak. Photomicrograph taken at 50x magnification using crossed polars with polariser and analyser at 45˚ to bedding and cleavage. Field of view (width) is 0.2 mm.

Sample 157369 (SB on Figure 4.6) from the eastern side of the Rocky Cape Block has been subjected to far more strain as demonstrated by the development of stronger cleavage and the measured KI values also indicate higher levels of metamorphism. Detrital micas in this sample are found both parallel to bedding and cleavage with the smaller white micas mostly parallel to cleavage. To be parallel with cleavage the detrital micas must have been rotated so it is possible that the smaller white micas may also have been rotated. Approximately 20% of the white micas are parallel to bedding and allowing for the possibility that others have been rotated it is reasonable to assume that burial metamorphism operated on this sample especially as there is a very close correlation between stratigraphic position and KI for all samples across the Rocky Cape Block.

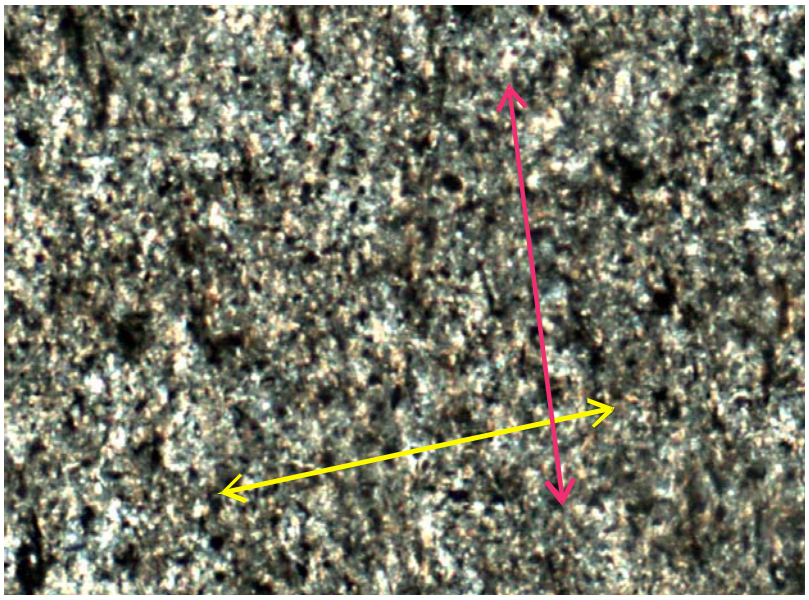

Figure 4.5. Photomicrograph of sample 157369, the location is shown as SB on Figure 4.6. This sample has been subjected to greater strain than sample 157374 as shown by the stronger cleavage of the latter. Large (40 micron long) detrital mica grains can be seen both parallel with bedding and cleavage, with those parallel to cleavage having been rotated. Rotation of detrital grains could indicate that neocrystalline white micas have also been rotated. Most of the smaller white micas are parallel to cleavage with approximately 20% parallel to bedding. Allowing for the probability that rotation has occurred to align white micas with cleavage, the alignment of the majority of white micas with bedding in sample 157374 and the

close correlation between stratigraphic depth and Kubler Index results indicates that burial metamorphism has been responsible for the metamorphic peak. Photomicrograph taken at 50x magnification using crossed polars with the polariser and analyser at 45˚ to the bedding and cleavage. Field of view (width) 0.2 mm.

On balance it appears that orientation of the white micas, generally parallel with bedding, supports the view that burial metamorphism is responsible for the metamorphic peak in the Rocky Cape Group samples.

4.4.5. Discussion of results.

Results of the Kubler Index survey show that regional metamorphism within the Rocky Cape Block has been close to greenschist facies and at this grade the organic-rich sediments found within it are post-mature for petroleum generation. The temperature contours derived from the Kubler Index survey follow the general shape of the Smithton Synclinorium with increasing temperatures on the limbs relative to the hinge. The temperature increases correlate well with stratigraphic depth below the Togari Group for example Tipunah Road (Cowrie Siltstone) measured 240°C and Sister's Beach (Irby Siltstone) measured 330°C with approximately 2 km stratigraphic difference between the two sites. This would imply that metamorphic peak was reached before folding occurred. If a geothermal gradient of 40°C/km was assumed then the maximum palaeotemperatures measured could have been generated by burial depths of ~7.5 km. Presently exposed Togari Group can account for 3.5 km burial and the Cowrie Siltstone sampled is stratigraphically ~3.2 km below the unconformity at the top of the Rocky Cape Group thus accounting for ~7 km burial depth. So allowing for 2 km of erosion it is reasonable to invoke burial for the level of metamorphism measured.

Estimates of maximum depth of burial are achieved by converting maximum temperature to an equivalent depth making assumptions regarding past heat flow. There is little direct evidence of the thermal gradient during peak thermal events that probably control the petroleum generation in Tasmania. Continental average geothermal gradients are about 25˚C/km. However, the modern Tasmanian geothermal gradient is much higher, with measured geothermal gradients in the range 30-40˚C/km (Green, 1989). O'Sullivan et al. (2000) noted that the Cretaceous thermal

peak in Bass Strait reached 45˚C/km and that this value has dropped back to 35˚C/km today. Evidence for the Cretaceous thermal event is also seen in other wells and a range of exposed lithologies around Tasmania (Bacon et al. 2000). This thermal pulse is the dominant influence on source rock maturity in the Tasmania Basin. Estimates for the geotherm during this event are all in the range 35-50˚C/km (Bacon et al. 2000, O'Sullivan et al. 2000) and as a result 40˚C/km has been used for modelling the Gondwanan petroleum system.

The geothermal gradient relevant to the Larapintine 2 petroleum system is more difficult to determine. The geothermal gradient in western Tasmania during the middle Devonian orogeny is generally regarded to be high based on the extensive granite intrusions. Burrett (1992) concluded a geothermal gradient of 75˚C/km was required to explain the metamorphic grade in western Tasmania. Patterson et al. (1981) estimated a pressure of 2.5 kbars at Renison Bell, in an area where the peak metamorphism was sub-greenschist (CAI =5) away from the affect of Devonian granites. This is compatible with a geothermal gradient above 40˚C/km. Patisson et al. (2001) demonstrated that the geotherm in NE Tasmania at peak metamorphism was 100˚C/100Mpa which, for a typical metasedimentary density, is equivalent to 38˚C/km. Based on these results a value of 40˚C/km is assumed for modelling the Larapintine 2 petroleum system.

During the Late Cambrian thermal peak the Rocky Cape Group, and other Proterozoic sedimentary rocks were exposed to a very high geothermal gradient associated with extensive rifting and volcanism in the Dundas trough. There is no direct evidence for the geotherm at this stage but it is likely to have been at least as high as geotherms associated with the Cretaceous rifting in the Bass Basin. During the middle Cambrian orogeny the autochthonous Proterozoic metasedimentary rocks at Strathgordon reached 400˚C at 350MPa (Raheim, 1977) suggesting a geothermal gradient over 40˚C/km. There are the large inherent errors in estimating the geothermal gradient associated with potential oil and gas generation in the Proterozoic sedimentary rocks. However, the relevant estimates suggest that the 40˚C/km used for modelling the younger sequences is also realistic for modelling of the Proterozoic provided the thermal maximum was during the Cambrian or Devonian.

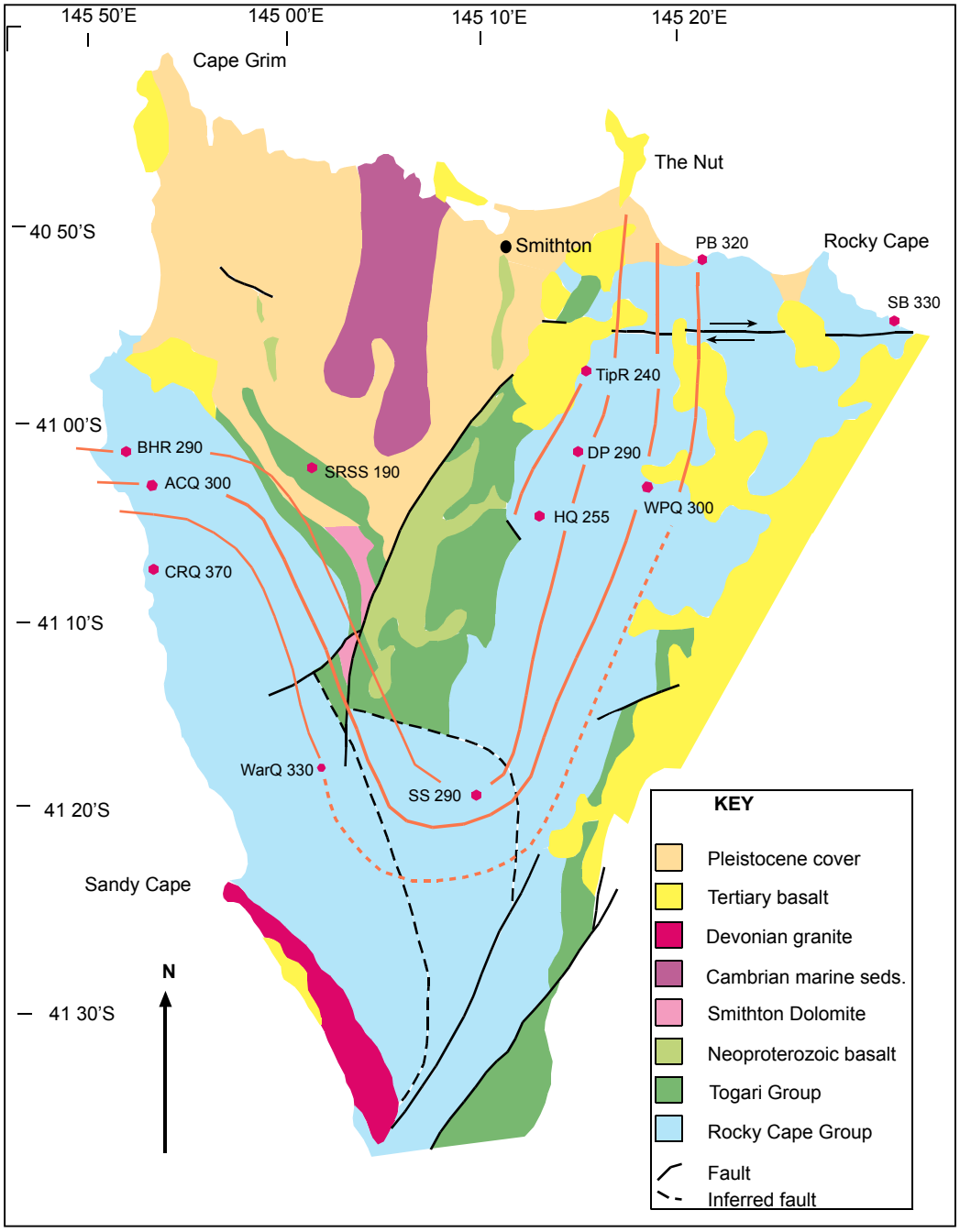

Figure 4.6. Map showing inferred palaeotemperature contours in northwestern Tasmania derived from Kubler Index measurements. Red marks indicate data points and full orange lines palaeotemperature contours inferred with some confidence, dashed orange lines are more speculative. Base map based on Geological Survey mapping.

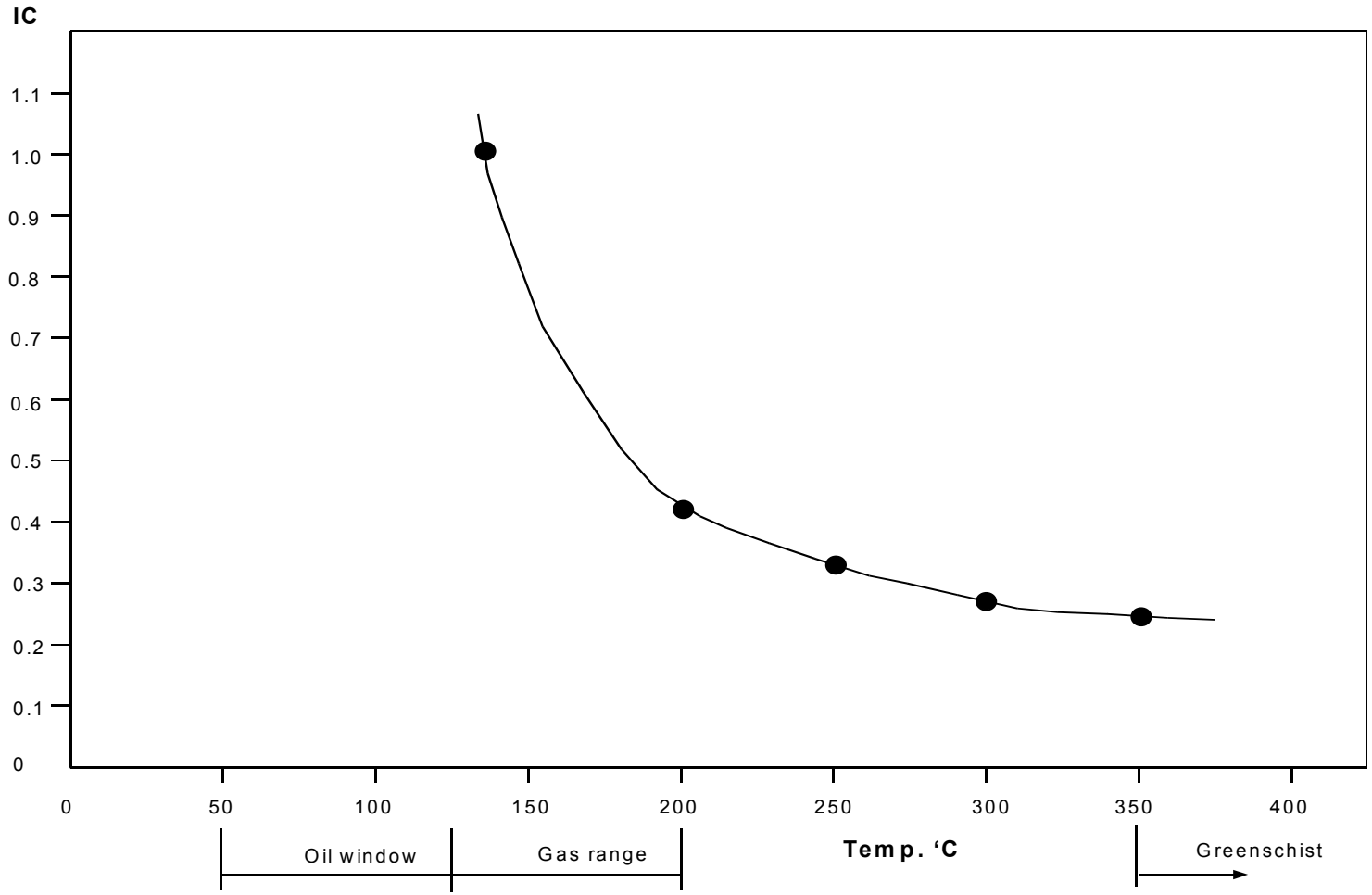

Figure 4.7. Correlation chart for Kubler Index and palaeotemperature. The relationship can only be regarded as approximate as explained in the text. Chart compiled from results published by Arkai (1991).

4.4.5.1. Discussion of the disparity between Rock-Eval pyrolysis maturity assessment and Kubler Index maturity assessment within the Rocky Cape Block.

There is a major discrepancy between the maturity assessments made by Rock-Eval pyrolysis and that of Kubler Index for the Rocky Cape Block. The results of Kubler Index indicate a maturity level close to that of the greenschist facies and this correlates well with assessments made by other workers using mineral assemblages (Everard et al., 2004; Herrman and Sumpton, 1982; Holm and Berry, 2002; Steele, 1983). There appear to be problems with the Rock-Eval pyrolysis results and so a close examination of these will be made to try and resolve the discrepancies in results between the two methods.

T_{max} and Production Index (PI) are the two parameters from Rock-Eval pyrolysis that can be used for maturity assessment and it is expected that there is a close correlation between these two measures. PI is normally ~0.1 when T_{max} is 435°C, marking the beginning of the oil window (Peters, 1986). The end of the oil window usually has a PI of ~0.4 with T_{max} at 470°C. When PI = 1.0 hydrocarbon generating capacity has been exhausted (Peters, 1986). The Rock-Eval pyrolysis results from the Rocky Cape Group show an obvious mismatch between PI and T_{max} suggesting that the results themselves are unreliable.

T_{max} is known to be unreliable when S_2 values are below 0.2 mg HC/gTOC (Peters, 1986) and on this basis four of the eight results can immediately be discounted. T_{max} values are also unreliable for oxidised samples and the Salmon River Siltstone sample with an OI of 303 must be considered unreliable. This leaves only three samples all taken in relatively close proximity near Cowrie Point where the maturity values would be expected to be virtually the same, however these samples have widely varying T_{max} values. There is also a mismatch between the PI and T_{max} values for these samples suggesting the results are erroneous.

Glikson et al., (1992) found that bitumens/pyrobitumens make a pronounced contribution to the organic matter in the Georgina and McArthur Basins and these have been shown to effect pyrolysis results by suppressing T_{max}. Where high concentrations of pyrobitumens occur with little or no alginite the bitumens provide the S_2 peak with an anomalously low T_{max} as a result. The error can be detected when

obtaining an exceptionally high PI and very low S_1/S_2 ratio. Sample CP3 gives an example of this with PI of 0.27 and S_1/S_2 ratio of 0.36, the T_{max} 402°C being a mismatch with PI.

Samples from the Georgina and McArthur Basins were also characterised by low HI and high OI and this is also characteristic of the samples from Cowrie Point. Thus it would seem that the Rock-Eval pyrolysis results from the Rocky Cape Block are not giving an accurate assessment of the maturity and by implication are also not giving an accurate assessment of source rock potential.

On the other hand Kubler Index results indicating maturity levels close to greenschist facies fit well with the observed schistose textures noted within Rocky Cape Block units in such places as Sisters Beach and other sites along the western margins of the Arthur Lineament. This suggests that the results of the Kubler Index survey are more reasonable in respect to maturity than those derived from Rock-Eval pyrolysis. From the results it can be concluded that the Rocky Cape Block is over mature everywhere for hydrocarbon generation.

4.6. Results of maturity analysis of the Ordovician Gordon Group.

An understanding of the maturity level of potential source rocks is critical to both an assessment of their potential for petroleum generation and also to predictions of whether oil or gas is likely to be generated. In the case of the Gordon Group, outcrops on the margins of the Tasmania Basin were sampled, as no samples are available from beneath the Parmeener Supergroup within the Tasmania Basin. Rock-Eval pyrolysis was used to determine maturity as well as source rock potential. A selected sample was also assessed using biomarker maturity as a crosscheck on the other methods of maturity assessment. Bitumen reflectance was used for maturity assessment of a sample of the Gordon Group from the west coast during investigations into the origins of bitumen found in the Comstock mine. Thin sections of Gordon Group samples were observed under fluorescent mode but no fluorescence was observed indicating the maturity of all samples is higher than the oil window. All of the physical and geochemical methods of maturity assessment used during this study were compared with previous regional CAI maturity results obtained by Burrett (1992) and also with some geochemical maturity assessments made during previous studies.

Rock-Eval pyrolysis methods are fully explained in Appendix A but for the purposes of maturity assessment there are two parameters of interest, T_{max} and Production Index (PI), and both are relatively crude measures of organic maturity. T_{max} is the temperature at which the maximum volumes of hydrocarbons are generated during pyrolysis. The Production Index (PI) is a measure of how far generation has progressed with a value of ~0.1 marking the beginning of the oil window and ~0.4 the end of the oil window. PI is calculated by $[S_1/(S_1 + S_2)]$. The results of Rock-Eval pyrolysis relevant to maturity assessment for Gordon Group samples are shown in Table 4.5.

Table 4.5. Rock-Eval pyrolysis results for the Gordon Group.

	Locality	**T_{max}**	**S_1**	**S_2**	**S_3**	**$S_1 + S_2$**	**PI**	**S_2/S_3**	**PC**	**HI**	**OI**	**TOC**
UL25	Florentine	469	0.02	0.26	0.40	0.28	0.07	0.65	0.02	33	51	0.78
CB13	" "	446	0.01	0.10	0.17	0.11	0.10	0.58	0.00	22	37	0.46
CB14	" "	467	0.01	0.04	0.19	0.05	0.25	0.21	0.00	3	16	1.16
SM1	" "	461	0.02	0.09	0.23	0.11	0.20	0.11	0.00	22	57	0.40
11RO1	" "	518	0.01	0.15	0.26	0.06	0.06	0.58	0.01	10	18	1.37
WQR1	" "	544	0.03	0.26	0.38	0.29	0.11	0.68	0.02	14	20	1.83
CB16	" "	545	0.03	0.43	0.51	0.46	0.07	0.84	0.03	74	87	0.58
CB26	" "	508	0.05	0.24	0.25	0.29	0.18	1.00	0.02	34	34	0.70
CB30	" "	488	0.03	0.19	0.33	0.22	0.14	0.57	0.01	44	76	0.43
CB32	" "	520	0.06	0.49	0.75	0.55	0.11	0.65	0.04	76	117	0.64
17/2	" "	522	0.01	0.31	0.28	0.32	0.03	1.10	0.02	54	49	0.57
17/16	" "	439	0.02	0.41	0.53	0.43	0.05	0.77	0.03	51	66	0.80
MC1	Lune Riv.	467	0.07	0.23	0.14	0.30	0.23	1.64	0.02	28	17	0.80
175	Florentine	465	0.12	0.51	0.43	0.63	0.19	1.18	0.05	106	89	0.48
LR2	Lune Riv.	496	0.14	0.24	0.16	0.38	0.37	1.50	0.03	34	22	0.70

Analyses by AMDEL.

In general it can be said that Rock-Eval pyrolysis has established the maturity level for the Gordon Group samples in southern Tasmania to be in the gas range and this correlates well with other methods such as CAI and biomarker maturity indexes. The wide range of results obtained does call into question the accuracy of the maturity determinations made by Rock-Eval pyrolysis and so a close examination of the results will be made to see if reasons can be found for the spread of results.

4.6.1. Discussion of Rock-Eval pyrolysis maturity results for the Gordon Group.

The maturity results for the Gordon Group as indicated by T_{max} cover an extremely wide range, which does not seem to be geologically reasonable considering that the samples were collected from a similar stratigraphic level with the expectation of closely matched maturity levels. In fact some samples were collected from a single stratigraphic level over a five-kilometre length of the Florentine Valley and had T_{max} values varying by over 85°C. Another problem evident with the maturity assessment as measured by Rock-Eval pyrolysis is a mismatch in many cases between the T_{max} and PI values, in fact only five samples have a reasonable match for these two parameters.

T_{max} varies from 439°C to 545°C, a far greater range than could reasonably be expected. Expectations of maturity for the Gordon Group from earlier CAI determinations would indicate a value greater than a T_{max} of 439°C but much less than T_{max} of 545°C. It is known that where $S_2 \leq 0.2$ mg/g that T_{max} values are unreliable (Peters, 1986). On this basis, five samples can be discounted as their S_2 values are below 0.2 mg/g and these in the main had low T_{max} so the very low maturity values are likely to be unreliable. Very high T_{max} values have been noted in other studies for oxidised samples and the same applies to some of the Gordon Group samples where high OI values coincide with high T_{max} values (Peters, 1986; Snowdon, 1995). Snowdon (1995) also found that erroneously high T_{max} values can result from samples being dominated by reworked organic material and this may also be a factor in the Gordon Group samples as organic matter separated for palynological examination proved to be amorphous matter and likely to have been reworked.

A number of samples have marginal S_2 values and these too may have given unreliable T_{max} values. Small S_2 and S_3 values can result in unreliable HI or OI values, particularly when TOC is also low, because calculating S_2/TOC and S_3/TOC involves dividing one small number by another. Determination of maturity using Rock-Eval pyrolysis on material of low generative potential is fraught with problems and results must be treated cautiously.

Further there should be a correlation between PI and T_{max} as both are indicators of maturity, however overall there is no correlation between these two parameters with

r = -0.2. Considered individually there are five samples with a reasonable correlation between PI and T_{max} but three of these must be discounted due to low S_2 values. One sample with a normal correlation between PI and T_{max} is a core sample (LR2 from DDH DLR5-4) suggesting that core samples may give more reliable results than using outcrop samples. Unfortunately for this study core samples were unavailable in the area of interest below the Tasmania Basin. A second sample (MC1) with a normal correlation between PI and T_{max} was taken from a recent deep road cut and this adds weight to the argument for core sampling being more effective than outcrop sampling for maturity assessment.

As many samples have been shown to give unreliable maturity assessments, only rough estimates of maturity can be made from the Rock-Eval pyrolysis results. The high T_{max} values, 500°C+, are probably due to oxidised samples and so can be discounted. T_{max} values less than 460°C are clearly unreliable due to low S_2 values so the possible range of maturity lies somewhere between 465°C and 496°C. A cluster of samples lies between 465°C and 470°C suggesting this may be close to the real maturity level. If a range of 465°C to 470°C was accepted then this would put the maturity of the Gordon Group within the wet gas range generation zone and this is supported by the presence of wet gas trapped within some samples. Maturity at this level is also supported by the lack of fluorescence, indicating maturity above the oil window. This range would also correlate with CAI 3 previously determined for samples from the same areas. A slightly larger range could be justified from the results with maturity from the wet gas range up into the dry gas range as late maturity in the dry gas range could account for the low generative potential as demonstrated by the Rock-Eval pyrolysis results. Maturity at this level would mean the main phase of hydrocarbon generation has been completed and that only low volumes of gas would currently be being generated, possibly too little to have enough pressure to migrate. The generative potential at various levels of maturity was determined by Demaison and Moore (1980) and is illustrated in Figure 4.8.

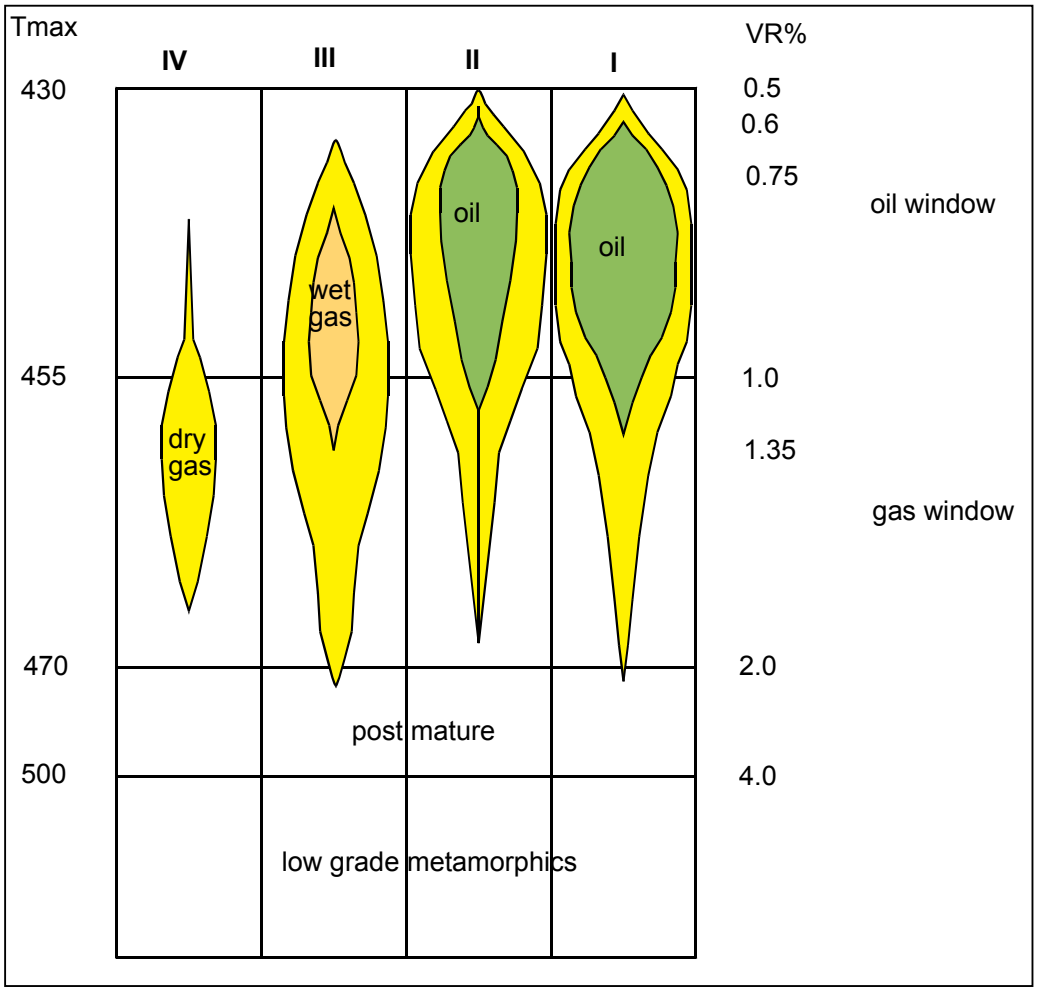

Figure 4.8. Diagrammatic representation of the hydrocarbon generative potential of source rocks containing different types of kerogen (I-IV) throughout their maturity ranges. The width of the coloured blocks is proportional to their generative potential and the colours represent the types of hydrocarbons generated at different temperatures, yellow for dry gas, green for oil and tan for wet gas. T_{max} temperature and vitrinite reflectance scales are shown to indicate maturity levels and the oil and gas windows are also shown. Diagram after Demaison and Moore (1980).

4.7. Discussion of possible reasons for high maturity values in Ordovician Gordon Group samples.

On the flanks of the Florentine Valley, the Siluro-Devonian Tiger Range Group (1150 m+) is exposed thus showing the pre-Carboniferous stratigraphy overlying the Gordon Group. Extrapolating upwards from the known geology of the Florentine Valley a re-constructed cross-section of the stratigraphy was drawn, as it would have been after Tabberabberan Orogeny and prior to Carboniferous erosion. This cross-

section, Figure 4.9, shows that approximately 4 km of overburden lay above the current ground surface before being eroded. Using the present geothermal gradient of 40°C/km, burial of 4 km equates to a maximum palaeotemperature of 160°C. This temperature is within the CAI 3 range (110-200°C) and equates well with palaeotemperatures determined from Rock-Eval pyrolysis. There is no need to invoke higher than modern geothermal gradients to achieve the inferred maximum palaeotemperatures measured for the Gordon Group in the Florentine Valley, however folding has effectively added to the burial depth. The implication is that maximum palaeotemperatures were achieved at or soon after the Tabberabberan Orogeny and before Carboniferous erosion.

It can reasonably be assumed that in other areas where Gordon Group has reached similar levels of maximum palaeotemperature, combinations of folding and thrust stacking have also operated. Hence CAI values are independent of the stratigraphic level and this explains why Burrett (1992) noticed no appreciable differences in CAI values between the tops and bottoms of Gordon Group stratigraphy.

CAI 4 was recorded for the Everlasting Hills and the probable overburden at this site comprised 2.0 km of Siluro-Devonian, Eldon Group, based on equivalent sequences in the lower Gordon River (Baillie, 1989). The implied depth of burial at this site using a geothermal gradient of 40°C/km is approximately 5 km. There is limited information available on stratigraphy and dips in the Everlasting Hills area from which to draw an accurate cross-section however the Gordon Group outcrop appears to form the western limb of a northwesterly trending syncline. Parmeener Group cover to the east rests unconformably on the Gordon Group indicating that erosion has completely removed the Eldon Group. Exposure of Denison Group conglomerates to the west is a further indication that the Everlasting Hills area was eroded more deeply than the Florentine Valley during the Carboniferous. Assuming a similar folded situation occurs in both the Everlasting Hills and Florentine Valley (see Figure 4.9) erosion 1 km deeper would completely remove the Eldon Group and expose a sequence effectively buried to a depth of 5 km. Burial at this depth would generate maximum palaeotemperatures of ~200°C, within CAI 4 range. This mechanism can probably be extended to other locations where CAI 4 has been recorded such as Isle Du Golfe and Judds Cavern.

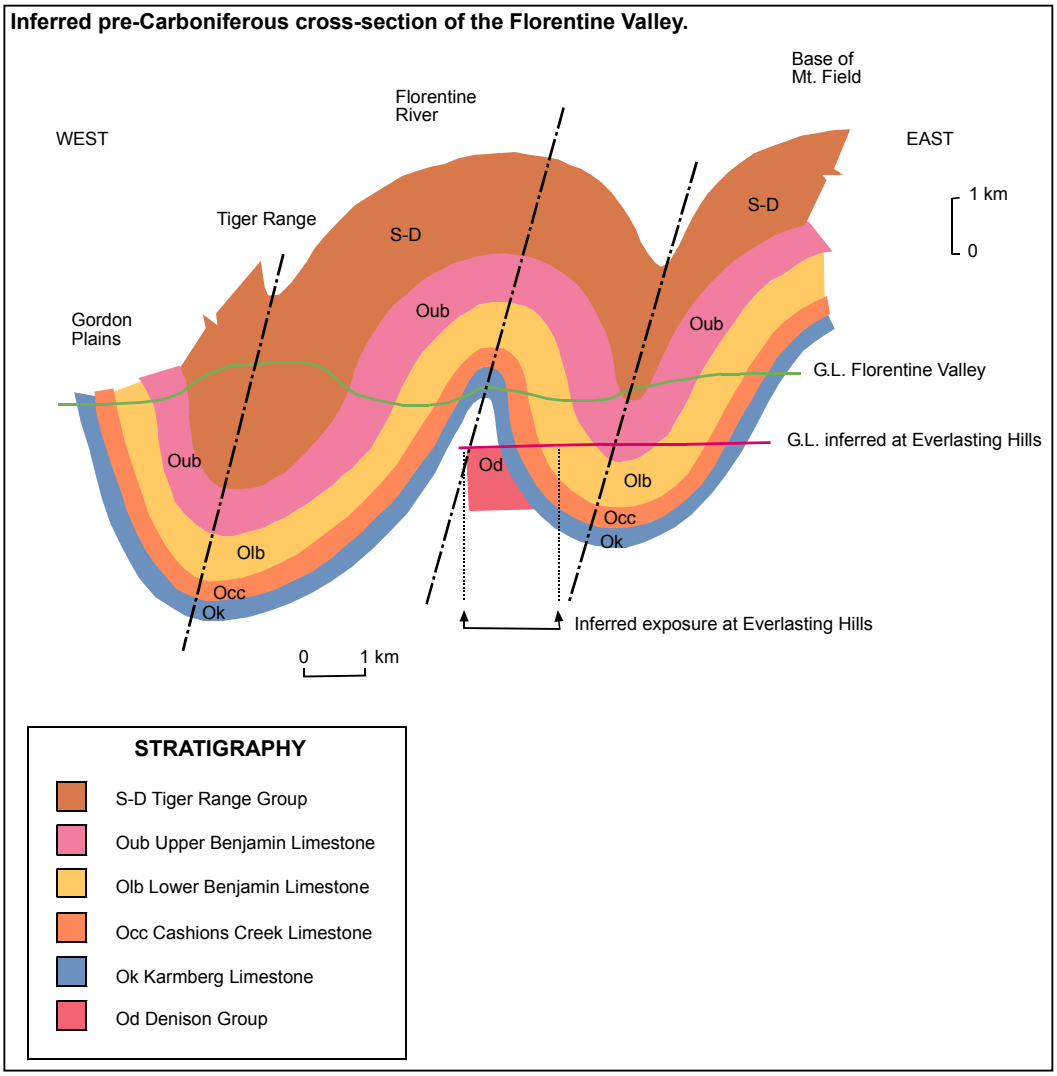

Figure 4.9. Inferred west to east cross-section of the Florentine Valley as it would have appeared before Carboniferous erosion. Cross section has been drawn by reference to mapping by Corbett (1964) and Banks and Baillie (1989), augmented by dip measurements made during personal fieldwork. Current ground line drawn from topographic detail on Tiger 1:25 000 map, TASMAP (1988). Inferred depth of burial for current ground level is ~4 km which equates to a palaeotemperature of 160°C, using a geothermal gradient of 40°C/km. The cross section shows that inferred burial depth was achieved through folding of pre-Carboniferous sequences and the inference can be drawn that maximum palaeotemperatures were achieved after the Devonian Tabberabberan Orogeny and prior to Carboniferous erosion.

(b) An exposure of Gordon Group limestone at the Everlasting Hills is inferred to have a similar folded structure to the Florentine Valley shown by an arrowed line on the cross section. The Everlasting Hills exposure has been eroded to ~5 km depth as shown by the inferred ground line so that maximum palaeotemperatures were ~200°C.

One low value of CAI 1.5 (50-90°C) was measured at Vanishing Falls and the position of the sample on the anticline may explain this. The sample was probably

taken from the top of an anticlinal fold where burial was in the range 1.5-2.0 km. Erosion has removed the overlying Eldon Group before deposition of Parmeener Supergroup. The sample was collected just below a dolerite sill (Burrett, 1992), which in this locality intruded at the base of the Parmeener Supergroup.

High maximum palaeotemperatures (300°C+) for the Gordon Group have been recorded in an arcuate zone from the western and northern margins of the Tyennan Nucleus and across to Beaconsfield. A map of the distribution of Devonian-Carboniferous maximum palaeotemperatures was plotted using data collated from the following sources and shown as Figure 4.8.

1. Burrett's (1992) CAI survey.
2. Patison et al., (2001) Kubler Index survey of northeastern Tasmania.
3. Kubler Index survey of northwestern Tasmania.
4. Palaeotemperatures inferred from metamorphic petrology at a number of sites.
5. Fluid inclusion studies.
6. Rock-Eval pyrolysis T_{max} determinations made during this study.

The details for numbered points shown on Figure 4.10 are given in Table 4.6. Included on the map are the following features, which may have had an influence on pre-Carboniferous palaeotemperatures.

1. Contours of the inferred crustal thickness of Tasmania.
2. Boundaries of inferred Devonian granites at 1 km depth.

It is most likely that a combination of factors has been responsible for the 300°C+ palaeotemperatures. The following discussion will consider each of the above factors in turn to see if they have influenced maximum palaeotemperatures, particularly in respect to the Gordon Group.

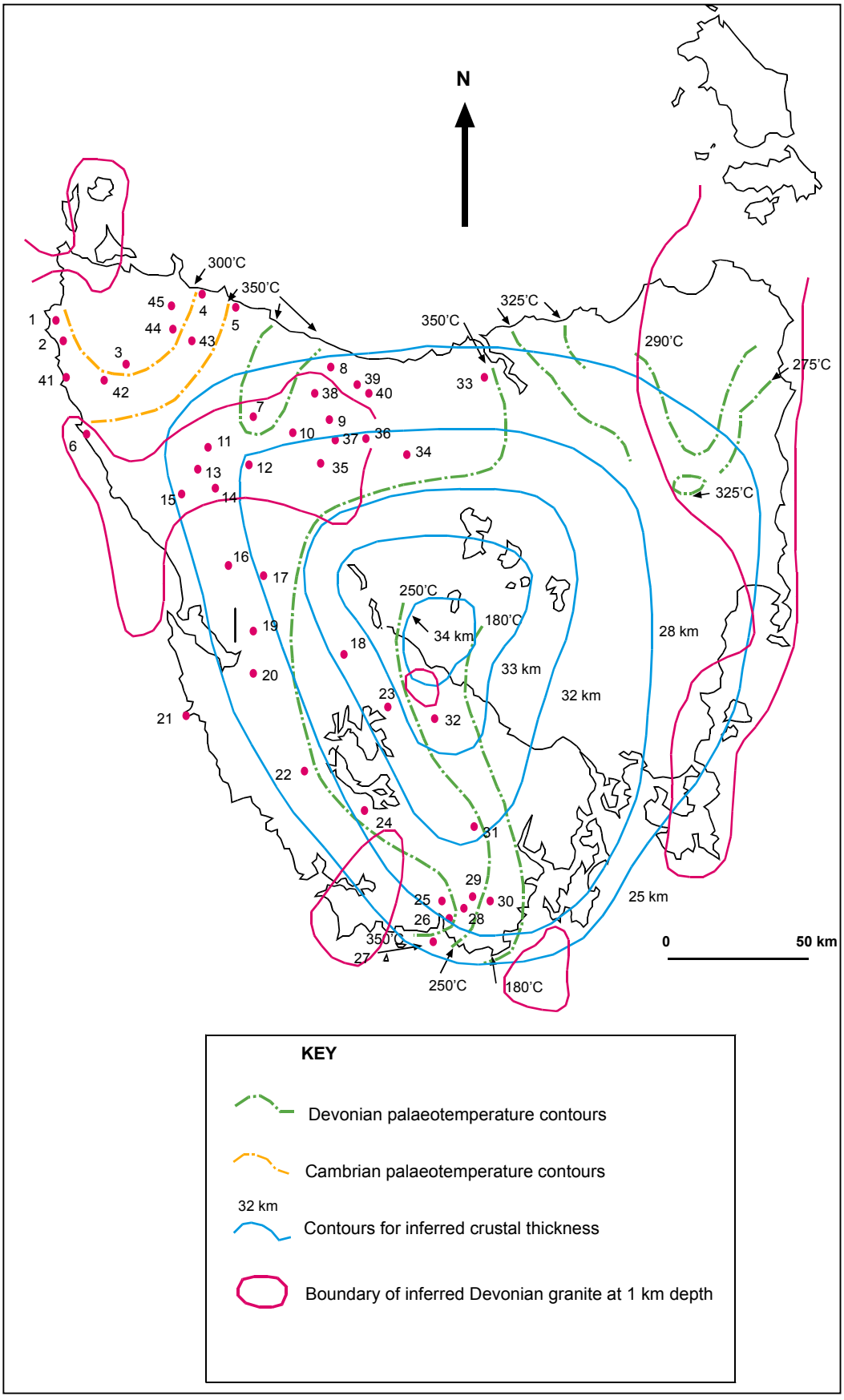
N
300'C
350'C
325'C
350'C
290'C
275'C
325'C
250'C
180'C
34 km
28 km
33 km
32 km
25 km
350'C
250'C
180'C
0
50 km
KEY
Devonian palaeotemperature contours
Cambrian palaeotemperature contours
32 km
Contours for inferred crustal thickness
Boundary of inferred Devonian granite at 1 km depth

Figure 4.10. Devonian/Carboniferous palaeotemperature contours for Tasmania plotted along with features that may have bearing on the palaeotemperature distribution. Palaeotemperature contours in northeastern Tasmania after Patison et al. (2001). Palaeotemperature data points are numbered and Table 4.6 indicates location name, inferred maximum palaeotemperature, method used to derive data and references. Inferred Devonian granite contours are from Leaman and Richardson (1992). Inferred crustal thickness contours after Leaman (1988b) with contributions from Vitesnik (1984) and Richardson (1980).

Thin crust can often have higher geothermal gradients than thick crust so plotting crustal thickness could be relevant to determining causes for palaeotemperature variations. The 350°C contour in central Tasmania tends to follow the northern and western edges of the 32 km crustal depth contour, however it cuts across crustal depth contours in the Beaconsfield area and also near Precipitous Bluff, as do the 250°C and 180°C contours. Maximum palaeotemperature contours in northwestern and northeastern zones do not appear to relate to overall thickness so it appears unlikely that crustal thickness has been the major controlling factor for maximum palaeotemperatures.

Burrett (1992) suggested that Devonian granitoid intrusions were the source of major heat input to Gordon Group, however the palaeotemperature contours shown on Figure 4.10 do not have any relationship to the underlying granites. Granites underlie both high temperature and lower temperature regions and high palaeotemperatures occur up to 50 km away from known granite margins.

Table 4.6. Details for numbered points shown on Figure 4.10.

Number	Location	Inf. °C	Method	Reference
1	Bluff Hill	290	KI	Own data
2	Alert Creek	300	KI	Own data
3	South Sumac Rd.	290	KI	Own data
4	Pegg's Beach	315	KI	Own data
5	Sister's beach	350	KI	Own data
6	Duck Creek	350	CAI	Burrett (1992)
7	Que River	250	Min. KI	(Offler and Whitford, 1992)
8	Eugenana	350	CAI	Burrett (1992)
9	Loongana	350	CAI	Burrett (1992)
10	Vale of Belvoir	350	CAI	Burrett (1992)
11	Huskisson Syncl.	350	CAI	Burrett (1992)
12	Sophia River	350	CAI	Burrett (1992)
13	Wilson River	350	CAI	Burrett (1992)
14	Rosebery	350	Minerals	(Green, 1983)
15	Zeehan	350	CAI	Burrett (1992)
16	Queenstown	350	CAI	Burrett (1992)
17	Bubs Hill	350	CAI	Burrett (1992)
18	Everlasting Hills	250	CAI	Burrett (1992)
19	Andrew River	350	CAI	Burrett (1992)
20	Low. Gordon River	300	CAI	Burrett (1992)
21	Point Hibbs	60-300	CAI	Burrett (1992)
22	Olga river	350	CAI	Burrett (1992)
23	McPartlan Pass	200-350	Minerals	(Williams, 1976)
24	Wilmot Range	320	Minerals	(Boulter, 1974)
25	Salisbury River	350	CAI	Burrett (1992)
26	Precipitous Bluff	350	CAI	Burrett (1992)
27	Isle Du Golfe	250	CAI	Burrett (1992)
28	Lake Sydney	500	CAI	Burrett (1992)
29	Judds Cavern	250	CAI	Burrett (1992)
30	Picton River	180	CAI	Burrett (1992)
31	Weld River	250+	Fluid Inc	(Taheri, 1990)
32	Florentine Valley	180	T_{max}	Own data
33	Flowery Gully	350	CAI	Burrett (1992)
34	Mole Creek	350	CAI	Burrett (1992)
35	Moina	350	CAI	Burrett (1992)
36	Liena	350	CAI	Burrett (1992)
37	Claude Creek	350	CAI	Burrett (1992)
38	Gunns Plains	350	CAI	Burrett (1992)
39	Melrose	350	CAI	Burrett (1992)
40	Railton	350	CAI	Burrett (1992)
41	Couta Rocks	370	KI	Own data
42	Waratah Creek	340	KI	Own data
43	Wedge Plains	300	KI	Own data
44	Dollie Pit	290	KI	Own data
45	Tipunah Road	230	KI	Own data

The 350°C contour from Beaconsfield through the Mole Creek area and down the west coast follows a trend with similar to that of the Mt Read Volcanic Belt and may reflect that Devonian structures were partly inherited from Cambrian structures. A Devonian granite ridge follows a trend from the Pieman Granite through to the Housetop Granite along a line sub-parallel to the northern parts of the Mt Read Volcanic Belt. This granite ridge correlates with the highest metamorphic grades in northern Tasmania indicating it has some control on metamorphic grades.

Stratigraphic overburden thickness, in northern Tasmania along the high palaeotemperature zone, is not thick enough to achieve burial temperatures of the order shown by CAI measurements. Maximum pre-Carboniferous burial depth for the Gordon Group in northern Tasmania, based on known stratigraphy, was ~1.5 km.

Woodward et al., (1993) interpreted the pre-Carboniferous structure in northern Tasmania, from outcrop exposures, to consist of a series of thrust stacks similar to that observed in the foreland of the Rocky Mountains in U.S.A. At least 10 km of shortening is documented in the Gog Range section (Woodward et al., 1993). Thrust slices of Precambrian basement, Cambrian oceanic suite and Ordovician through to Devonian cover occur above a northeast-dipping detachment (Woodward et al., 1993). The northeast dipping detachment has also been imaged by seismic reflection (Barton, 1999). Woodward et al., (1993) have drawn a cross-section through the Mole Creek and eastern Gog Range, which shows a shortening of ~40% across this section. To accommodate shortening of this order thrust stacking has occurred similar to that shown in Figure 4.11.

Figure 4.11 is an extrapolation upwards from the cross-section of Woodward et al., (1993) to determine likely burial depths in the Mole Creek region. From Figure 4.11 it can be seen that burial depths of 7.5 km+ are possible using the mechanism of thrust stacking hence 300°C+ palaeotemperatures could be achieved without invoking higher than modern geothermal gradients. As with lower maximum palaeotemperatures, the 300°C+ values were reached during or soon after the Tabberabberan Orogeny and prior to the Carboniferous erosion. Thrust stacking has also been demonstrated to achieve 300°C+ at Point Hibbs (Burrett, 1992; Carey and Berry, 1988).

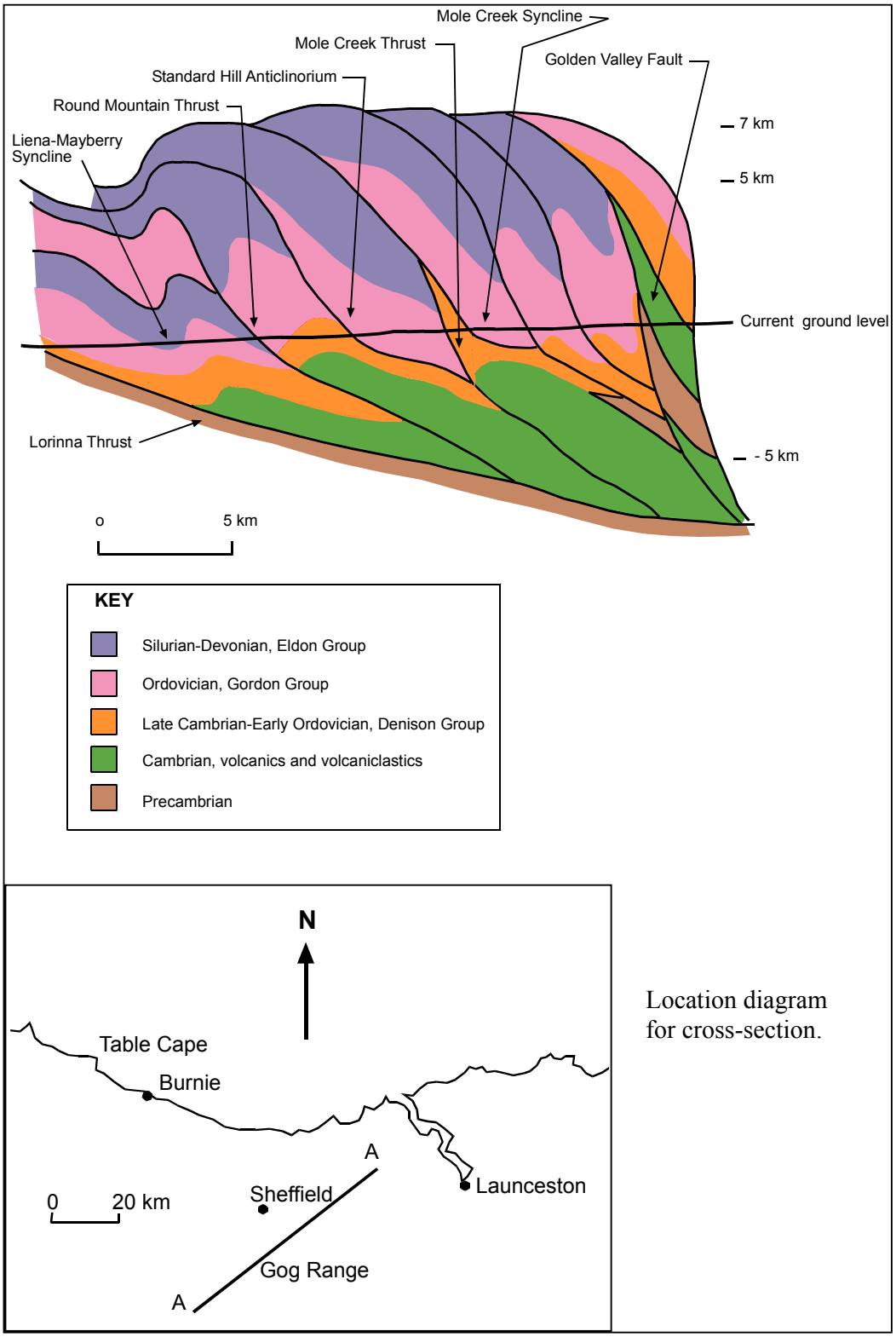

Location diagram for cross-section.

Figure 4.11. Inferred cross-section of the Mole Creek valley and eastern Gog Range drawn to represent situation after the Tabberabberan Orogeny and before Carboniferous erosion. This cross-section has been extrapolated upwards from a cross-section prepared by Woodward et al. (1993), based on the importance of

thrusting in this area. Thrust stacking of the type shown could effectively bury the current ground level below 7.5 km and thus generate maximum palaeotemperatures of 300°C+. This mechanism of tectonic metamorphism implies that maximum palaeotemperatures were achieved soon after the Tabberabberan Orogeny and before Carboniferous erosion.

Thrust stacking has also occurred in western Tasmania, with the Precambrian Oonah Formation thrust over Cambrian to Devonian aged rocks, including Gordon Group (Brown and Findlay, 1992). In the Zeehan region 300°C+ values were recorded from Gordon Group and the high palaeotemperatures could be due to deep burial from thrusting. The Oonah Formation thrust sheet is now only 300 m thick but it could have originally been much thicker before erosion. The 10th Legion Thrust in the Zeehan region has been intruded by the Heemskirk Granite, that from geophysical interpretation links with the Housetop Granite. The age of thrusting can be constrained between 330-380 Ma, the early phase of the Tabberabberan Orogeny, from ages derived from these granites (Brown and Findlay, 1992). Thrust stacking in the Mole Creek area involves sequences of similar age and so can also be attributed to the Tabberabberan Orogeny. If thrust stacking was assumed to be the major reason for high palaeotemperatures within the Gordon Group this would imply that maximum palaeotemperatures were reached in the mid-Devonian. Figure 4.12 shows the locations of features and places mentioned.

Thrust stacking has also been recognised on the Sorell Peninsula where thrust sheets of Precambrian age overlie Cambrian beds (McClenaghan and Findlay, 1989). Intra-Devonian thrusting occurs throughout the zone identified by the 350°C contours on Figure 4.10 and is a regionally significant mechanism, it is most likely responsible for the high palaeotemperatures.

Thrust stacking could also be a reasonable mechanism for achieving the CAI 5 values in the Queenstown, Andrew River and Bubs Hill areas because the apparently excessive thickness of Siluro-Devonian sequences in the upper King River area can best be explained as the results of thrust stacking. Berry (1993) analysed the structure of the region near Mt. Lyell, including the King River Valley, and the structural sections he drew have been used as the basis for determining maximum burial depths for the Gordon Group. The sections drawn by Berry (1993) have been extrapolated

upwards using average stratigraphic thicknesses from correlates in nearby regions. A structural interpretation of part of the Lyell 1: 50 000 geological map (Calver et al., 1987), drafted by Berry (1993), is shown as Figure 4.13. The positions of two sections are shown on this map as I and II. Figure 4.14 shows a NNE trending cross section through Victoria Pass where the maximum burial of currently exposed Gordon Group would have been ~7 km and the deepest burial ~10 km. A second section NNE along the main Owen Conglomerate is shown in Figure 4.15 where maximum burial of Gordon Group is ~7.5 km. These burial depths would give maximum palaeotemperatures of 300°C+ and this has been demonstrated by CAI values in this region. The same situation may apply in the lower Gordon River and the Olga Syncline, regions at the edge of the Tyennan Nucleus, and close to a possible structurally weak zone marked by the Mt Read Volcanics.

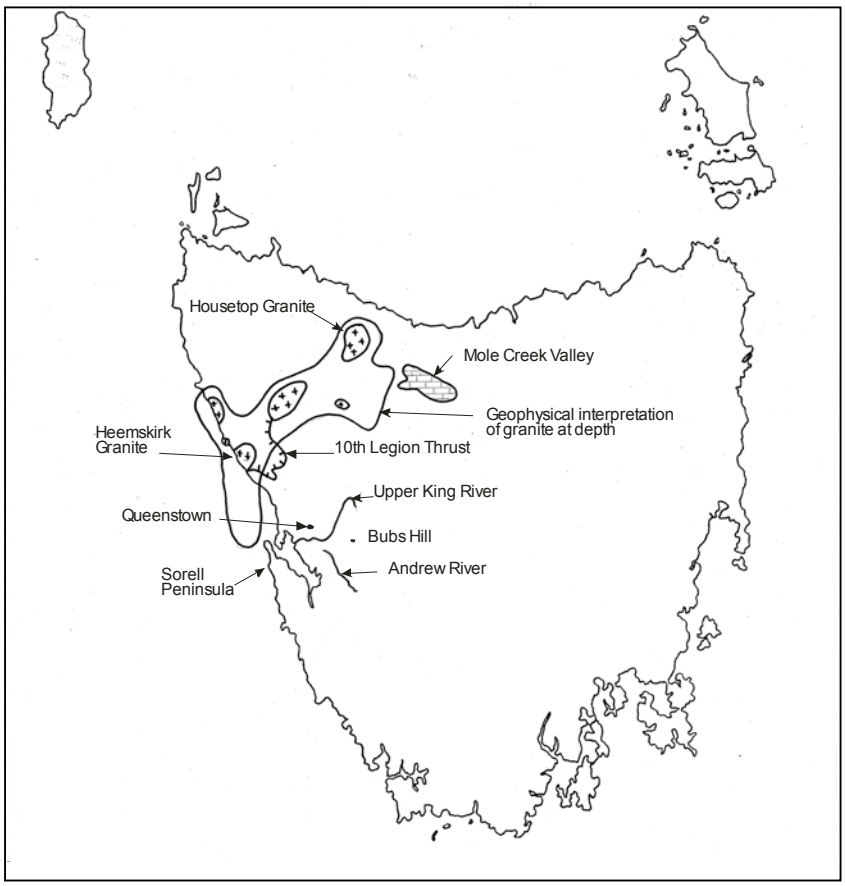

Figure 4.12. Map showing locations of features and places related to thrusts in western Tasmania. Geophysical interpretation from Leaman and Richardson (1992), position of 10th Legion thrust from Brown and Findlay (1992).

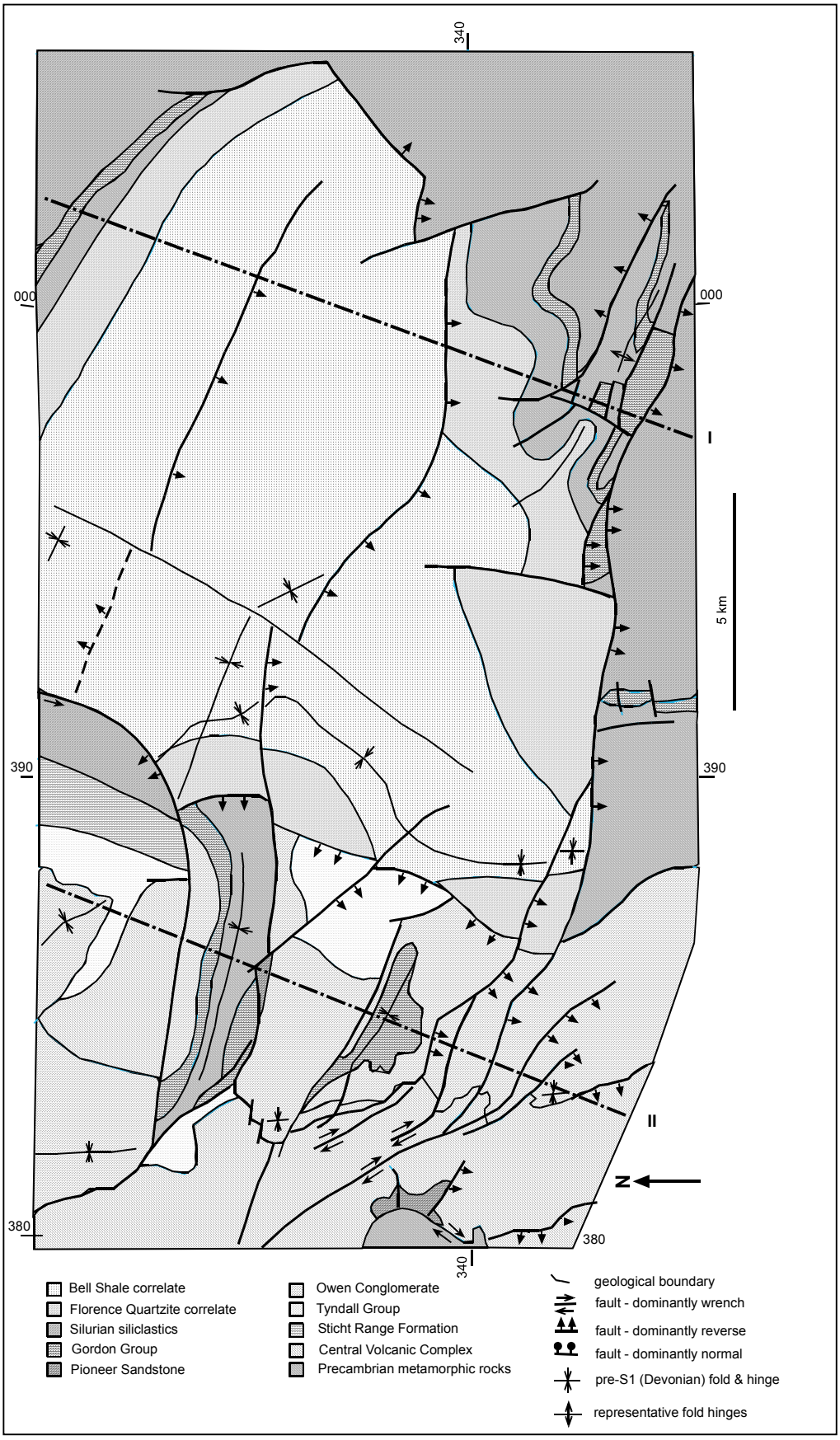
340
000
000
I
5 km
390
390
II
N
380
380
340
Bell Shale correlate
Florence Quartzite correlate
Silurian siliclastics
Gordon Group
Pioneer Sandstone
Owen Conglomerate
Tyndall Group
Sticht Range Formation
Central Volcanic Complex
Precambrian metamorphic rocks
geological boundary
fault - dominantly wrench
fault - dominantly reverse
fault - dominantly normal
pre-S1 (Devonian) fold & hinge
representative fold hinges

Figure 4.13. Structural interpretation of part of the Lyell 1:50 000 map (Calver et al., 1987). Structures within Bell Shale correlate are from domain analysis and from the sections shown assuming maximum thickness of the Bell Shale correlate of 3 km. (Berry, 1993). Lines I and II are the positions of sections shown in Figures 4.11 and 4.12.

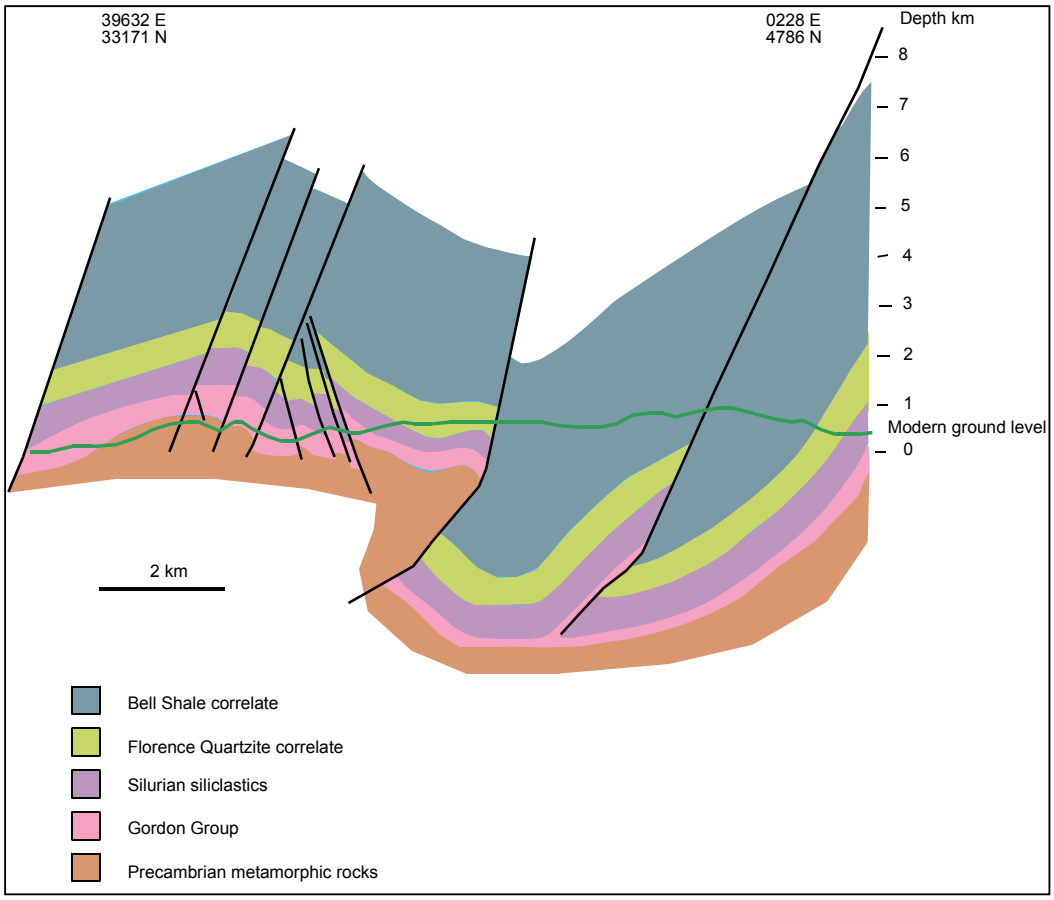

Figure 4.14. NNE trending cross section through Victoria Pass. Position of section is shown on Figure 4.10. The base cross section by Berry (1993) has been extrapolated upwards to show the probable maximum burial due to tectonic thickening, after Devonian folding and thrusting but before erosion commenced. Maximum burial of currently exposed Gordon Group would have been ~7 km and the deepest burial ~10 km.

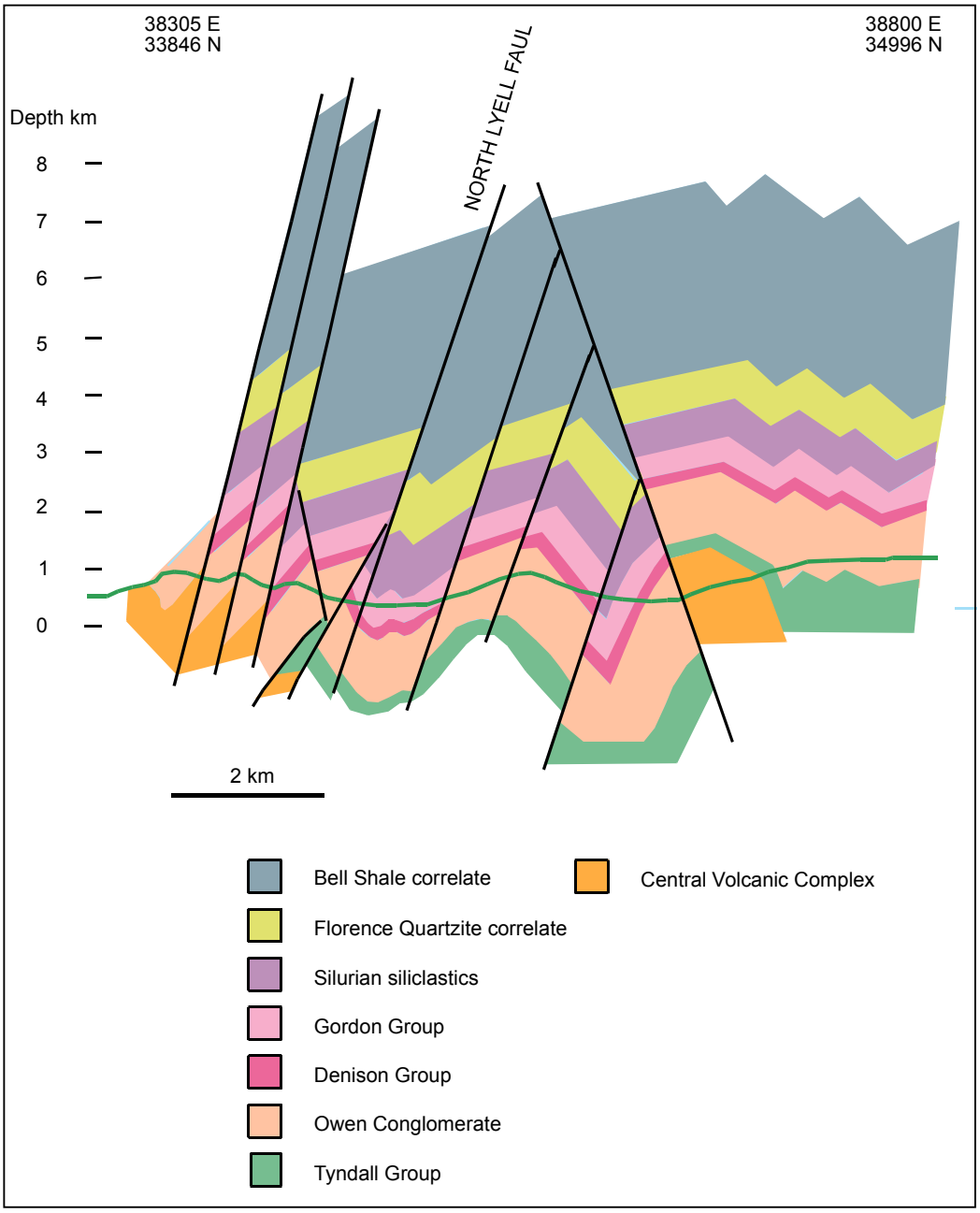

Figure 4.15. NNE trending section along the main range of Owen Conglomerate. Position of section shown on Figure 4.10. Base section by Berry (1993) has been extrapolated upwards to show the probable maximum burial of the Gordon Group due to tectonic thickening. Maximum burial along this section is ~7.5 km. Section has been drawn to represent maximum tectonic thickening after Devonian folding and thrusting but before erosion had commenced.

In southwestern Tasmania variations in CAI measurements have been recorded that are similar to those expected when tectonic thickening occurs. A transect from Picton

River to Isle Du Golfe shows variations from CAI 1.5 – 5 over a 50 km distance and 900 m vertical topographic difference. All samples were from Ordovician Gordon Group. Background values of CAI 3 can be gauged from measurements at Picton River, Point Cecil, Surprise Bay and Lune River, the first two points along the transect and the last two at a maximum of 20 km to the east. The most rapid changes along this transect occur between the Vanishing Falls and Precipitous Bluff where variations from CAI 1.5 to CAI 5 occur over a horizontal distance of 3 km and 230 m vertically. An east-west fault has been inferred to occur where the Salisbury River bends westwards (Dixon and Sharples, 1986) and this may separate the sites where CAI 1.5 and CAI 5 samples were collected. A currently active major fault occurs along the western side of Precipitous Bluff and this could be due to reactivation of basement structures. Figure 4.16 shows places mentioned and also the positions of a cross section of southern Tasmania.

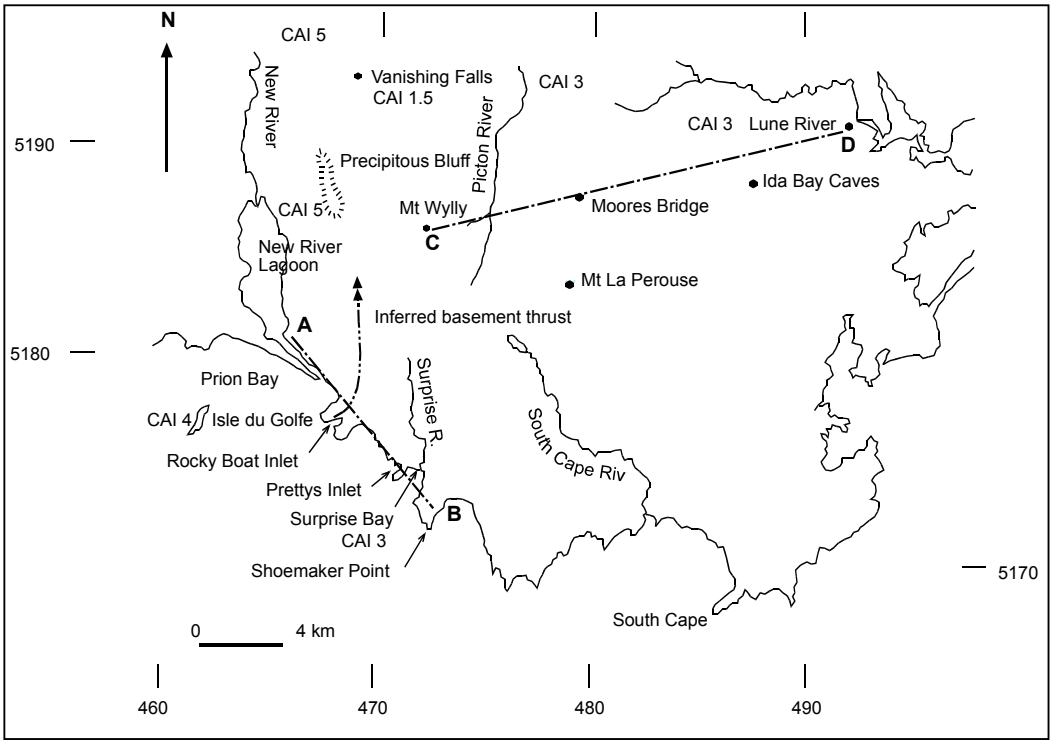

Figure 4.16. Map showing places mentioned in the south coast region of Tasmania and known CAI values. The positions for section shown in Figure 4.14 are shown as dashed lines labelled A-B and C-D. The inferred position of a major basement thrust is shown trending north from Rocky Boat Inlet. This inferred thrust separates area where CAI 3 values predominate from higher CAI values found elsewhere. The base map was drawn from the TASMAP, South Coast Walks map (1997). CAI values from Burrett (1992).

An inferred cross section of the probable post-Devonian structure in this region is shown in Figure 4.17. Geological mapping by Bischoff (1983) was used as the basis for the New River Lagoon to Shoemaker Point section. Geological mapping by Sharples (1979) and results of drilling by Summons (1981b) in the Lune River area was used for the Mt Wylly to Lune River sections. Inferences on burial depth were made based on results of CAI values by (Burrett, 1992). A folded section is shown on the east where CAI 3 values imply a similar structural situation to that in the Florentine Valley. Observations of the structural style of outcrops also show this to be the case. In the west CAI 5 values indicate that tectonic thickening occurred and geological mapping by Bischoff (1983) identified thrusts near Rocky Boat Inlet. The section has been drawn to show a thrust section overlying presently outcropping Gordon Group at Precipitous Bluff where CAI 5 values were obtained. The overlying thrust sheet, as drawn, contains Gordon Group currently exposed at Surprise Bay where CAI 3 values were measured. Gordon Group outcrops at Vanishing Falls, where CAI 1.5 was measured, probably occur near the crest of the anticline on the over riding thrust sheet.

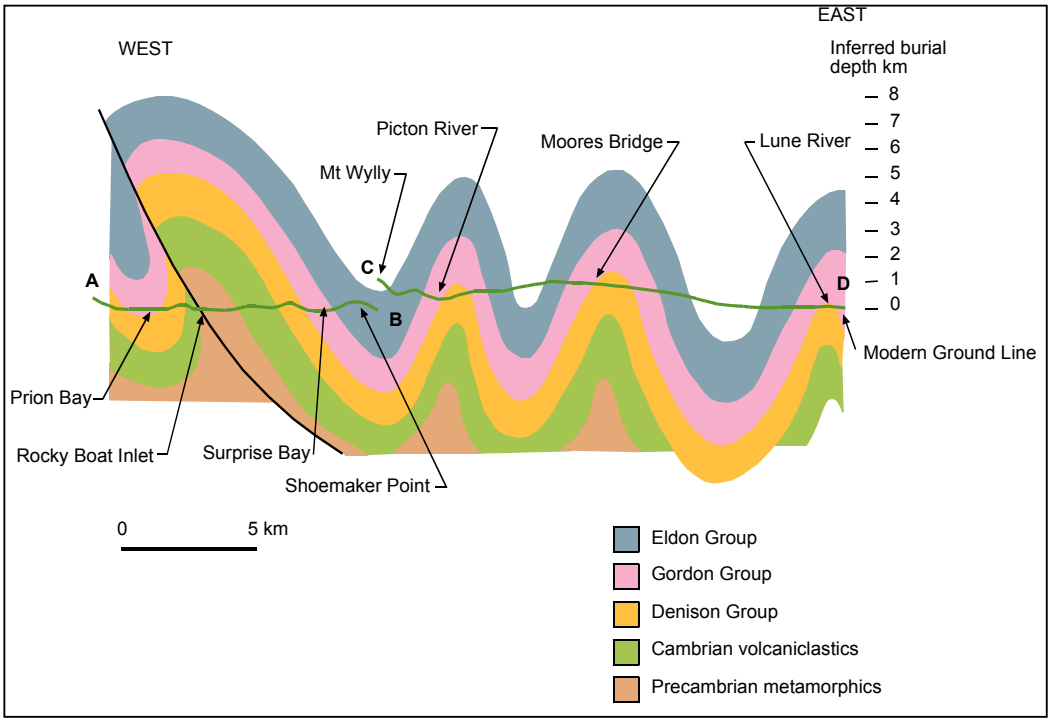

Figure 4.17. Inferred section across the south coast region of Tasmania directly after the Devonian folding and thrusting but before erosion commenced. Geology in the western section A-B was from mapping by Bischoff (1983). Geology on the eastern section C-D was based on Sharples (1979), drilling reported by Summons (1981) and

observations during this study. Burial depths were inferred from CAI values determined on Gordon Group by Burrett (1992). CAI 3 values from Lune River and folded exposures in the area led to an inference of folding similar to that of the Florentine Valley. CAI 5 values recorded in the west and CAI 1.5 values close by led to an inference of structure as shown. Identification of thrusts at Rocky Boat Inlet is further evidence for a structure of this style.

Only one location yielded CAI values above 5 and this was from a wollastonite-diopside-epidote hornfels adjacent to a Jurassic dolerite at Lake Sydney (Burrett, 1992).

4.8. Results of maturity investigations on the Upper Permian sediments within the Tasmania Basin.

Only Upper Permian sequences were considered in this study because other potential source rocks within the Permian system had already been assessed by Reid (2004) during a parallel study. Rock-Eval pyrolysis and vitrinite reflectance were used to assess maturity of potential source rocks from the Permian sequences. Interest in these sequences was initiated by the finding of bitumen associated with Upper Permian sandstone near the Badger River, south of Zeehan. Photographs of bitumen-stained sandstone outcrops at Badger River are shown in Figure 4.18. Investigations carried out on the site revealed the source of the bitumen to be organic-rich siltstone stratigraphically below the sandstone. The area was being investigated to try and find the source of bitumen found in the Proterozoic metasediments of the Comstock mine. Results of Rock-Eval pyrolysis for Permian sequences investigated are shown in Table 4.7.

Table 4.7. Permian Rock-Eval pyrolysis results.

Sample	T_{max}	S_1	S_2	S_3	$S_1 + S_2$	PI	S_2/S_3	PC	HI	OI	TOC
CCM2	539	0.17	0.69	0.00	0.86	0.20	-	0.07	4	0	14.30
MQ2	456	0.40	2.90	0.58	3.30	0.12	5.00	0.27	85	17	3.40
MQ3	457	0.35	3.33	0.33	3.68	0.10	10.09	0.30	102	10	3.25
MQC1	465	0.28	2.65	1.76	2.93	0.10	1.50	0.24	55	37	4.75
MQC2	496	0.25	1.43	1.35	1.68	0.15	1.05	0.14	23	21	6.15
590494	450	0.15	0.90	1.78	1.05	0.14	0.51	0.09	34	67	2.65
BR7	437	0.69	21.82	14.43	22.51	0.03	1.51	1.87	45	30	47.80
LC	497	0.20	2.29	5.69	2.49	0.08	0.40	0.20	6	17	32.90
BP1	431	0.40	0.05	0.08	0.09	0.50	0.62	0.00	1	2	3.24
Cat1	424	24.38	311.73	0.00	336.11	0.07	0.00	28.00	442	0	70.40
Cat2	432	8.09	256.03	6.33	273.12	0.03	41.86	22.76	354	8	74.80

Analyses by AMDEL.

Bitumen along bedding planes of Cygnet Coal Measures correlate sandstone at Badger River. Fifty cent piece coin for scale.

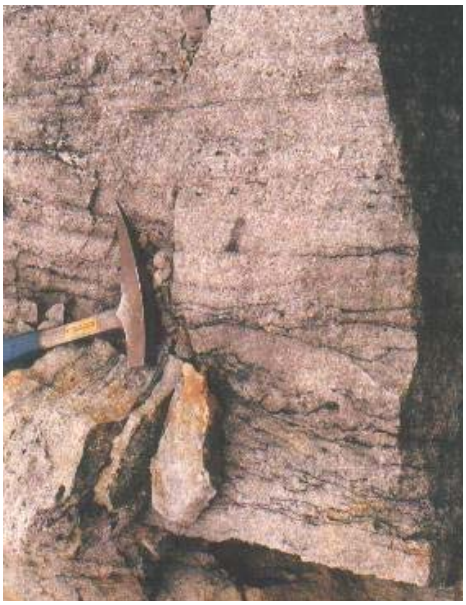

Figure 4.18. Bitumen along bedding planes and within pore spaces of sandstone of Cygnet Coal Measures correlates at Badger River, near Zeehan. Hammer head for scale.

Rock-Eval pyrolysis results from the siltstone and coal in the Badger River area show that the maturity of the siltstone is within the oil window and coals found nearby are within the gas window. These assessments were supported by vitrinite reflectance measurements, which average R_v 0.76% also indicating the oil window (Cook, 2004). Observations of thin sections under fluorescence mode showed strong yellow fluorescence also indicating maturity within the oil window as shown in Figure 4.19. The maturity assessment within the oil window is supported by observations of bitumen impregnation within sandstone immediately above the siltstone indicating that significant quantities of oil have been generated and expelled. Some of this material was still fresh when first collected.

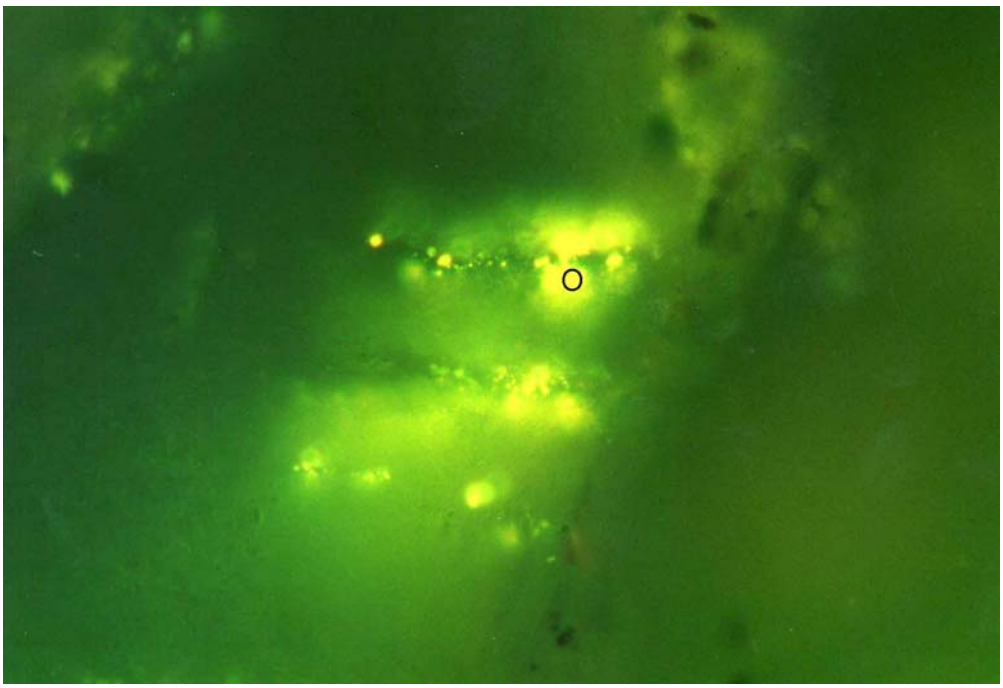

Figure 4.19. Fluorescence mode photomicrograph of thin section of Permian sandstone from Badger River area, a correlate of the Cygnet Coal Measures. Field of view 0.22 mm. Strong yellow fluorescence from oil inclusions indicates that maturity is within the oil window and that oil generation has occurred. Photograph taken by Alan Cook (Kieraville Konsultants).

Once it was realised that significant petroleum generation and migration had occurred in the western outlier of the Tasmania Basin a search was made within the main part of the basin for potential source rocks/evidence of generation at similar stratigraphic

levels. Previous studies (Bacon et al., 2000; Reid, 2004) had shown that the northern parts of the Tasmania Basin were immature for oil generation. A sample of high organic content siltstone from near Piper's River (BP1) had a T_{max} of 431°C indicating maturity just below the oil threshold. Two samples (Cat 1, Cat 2) from Catos Creek, north of St Marys, had T_{max} values of 424°C and 432°C also indicating maturity at the threshold of oil generation. Vitrinite reflectance measurements on the same samples gave values of R_v 0.46% and R_v 0.47% (Cook, 2004). Strong orange fluorescence from the vitrinite was also noted during observations in fluorescence mode indicating that some oil generation had occurred. These results correlate well with those obtained by Reid (2004) who found immature sediments north of a line near the latitude of St Marys.

A sample from South Cape Bay (CCM2) in southern Tasmania had a T_{max} of 539°C, which indicates maturity characteristic of rocks of low metamorphic grade, however this may have been due to nearby dolerite intrusions. A second sample from Leprena (LC), also in southern Tasmania, had T_{max} of 497°C at the end of the dry gas zone and these findings are consistent with Reid's (2004) findings that maturity for the Permian sediments is in the gas zone south of the Styx River.

Reid (2004) found the zone south of a line from the latitude of St Marys to the latitude of the Styx River was within the oil window of maturity. During this study, no suitable outcrop could be found in this zone to test the maturity of the Upper Permian sediments so some data was collated from company reports made during investigations into the coal resources of the Tasmania Basin. Using both vitrinite reflectance and calorific values an assessment was made for the Permian sediments and these results are shown in Figure 4.2. They clearly follow the pattern identified by (Reid, 2004) with an immature zone in the northeast and the boundary for the oil maturity zone approximately at the latitude of St Marys. The oil maturity zone identified in this study extends further south than defined by Reid (2004) to just south of Huonville. Further south from Huonville the maturity levels rise rapidly to low metamorphic grades but in some cases this could be due to the proximity of dolerite intrusions. Cretaceous igneous activity may also have had a significant influence on the maturity levels in this area.

Maturity for Permian rocks within the gas range in southern Tasmania implies deeper burial than has previously been recognised for this region. Assuming a geothermal gradient of 40°C/km for samples with vitrinite reflectance values of 1.5% implies burial of approximately 4 km. Known stratigraphy overlying the Cygnet Coal Measures comprising Triassic sandstone and Jurassic dolerite can only account for a maximum burial of 2 km. Bromfield (2004) has identified Jurassic sediments at Lune River and it is possible that Jurassic sediments may account for the missing section. There are unconfirmed reports of Jurassic sediments and volcanics present above the Triassic outcrops on Mt. La Perouse. Jurassic sandstone, mudstone and conglomerate of the Kawhia Series in New Zealand are up to 3 km in thickness (Kingma, 1974). Equivalent Jurassic sequences in Antarctica are 1+ km in thickness (Elliot and Hanson, 2001). Alexander Island has a 2.2 km thick sequence of Upper Jurassic-Lower Cretaceous conglomerates, sandstones and mudstones (Miller and MacDonald, 2004). Figure 4.20 shows the probable Jurassic palaeogeography of the region around Tasmania and the locations of currently exposed Jurassic outcrops.

This study has found that a significant portion of the Tasmania Basin is mature for oil and gas generation from Permian source rocks and that Upper Permian sources have generated oil in a western outlier of the Tasmania Basin. Maturity levels measured in southern Tasmania imply that much deeper burial has occurred in this region than has previously been recognised. The Jurassic palaeogeography indicates that deposition could have occurred and remnants of Jurassic aged rocks have been found close to where high maturity Permian samples were collected for this study. Indirect evidence, based on maturity levels of Permian aged samples and the known overburden, implies that approximately 2 km of Jurassic section covered southern Tasmania before being eroded.

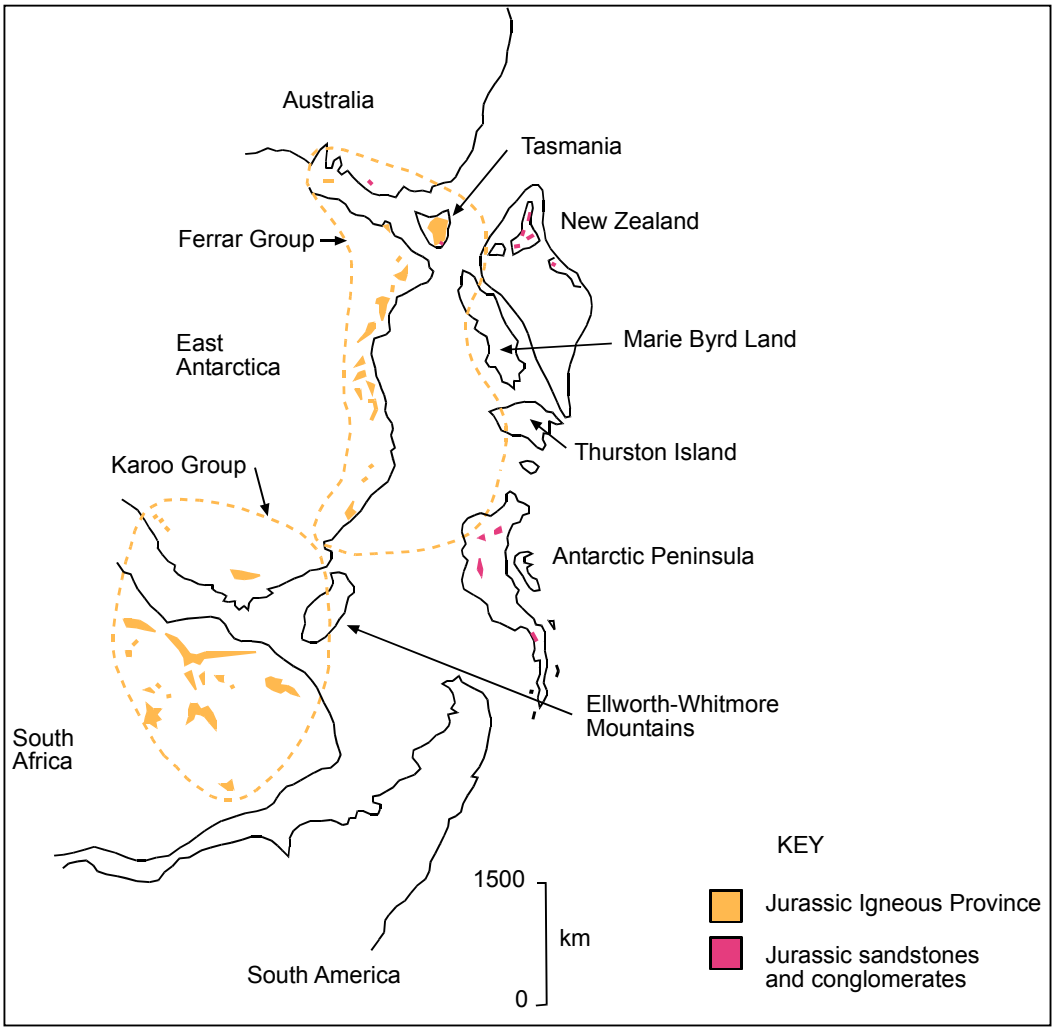

Figure 4.20. Jurassic palaeogeography of the parts of Gondwana adjacent to Tasmania during the Middle Jurassic. The geographic relationships between Tasmania, New Zealand and Antarctica at this time show that it possible that significant Jurassic sedimentary deposits could have occurred in southern Tasmania. Places where Jurassic outcrops of both igneous and sedimentary rocks currently occur are shown. Maturity assessment, as discussed in the text, indicates that at least two kilometres has been eroded from southern Tasmania and the probability is that much of this was Jurassic. Basic map from (Hergt et al., 1991) with additions from (Suggate, 1978), (Clarke et al., 1997), (Elliot et al., 1999), (Bromfield, 2004) and (Hunter et al., 2004).

4.9. Modern geothermal gradients in Tasmania.

Heat is generated in the earth's crust principally by the decay of radioactive trace elements but there are additional sources at depth including global accretion, core segregation, tidal deformation and core/mantle rotation (Cull, 1991). Lithology varies in its capacity to generate heat and Table 4.8 illustrates this by showing the heat capacities (Q) of a range of rock types along with the average content of uranium, thorium and potassium.

Table 4.8. Variations in heat capacity (Q) of a range of lithological types and their average content of radioactive trace elements.

Lithology	**U ppm**	**Th ppm**	**K wt.%**	**Q (αWm^{-3})**
Granite/Rhyolite	3.9	16.0	3.6	2.53
Granodiorite/Dacite	2.3	9.0	2.6	1.51
Diorite/Andesite	1.7	7.0	1.1	1.06
Gabbro/Basalt	0.5	1.6	0.4	0.29
Peridotite	0.02	0.06	0.0006	0.01
Undepleted mantle	0.02	0.09	0.02	0.01
Ocean island basalt	1.02	4.0	1.2	0.67
Limestone	2.0	1.5	0.3	0.66
Shales & siltstones	3.7	12.0	2.7	2.10
Quartzite	0.6	1.8	0.9	0.37

Data from (Haenel et al., 1988)

4.9.1. Modern measurement of geothermal gradients in Tasmania.

Modern measurements of geothermal gradients in Tasmania began with the work of Newstead and Beck (1953) who found a higher than normal geothermal gradient. Later work by Cull (1982), Cull and Conley (1983), Wronski (1977), Jaeger and Sass (1963) have verified Newstead and Beck's findings and Tasmania is now regarded as having an average heat flow of 90 mWm^{-2} against a world average of 60 mWm^{-2} (Cull, 1982). Geothermal gradient determination requires accurate temperature measurements to be made in deep drill holes, preferably within a single lithology. The International Heat Flow Commission collects data obtained under standard conditions and currently only four sites from Tasmania are held in their database. Data from other sites are available and supports the concept of high heat flow for Tasmania.

Data from onshore Tasmania are listed in Table 4.9 and these were used in conjunction with further data from Bass Strait oil wells, shown in Table 4.10, to draw geothermal gradient contours for Tasmania and shown in Figure 4.21.

Lithological variations encountered in the Tunbridge drill hole were shown to have had significant impact on the measured geothermal gradient. The section from 570 m to 680 m had a geothermal gradient of 60°C/km (Green, 1989). Overall the Tunbridge geothermal gradient was established at 41°C/km (Green, 1989). Similar geothermal gradient variations were noted due to lithological variations in the Glenorchy drill hole with the interval 250-650 m having a geothermal gradient of 34°C/km while the 650-1500 m interval had a geothermal gradient of 40°C/km (Green, 1989). The geothermal gradient changes in the Glenorchy drill hole relate to changes between siltstone and dolerite.

The geothermal gradient from Olga Ridge may be too low due to heat refraction effects as the drill hole was in close proximity to the contact between siltstone and quartzite. Significant underground water flow was also encountered and this most likely also reduced temperature readings (Wronski, 1977).

Data from petroleum exploration wells in Bass Strait were collated and these had an average geothermal gradient of 36°C/km, which compares well with an average of 35°C/km for Bass Strait oil wells quoted by Green (1989). Note however that in both of these figures no corrections have been made for the cooling effects of circulation

mud and if these were applied the geothermal gradient would probably be close to 40°C/km (Summons, 1981a).

Table 4.9. Geothermal gradients from Tasmanian onshore locations.

Locality	Easting	Northing	Geo. Grad. °C/km	Reference
Stanley	352 419	5479 735	28	(Green, 1989)
Storeys Ck.	562 433	5386 574	57	(Jaeger and Sass, 1963)
Rosebery	381 143	5374 755	35	(Cull, 1982)
Great Lake	466 857	5353 461	43	(Cull, 1982)
Tunbridge	524 791	5334 620	41	(Green, 1989)
Coles Bay	606 652	5337 189	28	(Cull, 1982)
Olga Ridge	400 188	5263 988	21	(Wronski, 1977)
Maydena	470 500	5264 100	39	(Summons, 1981a)
Glenorchy	520 433	5258 016	35	(Green, 1989)

Table 4.10. Geothermal gradients from Bass Strait petroleum explorations wells.

Well	Easting	Northing	BHT	Depth	G. grad.	Ref.
Barramundi	391414	14390971	87	2100	38	(Anon, 1999)
Yolla 1	397825	14410527	121	3347	33	(Cornell et al., 1985)
Squid 1	441070	14449986	89	2918	27	(Anon, 1984b)
Tas. Devil	429285	14509992	55	862	46	(Anon, 1985)
Pelican 1	401782	14466037	107	2790	36	(Culp, 1970)
Durroon 1	518078	14487067	80	3000	38	(Rigg, 1973)
Cape Sorell	337144	14666757	75	3524	29	(Anon, 1982)

Cull and Conley (1983) produced a map showing geothermal gradients as contours across Australia and over the Tasmania Basin they plotted a gradient of 35°C/km with lower values of 30°C/km to the west, which is in general agreement with Figure 4.21.

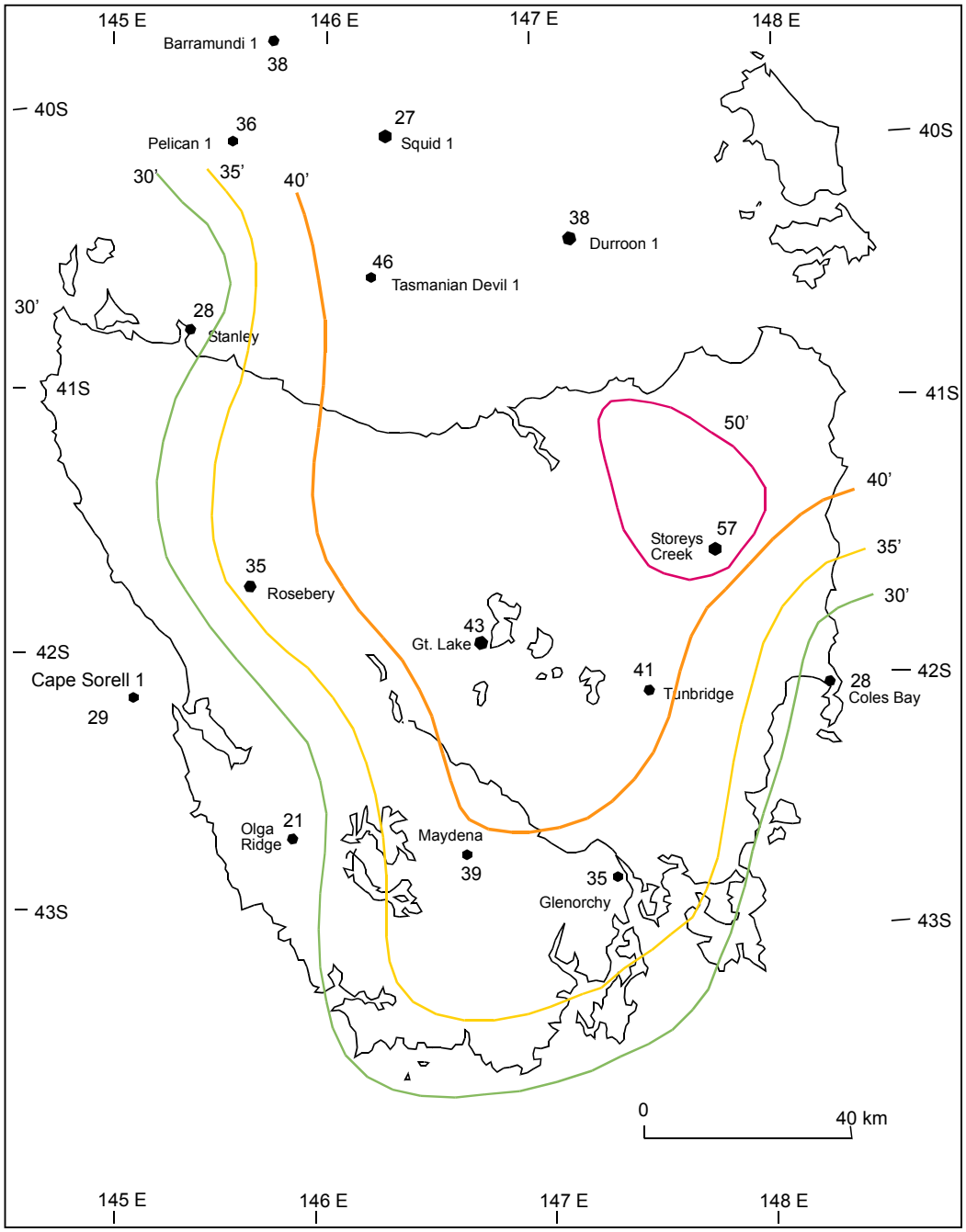

Figure 4.21. Contours of modern geothermal gradients interpreted from nine onshore locations and five Bass Strait oil exploration wells and one offshore west coast oil exploration well where geothermal gradients have been measured. The measurement at Olga Ridge may too low due to heat refraction effects as the site was close to the contact of siltstones and quartzite and strong water flows were also encountered in the drill hole. The Bass Strait geothermal gradients have been calculated from bottom hole temperatures without any corrections being applied for the cooling effects of mud circulation so these could also be 5°C/km below the real figure. Over the Tasmania Basin the geothermal gradient is currently 35-40°C/km.

The lower geothermal gradient values in western Tasmania probably reflect lower heat flow from Precambrian basement, which outcrops in that area. Further evidence of lower heat flows in western Tasmania comes from the Cape Sorell oil well drilled 12 km offshore where a geothermal gradient of 29°C/km was measured (Anon, 1982) and an even lower geothermal gradient of 27°C/km for the Clam 1 well in the Otway Basin (Lunt, 1969).

4.9.2. Possible reasons for high heat flows in Tasmania.

It has been demonstrated that lower geothermal gradients are found where older rocks are exposed on the surface with global average heat-flow ranges for Archean 41-46 mWm^{-2}, Proterozoic 49-54 mWm^{-2}, Phanerozoic 50-70 mWm^{-2} and ocean lithosphere 101 $\pm$2.2 mWm^{-2} (Pollack et al., 1993). The Tasmania Basin is included in the Eastern Province of Australian heat-flow fields where heat-flow averages 72 $\pm$ 27 mWm^{-2}, somewhat higher than global average (McLaren et al., 2003). Average Proterozoic heat-flow in Australia, which includes western Tasmania, has a higher than global average value of 82 $\pm$ 25 mWm^{-2} (McLaren et al., 2003).

If the shapes and positions of the contours for modern geothermal gradients (Figure 4.21) are compared with contours for crustal thickness in Tasmania (Figure 4.10) it can be seen that there is general agreement. This general agreement suggests that crustal thickness may be the major factor influencing modern heat flow in Tasmania with thicker crust having higher heat flow.

Higher heat flows in Bass Strait are probably due to younger cover, presence of granite, and recent volcanic and rifting activity. There has been some volcanism in northern Tasmania in the last 10 Myr. and this indicates an abnormally hot mantle (Sutherland et al., 1994).

O'Reilly and Griffin (1985; 1987) found that eastern Australia has been characterised by a very high geothermal gradient during at least the last 60 Myr. Sutherland and Hollis (1982) suggest that from xenolith data eastern Australia has had a high geothermal gradient from the Permian till the present however this would be difficult to prove. It can be demonstrated that high heat flows have occurred during the Jurassic, Cretaceous and during the last 60 Myr. based on volcanism.

4.9.2.1. Effects of granites.

Devonian granites in Tasmania are unusually enriched in U, Th and K and these radiogenic elements generate heat by decay so they also contribute to the geothermal gradient. Sandiford and McLaren (2002) have shown that heat producing elements concentrated in the upper 10-15 km of the lithosphere account for 50% or more of the measured heat flow at the surfaces of continents. Underlying high U granites may influence geothermal gradients in northeastern Tasmania. However granites at the surface have little effect on geothermal gradient as can be seen by the geothermal gradient at Coles Bay.

A number of granite suites in Tasmania are hosts to tin and tungsten mineralisation and granites of this type generally have abnormally high uranium and thorium contents. Examples are the Renison Granite with Uranium content of 23 ppm (range 6-97) and Thorium 41 ppm (range 12-90) (Bajwah et al., 1995) and Heemskirk Granite mean values of Th 44 ppm, U 9 ppm (red), Th 24 ppm, U 20 ppm (white) (Heirer and Brooks, 1966). These granites contain U and Th concentrations well above world averages (U, 4ppm and Th, 16 ppm) (Kranck and Eakins, 1965). Table 4.8 shows that there is a positive correlation between concentration of radiogenic elements and heat production capacity.

In the Rossarden-Storeys Creek district three uranium prospects have been located (Blissett, 1962). Pitchblende has been identified in veins near Storeys Creek and thucolitic hydrocarbons have also been found in Prospect Creek with both most likely derived from erosion of uranium-bearing granite.

Near the Great Lake, tholeiitic basalt was sampled and this had Th 3.2 ppm and U 0.8 ppm, compared to typical oceanic tholeiite basalt with Th 0.18 ppm and U 0.1 ppm (Gottfried et al., 1968). The widespread occurrences of rocks containing radiogenic elements must contribute to the higher than normal geothermal gradients in Tasmania.

4.9.2.2. Mantle plume.

A further influence on heat flow in Tasmania may be from the presence of a mantle plume beneath Bass Strait. A line of extinct volcanoes stretches from Cape Hillsborough, in northern Queensland, to Mt. Macedon, in southern Victoria, and these get progressively younger to the south. These extinct volcanoes trace the path of

a mantle plume, which currently lies under Bass Strait at approximately 40°S (Belfield, 2002). Volcanoes have only formed at intervals along the trace as mantle plumes have difficulty penetrating thick cold continental lithosphere but it still has the capacity to raise geothermal gradients.

Geothermal gradients in western Victoria follow a trend of higher heat flows to the south, which seems to be in accord with the passage of a mantle plume. Table 4.11 indicates geothermal gradients in western Victoria showing a trend for increasing heat flow to the south.

Table 4.11. Geothermal gradients in western Victoria.

Locality	Easting	Northing	Geothermal Gradient °C/km.
Horsham	589138	14079931	22.8
Warracknabeal	620928	14038406	23.6
Castlemaine	252485	14104042	24.2
Stawell	658577	14101906	27.1
Lancefield	301620	14111998	30.5
Mt. Gambier	489722	14178083	28.6
Portland	558265	14243010	30.7
Otway	517511	14228024	34.9

Data from Purvis and Cull (2001).

4.10. Potentially mature zones onshore Tasmania.

Precambrian rocks of onshore Tasmania, from the observations made during this study, are over mature for the generation of hydrocarbons. Although only the Rocky Cape Group was studied in detail, observations were also made of possible correlates in the upper Weld Valley and these appeared to be of low metamorphic grade therefore no hydrocarbon generation could be expected. Precambrian dolomite core samples from the Hunterston stratigraphic drill hole were checked for TOC levels and found to have very low organic content (below 0.2% TOC, AMDEL, 2002). No maturity measurements could be made due to the low levels of organic matter present. The intensely folded structures of the Precambrian sequence in the Hunterston drill core suggests maturity of metamorphic grade and it would be reasonable to interpret the deeply buried (1000 m+) Precambrian sequences below the Tasmania Basin to be of metamorphic grade when exposed correlates in northwestern Tasmania have low

metamorphic grade. From observations made during this study the Precambrian sequences onshore Tasmania can effectively be ruled out as having any potential for source rocks on the basis of maturity beyond the capacity to generate hydrocarbons.

Ordovician sequences in southern Tasmania appear to be at a maturity level within the gas range. Limited outcrop only allows maturity assessment along the western edge of the Tasmania Basin from the northern parts of the Florentine Valley south to the Lune River, with many areas in between not having any outcrop. The main area of interest from an exploration point of view is beneath the Tasmania Basin and because no drilling has intersected Ordovician sediments in this zone the presence of suitable rocks can only be inferred from the known exposed geology and geophysical interpretations. Unfortunately there are no currently available methods for determining maturity levels by geophysical means.

The gas range, from wet gas to the end of dry gas, is the level of maturity determined for the Gordon Group in southern Tasmania. The zone in which this occurs extends from the northern margins of the Florentine Valley south to the Lune River. The Gordon Group is exposed in the Florentine Valley and also in the Vale of Rasselas and so the area of petroleum exploration interest lies under cover to the east. Gordon Group sediments are not likely to be found east of the Tamar Lineament as basement in this zone is either Mathinna Group or granite. The zone interpreted to be within the gas zone for the Gordon Group is approximately 60 km west to east and 200 km north to south if suitable source rocks do in fact exist below the Tasmania Basin. If 20 km wide thrust stacked zones occur along the Tamar Lineament, as indicated by exposures in northern Tasmania, this area would be considerably reduced. The proposed prospective area is shown in Figure 4.20 but note that no actual measurements have been made on any samples as no drilling has yet intersected potential source rocks or even any Gordon Group sediments from this zone. Table 4.12 gives details of locations, lithology and references for basement interpretation used in Figure 4.22.

Table 4.12.

References, locations and lithology for southeast Tasmania basement interpretation.

Location	Reference	Lithology
Hunterston	Reid et al. (2003)	Precambrian dolomite
Tunbridge	Forsyth (1989)	PC cf. Badger Head Gp.
Ross	Forsyth (1989)	PC cf. Badger Head Gp.
The Quoin	Williams (1983)	Mathinna Beds
York Plains	Dickson et al. (1984)	PC phyllite, quartzite
Eldon	Sutherland (1977)	PC quartz schist
Acton	Sutherland (1976)	PC phyllite, qtz. Veins
Glenorchy	Everard (1976)	Cambrian
Woodbridge	Williams (1985)	PC phyllite, quartz
Cygnet	Gunn et al. (1997)	Mesozoic igneous intr.
Lune River	Gunn et al. (1997)	Lower Cambrian
Shittim, Bruny Is.	Anon (1997)	PC phyllite
East coast	Leaman and Richardson (1992)	Granite
South Cape	Subexposure	Gordon Lst.
Weld Valley	Seymour and Calver (1995b)	Precambrian
Florentine Valley	Corbett and Banks (1974)	Gordon Lst.
Flanking east coast	Inference	Mathinna Beds

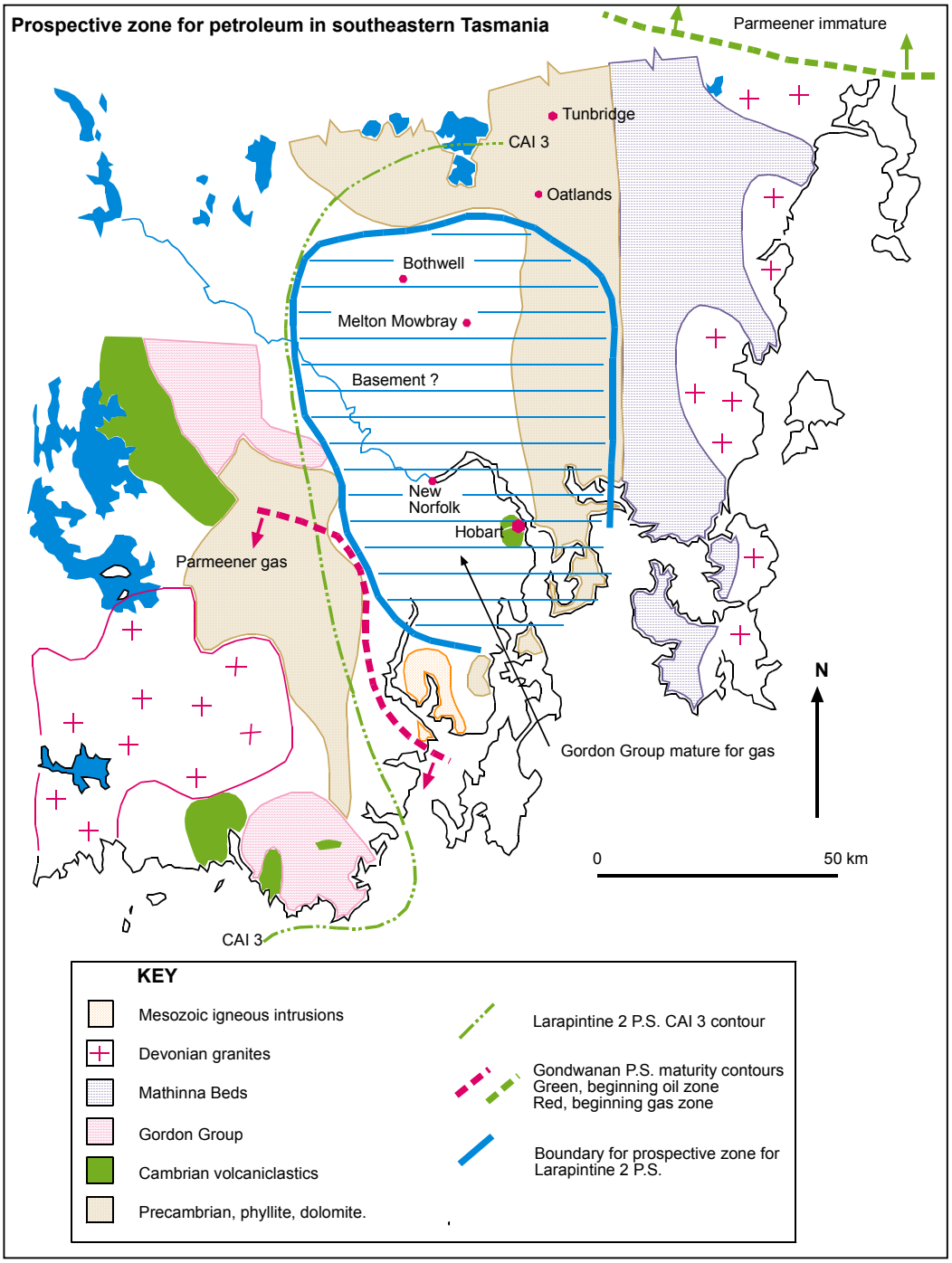

Figure 4.22. Map showing potential prospective zones for stacked petroleum systems in southeastern Tasmania. The prospective zone for the Gondwanan petroleum system, hosted by the Parmeener Supergroup, lies between the dashed green line at the north of the map and the dashed red line near the south. A dark blue line is the inferred boundary for the prospective zone for gas from the Larapintine 2 petroleum system. This area has been inferred as prospective on the basis of maturity within the gas zone and the possibility of source rocks being present below the Tasmania Basin. Inferred basement lithology is shown but it will be noted that much of the prospective zone for the Larapintine petroleum system is unknown and thus shown blank on the map. Inferred lithology below the far southern portions of the mature zone for gas for

the Larapintine petroleum system would suggest that it is largely unprospective for petroleum due to lack of suitable source rocks and structural complexities.

Upper Permian sediments are within the oil window of maturity in an outlier of the Tasmania Basin on the west coast of Tasmania, near Zeehan. From indirect evidence similar sediments, if present, would also be in the oil window of maturity in the main Tasmania Basin south from the latitude of St Marys to the latitude of Huonville. South of Huonville Upper Permian sediments are within the gas range of maturity and exposures on the south coast of Tasmania are of metamorphic grade. Figure 4.2 illustrates these zones of maturity on a map of Tasmania.

There is an overlap of areas where Permian sediments are mature for oil and possibly Ordovician sediments are mature for gas. This overlap area has the potential for stacked petroleum systems to operate in onshore Tasmania. It must be stressed however that maturity assessments of the Gordon Group show that they are in the last stages of petroleum generation where volumes are minimal and pressure for migration is limited. Another major difficulty is that the source rocks are only inferred.

On a maturity basis the Permian sediments would appear to have the most potential for hydrocarbon generation of any sediments identified as having source potential onshore Tasmania. The maturity of Permian sediments indicates both oil and gas potential.

CHAPTER FIVE.

EXPLANATIONS FOR BITUMEN OCCURRENCES ONSHORE TASMANIA.

5.1. Introduction, historical occurrences of bitumen and oil seeps onshore Tasmania.

The modern oil industry began in Pennsylvania, U.S.A., during the 1850's with the first successful drilling for oil by Drake in 1859 (Campbell, 1964). Up until that time fuel for lamps was obtained from whale oil and Tasmania was a major supplier of this commodity (Mercer, 2002). Whalers and sealers had collected stranded bitumen along the coasts of southern Australia during the 1800's and used it to caulk boats and to seal the floors of huts (Wilkinson, 1991). Government geologist Charles Gould reported bitumen strandings in 1871 and explorer and prospector T.B. Moore reported bitumen stranded in a number of places along the west coast of Tasmania between 1876 and 1895 (Bacon et al., 2000). Some bitumen strandings were mistaken for seeps and at least one syndicate was formed to exploit perceived resources on the basis of these reports (Twelvetrees, 1915).

Oil shale was discovered near Latrobe in northern Tasmania in 1851 and this was the initial indication of potential for oil onshore Tasmania (Rudd, 1951). Until the use of internal combustion engines became established there was little incentive to develop the oil shale deposits so these were not worked until 1910, at Railton (Wilkinson, 1991). Later the Tasmanite Shale Oil Company Limited continued production from the Latrobe deposits until 1935, selling fuel oil to the Tasmanian Government Railways and Mt Lyell Mining and Railway Company (Wilkinson, 1991). By 1935 the high sulphur content of the Tasmanian shale oil put it at a disadvantage to imported petroleum and so production ceased.

The first recorded drilling for oil in Tasmania was in 1915 at Bruny Island by the Bruny Island Petroleum Company, who drilled a 130 m well but found no oil (Wilkinson, 1991). Liquid petroleum had been reported to be exuding from the ground in the area but Dr. Arthur Wade, called in by the Mines Department, could not find any seeps (Wade, 1915). Traces of oil were noted from Johnson's Well and

Myles Creek, both sites on Bruny Island, in 1929, and these were considered to be genuine by the government geologist Alexander McIntosh Reid (Reid, 1929).

A number of exploration wells were drilled during the 1920's mainly on Cressy to Port Sorell structures. Alexander McIntosh Reid, government geologist, confirmed a number of oil and gas shows in 1923 by the Adelaide Oil Exploration Company however no commercial finds resulted (Reid, 1923). The oil seeps Reid confirmed in northern Tasmania appear to be related to oil shale deposits and the heating effects of dolerite intrusions on oil shales may have generated the oil he noted.

Many reports were made of oil and gas shows and seeps at various places around Tasmania but many of those investigated proved not to be genuine. Films of iron and manganese oxide on water can resemble oil, as can exudates from some plants and methane gas bubbles rise through water from the decomposition of organic matter. Pollution, such as oil run-off from roads after rain, can also lead to false reports of seeps. During this research four reported seep sites were investigated none of which were genuine. A reported gas seep at Marion Bay was found to be marsh gas and a reported oil seep on Bruny Island, near the ferry terminal, was found to be a spill of bitumen possibly from a passing ship. Anecdotal evidence from the ferry operator was that the bitumen came from a discarded drum that lay on the site for a number of years. Geochemical analysis of the Bruny Island bitumen suggested Middle East origins (Revill and Esmay, 1999). A reported seep near Temma, on the west coast of Tasmania, had a distinctive hydrogen sulphide odour and what appeared to be an oily film on water seeping from bedding planes. The hydrogen sulphide odour came from rotting plant debris in swamp deposits and the oil-like film proved to be iron oxides. A fourth site, on the Dazzler Range, had particles of muscovite floating on a pond that resembled an oil film. A map showing locations of seeps and reports of seeps is located in a pocket at the end of this thesis.

5.2. Evidence of petroleum expulsion and migration onshore Tasmania.

One oil seep has been verified by modern geochemical methods and this occurs through fractured dolerite at Lonnavale in southern Tasmania. Geochemical analysis showed this seep to have the characteristic tricyclic triterpane signature of Permian source rocks with *Tasmanites* as the main organic contributor (Bottrill, 1996).

Pyrobitumen has been found in association with lead-zinc mineralisation within Gordon Group limestone near Zeehan in western Tasmania (Morris and Taylor, 1995). Bituminous material has also been found near Bubs Hill also in association with lead-zinc mineralisation and Gordon Group limestone (Reid, 1964).

Bitumen has been found in the Comstock and Oceana mines near Zeehan along faults and fractures in Precambrian rocks and appears to have laterally migrated to these positions. During investigations into the possible sources for these occurrences further bitumen of the same type was found near the Badger River to the south of Zeehan and traced to Permian source rocks.

Oil inclusions were noted in core samples from Douglas River on the east coast of Tasmania (Bedi, 2003). These oil inclusions are likely to have been derived from Permian sources due to the presence of a number of possible source rocks such as carbonaceous Liffey Group, Woody Island Siltstone and Tasmanite oil shale in the 200 m sequence stratigraphically below the sample site (Calver, 1984). Unfortunately the oil inclusions were too small to allow any definitive analysis.

Bitumen was found during drilling of a stratigraphic hole at Forest, near Smithton, in northwestern Tasmania (Brown, 1985). The bitumen found in Forest 1 DDH was associated with Black River Dolomite. Further bitumen was located in amygdales within basalt at Kanunnah Bridge, also within the Rocky Cape Block (Legge, 2001). Both of these occurrences occur close to Black River Dolomite outcrops and also overlie Cowrie Siltstone so the bitumen in each case may possibly have been derived from the same Precambrian source and a discussion of possible sources follows in section 5.3.1.

5.3. Probable timing of petroleum expulsion events.

Verified occurrences of bitumen and oil onshore Tasmania are associated with rocks of a wide range of ages and this suggests that generation events may have occurred at widely different times throughout the geological history of Tasmania. The oldest rocks in which bitumen has been located are Neoproterozoic and possible source rocks for these occurrences could be of Mesozoic age. Pyrobitumen has been located in association with Ordovician rocks and generation of this petroleum may have occurred during the Early Devonian. The youngest verified occurrences of petroleum

onshore Tasmania have been generated from Permian source rocks with possible generation occurring during the Cretaceous. Probable timing of expulsion events will now be considered in more detail.

5.3.1. Proterozoic bitumen generation.

Bitumen was located within amygdales of the Spinks Creek Volcanics, part of the Kanunnah Subgroup of the Togari Group, at Kanunnah Bridge (Legge, 2001). The amygdales occur within basalt and all are less than 1 mm across. The bitumen appears opaque under transmitted light and mid-grey in reflected light. The cracked appearance of the bitumen suggests that lighter hydrocarbons may have been driven off leaving the desiccated remains now seen within amygdales in the basalt as shown in Figure 3.2. From the size of the trapped bitumen samples it would appear that only small quantities of hydrocarbons were generated.

In the immediate vicinity of the basalt flow there are turbiditic siltstones and mudstones and due to lack of organic matter these have no potential as source rocks for bitumen. To the west is a major fault, Roger River Fault, and beyond this fault is an outcrop of Salmon River Siltstone, which does have some potential as a petroleum source rock due to high organic content (TOC 0.85%). However the Salmon River Siltstone is stratigraphically higher and younger (Cambrian) than the basalt in which the bitumen is found so it is not the source rock for the Kanunnah Bridge occurrences. Sequences, stratigraphically below the basalt, are exposed close by to the east and these also appearing to have some potential as petroleum source rocks based on TOC results. Two sequences, separated by a low-angle unconformity, both with some petroleum source potential occur to the east and these are the Cowrie Siltstone and the Black River Dolomite. Both Cowrie Siltstone and Black River Dolomite are also exposed to the west of the Roger River Fault and it could be assumed that continuous extent of these lithologies occurs at depth, although now faulted.

It is probable that the basalt has intruded one or more of these potential source rocks and heat from the intrusion has generated bitumen from possibly immature organic matter. The basalt has then trapped the newly generated bitumen within amygdales so that it has been preserved until the present. It is also possible that other petroleum was generated in the same event but not trapped within the basalt and migrated elsewhere. The only other evidence for bitumen, of comparable age in the region, was located at

depth in the Forest 1 stratigraphic drillhole some 30 km to the north of Kanunnah Bridge. The Forest 1 bitumen was found in association with Black River Dolomite suggesting that this was the source for both occurrences. There is no evidence for cover sequences in this area, which could have provided reservoir sequences, and the present folding appears to have occurred during the Cambrian so that trap structures were unlikely to have been present at the time of hydrocarbon generation.

The potential source rocks for the bitumen located at Kanunnah Bridge and Forest 1 DDH are now all over mature, as shown in Chapter Four, but during the Proterozoic it is likely they were still immature. Major discrepancies are evident in the current maturity data derived from Rock-Eval pyrolysis and those from Kubler Index measurements for the Cowrie Siltstone so source potential will be based on total organic content. Due to the current high maturity of these siltstones other source potential indicators do not give a true indication of the original source potential. Total organic content and source potential as indicated by Rock-Eval pyrolysis S_1, S_2 and Hydrogen Index are shown in Table 5.1 for three potential source rocks identified for the bitumen noted in northwest Tasmania. Kubler Index measurements indicate a current maturity close to greenschist for this region, a palaeotemperature approximately 150°C higher than that indicated by Rock-Eval pyrolysis T_{max}. S_1 and S_2 figures indicate low potential but this is most likely due to the high maturity of the samples. TOC and HI figures do suggest some potential as source rocks, particularly during a lower maturity phase as was likely during the Neoproterozoic.

Table 5.1.

Potential source rocks in northwest Tasmania.

Potential Source rock	**TOC**	**S_1**	**S_2**	**HI**
Salmon River Siltstone *	0.85	0.07	0.47	55
Black River Dolomite JR1	2.08	0.02	0.03	1
Black River Dolomite Sumac 4	0.25	-	-	-
Cowrie Siltstone CS1	1.45	0.06	0.32	22
Cowrie Siltstone CP2	0.64	0.02	0.49	76
Cowrie Siltstone CP3	1.37	0.28	0.77	56
Cowrie Siltstone CP4	0.70	0.03	0.16	22

Data from AMDEL 2003-2005. * Cambrian

Data shown in Table 5.1 indicates that Cowrie Siltstone had potential to be source rocks for the bitumen found in northwest Tasmania. Black River Dolomite samples, although selected, demonstrate low potential as source rocks.

The timing of the generation event, if related to eruption of Kanunnah Volcanics as indicated by trapped bitumen, was late Neoproterozoic ~600-650 Ma (Logan et al., 1999). A diagrammatic representation of the Centralian petroleum system, on shore Tasmania, is shown in Figure 5.1.

CENTRALIAN PETROLEUM SYSTEM

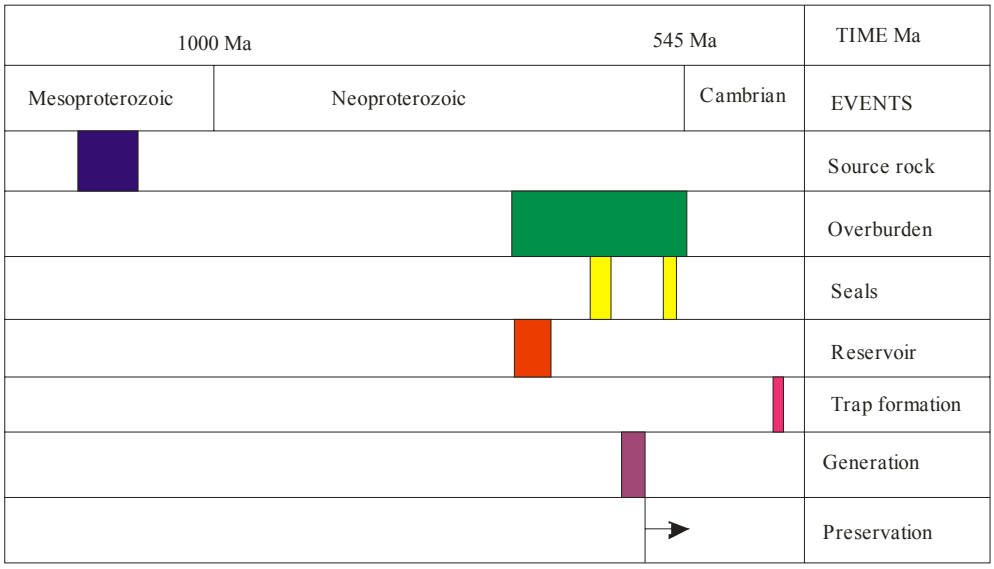

Figure 5.1. Centralian petroleum system diagram, for on shore Tasmania, showing the relative timings for key petroleum system elements.

5.3.2. Petroleum generation from Ordovician sources.

There is evidence for only minor generation of petroleum from Ordovician sources onshore Tasmania and mostly now in the form of pyrobitumen. Pyrobitumen has been found associated with Pb-Zn mineralisation in a region south of Zeehan through to Bubs Hill. In thin sections from Grieves Siding and Oceana prospects, pyrobitumen appears as fine traces (>0.1 mm wide) along the edges of veins containing galena and sphalerite. In rare core sections, pyrobitumen vein fill is up to 5 mm wide. A photomicrograph of pyrobitumen within Gordon Group from Grieves Siding is shown in Figure 5.2. The close association of Pb-Zn mineralisation and pyrobitumen suggests that petroleum generation and migration occurred simultaneously with the

deposition of sulphide minerals and so if the timing of Pb-Zn mineralisation can be determined it would also establish the timing of hydrocarbon generation from Ordovician sources onshore Tasmania.

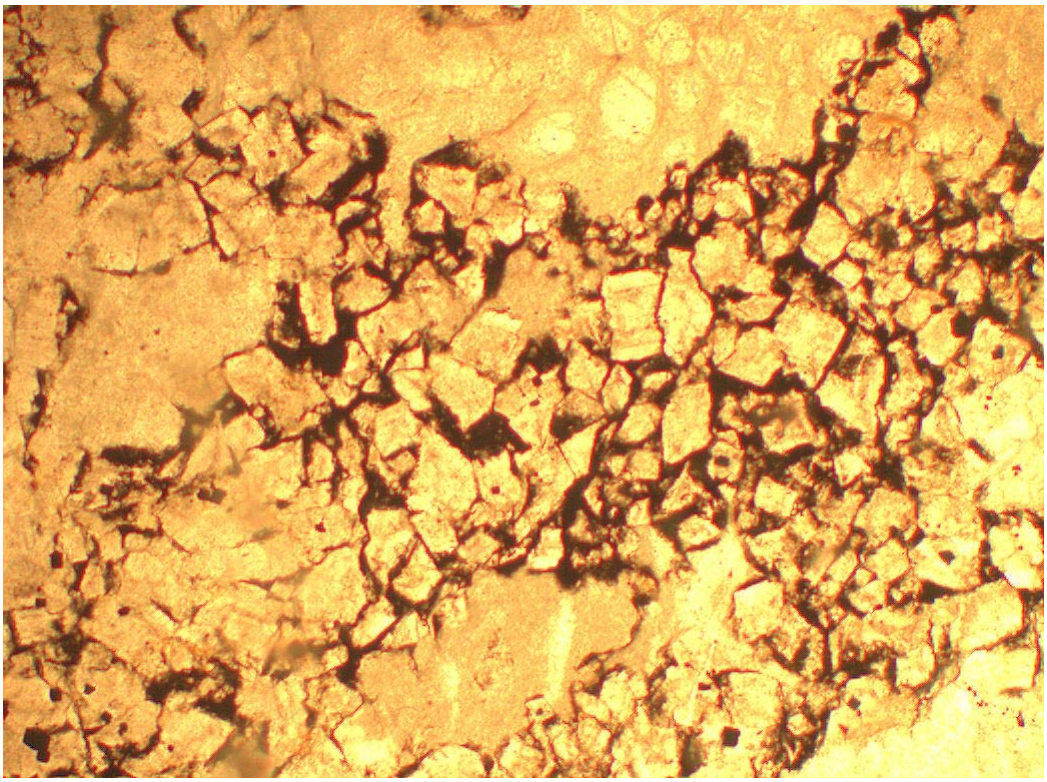

Figure 5.2. Photomicrograph showing part of thin section of Gordon Group from Grieves Siding where pyrobitumen fills pores between grains. Thin section by Ellis (1984), cut from core of DDH Zt-80-4 at 340.6 m depth. Field of view 2 mm, PPL.

A range of ore formation mechanisms and timings have been suggested for the Grieves Siding and Oceana prospects ranging from syndiagenetic replacement (Irish-style) during the Ordovician (Taylor, 1983; Taylor and Mathison, 1990), to Mississippi Valley-type epigenetic mineralisation during the Devonian (Groves and Solomon, 1971; Morris and Taylor, 1995). As the Zeehan mineral field in general has been subjected to mineralisation by granitic fluids during intrusion of the Heemskirk Granite, Late Devonian, this possibility must also be considered.

Syndiagenetic replacement as a mechanism for the sulphide mineralisation at Grieves Siding and Oceana can be ruled out on the basis of crosscutting textures visible in thin sections. Examination of thin sections prepared by Ellis (1984), McGilvray (2003)

and Glover (1996), showed sulphide and pyrobitumen-filled veins cross-cutting earlier carbonate veining (Fig. 5.3). Crosscutting textures such as these are definite indicators of epigenetic mineralisation. Some of the earlier stage veins were also displaced by shear veins indicating that the host rock was brittle before the sulphide and bituminous veining event. Pyrobitumen-filled veins also cut sedimentary stylolites indicating that compaction and early diagenesis had occurred prior to the bituminous veining event. On the evidence of mineral textures, sulphides have replaced carbonates because galena pseudomorphs of siderite are visible and both galena and sphalerite fill voids between siderite crystals. Ellis (1984) determined a three-stage sequence of mineralisation at Oceana, dolomitisation then sphalerite, siderite and calcite followed by galena, calcite and minor chalcopyrite. At Grieves Siding, Glover (1996) determined a sequence consisting of dolomite, then siderite, then sphalerite, pyrite and galena followed by calcite. These paragenetic mineralisation sequences are typical of those expected for MVT deposits where dolomite is formed first and then replaced by sulphides (Sass-Gustkiewicz et al., 1982). A photomicrograph showing galena and pyrite replacing siderite is shown in Figure 5.4.

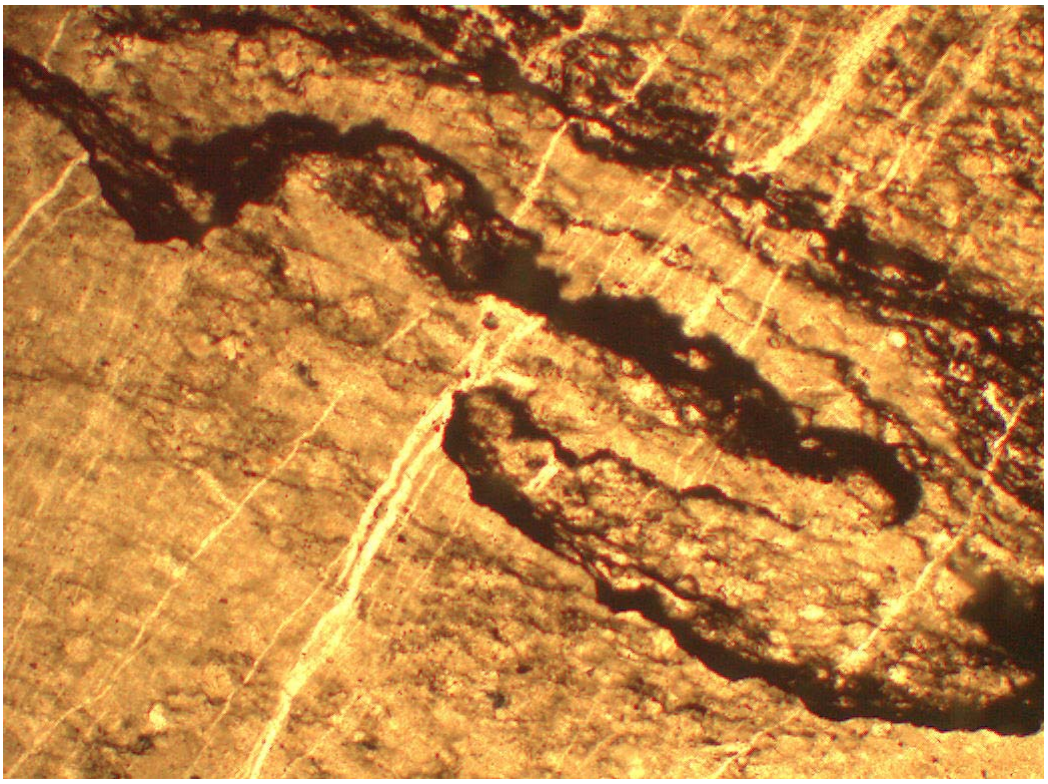

Figure 5.3. Photomicrograph showing part of a thin section of Gordon Group from Grieves Siding with pyrobitumen-filled stylolites crosscutting earlier carbonate veining. Crosscutting texture indicates the epigenetic timing of the bituminous generation event. Thin section made by Ellis (1984) and cut from core of DDH Zt-80-4 at 102 m depth. Field of view 2 mm, PPL.

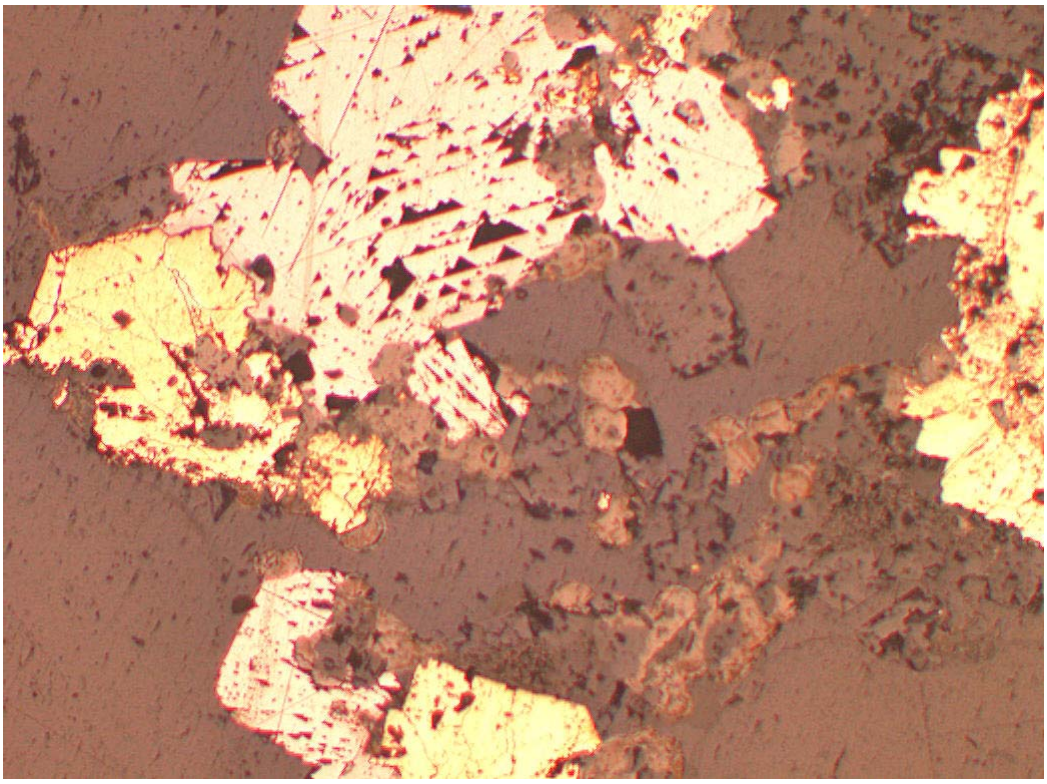

Figure 5.4. Photomicrograph showing sulphide mineralisation associated with bituminous veining within Gordon Group from Grieves Siding. Galena and pyrite fill voids between siderite crystals, typical of MVT deposits. Thin section prepared by Glover (1996) from core section of ZG 1007 at 726 m. Photograph taken using reflected light, field of view 2 mm.

Saxon (1994), points out that the sulphide mineralisation could not have survived the high-energy, oxygenated conditions demonstrated by the host rock sedimentology if they had been emplaced syndiagenetically. Bioturbation is present in the host sediments as evidence of oxygenated conditions.

Fluid inclusions from Grieves Siding gave average homogenisation temperatures of 150˚C similar to that expected from Mississippi Valley-type (MVT) deposits (80˚C-200˚C) and below both magmatic and metamorphic water values (Glover, 1996). Salinity for the fluid inclusions was in the range 2.5 to 4.3 wt. % NaCl, consistent with mixed meteoric and seawater sources and just outside the range for connate brines (Glover, 1996). On the basis of the mineral assemblages of galena and sphalerite with calcite and barite, Groves and Solomon (1971) determined that Bubs Hill mineralisation was MVT. The mineralisation at Bubs Hill was deposited

primarily in solution collapse breccias, close to the contact of Gordon Group with the overlying Crotty Quartzite (Groves and Solomon, 1971). Mineralisation at Bubs Hill is related to major east-west faults (Scott, 1957), so there are similarities to the deposits at Oceana and Grieves Siding and probably the three sites are genetically related.

Evidence presented suggests that mineralisation at Grieves Siding, Oceana and Bubs Hill was epigenetic and probably occurred after the deposition of the Eldon Group, because there must have been at least 700 m overburden for sedimentary stylolites to form (Bathurst, 1971; Nicolaides and Wallace, 1996). Isotopic, mineralogical and structural evidence indicates that mineralisation took place prior to Devonian granite intrusion and prior to the Mid-Devonian Tabberabberan Orogeny.

The best estimate for timing of mineralisation is that it occurred during the Early Devonian and that fluids transporting the lead and zinc also transported the petroleum that is now present as pyrobitumen. Burial of the Gordon Group, in western Tasmania, would have been ~2 km during the Early Devonian, based on estimates of Eldon Group stratigraphy. At this level of burial and with a probable geothermal gradient of 40°C/km any organic material present, within the Gordon Group, would have been mature for oil generation. Ore fluid temperatures of ~150°C, determined from fluid inclusions, were achieved through deeper circulation through the Crimson Creek and Oonah Formations as implied by lead isotope values. Hydrothermal fluids may have triggered petroleum generation and fluid flow provided a transport mechanism. It is unlikely that the minor amounts of petroleum generated would have achieved enough pressure to migrate without an external drive.

Hydrocarbons within the ore fluid may have provided a reductant to help in the precipitation of the sulphides and carbonate rocks also preserve the reducing capacity of hydrocarbons better than sandstones (Anderson, 1991). Research is on-going in regard to the role played by hydrocarbons in transporting metals in ore fluids however Etminan and Hoffmann (1989) have found that hydrocarbon fluid inclusions, found in sphalerite and dolomite intimately associated with MVT deposits in the Canning Basin, Western Australia, have different biomarkers and are more mature than those found in host rocks. The implication is that ore fluids have transported hydrocarbons from deep within the basin and that the source rocks may not be the host rocks as first

supposed. If this is the case it may explain the hypothesis of Anderson and Macqueen (1982) that oil basins are not good MVT basins and vice versa. If the ore fluids have introduced the minor amounts of pyrobitumen noted in association with Pb-Zn mineralisation hosted by Gordon Group from deeper in the basin, then this may explain why hydrocarbons have not been noted elsewhere related to Gordon Group.

Driving mechanisms for the fluids responsible for MVT deposits are controversial but three main mechanisms have been proposed, sediment compaction, topographic relief and tectonic deformation (Garven et al., 2001). Compaction-driven flow rates are known to be orders of magnitude slower than the other mechanisms (Neuzil, 1995) and therefore unlikely to lead to commercially important deposits. No significant tectonic event is recognised for Tasmania in the interval determined to be likely for the mineralisation at Grieves Siding, Oceana and Bubs Hill so perhaps compaction or topographic relief may have been responsible for the fluid flow. The low tonnage of sulphide mineralisation in these deposits may relate to low volume of fluid flow and may also indicate compaction or topographic relief as a mechanism for fluid flow.

Basinal brines from which MVT deposits have formed in various parts of the world have been found to contain small quantities of hydrocarbons even though the basins from which they have been derived could not be considered prospective for petroleum. Tasmania is no exception to this situation and the significance for oil exploration, onshore Tasmania, from the western Tasmanian possible MVT deposits, is that oil generation from Ordovician sources appears to have occurred during the Early Devonian and prior to the formation of significant traps during the Tabberabberan Orogeny. If commercial quantities of petroleum were generated from the Gordon Group at this time, which from the evidence appears unlikely, it would have been lost due to the lack of trap structures.

A Tasmanian example where mineralising fluids flowing through non-petroleum prospective country rocks have also carried hydrocarbons is in north eastern Tasmania. At the Aberfoyle tin-tungsten deposit, biogenic hydrocarbons have been found in fluid inclusions and these were probably formed by interaction of mineralising fluids with sedimentary country rocks (Hoffman et al., 1988). The Mathinna Group sedimentary country rocks near the Aberfoyle mine are not considered likely hydrocarbon source rocks, yet they obviously had enough organic

matter to form minor amounts of hydrocarbons. This would suggest that the Gordon Group limestones also have the potential to generate the small amounts of bituminous material noted in association with lead-zinc mineralisation in western Tasmania.

Petroliferous odours have been noted emanating from freshly broken Gordon Group limestone, particularly from near the top of the Upper Benjamin Limestone and this is in-situ gas generated due to burial of the limestone. An analysis of this gas was detailed in Chapter Three section 3.4.5. Migration has not occurred due to the low volume of gas generated and the tight nature of the limestone matrix. Hydrocarbon gases are confined to areas, such as the Florentine Valley and Lune River, where burial has not pushed temperatures above the gas preservation limit.

Figure 5.5 shows the overall Larapintine petroleum system elements and relative timings of important events.

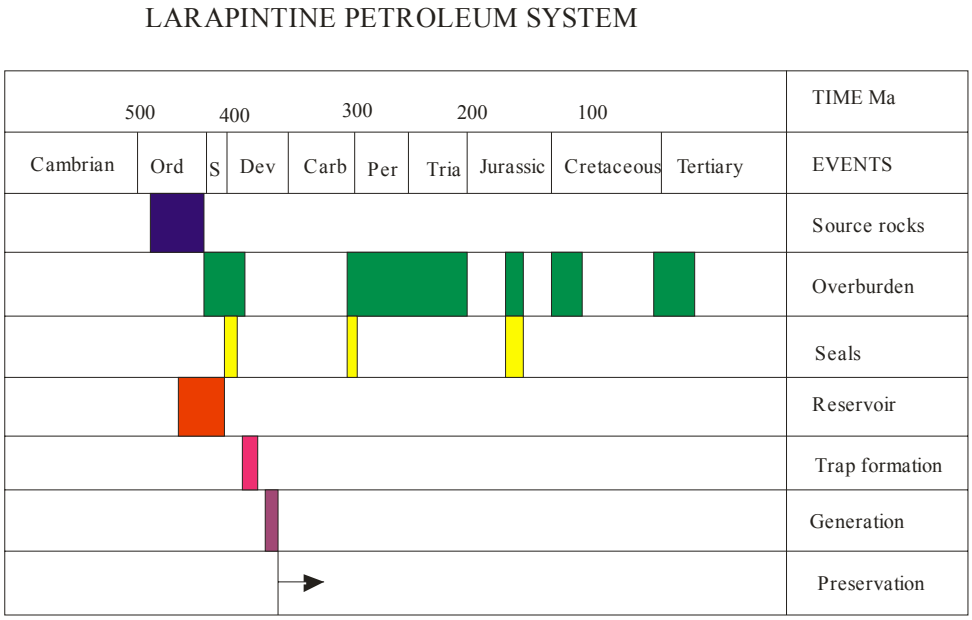

Figure 5.5. Larapintine petroleum system diagram showing the relative timings for key petroleum system elements.

5.3.3. Petroleum generation from Permian sources.

The most promising evidence for petroleum generation from an exploration point of view is provided by Permian sources onshore Tasmania. The only oil seep confirmed by modern geochemical methods occurs at Lonnavale in southern Tasmania and

samples of oil and bitumen from this seep were analysed by the CSIRO Marine Research Laboratory in Hobart (Revill, 1996) and also AMDEL (Wythe and Watson, 1996). The bitumen is dark brown to black, vitreous, soft and sticky when fresh, but hardens and darkens to a dull black on exposure to air. The bitumen readily leaves oil stains on paper, indicating a moderate content of low to moderate weight hydrocarbons (Bottrill, 1996). The analysis showed an unusual feature in that the samples lacked appreciable concentrations of hopanes. Similar proportions of C_{27} and C_{29} steranes were present along with moderate amounts of diasteranes. These characteristics and the abundance of tricyclic terpanes suggest a close affinity to the tasmanite oil shale (Volkman, 1999).

GC and GC-MS analysis by Wythe and Watson (1996) showed that the lightly biodegraded bitumen and oil located at Lonnavale have been derived from a moderately mature (0.8 VR_{eq}) source. The analyses also show the oil and bitumen to have been derived from a mixed algal/terrestrial source, deposited in an anoxic nearshore environment and rich in *Tasmanites.* Note that the maturity of the oil and bitumen is below the expected background level for this locality as shown in Figure 4.2. Tasmanite oil shale is located well down in the stratigraphic sequence near Lonnavale.

The geochemical characteristics indicating the oil and bitumen have been derived from Tasmanite oil shale and the lower than background maturity levels suggest that migration has occurred. Maturity for Permian potential source rocks increases towards the south (Reid, 2004) and this trend has been confirmed during the course of the present study. The Lonnavale seep is evidence that oil generation is possible from suitably mature sections of *Tasmanites* containing shales onshore Tasmania.

There is some anecdotal evidence that sawmillers used oil from this seep as lubricants and if so the seep may have been more active in the past than it is at present. The site of the seep is in a dolerite quarry and quarrying operations may have disrupted the flow paths and thus effectively shut off the seep. As will be explained in section 5.4, seismic pumping may also have been a factor in activating seeps and during the present seismically quiet period this effect has been absent so flow has been negligible.

Further evidence of petroleum generation from Permian sources has come from the Zeehan region. During developmental work at Comstock mine in 2001 bitumen was found along faults and fractures within the Proterozoic Oonah Formation. Initially it was assumed that Ordovician Gordon Group limestone was the source for this bitumen as there is direct contact between this group and Oonah Formation however investigations during this study have revealed it has been sourced from Permian Cygnet Coal Measures. In 2003 fresh samples of albertite bitumen were collected from the Comstock mine so that petrographic and geochemical analysis could be conducted to determine the source of the bitumen. Maturity of the Comstock bitumen was determined by reflection measurements and found to average R_v 0.75% which is within the oil window. Reflectance measurements on bitumen derived from western Tasmanian Gordon Group limestone average R_v 2.7%, which is within the dry gas range. Rock-Eval pyrolysis T_{max} temperatures and biomarker maturity indexes from Gordon Group samples all support maturity assessment within the dry gas range.

As well as major differences in maturity there are differences in the organic source matter for the Comstock and Gordon Group limestone derived bitumen. Organic geochemical analysis shows that Comstock bitumen has plant affinities whereas Gordon Group limestone bitumen has marine algal affinities. A comparison of the GC-MS traces from analysis of Comstock and Gordon Group derived bitumen samples is shown in Figure 5.6 where it can be seen that each sample has different chemical characteristics implying that they have been derived from separate sources.

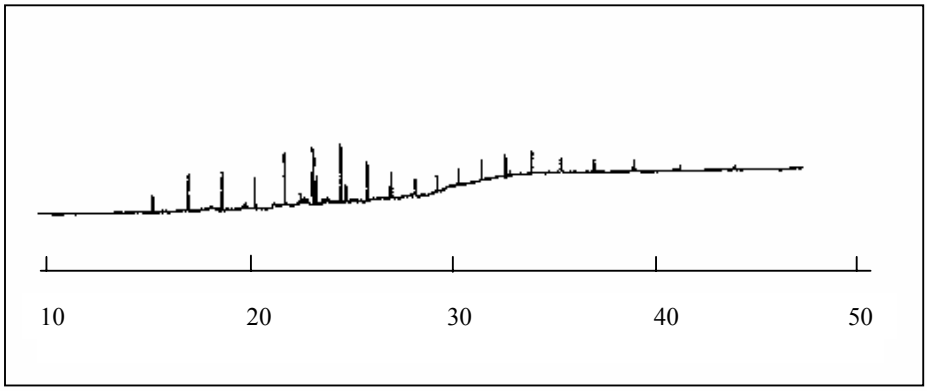

GC-MS trace of saturates from sample of Badger River bitumen. Analysis by AMDEL.

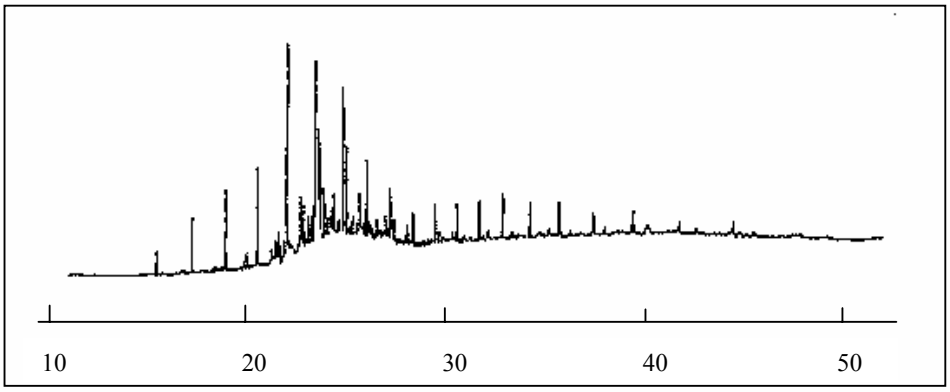

GC-MS trace of saturates from sample of Gordon Limestone, Florentine Valley. Analysis by AMDEL.

Figure 5.6. GC-MS traces of bitumen samples from Permian Cygnet Coal Measures from the Badger River and of Gordon Limestone from Florentine Valley.

These results indicate that the Comstock bitumen was not sourced from Gordon Group limestone and the low maturity suggests that the source is most likely younger. Investigations were made of Permian outcrops to the south of Zeehan along the Badger River and bitumen saturated coarse-grained quartz sandstone was located. Oil inclusions containing some gas bubbles were found in samples from these outcrops as shown in the photomicrograph, Figure 4.16. The sandstone outcrops form the upper parts of the Cygnet Coal Measures and lower in the sequence thin coal beds and thick,

black beds of siltstone are located. Rock-Eval pyrolysis of samples from these possible source beds indicates that the siltstone has the potential to generate oil and gas. A chart, Figure 5.7, comparing Rock-Eval pyrolysis results from both siltstones and coals of the Cygnet Coal Measures show that coals have distinctly higher T_{max} values than the siltstones and also lower HI values indicating that the coals have lower source potential.

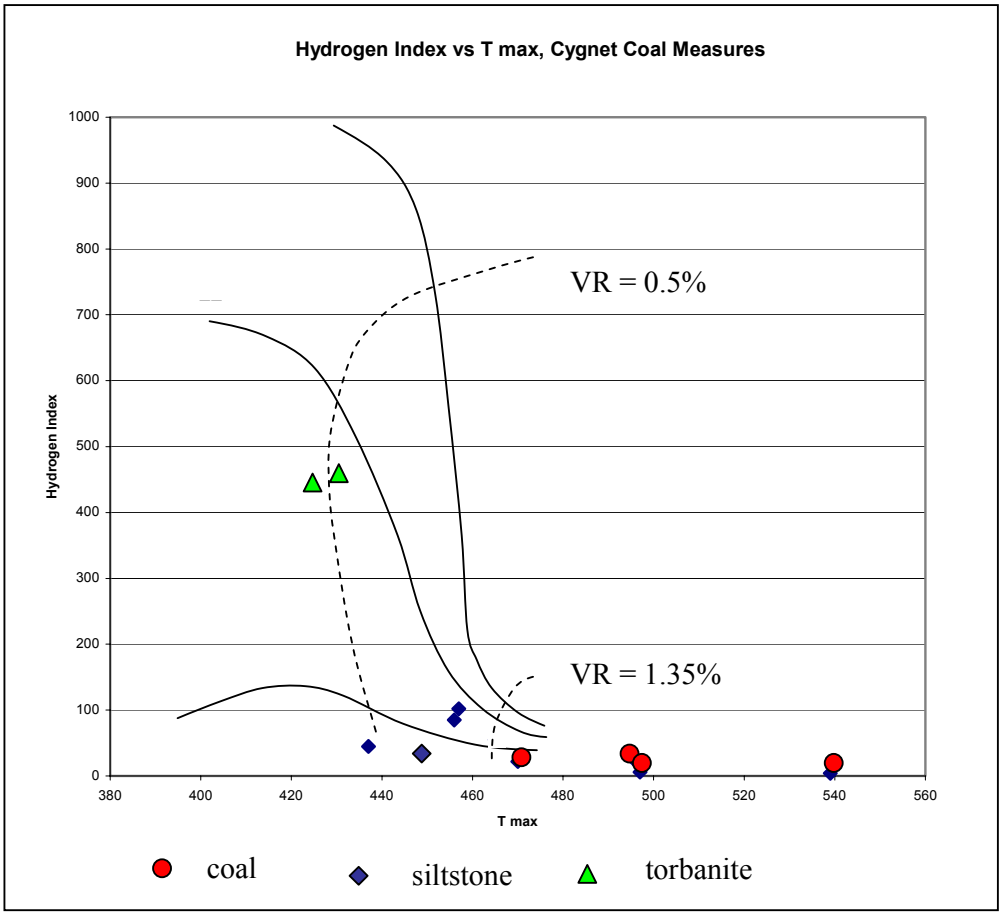

Figure 5.7. Chart showing a comparison in Rock Eval pyrolysis results from Permian coal and siltstone samples across Tasmania. Cygnet Coal Measures coal samples are shown in red and siltstone in blue to highlight differences in samples taken from similar stratigraphic levels. Note that coal samples show high T_{max} values and low HI indicating very low potential as source rocks. The siltstone samples fall within the "oil window" of maturity and have HI values indicating gas potential as source rocks. Lower Freshwater torbanite samples, shown in green, are of marginal maturity but HI values indicate good potential as source rocks. Analysis by AMDEL.

The Cygnet Coal Measures are the source beds for the bitumen found at Comstock mine and migration has occurred along faults. The source beds are likely to have had a much wider original distribution than at present, as there is evidence of deep and

widespread erosion in this area. Siltstone within the Cygnet Coal Measures can be considered to be the source of a considerable volume of oil and gas generated near Zeehan and bitumen-stained sandstone sequences can be seen between the Badger and Henty rivers. Cygnet Coal Measures outcrop over a wide area of Tasmania (Bacon, 1991), as shown in Figure 5.8, but as yet no other reports have been made of oil or gas generated from this source. The high stratigraphic level at which these sediments were deposited has probably not allowed deep enough burial for maturity to reach a level where hydrocarbon generation could occur in the main part of the Tasmania Basin. A second factor may be that organic-rich siltstones, correlates of the Cygnet Coal Measures, within the main Tasmania Basin are too thin and discontinuous to be capable of generating significant amounts of hydrocarbons.

A likely contributing factor to the generation and migration of oil/gas near Zeehan was the high heat flow in the region during rifting events associated with the separation of Tasmania and Antarctica (Kohn et al., 2002). In areas away from coastal zones heating effects from rifting may not have been as great and so source rocks did not reach maturity. Deep erosion has also occurred as evidenced by only scattered remnants of Permian-Triassic sediments remaining in the west coast region. Fission track studies also indicate that kilometre scale denudation may have occurred in this area during the Late Cretaceous (Kohn et al., 2002). Further evidence of extensive erosion in this area can be deduced from the sedimentary fill in the offshore Strahan and Port Davey Sub Basins where sedimentation started in the Late Cretaceous (Moore et al., 1992). The thickness of these offshore sediments is also evidence to the depth of erosion that must have occurred onshore and the possibility of deeper burial than has been postulated until now. Maturity measurements of Badger River samples imply a burial depth, using 30°C/km geothermal gradient, of 2 km+.

An overall representation of the Gondwanan petroleum system, onshore Tasmania, is shown in Figure 5.9.

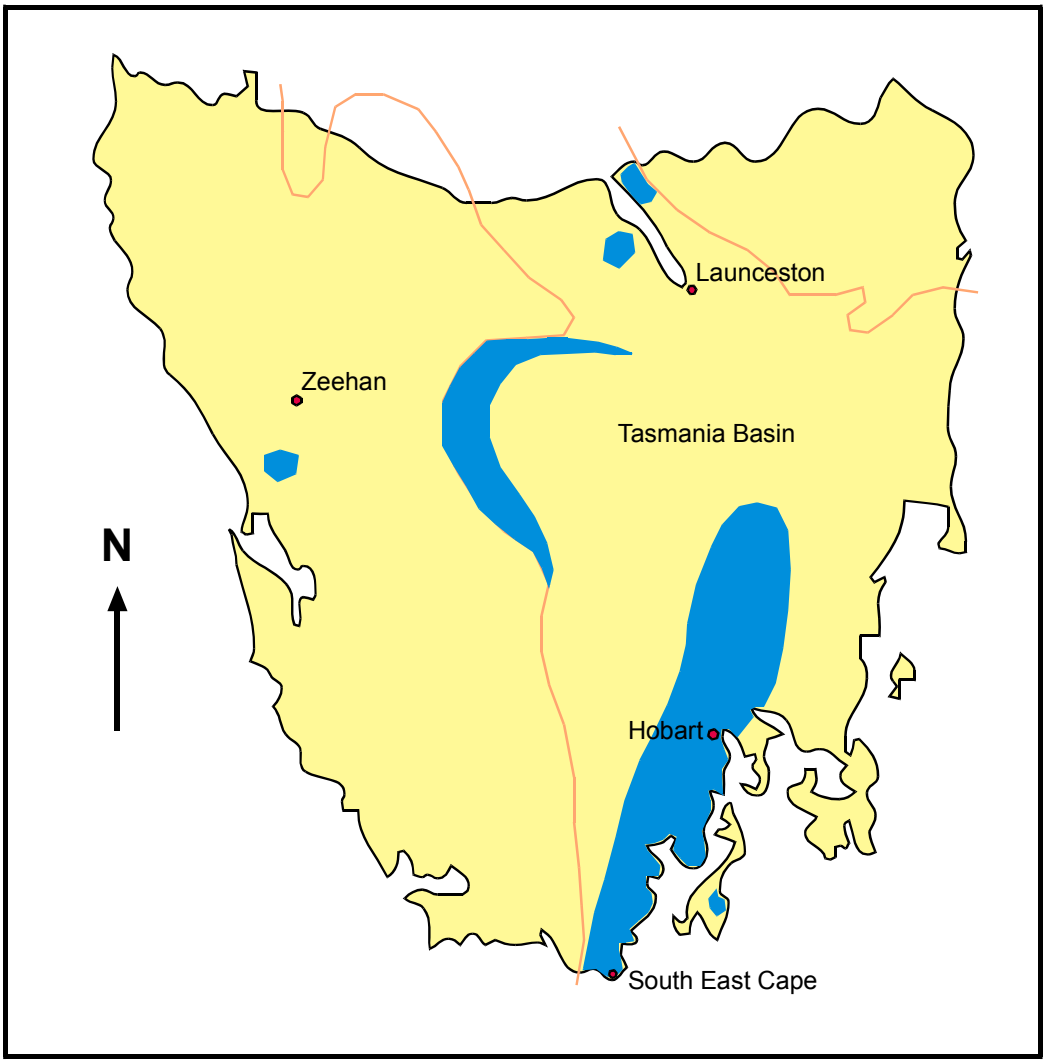

Figure 5.8. Map showing the distribution of Cygnet Coal Measures and correlates, shown as blue areas, in Tasmania. The map is a projection of underground coal found as thin, discontinuous seams. Coal beds in parts of the basin were eroded prior to deposition of overlying sequences. Orange lines indicate the margins of the Tasmania Basin. After Bacon, 1991.

GONDWANAN PETROLEUM SYSTEM

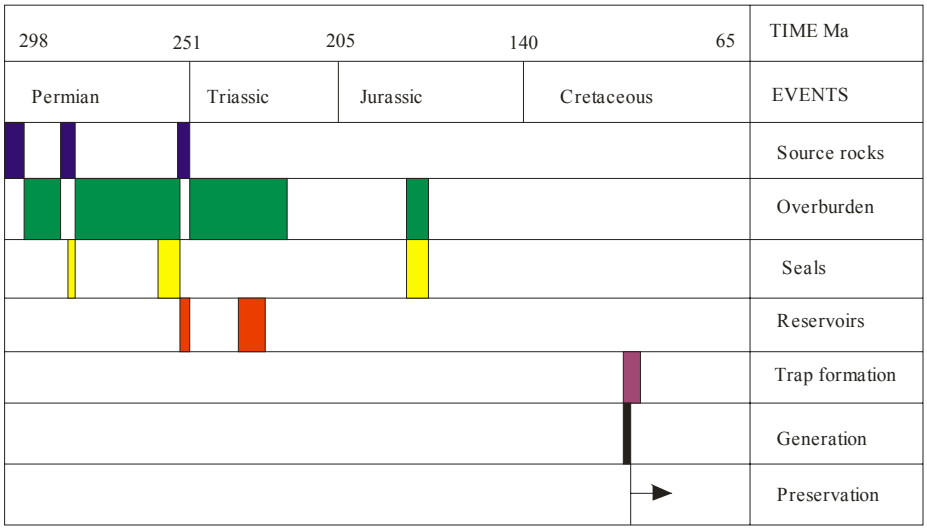

Figure 5.9. Gondwanan petroleum system diagram, for onshore Tasmania, showing the relative timings for key petroleum system elements.

5.4. Relationships between sightings of seeps and seismic events.

Tasmania has recently had a quiet period for earthquake events however swarms of these events occurred towards the end of the nineteenth century and early twentieth century until the 1930's and these periods coincide with the most frequent reporting of seeps or presumed seeps (Leaman, 1988a). First hand records of these events were recorded by Shortt (1884; 1885), who was the official meteorological observer in Tasmania at the time. Carey (1960) catalogued 2540 seismic events between 1883-1886 and further seismic activity continued intermittently until 1892. Michael-Leiba (1989) used contemporary reports to determine the magnitude and probable epicentres of the largest earthquakes from this period to help in constructing earthquake risk maps for Tasmania. It is possible that seismic pumping allowed petroleum to migrate to the surface along tight migration paths, particularly in the period 1883-1892 when earthquake events occurred at the rate of one event per month (Michael-Leiba, 1989).

Bendall (1990) collated reports of seeps and presumed seeps and plotted these on a map of Tasmania where they form NW/SE, NE/SW trends. These trends suggest that deep crustal lineaments are still active and may form migration routes for hydrocarbons (Bendall et al., 1991). Experienced petroleum geologists verified very few of these reports and so many may not in fact have been genuine oil or gas seeps.

It is of interest however that deep crustal lineaments have been identified by these seeps.

It is generally considered a good sign for potential petroleum exploration that oil or gas seeps are present. However, even the presence of seeps does not always indicate that commercially viable reservoirs are present. If petroleum reservoirs were present then the lack of seeps would suggest that very effective seals are in place and that these only intermittently leak during seismic events. As gas is potentially being generated below the Tasmania Basin gas seeps could likely be operating and these would be more difficult to detect than oil seeps. No systematic search has been made for gas seeps.

5.4.1. Seep detection.

The usual method for seep detection on land is to drive a hollow probe into the ground to a depth of 1 m+ and draw off all gases present through a seal at the top with a syringe. The sample collected can then be analysed in a gas chromatograph and any hydrocarbon levels above the normal background constitute an anomaly. For a first pass over a basin where gas seeps have not previously been detected this method may prove to be too slow and not cost effective.

Airborne detection methods may prove to be more effective for a first pass and then if anomalies are identified ground methods could be used as a follow up process. Low flying aircraft are able to collect air samples and pass these through an on board chromatograph in an attempt to detect gas haloes (Jones et al., 1999). This method may be useful over the Tasmania Basin, much of which is used for agriculture so that there are very few sources of introduced hydrocarbons that could produce anomalies to make interpretation of the results difficult.

Another potentially effective method of seep detection would be to use a gamma ray spectrometer and detect radiation emanating from concentrations of uranium and thorium. The gamma ray spectrometer could be either carried by an aircraft flown in a pattern over the Tasmania Basin or else use a satellite mounted system.

Uranium is mobile and being soluble is easily transported by groundwater. When uranium encounters organic matter, such as subsurface hydrocarbons, the ions become

insoluble and immobile. Hence higher than background levels of gamma rays may indicate the presence of a hydrocarbon trap or seeps from a hydrocarbon reservoir. Anomalies detected during a radiometric survey, not obviously related to underlying geology, could be followed up by more intensive detection methods to determine if seeps were present. This method could serve as a cost effective first pass for the detection of possible hydrocarbon seeps.

Hyperspectral imagery can also detect subtle changes caused by hydrocarbons on soil by using the spectral signatures from visible, near-infrared and short wave-infrared light (Gruber, 1999). Note that no one method should be used in isolation and results should be interpreted in the light of known geology and structures.

5.5. Potential reservoirs for the Larapintine 2 petroleum system, onshore Tasmania.

If seismic pumping has been responsible for oil seeps onshore Tasmania it is possible that petroleum reservoirs are present from which oil has been pumped and so a brief consideration will be given to potential reservoirs. A survey was made of the Tiger Range Group, which overlies the Gordon Group in the Florentine Valley area, to search for possible reservoir facies. Only the Arndell Sandstone had any reservoir potential with 2% apparent porosity. However the Arndell Sandstone is fine-grained with little permeability and on this basis cannot be considered as a viable reservoir facies. Other units within the Tiger Range Group appeared to offer potential as seal units if a reservoir did exist below.

5.5.1. Potential palaeokarst reservoirs.

Another reservoir possibility considered was palaeokarst as other carbonate hydrocarbon petroleum systems contain giant-sized petroleum accumulations in palaeokarst reservoirs such as in the Lower Ordovician, Puckett Field in west Texas and the Lower Cretaceous Lane Field in eastern Mexico (Loucks, 1999). Other palaeokarst reservoirs are found in the North China Basin, Rospo Mare Field in Italy and the west Texas, Ellenburger Field, hence the possibility for reservoirs of this type within the Gordon Group cannot be ignored. Modern karst features are widespread within the Gordon Group and this indicates the potential for any sub-aerially exposed parts during earlier epochs to also have become karstified (Kiernan, 1995).

Structural systems such as joints, faults, folding and bedding have a profound influence on the evolution of modern karst systems in Tasmania. The fold structure of the pre-Carboniferous rocks of western Tasmania, generated by compressive forces have been particularly important in this respect because fissure frequency is a principal determinant of the form cave cavities take (Ford and Williams, 1989). In order for karst landforms to be produced the carbonate rocks involved have to be sub-aerially exposed to allow meteoric waters access so that dissolution processes can occur.

If present karst systems within the Gordon Group can be shown to be of great age there is the possibility that some of these older systems may have been buried and become palaeokarst. There is also the possibility that karst systems developed before the deposition of the Parmeener Supergroup and it is systems such as these, which could provide the most potential for suitable hydrocarbon reservoirs. Palaeokarst sediments of Devonian age have been found at Eugenana (Banks and Burns, 1962). Kiernan (1995) suggests that the presence of palaeokarst phenomena of Devonian age at Eugenana provides strong grounds for suspecting karstification at least that early elsewhere in Tasmania. Kiernan (1995) also states that palaeokarst sediments are widespread within exposures in the Exit Cave Quarry and Osborne and Cooper (2001) have shown that at least two episodes of karstification leading to palaeokarst deposits have occurred at this site. The first of these events occurred during the Early Carboniferous and the second occurred during the Late Carboniferous (Osborne and Cooper, 2001). A small outcrop near Moina, in the valley of the Lea River, is a skarn of Devonian age, which has possible palaeokarst cavities predating the skarn event (Hughes, 1957).

Calver (1992) reported two underground cavities when drilling the Benjamin Limestone (Gordon Group) at Tyenna. Clay and brecciated limestone in a sandstone matrix were also encountered in this drill hole and these may represent palaeokarst sediments. Cave breccia has also been found at the surface near Settlement Road in the Florentine Valley and this may be another example of palaeokarst, which has become exposed (Goede, 1976). Palaeokarst cave fill deposits have been reported from the Growling Swallet cave in the Florentine Valley where passage development

appears to follow old deposits embedded in the walls and in other cases skirts highly lithified deposits (Clarke, 1995).

Mississippi Valley-type mineralisation occurs in three 2-3 m thick dolomitised horizons in the Gordon Group at Bubs Hill (Taylor, 1989). This style of mineralisation also occurs near Zeehan (Morris and Taylor, 1995) and it is highly likely that palaeokarst is associated with these areas as MVT mineralisation often occurs within palaeokarst of carbonate host rocks (Rhodes et al., 1984). Karstic structures exhibiting the largest cavity development and consequently the greatest amounts of infill sediments commonly host the best grades of mineralisation.

Osborne and Armstrong (1996) propose that many of the Eastern Australian cave systems have formed due to weathering of pyrite-bearing palaeokarst or other ore bodies in the limestone. To back up their claims they say that many eastern Australian cave systems feature large chambers, which appear to be out of scale with the size of cave passages connecting them and the size of presently active streamways in the caves. Weathering of palaeokarst hosted sulphide deposits will release sulphuric acid into the groundwater system, which would rapidly dissolve the limestone. Osborne and Armstrong (1996) have found weathered pyrite in dolomitic palaeokarst deposits of at least two phases at Jenolan Caves, NSW. The first phase was Late Carboniferous and the second latest Carboniferous to earliest Permian. Considerable portions of the Jenolan Caves system are ancient caves (Permo-Carboniferous) from which sulphide-bearing palaeokarst deposits have been removed by weathering.

At Wyanbene, NSW, Rowling (1995) has described how north-south trending joint sets were filled with sulphide-bearing palaeokarst sediments and these zones of possibly hydrothermally deposited materials have controlled the development of the modern cave system. Degeling (1982) described a skarn body known as Garnet Hill, near Yarrangobilly Caves, NSW, which had chalcopyrite, galena, pyrite, magnetite, chalcocite, malachite and native copper present. Degeling (1982) suggested that the original caves were either hydrothermal features filled by ore deposits or meteoric features in which ore deposits were emplaced.

A series of other cave systems in eastern Australia, Wombeyan, Bendithera, Colong, Coolemon, Mitta Mitta have occurrences of sulphide mineralisation associated with

them which seems to show a link between sulphide mineralisation and cave development. Sulphide-bearing palaeokarst has also been found at Ida Bay caves in Tasmania and these may have been emplaced during hydrothermal events either in the Permo-Triassic related to basinal fluid flow from the Tasmania basin or in the Jurassic related to doleritic magmatism (Osborne and Cooper, 2001).

Jennings (1982) says that buried karst can be difficult to recognise but gives as an example the plan of a zinc mine at Jefferson City, Tennessee where MVT mineralisation has filled what appears to be palaeokarst breccias in which two levels of the network partly overlie each other. Palaeokarst breccias of this type would provide ideal hydrocarbon reservoirs. An eastern Australian example of a possible MVT deposit is associated with the Coolemon caves in NSW. Ashley and Creelman (1975) concluded that this deposit had developed by sulphides replacing a palaeokarst breccia and they also found that bituminous material commonly occurred in fluid inclusions.

Kiernan (1989) has implied that the karst system near Lake Sydney may be a reactivated palaeokarst, which was blocked by glacial sediment. He further states that the potential exists for the occurrence of palaeokarst from Cambrian to Tertiary age to exist in Tasmania.

Loucks (1999) shows that hydrocarbon reservoirs of palaeocave origin are commonly the products of coalesced collapsed-palaeocave systems. Often cave systems form a series of levels such as the three levels of the tourist caves at Yarrangobilly, NSW (Jennings, 1982). Wherever possible water tends to find lower ways through karst and in so doing enlarges the conduits, eventually earlier higher levels are replaced and a vertical sequence of caves is generated. This sequence may be the product of climatic or tectonic conditions. For example a single uplift may be followed by a progressive dissolution of cave systems or a succession of uplifts may generate a similar system. Cyclical climatic changes could also generate a similar pattern.

If a system such as this is buried by later sedimentation the overburden pressure can lead to collapse breccias filling the former cave chambers and passages. This combination of processes can form spatially complex reservoirs that can be hundreds to thousands of metres across, commonly forming large exploration targets. Loucks

(1999) states that hard, quantitative data about the sizes of such reservoirs is difficult to access as well exposed outcrops of palaeocave systems are relatively rare.

Much of the Gordon Group lies buried beneath Parmeener Supergroup cover and the potential for palaeokarst to exist beneath this cover is quite high based on the number of palaeokarst examples found in the limited exposed outcrop. This implies that there is potential for palaeokarst reservoirs to be found within Gordon Group provided that there are mature source rocks to supply the hydrocarbons.

Palaeokarst makes up only a small proportion of the volume of its enclosing limestone. An area of 9 square kilometres was considered at Ida Bay encompassing the cave systems around Marble Hill and mapped by Kiernan (1993). In map view, as shown in Figure 5.10, the known caves make up 0.5 square kilometres or 5.5% of the area. To consider this in three dimensions the limestone is 350 m thick in this area and the cave passages average less than 3 m in diameter. Volumetrically the caves represent 0.05% of the volume of the enclosing limestone in this highly karstified area. A palaeokarst reservoir would likely be a collapse breccia and so represent an even lower percentage of volume, as the whole system is unlikely to collapse.

Mole Creek karst area is approximately 250 square kilometres in area and known caves are approximately 2 square kilometres in area representing 0.8% of the total. In volume terms this is less than 0.02% of the limestone. This suggests that Gordon Group potential karst reservoirs may be very small target zones and difficult to find beneath cover.

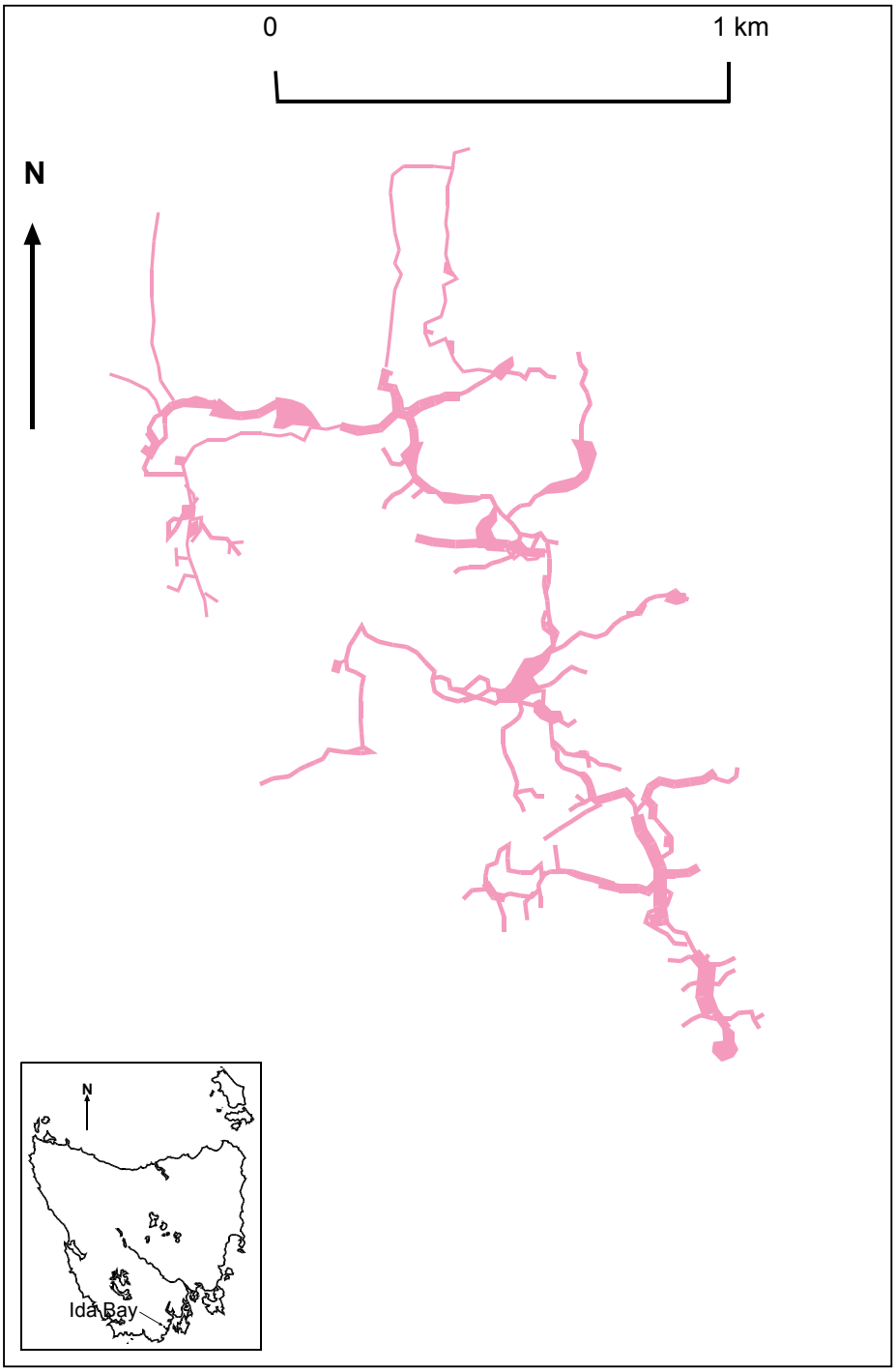

Figure 5.10. Map of the Mystery Creek cave system near Ida Bay, plotted by Kiernan (1993). A typical example of the patterns observed in Gordon Group cave systems. The volume of the cave passages represents only 0.05% of the volume of the enclosing limestone and so represents a small target if considered as a petroleum reservoir. Inset shows location of Ida Bay on map of Tasmania.

No evidence has been found of any palaeokarst reservoirs within the Gordon Group so reservoirs of this type onshore Tasmania remain as hypothetical possibilities. Palaeokarst breccia would certainly provide the necessary porosity for an ideal reservoir within an otherwise tight limestone. However it must be stated that there is no real evidence that seismic pumping has in fact occurred from reservoirs, the small amounts of oil noted by Reid (1923) appear to have been locally derived from material collected along faults and bedding planes and not from pre-Carboniferous sources.

5.5.2. Potential for fractured reservoirs.

Fine grained rocks often do not have the capacity to form petroleum reservoirs due to a lack of porosity however if these same rocks are fractured spaces formed between the rock fragments do permit these rocks to become ideal reservoirs. Fluids can flow through fractured zones and if suitable seals are in place, over and at the ends of fractured zones, petroleum can be trapped.

The tectonic history of Tasmania has provided a number of opportunities for fault and fracture zones to develop and many such zones can be seen throughout Tasmania. This would suggest that fault and fracture zones also exist below the Tasmania Basin where they could provide reservoirs for hydrocarbons possibly generated in that region. Fault and fracture zones formed in fine grained rocks would have ideal seals on each side formed by the non-fractured, fine grained rock. To form a reservoir the ends and top of such a zone would also need to be sealed. A number of potential sequences occur within the Parmeener Supergroup that could act as suitable top seals. Dolerite has also been intruded right across the Tasmania Basin and it too could act as a top seal for fractured or faulted petroleum reservoirs.

Fault zones are often intersected by later faulting in another direction and movement along the later faults can cause the ends of the original fault to become sealed by lateral movement of fine grained rocks across the faulted zone. Fault zones also tend to have finite lengths and if formed from fine grained rocks and the top is sealed any fluids entering the zone from below will be trapped.

It is highly likely fault and fracture zones occur below the Tasmania Basin and could provide ideal petroleum reservoirs. Seismic methods could be used to identify these zones during any potential exploration program.

5.6. Conclusions regarding petroleum generation onshore Tasmania.

Evidence of petroleum having been generated at different stratigraphic levels and different times throughout Tasmania's geological history has been presented. The examples from Proterozoic sequences are in areas where no known reservoir sequences occur and where the likelihood of trap structures being present is limited. The metamorphic grades of these Proterozoic sequences, even in areas considered to be of low metamorphic grade, are such that any hydrocarbons generated would likely to be degraded and no current generation could be expected. Drilling and geophysical evidence suggests that similar sequences may be present below the Tasmania Basin (Leaman, 2001; Reid et al., 2003). If Proterozoic source rocks were present below the Tasmania Basin, where trap structures and reservoir beds may be present, there could be some potential for past generation in this area and this is the reason that sequences in northwest Tasmania were investigated.

The evidence of petroleum generation from Ordovician sequences is limited and it is likely that only small amounts of petroleum were generated, probably in situations where hydrothermal fluids were active as all known occurrences are associated with sulphide mineralisation. Petroliferous odours have been detected from freshly broken Gordon Group limestone however the small amounts of hydrocarbons involved could have been generated from minor amounts of organic matter as indicated by hydrocarbons derived from the Mathinna Group in the Aberfoyle mine.

There is evidence in western Tasmania for considerable quantities of hydrocarbons having been generated from Permian sources. It is possible that a reservoir existed in the Zeehan region and that erosion removed the cap so that the contents escaped. An oil seep at Lonnavale and evidence of oil inclusions at other sites indicates that generation of hydrocarbons from Permian source rocks may have been widespread onshore Tasmania.

The small amounts of hydrocarbons noted from Neoproterozoic and Ordovician source rocks during the course of this study have been generated by localised events

and do not indicate any potential for commercially viable reservoirs of oil or gas being derived from these sources. Evidence of a probable breached reservoir with oil and gas derived from Permian source rocks is the best available evidence for potential exploration prospects onshore Tasmania. The presence of one oil seep with bitumen present probably derived from Permian source rocks do not necessarily mean that commercial quantities of hydrocarbons have been trapped. It is probable the oil and gas shows confirmed by Reid in the 1920's in the Port Sorell region may also have been derived from Permian sources, however no geochemical analysis is available to confirm this assumption. Current thermal maturity determinations for the Permian sequences in the Port Sorell region indicate immature source rocks but this does not preclude localised variations where minor generation may have occurred.

There is no evidence currently available to indicate that any petroleum has been trapped in reservoirs however there is enough evidence to show that hydrocarbons have been generated and have in some instances migrated onshore Tasmania.

CHAPTER SIX.

CONCLUSIONS IN RESPECT TO THE HYDROCARBON EXPLORATION POTENTIAL OF THE SEQUENCES INVESTIGATED ONSHORE TASMANIA.

6.1. Larapintine 2 petroleum system.

The Larapintine 2 petroleum system takes its name from the Early Ordovician Larapintine Seaway (Nicoll et al., 1988) in which excellent marine source rocks were deposited (Bradshaw, 1993). This study was based on the model that during the Ordovician, the Larapintine Seaway as shown in Figure 6.1 covered significant parts of Tasmania. Shallow tropical, platform carbonates of the Gordon Group were deposited during this time and potentially formed hydrocarbon source rocks. Overlying siliclastics of the Eldon Group potentially form reservoir and seal facies. These Palaeozoic formations were deformed into a fold and thrust belt during the Middle Devonian forming possible traps.

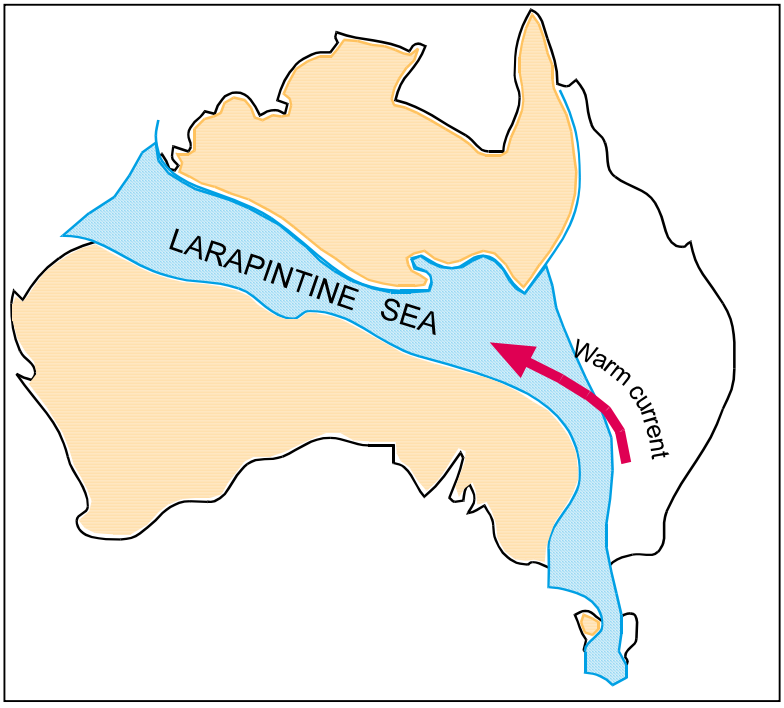

Figure 6.1. The Larapintine Seaway as it appeared across Australia during the Ordovician. After Webby (1978).

The Gordon Group has been considered during this study and as discussed in Chapter Three, the source potential is very low and source beds are thin (<200 mm) and discontinuous. In Chapter Four the maturity of potential source beds is shown to be in the late stages of the gas window. Due to the current high levels of maturity the present generative capacity is too low to build the pressures required for migration to occur so any commercial reservoirs would have had to be filled during earlier stages of migration. Migration pathways are usually stained by bitumen and the only evidence of this, within the Gordon Group, occurs in possible MVT prospects in western Tasmania. As described in Chapter Five petroleum migration probably occurred during the Early Devonian and the petroleum noted, now pyrobitumen, may have come from deeper in the basin and not from the Gordon Group.

Oil generated from the Gordon Group during the Early Devonian could not have been preserved because trap structures were not in place. Events such as the Tabberabberan Orogeny, Jurassic dolerite intrusions, Cretaceous igneous intrusions, Tertiary rifting and igneous intrusions would all have had deleterious effects on any reservoirs of petroleum generated before the mid-Devonian.

The basement below the Tasmania Basin is known to have undergone complex folding, thrusting and faulting as shown on seismic interpretations (Blackburn, 2004; Stacey, 2004). Exposures of basement structures outside the Tasmania Basin also indicate the probable complexity hidden under Parmeener Supergroup cover. Such complex structures are likely to allow only limited drainage into any potential gas reservoirs, assuming gas generation has occurred since Devonian deformation, so any potential reservoirs would be small.

Near most oil or gas fields seeps are noted in the vicinity (Hunt, 1995), but no such seeps have been detected from Ordovician source rocks, onshore Tasmania. This does not rule out the possibility of commercially viable reservoirs being found but it does suggest that the possibility is low. The probability is that gas would be the main hydrocarbon generated by Ordovician source rocks, onshore Tasmania, and seeps from a gas reservoir would be more difficult to detect than oil seeps. The potential prospective zone is below closely settled farmland so it is likely than any seep of note would have been detected.

A further problem with the Larapintine 2 petroleum system, onshore Tasmania, is that there is no direct evidence that Gordon Group rocks occur in the area inferred to be mature for gas beneath the Tasmania Basin. It is assumed that Gordon Group extends at depth from outcrops on the western side to below the Tasmania Basin and geophysical interpretations based on gravity and magnetics support this interpretation. However as shown in Figure 4.20 the basement lithology below the potential prospective zone for the Larapintine petroleum system is largely unknown.

The results of this investigation, considering source rock potential and source rock maturity, show that it is unlikely for commercially viable reservoirs of hydrocarbons to be located onshore Tasmania from the Larapintine 2 petroleum system.

6.2. Potential for Neoproterozoic hydrocarbon source rocks, onshore Tasmania.

The Centralian 1 petroleum system is hosted within Neoproterozoic carbonates, evaporates and shales in the Amadeus, Ngalia, Georgina, Officer, Birrindudu and Savory Basins of mainland Australia. These basins were all once part of the Centralian Superbasin, which covered much of Australia although the extent is not fully known (Logan et al., 1999). A map of the Centralian Superbasin, Figure 6.2, shows possible Tasmanian components. Preiss (2000) presents evidence showing connections between the Centralian Superbasin, the Adelaide Geosyncline, Tasmania and the Ross Orogen thus suggesting that a much greater area for the Centralian deposition than just the dismembered basins mentioned above. Oil and gas shows have been discovered within this system but as yet no commercial discoveries have been made. The system has analogs in Siberia and Oman where commercial fields are currently producing from Precambrian source rocks.

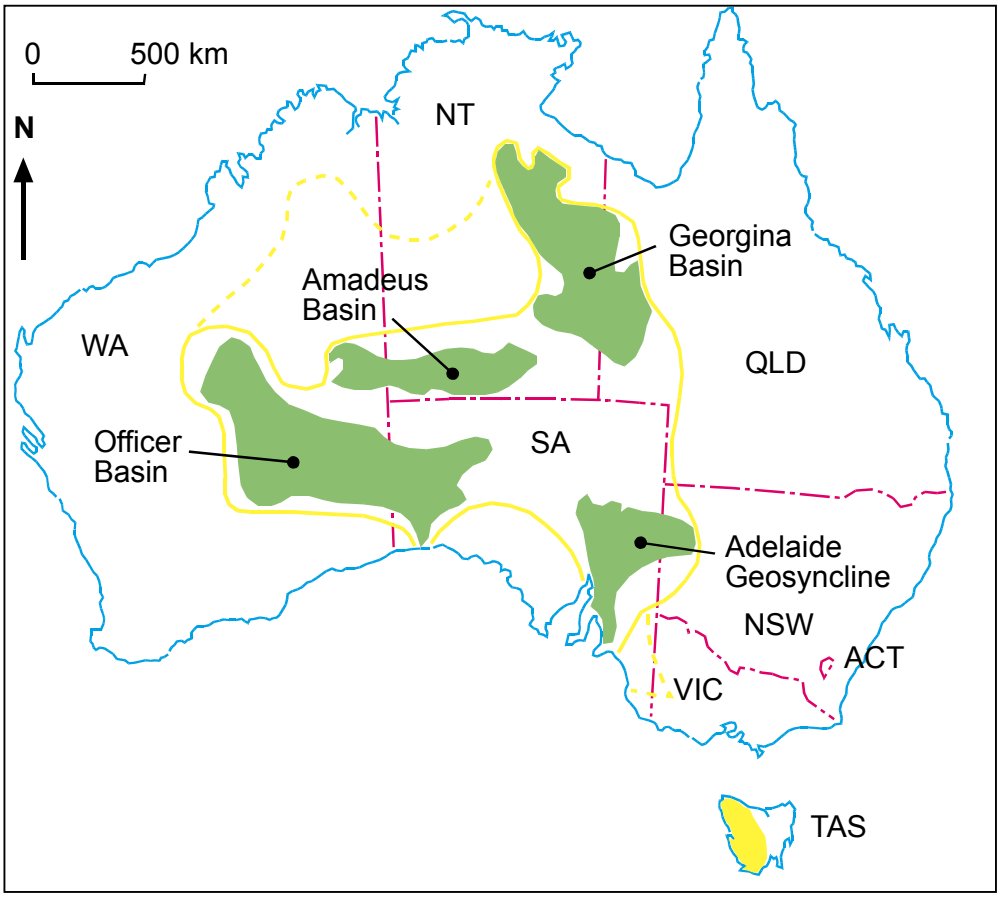

Figure 6.2. Component basins of the Centralian Superbasin are shown in solid green with the outline of the accepted extent of the superbasin shown as a yellow continuous line. Dashed yellow lines show possible extensions to the superbasin, as suggested by Preiss, in northwestern Australia and near the South Australian-Victorian border. Possible extent of the superbasin in Tasmania is shown in solid yellow. Map based on Logan et al., (1999) and Preiss (2000).

The location of Tasmania during the Neoproterozoic is unknown but Calver and Walter (2000) have noted similarities between sediments of this age on King Island and the Adelaide Fold Belt. Li and Powell (2001) have suggested that the Precambrian parts of Tasmania may have been part of a southern extension of the South China Block, which broke away from the rest of Australia during the break-up of Rodinia. Tasmania later broke away from the South China Block and was transported to its present position by at least the Early Ordovician. Recent age determinations from metamorphic rocks on western King Island indicate possible Mesoproterozoic basement in southeastern Australia and this removes a major problem in the correlation of the Adelaide Fold Belt with northwestern Tasmania.

Deformation ages of 1300 Ma for King Island may correlate with similar aged events in the Musgrave Block and also with a metamorphic belt hidden beneath the Transantarctic Mountains (Berry et al., 2005). These correlations would suggest that northwestern Tasmania has remained near its present position since the Mesoproterozoic. There are definite correlations between Neoproterozoic sediments on King Island and some within the Rocky Cape Block of northwestern Tasmania and it is possible these were once all part of the Centralian Superbasin. Correlations have also been made between Rocky Cape Block units and other Precambrian units in Tasmania such as the Weld River Group and the Savage River Dolomite.

In Chapter Four it was shown that the maturity levels of Neoproterozoic potential source rocks in northwestern Tasmania are almost to greenschist facies and so have no capacity to generate hydrocarbons. Potential correlates of Neoproterozoic sequences in northwestern Tasmania may occur beneath the Tasmania Basin but these would also be expected to have at least greenschist facies levels of maturity. The long and turbulent geological history these Neoproterozoic rocks have undergone also reduces the potential for preservation of any hydrocarbons generated during times when potential source rocks may have been mature for generation.

From the results of drilling and geophysical investigations it would appear that sediments of Neoproterozoic age are widespread but due to their high maturity they have no potential as source rocks. The results of this investigation demonstrate that it would be futile to explore for hydrocarbons generated from Neoproterozoic source rocks, onshore Tasmania.

6.3. Hydrocarbon potential of Permian coals and associated siltstones, onshore Tasmania.

As shown in Chapter Three, the Permian coals and associated siltstones investigated during this study have good to excellent source potential. Maturity, as shown in Chapter Four, ranges from immature in northern Tasmania to marginal oil maturity near St Marys and then to oil maturity across the southern Tasmania Basin. In the far southern Tasmania Basin these rocks are within the gas range of maturity as shown in Figure 4.2.

Permian coal and siltstone source rocks have generated and expelled both oil and gas in a western outlier of the Tasmania Basin, near Zeehan, as described in Chapter Five. A likely contributing factor to the generation and migration of oil/gas near Zeehan was the high heat flows in the region during rifting events associated with the separation of Tasmania and Antarctica (Kohn et al., 2002). Deep erosion has also occurred as evidenced by only scattered remnants of Permian-Triassic sediments remaining in the west coast region. Measured maturity of potential Permian petroleum source rocks is further evidence for deep erosion showing that up to two kilometres of overburden is now missing. Fission track studies also indicate that kilometre scale denudation may have occurred in this area during the Late Cretaceous (Kohn et al., 2002). Further evidence of extensive erosion of this area can be deduced from the sedimentary fill in offshore Strahan and Port Davey Sub Basins where sedimentation started in Late Cretaceous (Moore et al., 1992).

The Permian source rocks considered in this study appear to have limited distributions within the Tasmania Basin and occur only as thin discontinuous beds (<700 mm). No evidence was found during this study for petroleum generation within the Tasmania Basin from the coal or siltstone source rocks investigated.

6.4. Conclusions in regard to overall petroleum prospectivity, onshore Tasmania.

Source rock potential and maturity of three potential petroleum systems have been investigated onshore Tasmania. All three petroleum systems appear to have components either within or below the Tasmania Basin. The Centralian petroleum system has no suitable source rocks because the maturity levels are too high for hydrocarbons to be generated.

The Larapintine 2 petroleum system has only very thin potential source beds with low generative potential and maturity in the late gas window. No evidence has been found for seeps from this system and the only evidence for migration is from possible MVT prospects for Pb-Zn where it is debatable whether the petroleum involved actually came from Ordovician sources. Only inferences have been made about the existence of Gordon Group in the zone inferred to be mature for gas generation from this petroleum system. Generation of petroleum is inferred to have commenced before

traps were in place, as explained in Chapter Five, and the post-generative tectonic events have not been conducive to hydrocarbon preservation.

The results of this investigation would suggest that there is no potential for commercially viable hydrocarbon reservoirs to be hosted from the Larapintine 2 petroleum onshore Tasmania.

The Gondwanan petroleum system has some potential, onshore Tasmania, as there has been positive evidence of petroleum being generated and expelled from this system. Examples of petroleum generated from this system include a seep at Lonnavale and oil inclusions within rocks from a variety of places in southern Tasmania. Bitumen impregnated rocks near the Badger River, south of Zeehan, indicate that a possible breached reservoir occurs and geological, source rock maturity and geochemical evidence indicates a Permian source.

Source rocks for the Gondwanan petroleum system have been deposited widely across the Tasmania Basin however the coal and siltstone source rocks considered in this study appear to have limited distributions and thin beds so that the potential volume of petroleum that could be generated would be too low for commercial viability. No suitable trap structures have been identified in the essentially flat lying and complexly faulted Parmeener Supergroup in the southern Tasmania Basin. The evidence that suitable source rocks are present and that hydrocarbon generation has actually taken place does justify a search for suitable trap structures.

APPENDIX A.

Rock-Eval pyrolysis.

Rock-Eval pyrolysis is a method used to rapidly evaluate the petroleum-generative potential and thermal maturity of rocks developed by Espitalie et al. (1977) .The technique involves heating pulverised rock under an inert atmosphere and analysing the evolved gases. Quantitative and reproducible parameters from this process allow comparison of samples rapidly and inexpensively and the data obtained can be readily compared to other methods, such as elemental analysis for source rock potential and vitrinite reflection for maturity.

The technique involves passing a stream of helium through 100 mg of pulverised rock heated initially at 300°C. The temperature is then programmed to increase at about 25°C/min up to 550°C. The vapours are analysed with a flame ionisation detector (FID), resulting in peaks as shown in Figure A.1. The first peak represents any free hydrocarbons in the rock that were either present at the time of deposition or were generated from the kerogen since deposition and these are reported as S_1. Heating at 300°C simply distils the free hydrocarbons out of the rock (Hunt, 1995).

The carboxyl groups in the kerogen break off between 300°C and 350°C, yielding CO_2, which is trapped and analysed later during the cooling cycle using a thermal conductivity detector (TCD) and reported as S_3. Between about 350°C and 550°C, hydrocarbons are generated by cracking the kerogen until only residual non-generating carbon remains and reported as S_2. In addition high molecular-weight bitumen that was not distilled out and reported in S_1 is cracked into smaller molecules and included in S_2.

The areas under the curves are labelled S_1, S_2 and S_3 respectively with S_1 and S_2 being proportional to the flame ionisation detector (FID) carbon in the vaporized products. Results are reported as milligrams of hydrocarbon based on calibrating the detector with standards. The TOC value is calculated separately.

The ratio of mg HC in S_2/g TOC is called the Hydrogen Index (HI). The ratio of mg CO_2 in S_3/g TOC is called the Oxygen Index (OI). Hydrogen Index can be roughly

correlated with atomic H/C ratio and Oxygen index (OI) with the atomic O/C ratio of the van Krevelen diagram.

As kerogen breaks down and loses hydrocarbons with greater burial, peak two gets smaller and peak one, which represents the released hydrocarbons, gets larger. Dividing the area (S_1) by the combined areas S_1 and S_2 yields the Production Index (PI). This value increases steadily during hydrocarbon generation and the beginning of significant oil generation is around a PI of 0.1 and the end of oil generation around 0.4.

As generation proceeds, higher temperatures are required to crack the remaining kerogen but the temperature at which maximum hydrocarbon generation occurs is recorded as T_{max}. The beginning of oil generation starts at around T_{max} 430°C and ends at around T_{max} 460°C. Rock-Eval pyrolysis T_{max} is frequently used as a maturity indicator, because as the maturity of the kerogen increases the temperature at which maximum pyrolysis occurs also increases. Actual T_{max} temperatures are dependent upon kerogen type so when comparing maturity values with other maturity measurements the type of kerogen must be considered. T_{max} values for small S_2 peaks (<0.2 mg HC/g TOC) are unreliable.

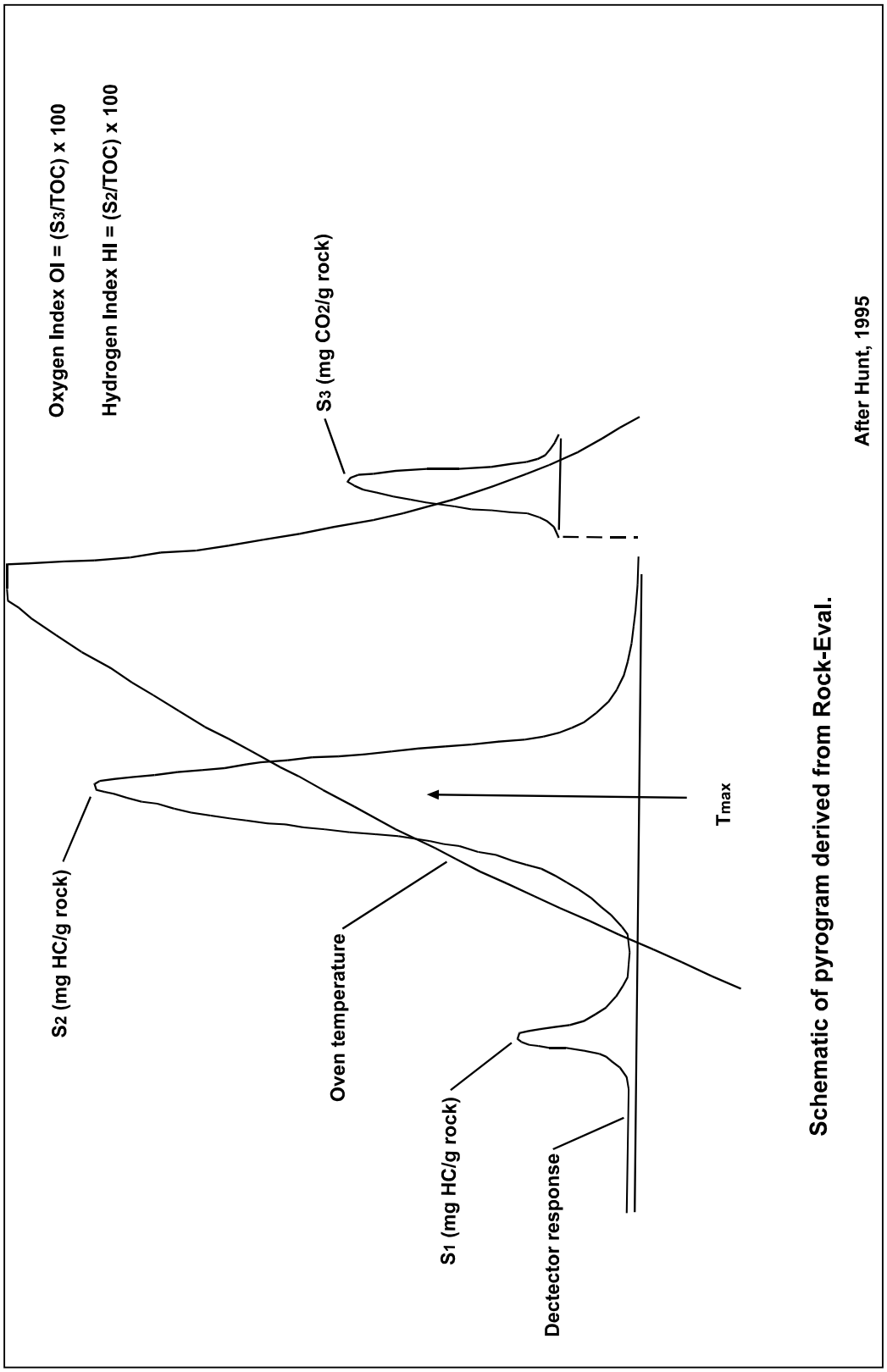

Figure A.1. Schematic representation of the pyrogram derived from Rock-Eval pyrolysis. Peak S_1 indicates the hydrocarbons distilled from the sample at 300°C. Peak S_2 are the hydrocarbons generated during pyrolysis and the temperature at which

the maximum hydrocarbons are generated is termed T_{max}. The total of S_1 and S_2 give an estimate of the generative potential of the sample. S_3 is a measure of the organic CO_2 generated by the sample up to 390°C. The flat-topped curve illustrates the oven temperature during pyrolysis. TOC is determined separately so that HI and OI can be calculated. After Hunt, (1995).

Rock-Eval pyrolysis reports.

The results of Rock-Eval pyrolysis are reported using a set of parameters based on the peaks of the pyrogram as explained above. The figures reported are listed below with the units as shown.

Parameter	**Unit**
T_{max}	°C
S_1- Volatile hydrocarbons	mg/g
S_2-HC generating potential	mg/g
S_3- Organic carbon dioxide	mg/g
$S_1 + S_2$- Potential yield	mg/g
PI-Production Index	
S_2/S_3	
PC-Pyrolysized carbon	mg/g
HI-Hydrogen Index	
OI-Oxygen index	
TOC- Total organic carbon	Weight %

The results are normally displayed as a plot of Hydrogen index versus T_{max}, which allows visualisation of kerogen type and maturity on the one plot. Figure A.2 shows a sample plot of Hydrogen index versus T_{max} with indications of ranges for oil generation and maturity limits.

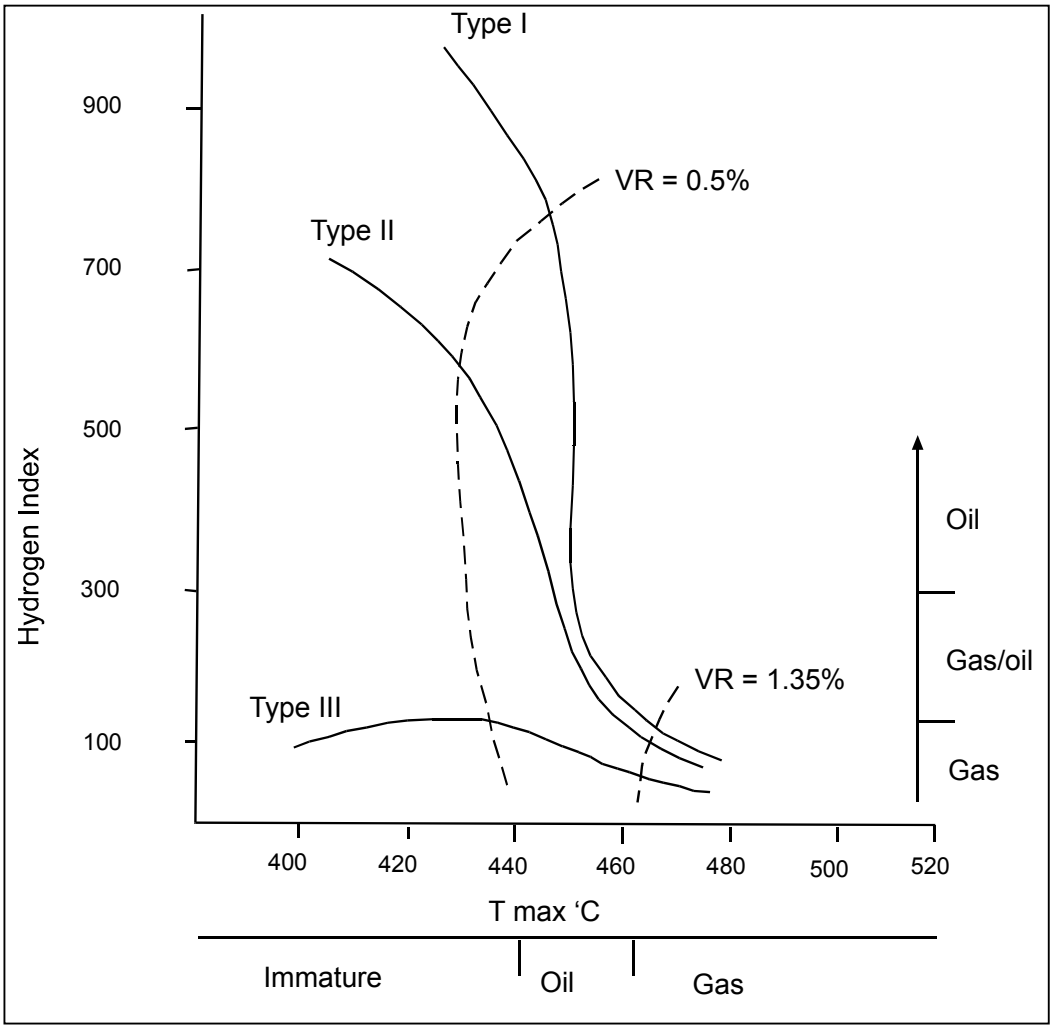

Figure A.2. Sample Hydrogen Index versus T_{max} plot as used to display data from Rock-Eval pyrolysis. Horizontal scale indicates maturity as defined by T_{max} and lower scale indicates maturity ranges for immature, oil and gas. Vertical scale uses Hydrogen Index to show source rock potential and scale on right hand side of diagram indicates likely hydrocarbons to be generated over particular ranges of Hydrogen Index values. Curved lines indicate the theoretical maturation pathways for Types I, II and III kerogen. Dashed curved lines indicate approximate equivalent vitrinite reflection maturity for the beginning and end of oil generation. The position a sample plots on this chart enables a direct assessment of source potential, maturity and kerogen type to be made.

Evaluation of the Rock-Eval pyrolysis parameters.

Generative potential.

Potential	**TOC**	**S_1**	**S_2**
Poor	0-0.5	0-0.5	0-2.5
Fair	0.5-1.0	0.5-1.0	2.5-5.0
Good	1.0-2.0	1.0-2.0	5.0-10.0
Very good	2.0+	2.0+	10.0+

Type of hydrocarbon likely to be generated.

Type	**HI (Hydrogen Index)**	**S_2/S_3 (Type Index)**
Gas	0-150	0-3
Gas and oil	150-300	3-5
Oil	300+	5+

Level of thermal maturation.

Maturation	**PI**	**T_{max} (°C)**	**R_o (%)**
Begin oil gener.	~0.1	~435	~0.6
End oil gener.	~0.4	~470	~1.4

Note: many maturation parameters depend on type of organic matter.

Type Index (S_2/S_3).

<2 gas, >5 oil.

Kerogen Types.

Type I, highly oil prone.

Type II, oil prone.

Type III, gas prone.

Type IV, inert.

(Peters, 1986).

References.

Espitalie, J. M., M. Madec, B. P. Tissot, J. J. Mennig, and P. Leplat, 1977, Source rock characterisation method for petroleum exploration: 9th Annual Offshore Technology Conference, p. 439-448.

Hunt, J. M., 1995, Petroleum geochemistry and geology: New York, W.H.Freeman and Company, 743 p.

Peters, K. E., 1986, Guidelines for evaluating petroleum source rock using programmed pyrolysis: American Association of Petroleum Geologists Bulletin, v. 70, p. 318-329.

APPENDIX B.

Rock-Eval pyrolysis data.

Sample	Site	Tmax	S1	S2	S3	S1 + S2	PI	S2/S3	PC	HI	OI	TOC
Rocky Cape Block												
SRSS	Salmon R	501	0.07	0.47	2.55	0.54	0.13	0.18	0.04	55	303	0.85
CS1	Cowrie Pt	470	0.06	0.32	0.33	0.38	0.16	0.96	0.03	22	22	1.45
CP2	Cowrie Pt	489	0.02	0.49	0.21	0.51	0.04	2.33	0.04	76	32	0.64
CP3	Cowrie Pt	402	0.28	0.77	0.14	1.05	0.27	5.5	0.08	56	10	0.64
CP4	Cowrie Pt	497	0.03	0.16	0.5	0.19	0.17	0.32	0.01	22	71	0.7
AR1	Apiary R	475	0.04	0.13	0.57	0.17	0.25	0.22	0.01	3	14	3.24
TB1	Tayatea B	458	0.02	0.06	0.25	0.08	0.25	0.24	0	3	13	1.85
JR1	Julius R	439	0.02	0.03	0.32	0.05	0.5	0.09	0	1	15	2.08
Gordon Group												
UL25	Florentine	469	0.02	0.26	0.4	0.28	0.07	0.65	0.02	33	51	0.78
CB13	Florentine	446	0.01	0.1	0.17	0.11	0.1	0.58	0	22	37	0.46
CB14	Florentine	467	0.01	0.04	0.19	0.05	0.25	0.21	0	3	16	1.16
SM1	Florentine	461	0.02	0.09	0.23	0.11	0.2	0.39	0	22	57	0.4
11R1	Florentine	518	0.01	0.15	0.26	0.06	0.06	0.58	0.01	10	18	1.37
WQR1	Florentine	544	0.03	0.26	0.38	0.29	0.11	0.68	0.02	14	20	1.83
CB16	Florentine	545	0.03	0.43	0.51	0.46	0.07	0.84	0.03	74	87	0.58
CB26	Florentine	508	0.05	0.24	0.24	0.29	0.18	1	0.02	34	34	0.7
CB30	Florentine	488	0.03	0.19	0.33	0.22	0.14	0.57	0.01	44	76	0.43
CB32	Florentine	520	0.06	0.49	0.75	0.55	0.11	0.65	0.04	76	117	0.64
17 2	Florentine	522	0.01	0.31	0.28	0.32	0.03	1.1	0.02	54	49	0.57
17 16	Florentine	439	0.02	0.41	0.53	0.43	0.05	0.77	0.03	51	66	0.8
MC1	Florentine	467	0.07	0.23	0.14	0.3	0.23	1.64	0.02	28	17	0.8
LR2	Lune Riv	496	0.14	0.24	0.16	0.38	0.37	1.5	0.03	34	22	0.7
Cygnet Coal Measures and correlates												
BP1	Piper's R	431	0.04	0.05	0.08	0.09	0.5	0.62	0	1	2	3.24
BR7	Badger R	437	0.69	21.82	14.4	22.51	0.03	1.51	1.87	45	30	47.8
LC1	Leprana	497	0.2	2.29	5.69	2.49	0.08	0.4	0.2	6	17	32.9
59 494	Badger R	450	0.15	0.9	1.78	1.05	0.14	0.51	0.09	34	67	2.65
MQ2	Mallana	456	0.4	2.9	0.58	3.3	0.12	5	0.27	85	17	3.4
MQ3	Mallana	457	0.35	3.33	0.33	3.68	0.1	10.09	0.3	102	10	3.25
MQC1	Mallana	465	0.28	2.65	1.76	2.93	0.1	1.5	0.24	55	37	4.75
CCM2	Sth Cape	539	0.17	0.69	0	0.86	0.2		0.07	4	0	14.3
MQC2	Mallana	496	0.25	1.43	1.35	1.68	0.15	1.05	0.14	23	21	6.15
Cotas Creek torbanite												
Cat 1	Cotas C	424	24.4	311.7	0	336.11	0.07	0	28	442	0	70.4
Cat 2	Cotas C	432	8.09	265	6.33	273.12	0.03	41.86	22.76	354	8	74.8

All analyses by AMDEL.

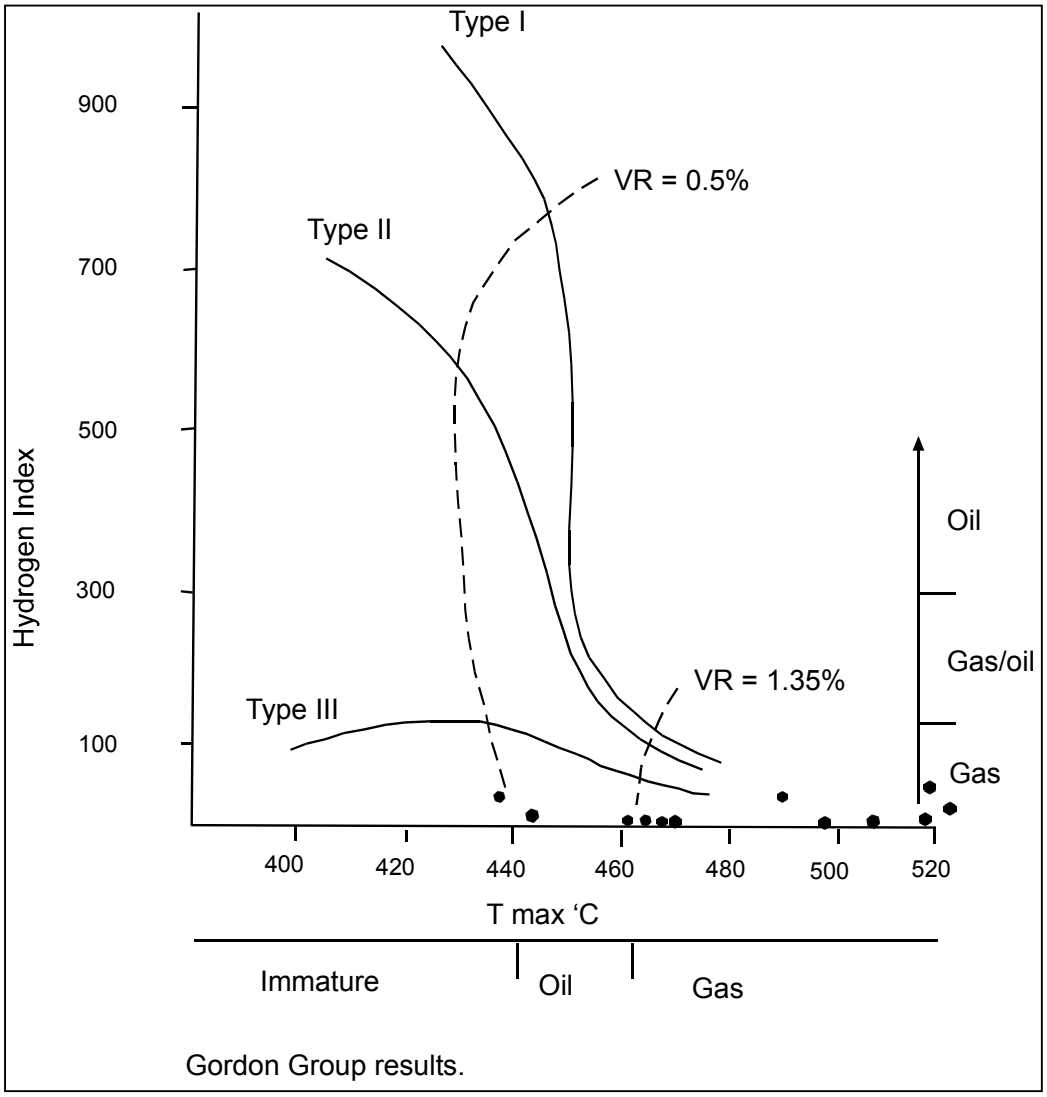

Figure B.1. Rock-Eval pyrolysis results for Gordon Group samples portrayed as a Hydrogen Index vs T_{max} chart.

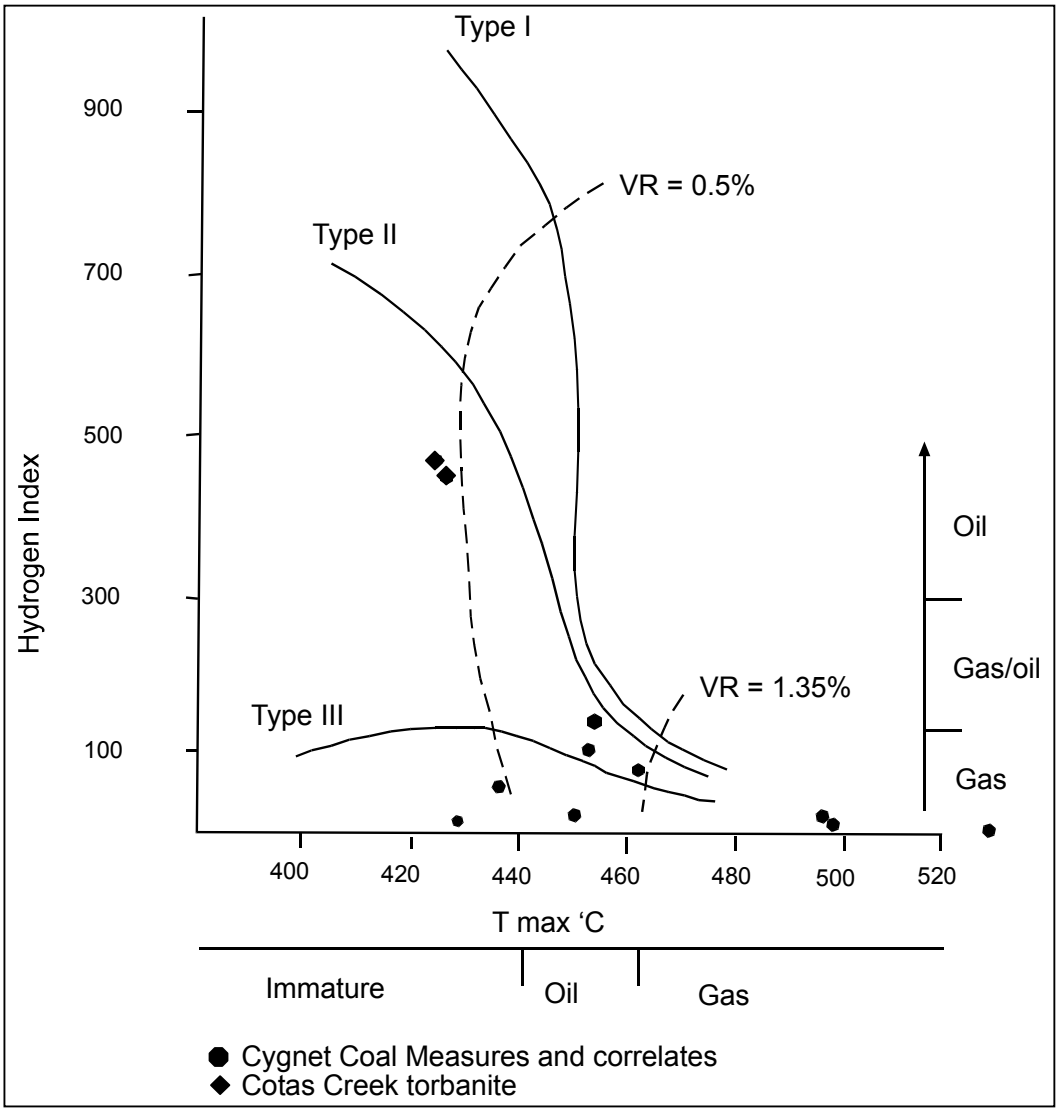

Figure B.2. Rock-Eval pyrolysis results for samples from the Cygnet Coal Measures and correlates, plus the Cotas Creek torbanite samples portrayed as a Hydrogen Index vs T_{max} chart.

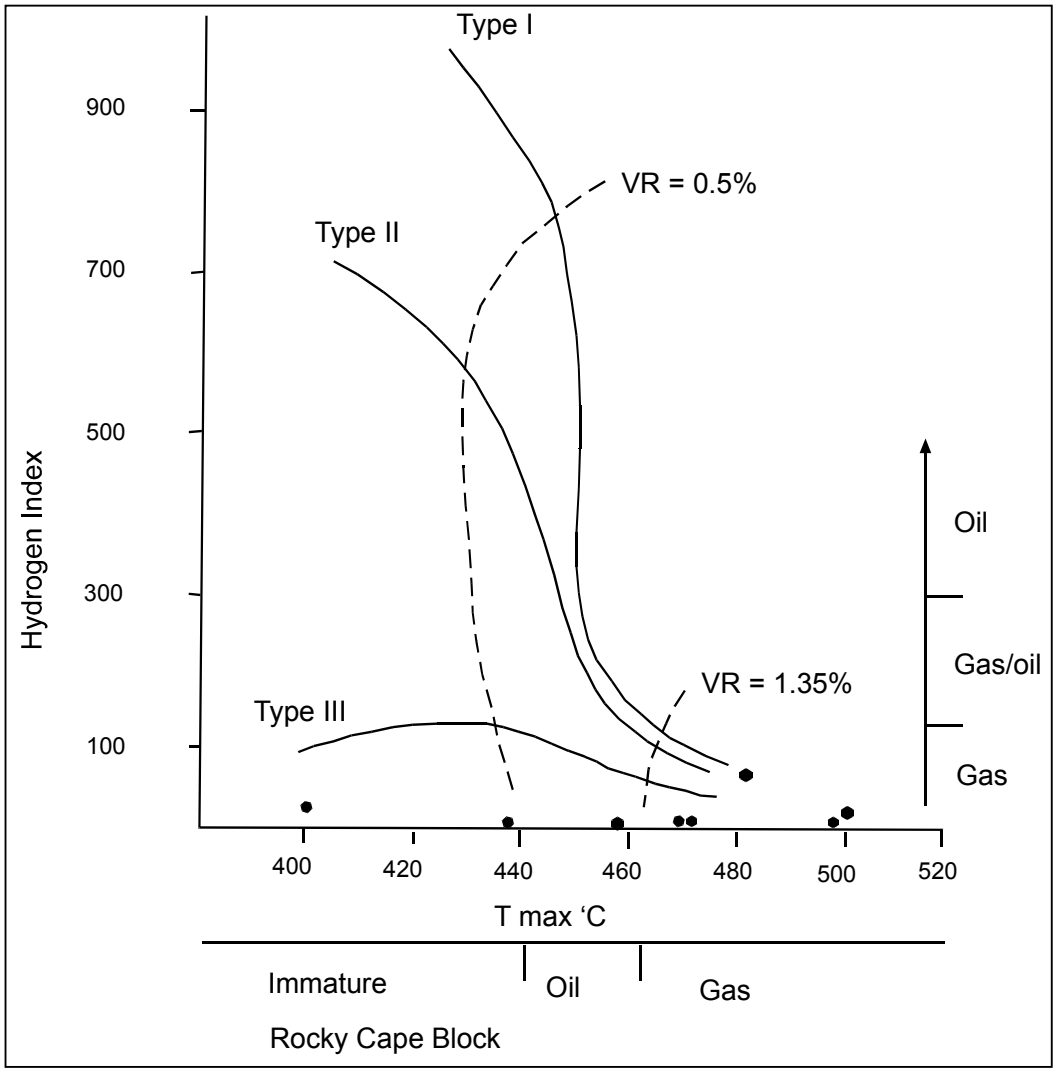

Figure B.3. Rock-Eval pyrolysis results for samples from the Rocky Cape Block portrayed as a Hydrogen Index vs T_{max} chart. These results are however erroneous probably due to contained bitumens/pyrobitumens suppressing T_{max} during pyrolysis as described in Chapter 4. Four of the eight samples also have S_2 values below 0.2 mg HC/gTOC rendering the results unreliable.

APPENDIX C

Sample locations.

ID	Lith.	Easting	Northing	DDH	Depth	Thin	Age	UTAS
H1	Dol.	495600	5326300	Hunterston	977.8	TS	PC	157291
H2	Dol.	495600	5326300	Hunterston	984.8	TS	PC	157292
H3	Dol.	495600	5326300	Hunterston	1010.5	TS	PC	157293
H4	Dol.	495600	5326300	Hunterston	1020.5	TS	PC	157294
H5	Dol.	495600	5326300	Hunterston	1025.9	TS	PC	157295
H6	Dol.	495600	5326300	Hunterston	1041.9	TS	PC	157296
H7	Dol.	495600	5326300	Hunterston	1098.6	TS	PC	157297
H8	Dol.	495600	5326300	Hunterston	1181.0	TS	PC	157298
H9	Dol.	495600	5326300	Hunterston	1291.0	TS	PC	157299
H10	Dol.	495600	5326300	Hunterston	1301.9	TS	PC	157300
UL1	L'st.	459200	5279200				Ord.	157301
UL2	L'st.	459200	5279100				Ord.	157302
UL3	L'st.	459200	5279100				Ord.	157303
UL4	L'st.	459200	5279100				Ord.	157304
UL5	L'st.	459200	5279100				Ord.	157305
UL6	L'st.	459000	5279000				Ord.	157306
UL7	L'st.	458900	5279200				Ord.	157307
UL8	L'st.	458900	5279200				Ord.	157308
UL9	L'st.	458800	5279200				Ord.	157309
UL10	L'st.	458800	5279000				Ord.	157310
UL11	L'st.	458800	5278500			TS	Ord.	157311
UL12	L'st	458800	5278400				Ord.	157312
UL13	L'st.	458800	5278500				Ord.	157313
UL14	L'st.	459000	5278700				Ord.	157314
UL15	L'st.	458900	5278500				Ord.	157315
UL16	L'st.	459000	5278400				Ord.	157316
UL17	L'st	459000	5278400				Ord.	157317
UL18	L'st.	458900	5278500				Ord.	157318
UL19	L'st.	458800	5278500				Ord.	157319
UL20	L'st.	458800	5278500				Ord.	157320
UL21	L'st.	459300	5278100				Ord.	157321
UL22	L'st.	459400	5278100				Ord.	157322
UL23	L'st.	459300	5278100				Ord.	157323
UL24	L'st.	459400	5278100				Ord.	157324
UL25	L'st.	459300	5278100				Ord.	157325
UL26	L'st.	459300	5278000				Ord.	157326
UL27	L'st.	459100	5277900				Ord.	157327
UL28	L'st.	459100	5277900				Ord.	157328
UL29	L'st.	459100	5277900			TS	Ord.	157329
UL30	L'st.	459000	5277900				Ord.	157330
UL31	L'st.	458900	5278900				Ord.	157331
UL32	L'st.	458900	5278900				Ord.	157332
UL33	L'st.	458800	5278900				Ord.	157333
UL34	L'st.	458800	5278800				Ord.	157334

UL35	L'st.	458800	5279200				Ord.	157335
UL36	L'st.	458900	5279300				Ord.	157336
UL37	L'st.	458900	5279400				Ord.	157337
UL38	L'st.	458900	5279400				Ord.	157338
UL39	L'st.	459100	5279200				Ord.	157339
UL40	L'st.	459100	5279200				Ord.	157340
LR2	L'st.	488775	5187105	DLR5-4	70.6		Ord.	157341
LR3	Shale	488705	5187555	DLR7	439.8	TS	Ord.	157342
LR4	L'st.	488775	5187105	DLR5-4	16	TS	Ord.	157343
SM1	L'st.	452500	5287400				Ord.	157344
11R1	L'st.	453300	5284215				Ord.	157345
WQR1	Shale	458000	5277600				Ord.	157346
172	Shale	453300	5280600				Ord.	157347
1716	Shale	453300	5280400				Ord.	157348
MC1	L'st.	487350	5187650				Ord.	157349
175	L'st.	453000	5281900				Ord.	157350
MQ2	Sil'st.	359400	5348800				Perm	157351
MQ3	Sil'st.	359400	5348800				Perm	157352
MQC1	Coal	359400	5348800				Perm	157353
MQC2	Coal	359400	5348800				Perm	157354
590494	Sil'st.	359000	5349400				Perm	157355
BR7	Sil'st.	358620	5349015				Perm	157356
LC	Coal	489700	5180200				Perm	157357
BP1	Sil'st.	511000	5437650			Palyn	Perm	157358
Cat1	Coal	597000	5402700				Perm	157359
Cat2	Coal	597000	5402700				Perm	157360
CCM2	Coal	485645	5171350				Perm	157361
PB1	Sil'st	361000	5476300				NeoP	157362
PB2	Sil'st	361000	5476300				NeoP	157363
PB3	Sil'st	361000	5476300				NeoP	157364
PB4	Sil'st	361000	5476300				NeoP	157365
PB5	Sil'st	361000	5476300				NeoP	157366
SB1	Sil'st	377350	5470400				NeoP	157367
SB2	Sil'st	377350	5470400				NeoP	157368
SB3	Sil'st	377350	5470400				NeoP	157369
SB4	Sil'st	377350	5470400				NeoP	157370
SB5	Sil'st	377350	5470400				NeoP	157371
BHR1	Sil'st	303800	5457550				NeoP	157372
BHR2	Sil'st	303800	5457550				NeoP	157373
BHR3	Sil'st	303800	5457550				NeoP	157374
BHR4	Sil'st	303800	5457550				NeoP	157375
BHR5	Sil'st	303800	5457550				NeoP	157376
ACQ1	Sil'st	306425	5450250				NeoP	157377
ACQ2	Sil'st	306425	5450250				NeoP	157378
ACQ3	Sil'st	306425	5450250				NeoP	157379
ACQ4	Sil'st	306425	5450250				NeoP	157380
ACQ5	Sil'st	306425	5450250				NeoP	157381
CRQ1	Sil'st	306990	5439400				NeoP	157382

CRQ2	Sil'st	306990	5439400				NeoP	157383
CRQ3	Sil'st	306990	5439400				NeoP	157384
CRQ4	Sil'st	306990	5439400				NeoP	157385
CRQ5	Sil'st	306990	5439400				NeoP	157386
WarQ1	Sil'st	327100	5424700				NeoP	157387
WarQ2	Sil'st	327100	5424700				NeoP	157388
WarQ3	Sil'st	327100	5424700				NeoP	157389
WarQ4	Sil'st	327100	5424700				NeoP	157390
WarQ5	Sil'st	327100	5424700				NeoP	157391
DP1	Sil'st	350250	5455300				NeoP	157392
DP2	Sil'st	350250	5455300				NeoP	157393
DP3	Sil'st	350250	5455300				NeoP	157394
DP4	Sil'st	350250	5455300				NeoP	157395
DP5	Sil'st	350250	5455300				NeoP	157396
WPQ1	Sil'st	356200	5453600				NeoP	157397
WPQ2	Sil'st	356200	5453600				NeoP	157398
WPQ3	Sil'st	356200	5453600				NeoP	157399
WPQ4	Sil'st	356200	5453600				NeoP	157400
WPQ5	Sil'st	356200	5453600				NeoP	157401
TipR1	Sil'st	351000	5467700				NeoP	157402
TipR2	Sil'st	351000	5467700				NeoP	157403
TipR3	Sil'st	351000	5467700				NeoP	157404
TipR4	Sil'st	351000	5467700				NeoP	157405
TipR5	Sil'st	351000	5467700				NeoP	157406
SS1	Sil'st	336800	5426650				NeoP	157407
SS2	Sil'st	336800	5426650				NeoP	157408
SS3	Sil'st	336800	5426650				NeoP	157409
SS4	Sil'st	336800	5426650				NeoP	157410
SS5	Sil'st	336800	5426650				NeoP	157411
SRSS1	Sil'st	319250	5453155				Camb	157412
SRSS2	Sil'st	319250	5453155				Camb	157413
SRSS3	Sil'st	319250	5453155				Camb	157414
SRSS4	Sil'st	319250	5453155				Camb	157415
SRSS5	Sil'st	319250	5453155				Camb	157416
HQA	Sil'st	349850	5449800				NeoP	157417
HQB	Sil'st	349850	5449800				NeoP	157418
HQC	Sil'st	349850	5449800				NeoP	157419
HQD	Sil'st	349850	5449800				NeoP	157420
HQE	Sil'st	349850	5449800				NeoP	157421
JR1	Sil'st	334850	5443215				NeoP	157422
CS1	Sil'st	362090	5476280				NeoP	157423
CP2	Sil'st	362090	5476280				NeoP	157424
CP3	Sil'st	362090	5476280				NeoP	157425
CP4	Sil'st	362090	5476280				NeoP	157426
AR1	Sil'st	349125	5456150				NeoP	157427
TB	Sil'st	348395	5452500			Palyn	NeoP	157428
Coms	Bitum	357450	5360350				Perm	157429
AS	San's	455150	5218800			TS	Silur	157430

MCC1	Palkar	484880	5118800			TS	?	157431

TS, thin section
Palyn, palynological preparation

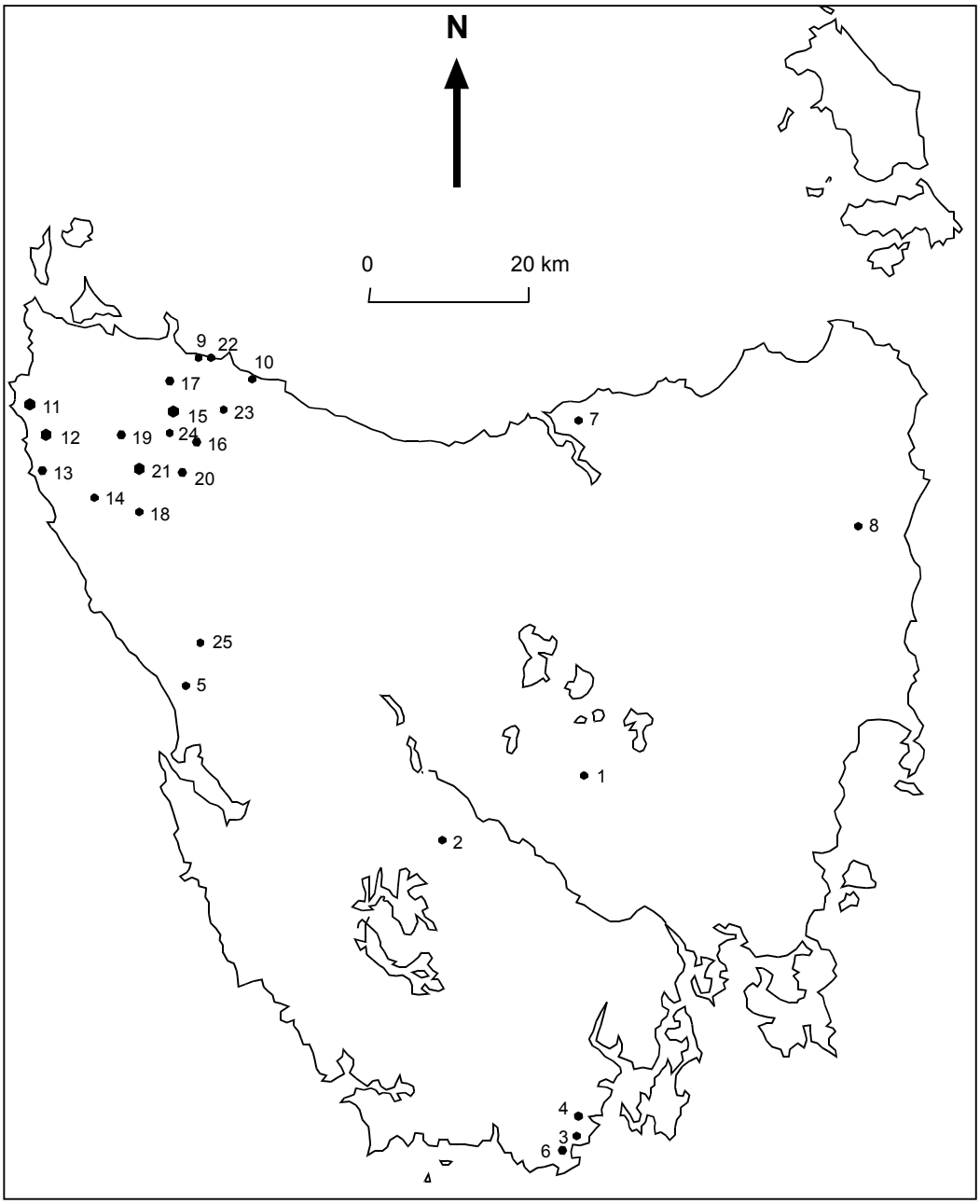

Figure C.1. Location map for samples mentioned in this thesis. Key to locations is in Table C.1.

Table C.1.

Key for numbers on sample locality map.

Number	ID	Lithology	Locality
1	H1-H10	Dolomite	Hunterston
2	UL1-40, SM1, 11R1, WQR1, 172, 17 16, 175, AS	Limestone/shale, sandstone	Florentine Valley
3	LR2, LR3, LR4, MCC1	Limestone	Lune River
4	MC1	Limestone	Ida Bay
5	MQ2, MQ3, MQC1, MQC2, 590494, BR7	Siltstone, coal	Mallana
6	LC, CCM2	Coal	Leprena
7	BP1	Siltstone	Bangor
8	Cat1, Cat2	Coal	Catos Creek
9	PB1-5	Siltstone	Peggs Beach
10	SB1-5	Siltstone	Sisters Beach
11	BHR1-5	Siltstone	Bluff Hill
12	ACQ1-5	Siltstone	Alert Creek
13	CRQ1-5	Siltstone	Couta Rocks
14	WarQ1-5	Siltstone	Waratah Creek
15	DP1-5	Siltstone	Dollie Pit
16	WPQ1-5	Siltstone	Wedge Plains
17	TipR1-5	Siltstone	Tipunah Rd.
18	SS1-5	Siltstone	South Sumac Rd.
19	SRSS1-5	Siltstone	Salmon River
20	HQA-E	Siltstone	Holder Quarry
21	JR1	Siltstone	Julius River
22	CS1, CP2-4	Siltstone	Cowrie Point
23	AR1	Siltstone	Apiary Road
24	TB	Siltstone	Tayatea Bridge
25	Comstock	Bitumen	Comstock Mine

APPENDIX D.

Kubler Index Results.

Analysis by X-Ray Diffraction with results reported as width in °2θ measured at half peak height.

Sample	AD	EG	Av AD	Av EG	Est. Temp.	
PB1	0.25	0.26				
PB2	0.25	0.25				
PB3	0.28	0.29				
PB4	0.27	0.27				
PB5	0.26	0.26	0.26	0.27	320	
SB1	0.26	0.26				
SB2	0.25	0.25				
SB3	0.25	0.25				
SB4	0.26	0.25				
SB5	0.25	0.26	0.25	0.25	330	
BHR1	0.25	0.26				
BHR2	0.31	0.32				
BHR2(rpt)	0.3	0.32				
BHR3	0.26	0.25				
BHR4	0.29	0.29				
BHR5	0.28	0.25	0.28	0.28	290	
ACQ1	0.26	0.25				
ACQ2	0.29	0.26				
ACQ3	0.26	0.28				
ACQ3(rpt)	0.27	0.28				
ACQ4	0.28	0.27				
ACQ5	0.26	0.26	0.27	0.27	300	
SS1	0.27	0.31				
SS2	0.3	0.29				
SS3	0.27	0.28				
SS4	0.28	0.29				
SS5	0.26	0.25	0.28	0.28	290	
HQA	0.34	0.31				
HQB	0.37	0.3				
HQC	0.28	0.28				
HQD	0.3	0.29				
HQE	0.31	0.29	0.32	0.29	255	
SRSS3	0.43	0.5	0.43	0.5	190	Note unreliable result.
CRQ1	0.25	0.24				
CRQ2	0.23	0.22				
CRQ3	0.24	0.23				
CRQ4	0.22	0.22				
CRQ5	0.27	0.25	0.24	0.23	400	
WarQ1	0.25	0.29				
WarQ2	0.26	0.26				
WarQ3	0.26	0.26				
WarQ4	0.24	0.25				
WarQ5	0.25	0.25	0.25	0.26	320	

DP1	0.29	0.25			
DP1 (rpt)	0.28	0.26			
DP2	0.26	0.27			
DP3	0.27	0.29			
DP4	0.28	0.28			
DP5	0.27	0.28	0.28	0.27	300
WPQ1	0.28	0.25			
WPQ2	0.27	0.27			
WPQ3	0.28	0.29			
WPQ4	0.27	0.26			
WPQ5	0.27	0.25	0.27	0.26	320
TipR1	0.37	0.36			
TipR2	0.36	0.35			
TipR3	0.35	0.33			
TipR4	0.34	0.33			
TipR5	0.38	0.37			
TipR5 (rpt)	0.36	0.35	0.36	0.35	240

AD = air-dried mount
EG = same mount treated with Ethylene Glycol
Width corrections made by calibration against 1994 Warr and Rice standards:-
AD, corrected = 1.167raw + 0.049; EG, corrected = 1.297raw + 0.022

Results shown are corrected values.

Note: Samples SRSS1, 2, 4 and 5 did not contain sufficient mica to produce a readable peak. SRSS3 produced a peak that yielded a result of uncertain reliability after manual measurement.

APPENDIX E.

Biomarker Geochemistry Results.

An outcrop sample (ID 175) from the Gordon Group was collected in the Florentine Valley at 453000 mE, 5281900 mN. This sample is a typical example of the black shale interbeds exhibiting the properties of petroleum source rocks and this is the reason that biomarker geochemistry was determined from this sample.

TOC, 0.48%.

Yield of extracted organic matter, 56mg/kg.

Alkane Ratios.

Norpristane/Pristane	0.48
Pristane/Phytane	1.39
Pristane/n-heptadecane	0.58
Phytane/n-octadecane	0.53

Results of referred rests are shown on separate pages.

Liquid chromatography of extracted organic matter.

Total saturates	38%
Total aromatics	19%
Total NSO	43%

Biomarker parameters of source, maturity, migration and biodegradation, ATP-269-P(1) oils.

SAMPLE	STERANES							TERPANES					ACYCLIC ALKANES			
	PARAMETER															
	1	2	3	4	5	6	7	8	9	10	11	12	13	14	15	16
175	30	1.55	1.91	1.01	1.24	1.03	0.30	0.26	0.33	0.65	0.20	1.36	0.13	1.39	0.58	0.53

Key to biomarker parameters of source, migration and biodegradation.

Parameter	Derivation*	Specificity
1	C_{27}:C_{28}:C_{29}5α(H)14α(H)17α(H)20R steranes	Source
2	C_{29}5α(H)14α(H)17α(H)20R sterane/C_{27}5α(H)14α(H)17α(H)20R sterane	Source
3	C_{29}13β(H)17α(H)20R diasterane/C_{27}13β(H)17α(H)20R diasterane	Source
4	C_{29}5α(H)14α(H)17α(H)20S sterane/C_{29}5α(H)14α(H)17α(H)20R sterane	Maturity, biodegradation
5	C_{27}13β(H)17α(H)20S diasterane/C_{27}13β(H)17α(H)20R diasterane	Maturity
6	C_{29}5α(H)14β(H)17β(H)20R sterane/C_{29}5α(H)14α(H)17α(H)20R sterane	Maturity, migration
7	C_{29}13β(H)17α(H)20R +20S diasteranes/C_{29}5α(H) steranes	Migration, source
8	18α(H)-30-norneohopane (C_{29}Ts)/C_{29}17α(H) hopane + C_{29}Ts	Maturity, source
9	17α(H) diahopane/18α(H)-30-norneohopane (C_{30}*/C_{29}Ts)	Source, maturity
10	C_{27}18α(H)-22,29,30-trisnorhopane (Ts)/C_{27}17α(H)-22,29,30-trisnorhopane (Tm) + Ts	Maturity, source
11	Ts/C_{30}17α(H)21β(H) hopane	Maturity
12	C_{32}17α(H)21β(H)22S homohopane/C_{32}17α(H)21β(H)22R homohopane	Maturity
13	C_{30}17β(H)21α(H) moretane/C_{30}17α(H)21β(H) hopane	Maturity
14	Pristane/phytane	Source
15	Pristane/n-heptadecane	Source, biodegradation, maturity
16	Phytane/n-octadecane	Source, biodegradation, maturity

Ratios calculated from peak areas as follows:

Parameters 1-7 m/z = 217, 218, 259 mass fragmentograms
Parameters 8-13 m/z = 191 mass fragmentogram
Parameters 14-16 capillary gas chromatogram of alkanes or whole oil/extract

Aromatic maturity data

Sample	MPI	MPR	DNR	MPDF	VR Calc. (%)					
					A	B	C	D	E	F
175	0.781	1.707	____	0.582	0.87	1.83	1.17	___	0.77	1.14

Key to aromatic maturity indicators.

Methylphenanthrene index (MPI), methylphenanthrene ratio (MPR), dimethylnaphthalene ratio (DNR) and calculated vitrinite reflectance ($VR_{calc.}$) are derived from the following equations (after Radke and Welte, 1983; Radke et al., 1984)

$$MPI = \frac{1.5(2\text{-MP} + 3\text{-MP})}{P + 1\text{-MP} + 9\text{-MP}}$$

$$VR_{calc}(a) = 0.6MPI + 0.4 \text{ (for VR} < 1.35\%)$$

$$VR_{calc}(b) = -0.6MPI + 2.3 \text{ (for VR} > 1.35\%)$$

$$MPR = \frac{2\text{-MP}}{1\text{-MP}}$$

$$VR_{calc}\,(c) = 0.99 \log_{10} MPR + 0{,}94 \text{ (VR} = 0.5 – 1.7\%)$$

$$DNR = \frac{2,6\text{-DMN} + 2,7\text{-DMN}}{1,5\text{-DMN}}$$

$$VR_{calc}\,(d) = 0.46\ DNR + 0.89 \quad (\text{for VR} = 0.9 – 1.5\%)$$

Where P = phenanthrene
1-MP = 1-methylphenanthrene
2-MP = 2-methylphenanthrene
3-MP = 3-methylphenanthrene
9-MP = 9-methylphenanthrene
1,5-DMN = 1,5-dimethylnaphthalene
2,6-DMN = 2,6-dimethylnaphthalene
2,7-DMN = 2,7-dimethylnaphthalene

Peak areas measured from m/z 156 (dimethylnapthalene), m/z 178 (phenanthrene) and m/z 192 (methylphenanthrene) mass fragmentograms of diaromatic and triaromatic hydrocarbon fraction isolated by thin layer chromatography.

Recalibration of the methylphenanthrene index using data from a suite of Australian coals has given rise to another equation for calculated vitrinite reflectance (after Boreham et al., 1988):

VR_{calc} (e) = 0.7 MPI + 0.22 (for VR < 1.7%)

The methylphenanthrene distribution ratio (MPDF) and calculated vitrinite reflectance VR_{calc} (f) is derived from the following equation (after Kvalheim et al., 1987):

$$MPDF = \frac{(2\text{-MP} + 3\text{-MP})}{(2\text{-MP} + 3\text{-MP} + 1\text{-MP} + 9\text{-MP}}$$

VR_{calc} (f) = -0.166 + 2.242 MPDF

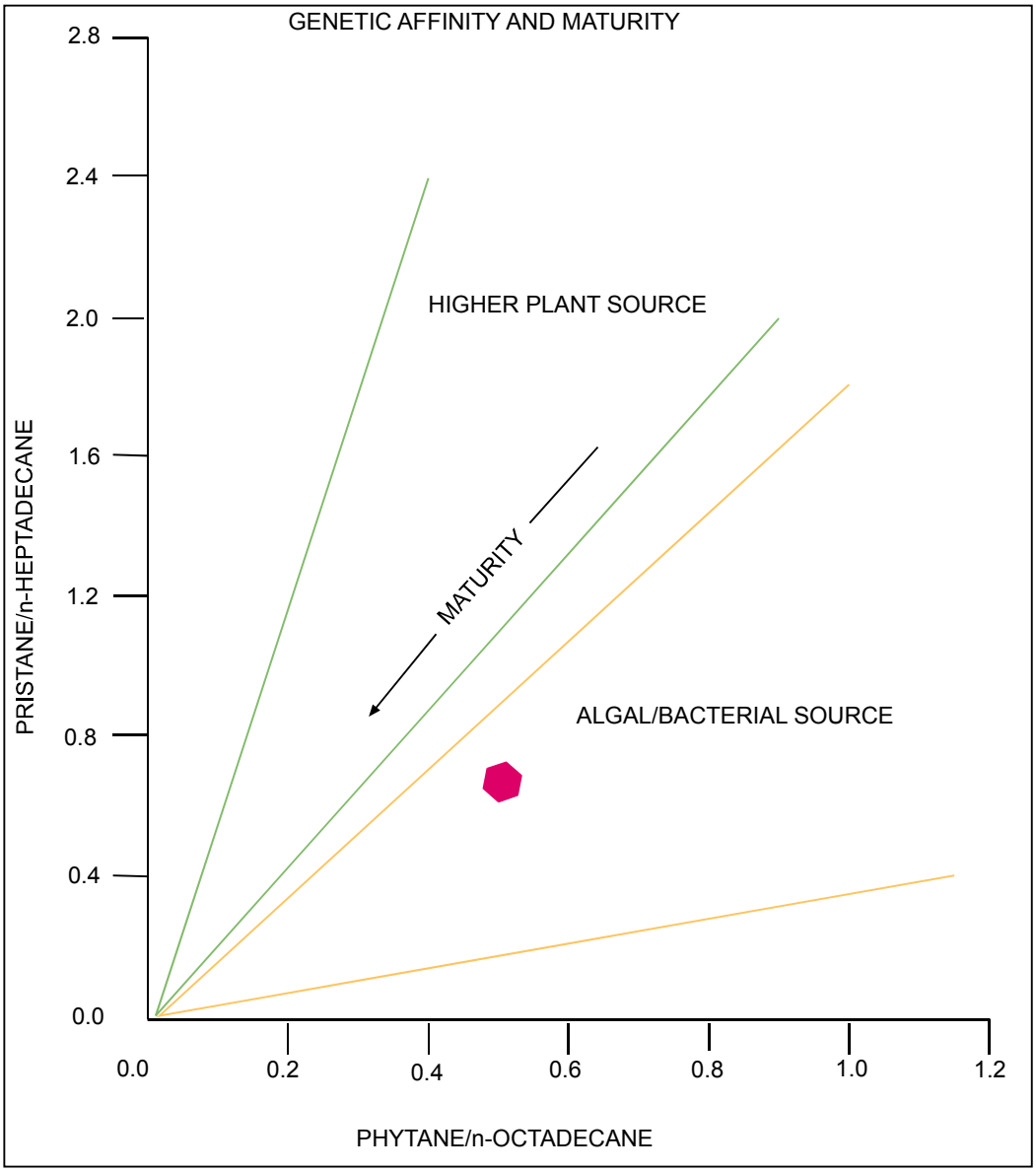

Figure E.1. Genetic affinity and maturity plot for sample 175.

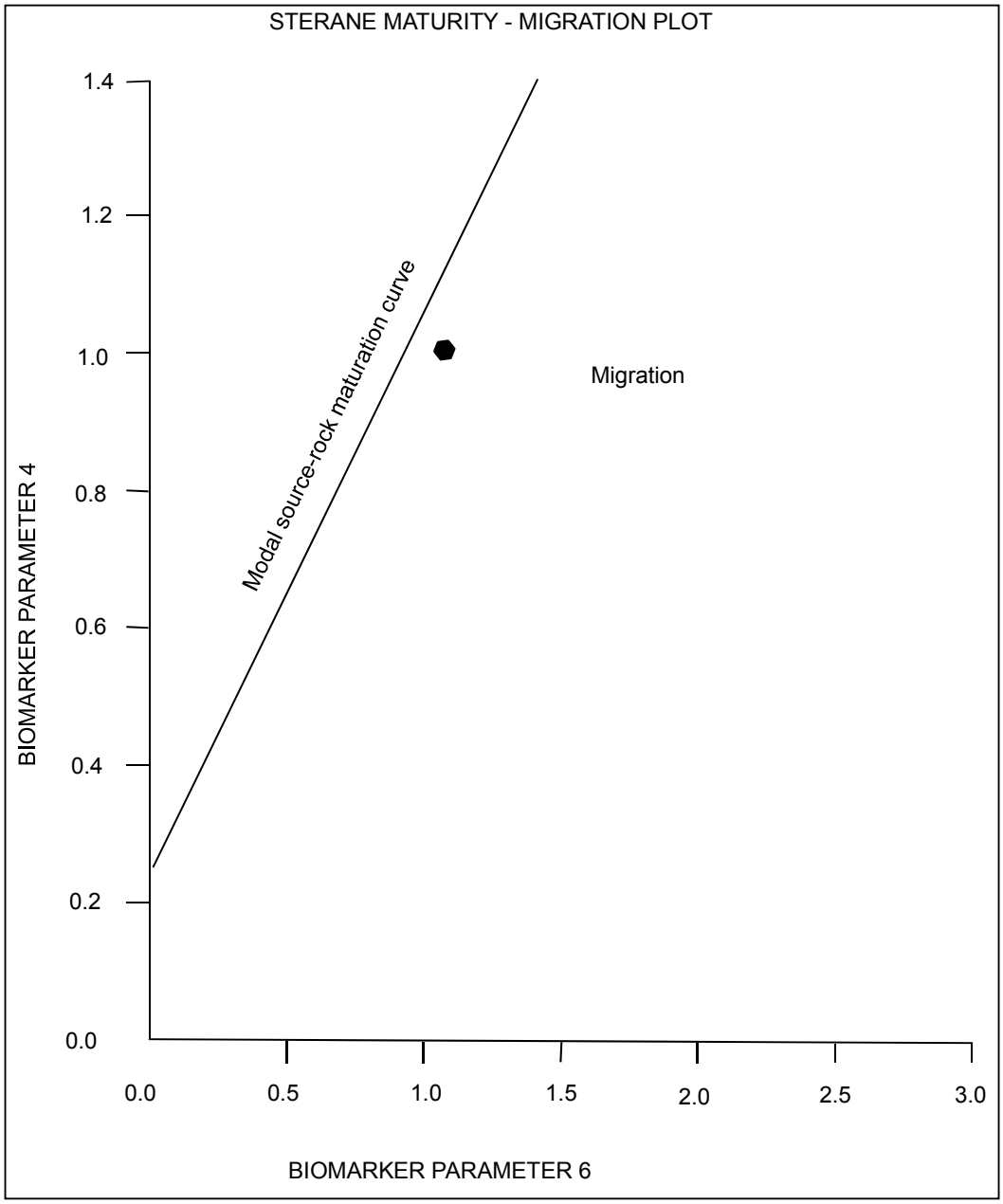

Figure E.2. Sterane maturity – migration plot for sample 175.

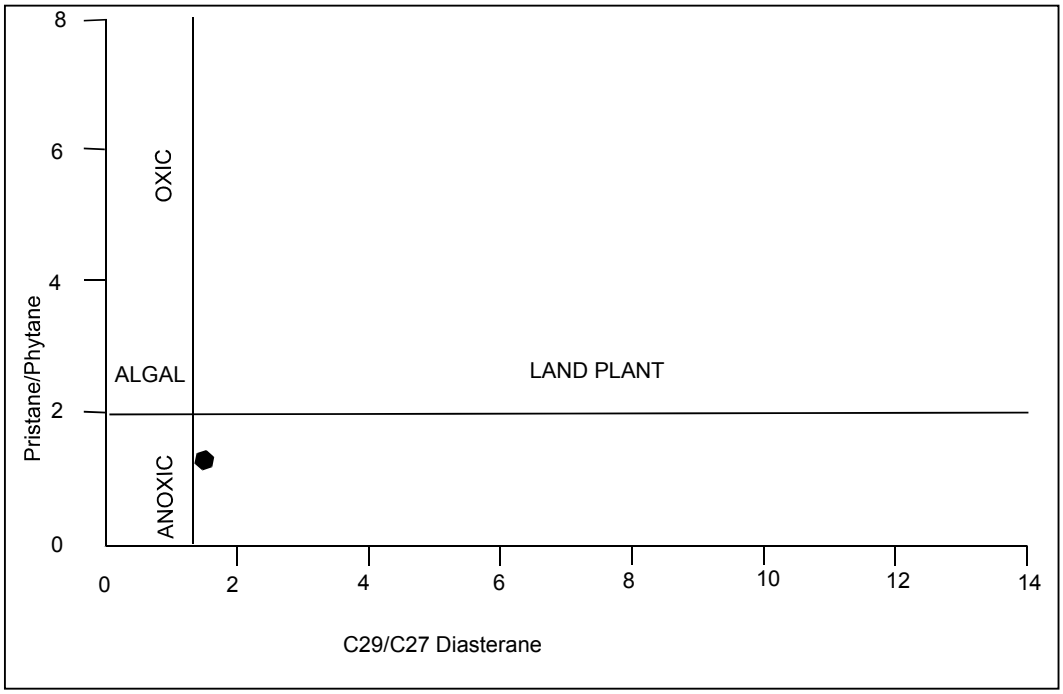

Figure E.3. Oil source affinity plot for sample 175.

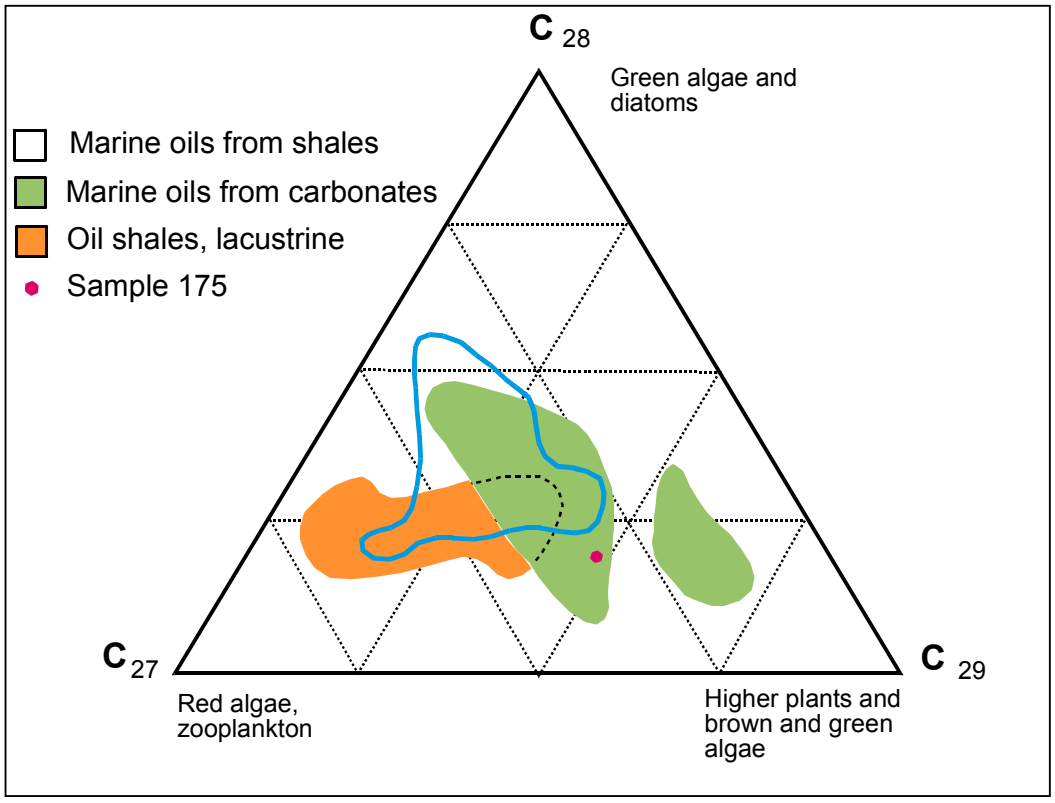

Figure E.4. Sterane distributions plot for sample 175 and also showing distributions for typical depositional situations. Sample 175 is clearly marine oil from carbonate source.

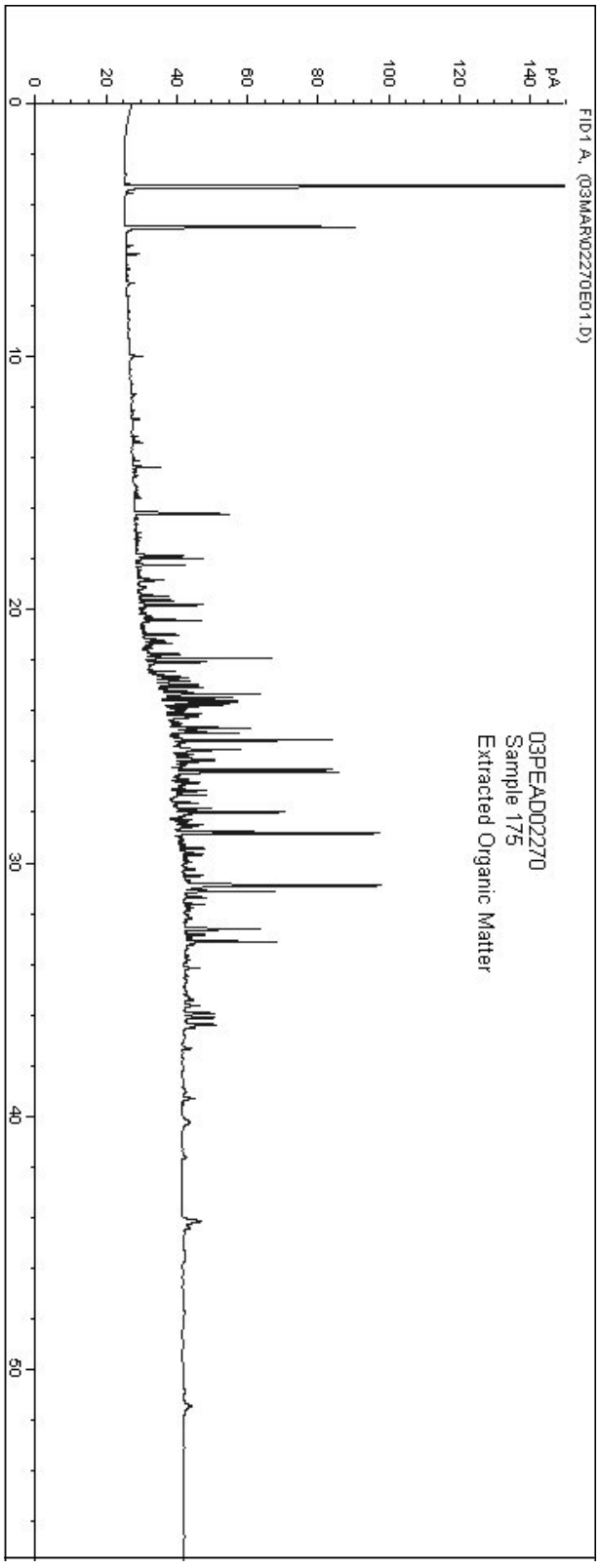

Figure E.5. Gas chromatogram showing the extracted organic matter from sample 175.

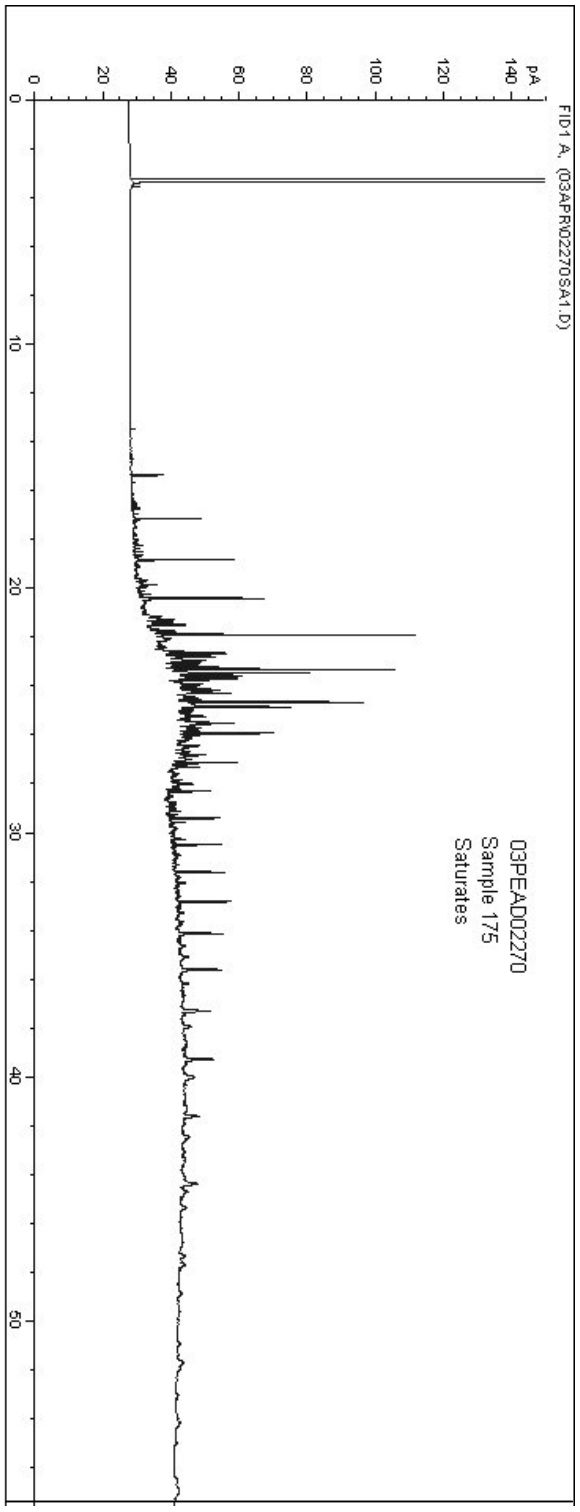

Figure E.6. Gas chromatogram of saturates extracted from sample 175.

APPENDIX F.

I. Organic matter in samples from an Ordovician limestone from Florentine Valley, Tasmania.

II. Bitumen from Comstock Mine, Zeehan, Tasmania.

III. Carbonaceous samples from Permian outcrops near Zeehan, Tasmania.

Report by Alan Cook.

I. ORGANIC MATTER IN SAMPLES FROM AN ORDOVICIAN LIMESTONE FROM FLORENTINE VALLEY, TASMANIA.

II. BITUMEN FROM COMSTOCK MINE, ZEEHAN, TASMANIA.

III. CARBONACEOUS SAMPLES FROM PERMIAN OUTCROPS NEAR ZEEHAN, TASMANIA

REPORT PREPARED FOR

ALAN CHESTER

by

ALAN C COOK

KEIRAVILLE KONSULTANTS

7 Dallas St
Keiraville, NSW, 2500
Australia

November 2003

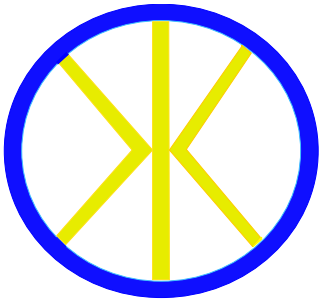

KEIRAVILLE KONSULTANTS
PTY LTD

I. ORGANIC MATTER IN SAMPLES FROM AN ORDOVICIAN LIMESTONE FROM FLORENTINE VALLEY, TASMANIA.

Alan Cook

A whole-rock sample of a shaly limestone of Ordovician age from the Upper Benjamin Limestone, Florentine Valley in Tasmania was sent by Alan Chester for determination of the level of organic maturation, together with slides (strew mounts) of organic matter concentrates and two vials containing suspensions of the organic matter concentrates. The sample was collected from the Florentine Valley, Tiger 1:25 000 map 4227, grid ref DN 585 790.

The whole-rock sample was mounted in polyester resin and some of the suspended organic matter concentrates was dried and prepared as polished blocks for examination in reflected light. The thin sections were examined in the form that they were received.

THIN SECTIONS

The dominant component within the strew mounts is unstructured material that appears to show weak dull brown transmission colours. Both of the slides also contain some equant to angular fragment of organic matter that are opaque, even at the margins. Examination of the whole rock and polished sections of the organic matter concentrates suggests that most of the opaque component represents pyrobitumens.

WHOLE-ROCK SAMPLE

Organic matter is sparse (less than 0.5% but >0.1%) in the limestone. The most prominent occurrences are of bitumens. These occur along stylolitic partings (Plate I.1) and within voids in sparry patches of carbonate and as more massive lenses (Plate I.2). Graptolite remains were also found (Plates I.3 and I.4) but they proved to be relatively rare compared to the bitumens. The graptolites show strong bireflectance. No evidence of coke structured was found in the bitumens. This suggests that the rate of maturation associated with the formation of the bitumens was relatively slow. Where higher rates of heating have occurred, bitumens are usually the first component to develop coke structures.

POLISHED BLOCKS MADE FROM ORGANIC MATTER CONCENTRATES

Two polished blocks were prepared from the organic matter concentrates. The organic matter within these samples is broadly similar and consists of grains of presumed bitumen ranging up to 30 microns in greatest diameter. The bitumens show mean reflectances of 2.74 and 2.63%, values very similar to the bitumen population reported for the whole-rock sample. Most of the grains show embayed margins and these may relate to bitumens that occur within sparry carbonate. The drying of the samples has lead to the agglomeration of the unstructured material that was found to be the dominant component within the thin sections. In the block prepared from the material labelled kerogen concentrate, the matrix has taken a moderately good polish and shows a reflectance of 1.95% (Plates I.5 and I.6). The sample labelled Organic Matter concentrate showed a similar matrix material (Plate I.7) but in this sample it is much more diffuse and the reflectances obtained were variable depending upon the apparent density at the point measured. Mean reflectances for this component were not determined for T9343.

Graptolites are presumably present within the organic matter concentrates but it was not possible to distinguish any. It is possible that they had become fragmented during demineralization, but it is more probable that they were oriented parallel with bedding and in this position the morphology is much less distinctive compared with sections perpendicular to bedding.

MATURATION LEVELS

The bitumen reflectances can be taken as being representative of the levels of maturation and are likely to approximate the vitrinite reflectance values that would be found if vitrinite were present in the section. The section currently lies within the dry gas window. The subsequent examination of samples from the Permian suggests that the main phase of maturation occurred prior to the deposition of the Permian. Although the level of maturation that is present within the Permian, the effect of this later phase of heating would have been relatively minor on the Ordovician section. It is probable that the bitumens were of a sufficiently high level of maturation that they would not develop coke structures and textures where they were affected by metamorphic aureoles from the Mesozoic intrusions that are present over much of Tasmania. Contact alteration would, however, produce higher reflectances but without coke textures.

PLATES – SECTION I

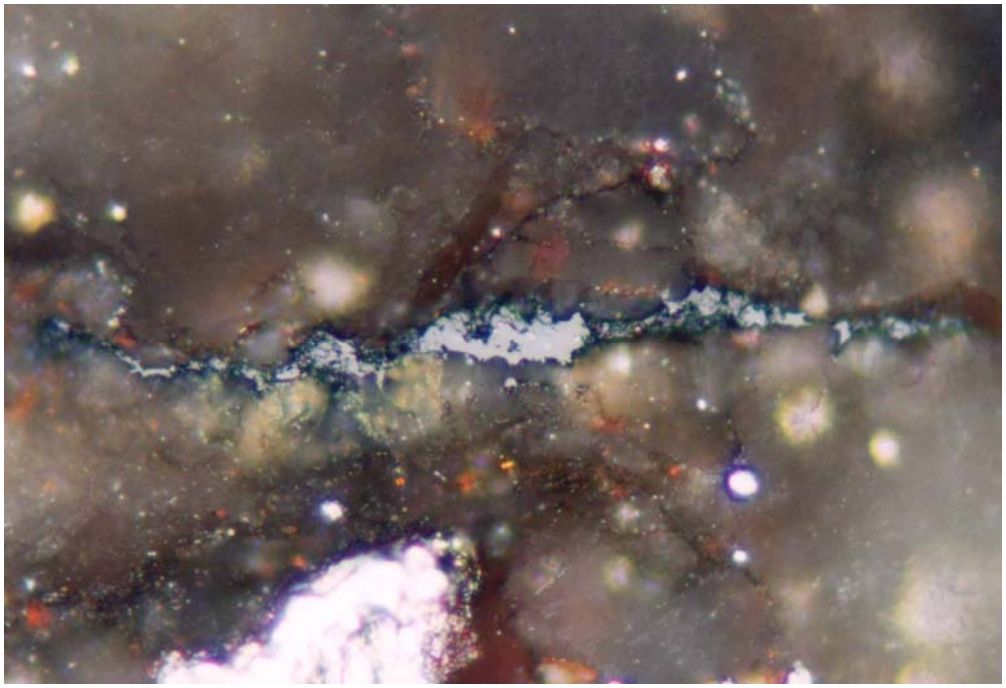

Plate I.1. T9341. Florentine Valley Limestone, whole rock mount. Bitumen occurring along stylolitic parting but probably emplaced after the development of the styolite, reflectance 2.94%. Reflected white light, field width 0.22 mm

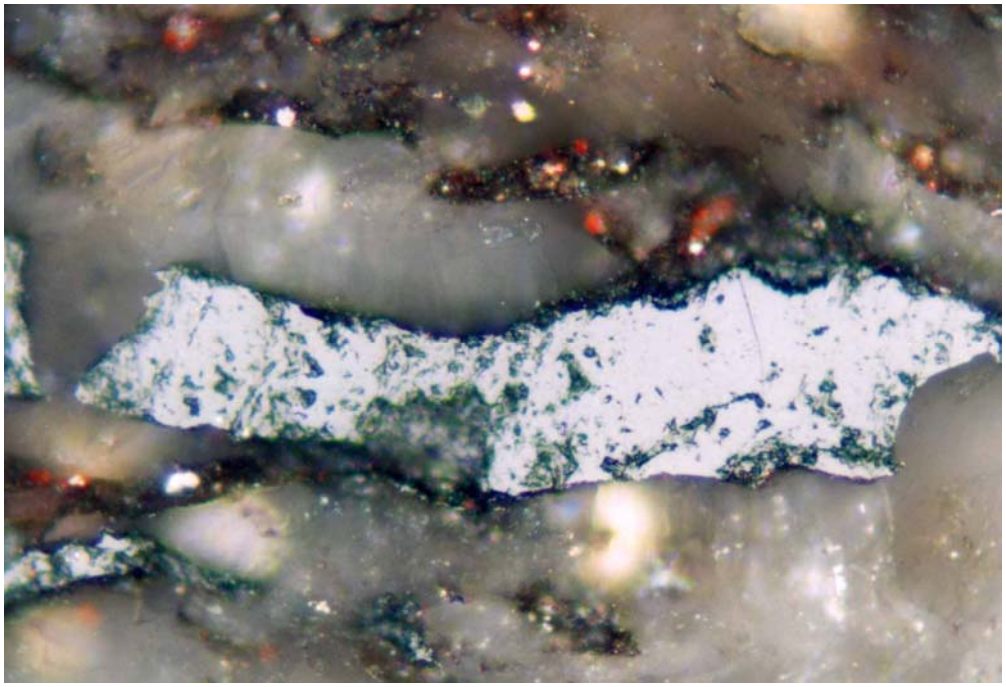

Plate I.2. T9341. Florentine Valley Limestone, whole rock mount. Probable bitumen occurring within sparry calcite, reflectance 2.58%. Reflected white light, field width 0.22 mm

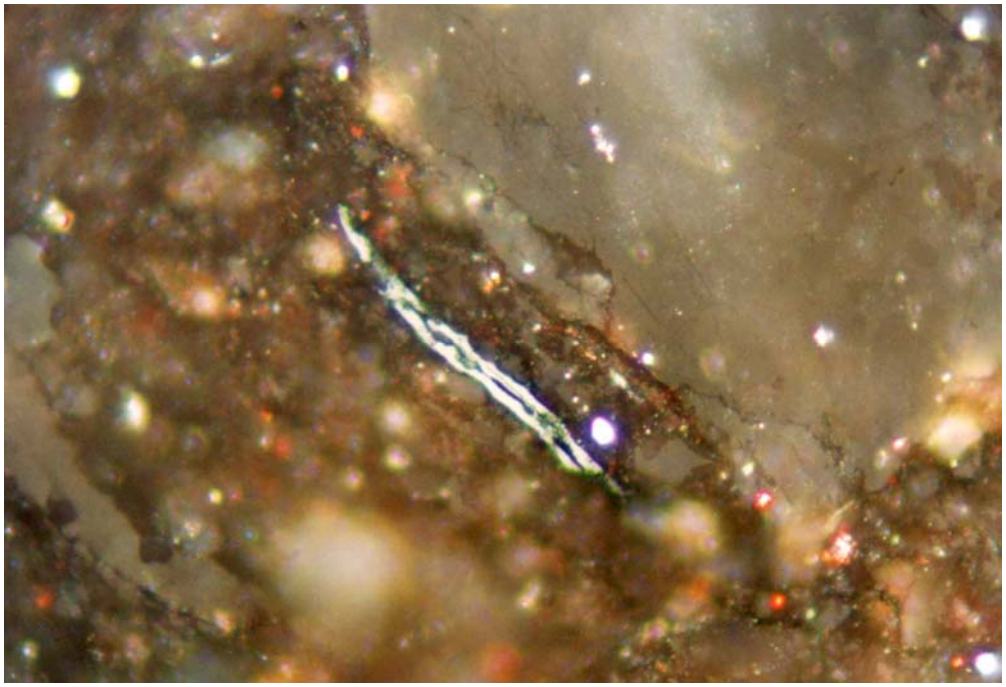

Plate I.3 T9341. Florentine Valley Limestone, whole rock mount. Graptolite in the orientation that yields maximum reflectance, 2.95% for this field. Reflected white light, field width 0.22 mm

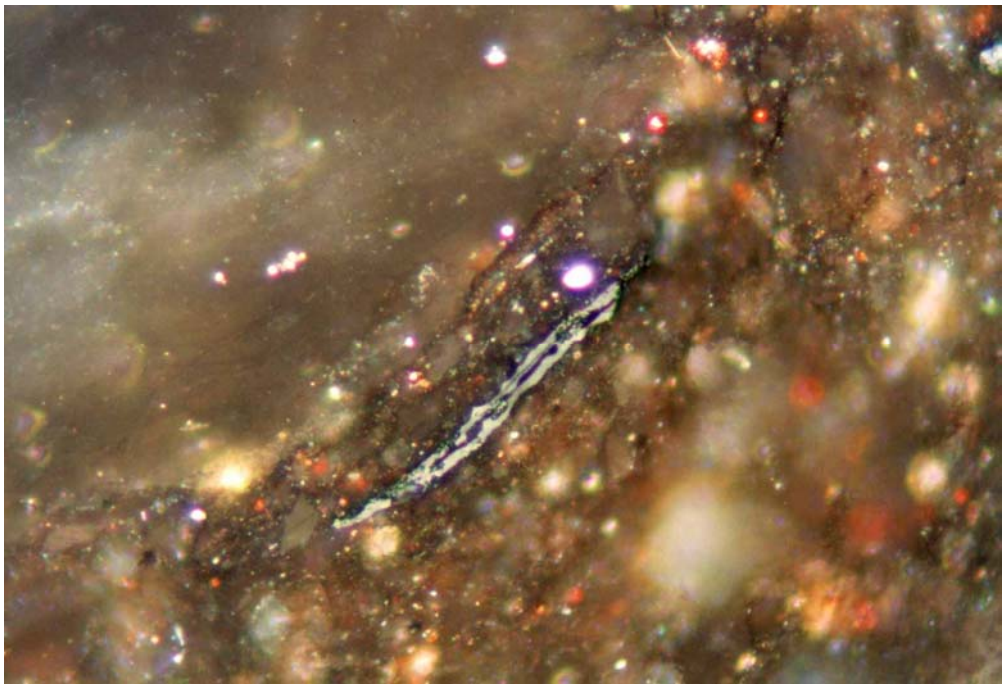

Plate I.4 T9341. Florentine Valley Limestone, whole rock mount. Graptolite in the orientation that yields minimum reflectance, 1.12%. Reflected white light, field width 0.22 mm

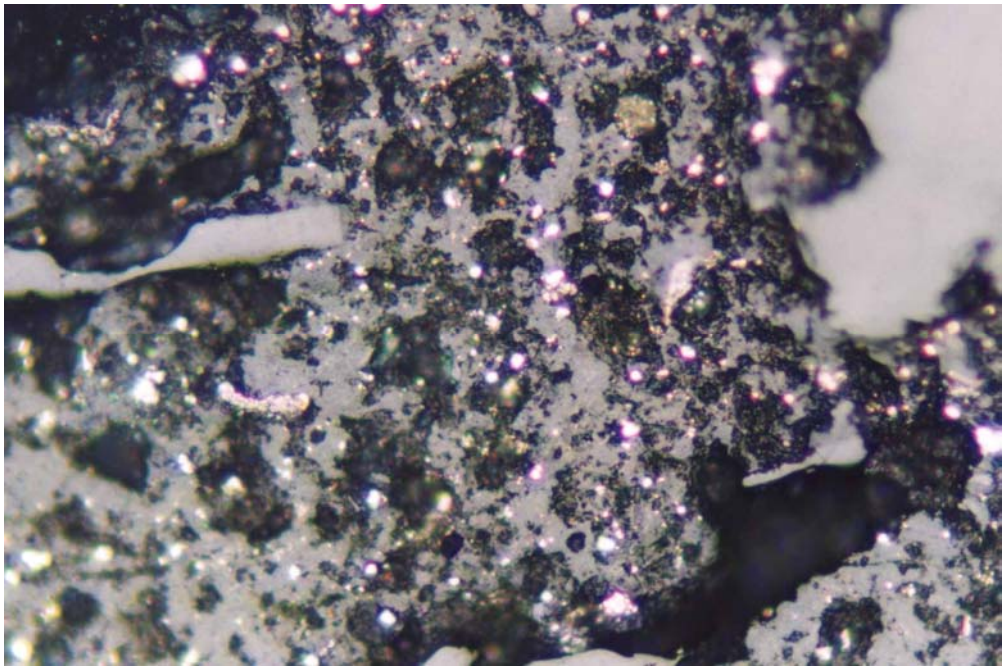

Plate I.5. T9342. Florentine Valley Limestone, "kerogen concentrate". Large fragments of bitumen (3.17%) set in a matrix of material having affinities to amorphinite, the matrix is compact and yields consistent reflectance values of about 1.90% for this field. Reflected white light, field width 0.22 mm

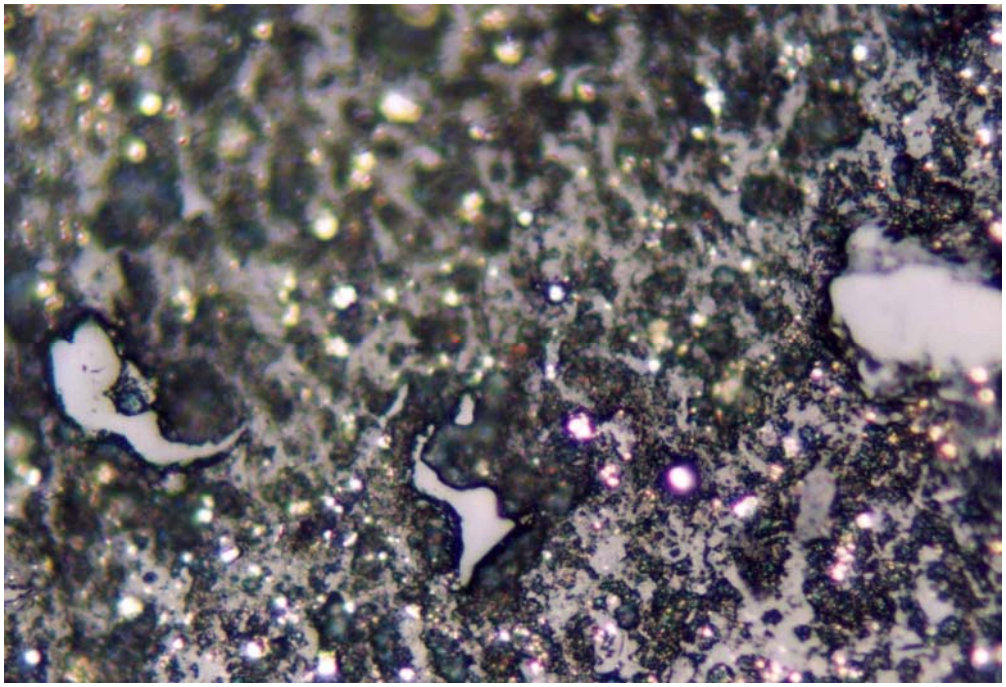

Plate I.6 T9342. Florentine Valley Limestone, "kerogen concentrate". Large fragments of bitumen (2.70%) set in a matrix of material having affinities to amorphinite, the matrix is compact and yields consistent reflectance values of about 1.90% for this field. Reflected white light, field width 0.22 mm

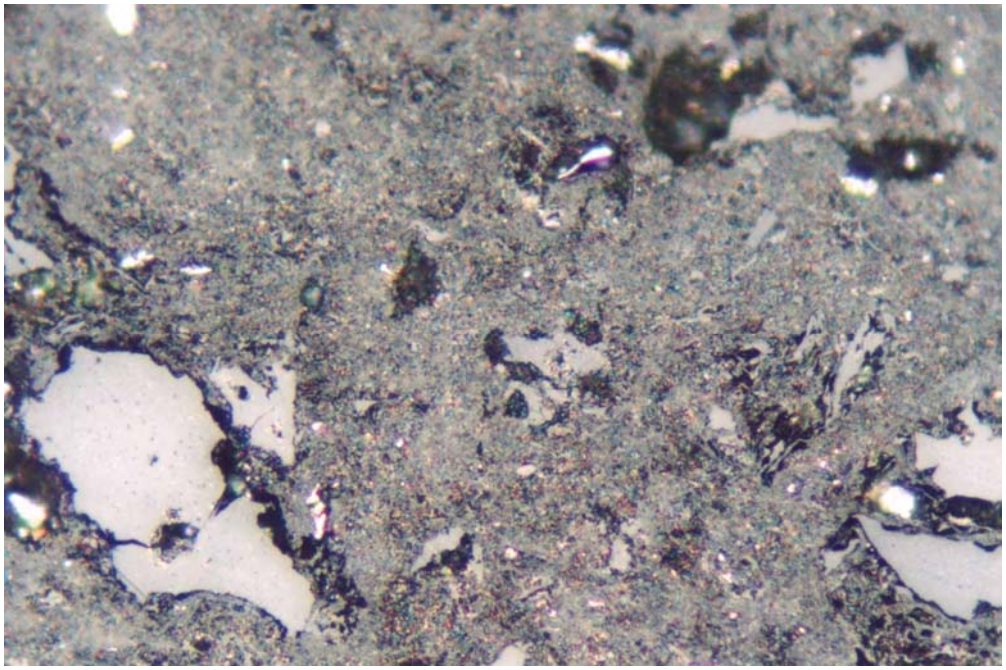

Plate I.7 T9342. Florentine Valley Limestone, "organic matter concentrate". Large fragments of bitumen (2.10, 2.73 and 2.44%) set in a matrix of material having affinities to amorphinite. The matrix is not compact and yields variable reflectance values of about 1.45% for this field. It appears to have the same optical properties as the matrix shown in Plate I.6 but has become less compacted during the process of drying. Reflected white light, field width 0.22 mm

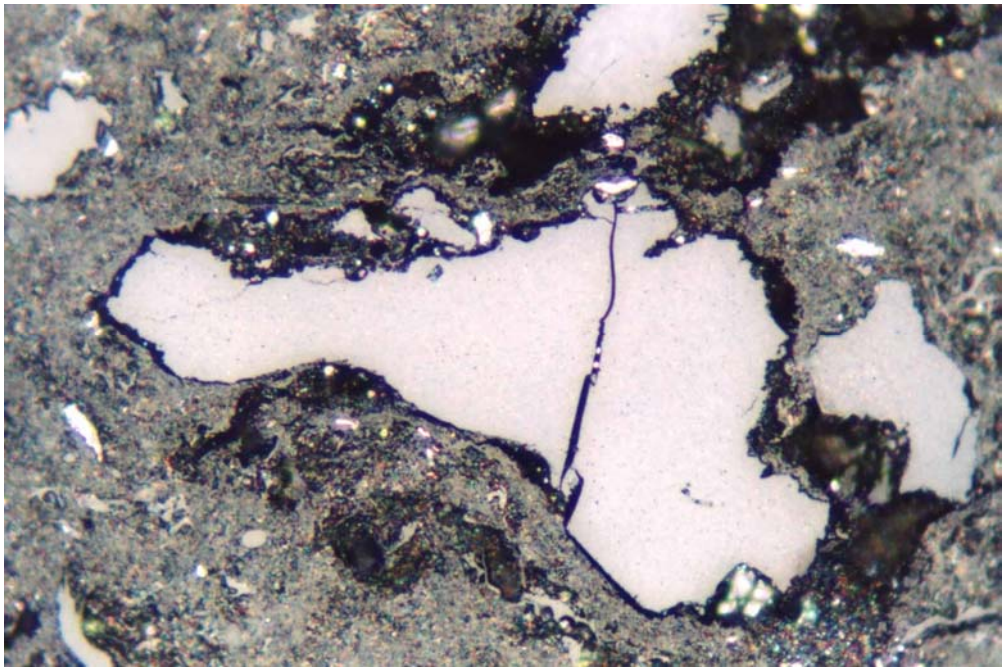

Plate I.8 T9342. Florentine Valley Limestone, "organic matter concentrate". Large fragments of bitumen (2.63%) set in a matrix of material having affinities to amorphinite. The matrix is not compact and yields variable reflectance values of about 1.43% for this field. Reflected white light, field width 0.22 mm

ORDOVICIAN - FLORENTINE VALLEY

KK # Ref #.	Depth (m) /Type	$R_v$max Mean	Range	SD	N	Sample description including liptinite fluorescence, maceral abundances, mineral fluorescence
						WHOLE ROCK
T9341 Outcrop	O/C	2.70	2.21-3.10	0.235	29	Fluorescing liptinite absent. (Shaly fossiliferous limestone. (Dom rare, "V" only. Some of the bitumens have clear bitumen morphology, but some occurrence are elongate. The faunal remains are thin (<5 microns) and show variable bireflectance. The bitumens are close to isotropic. The bitumens show no evidence of coke textures. Iron oxides are derived from alteration of framboidal pyrite and are common. Pyrite sparse.)
	F'nal R_{max}	2.85	2.37-3.42	0.284	10	
	F'nal R_{min}	1.46	0.73-2.05	0.381	10	
						STREW MOUNTS -
T9342 "Ker" conc	O/C Bit "Amorph"	2.74	2.30-3.70	0.308	27	Fluorescing liptinite absent. (Organic matter concentrate. The Main component of the organic matter is structureless material that corresponds with so-called amorphous kerogen in lower rank rocks. In the thin sections, it is weakly translucent brown and non-fluorescing. Its origin is not clear. The bitumen occurs as equant to elongate grains up to 200 microns across but more typically about 40 microns in greatest dimension. The bitumen corresponds with the component identified as bitumen in the whole rock sample. Pyrite abundant.)
		1.95	1.80-2.15	0.110	14	
T9343 "OM" conc	O/C Bit ?Faunal Rem	2.63	2.26-3.24	0.224	38	Fluorescing liptinite absent. (Organic matter concentrate. The Main component of the organic matter is structureless material that corresponds with so-called amorphous kerogen in lower rank rocks. It is more diffuse compared with T9342 and the reflectances of about 1.5% appear to be influence by small holes. The bitumen is similar to that in T9342 but is more abundant. A lower reflecting population represents in part faunal remains but could include a separate population of bitumen. The higher reflecting bitumen corresponds with the component identified as bitumen in the whole rock sample. Pyrite abundant.)
		2.13	2.02-2.27	0.083	16	

The bitumen reflectances are relatively consistent. It is possible that the cause of the lower bitumen reflectance for T9343 is the inclusion of faunal remains within that reading as the differentiation between those components is less clear compared with the whole rock sample. The difference between the reflectances of the faunal remains for the whole rock and that for the organic matter concentrate are not clear and the component found in the concentrate may be a different component from that found in the whole rock sample.

The bitumens are impsonitic in type and their reflectances will be close to those of vitrinite if normal higher plant derived vitrinite was present within the samples. This indicates that the maturation level lies within the dry gas window, but some higher homologues would still be expected so the reflectance data are probably consistent with the presence of gases up to pentane. I would expect the ratio of C_{2+} to methane would be low for the full gas, but methane and ethane will have been lost selectively near the outcrop. Measurement of the carbon isotopic composition will probably indicate biochemical alteration due to the current weathering cycle.

ACC 10 October 2003

II. BITUMEN FROM COMSTOCK MINE, ZEEHAN, TASMANIA.

Alan Cook

A hand specimen of bitumen collected in the Comstock Mine Zeehan, Tasmania was sent by Alan Chester for examination and comparison with bitumens found in a limestone sample from the Florentine Valley. The Comstock Mine is located west of Zeehan on the Pieman 100 000 map, grid ref CP 573 604.

In hand specimen, the bitumen has a vitreous lustre and is black in colour. Part of the sample was crushed preparatory to mounting and it was noted that the bitumen is soft and shows pronounced conchoidal fractures (Plate 2). During polishing, it became apparent that the bitumen is very soft and some of the grains developed fractures during preparation. Some of these could be due to shrinkage following exposure to the atmosphere.

The bitumen took a good polish and proved to show very low reflectances and a mean value of 0.19% was obtained with a very small range being found. The bitumen appears massive at low magnifications (Plates II.1 and II.2) and at higher magnification (Plate II.3).

The bitumen essentially lacks fluorescence. On exposure to the fluorescence excitation beam, a lowering of reflectance was observed. Plate II.3 illustrates this feature with the outer part of the field having been protected from irradiation by closing the field stop during illumination with the fluorescence excitation beam for 25 minutes. The illumination was then restored to reflected white light and the stop opened up again. The outer part of the field shows the original reflectance of 0.20% to 0.19% and the central irradiated part of the field a much lower reflectance of 0.09%. The photochemical etching has also brought out some structures within the bitumen. These are probably associated with flow in the bitumen.

The bitumen is asphaltic in type and is referable to albertite.

PLATES – SECTION II

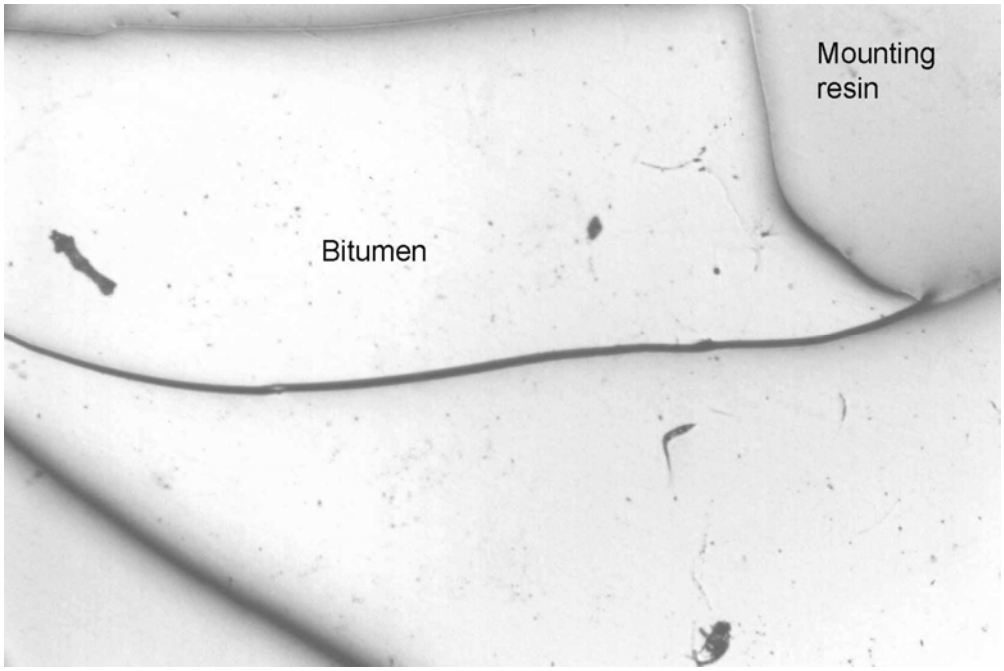

Plate II.1. Bitumen set in polyester resin. Cracks have developed within the bitumen after setting probably due to evaporation of "light ends" from the bitumen. Reflected white light, air lens, field width 1.12 mm.

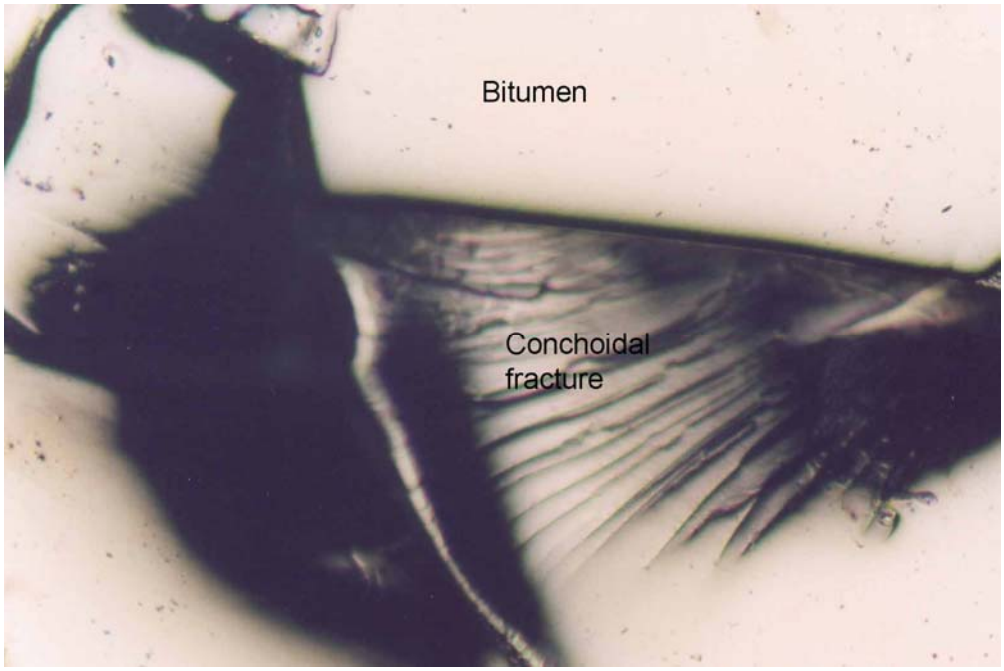

Plate II.2. Bitumen, the cracks show strong conchoidal features. Reflected white light, air lens, field width 1.12 mm.

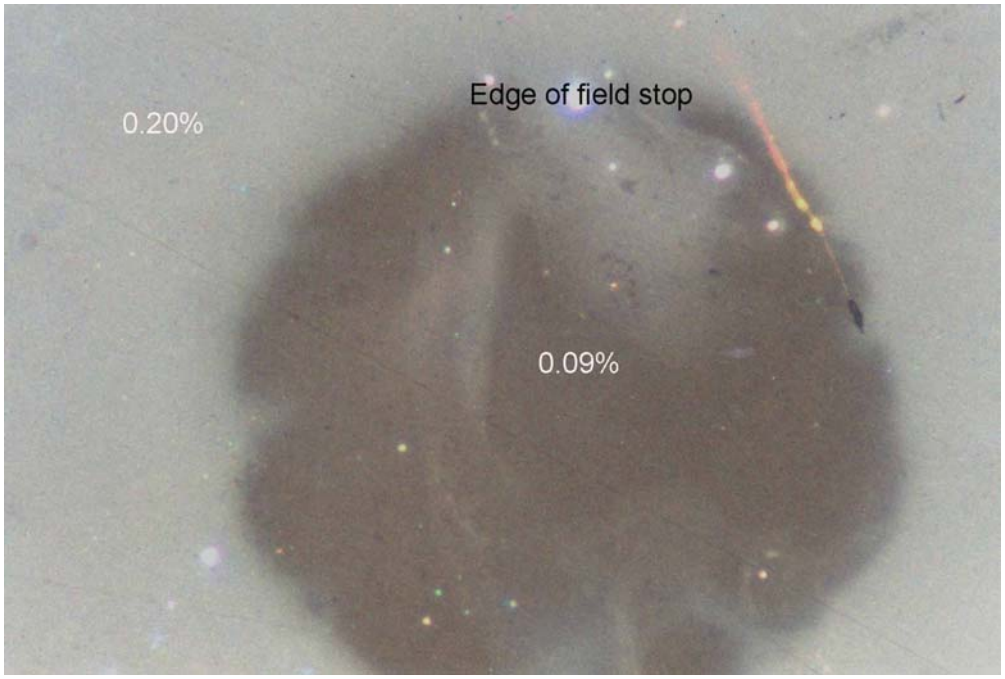

Plate II.3 Bitumen, photographed in oil immersion after the central part of the field had been irradiated with the fluorescence excitation beam for 25 minutes.. The stop was then opened up and the photographs taken in reflected white light. Reflected white light, field width 0.22 mm

BITUMEN - COMSTOCK MINE ZEEHAN

KK #	Depth (m)		$R_v$max			Sample description including liptinite fluorescence,
Ref #.	/Type	Mean	Range	SD	N	maceral abundances, mineral fluorescence
						HAND PICKED BITUMEN
T9385	?	-	-	-	-	Fluorescing liptinite absent. (Massive bitumen with strong
Mine	Bitumen	0.19	0.17-0.20	0.010	20	conchoidal fracture. Some internal structures are present within the bitumen. It appears to be losing some volatile components as some shrinkage occurred after polishing. Reflectance decreases slightly on immersion in oil, and this effect is accelerated by irradiation with fluorescence excitation beam. A reflectance of 0.20% was found to decrease to 0.09% after irradiation for 25 minutes. Fluorescence is weak to absent. It shows a slight increase on prolonged irradiation but is still weak. Pyrite rare.)

This bitumen does not appear to be related to those found in samples T9341 to T9343. The bitumen is referable to a suite of non-fluorescing bitumens and its low reflectance indicates a low level of maturation and would normally be expected to occur in association with a vitrinite reflectance of between 0.4% and 0.9%.

III. CARBONACEOUS SAMPLES FROM PERMIAN OUTCROPS NEAR ZEEHAN, TASMANIA

After it was established that the bitumen within the Comstock Mine was not related to the bitumens found in the Ordovician section, three samples from the Permian were sent for examination. These came from the Badger River near Firewood siding, south of Zeehan, 145 17.5' E, 42.00' S. Pieman 1:100 000 map 7914, grid ref CP 585 493. They consisted of carbonaceous shale grading to a shaly coal, and two sandy samples that were thought to contain possible bitumens.

All three of the samples were examined as whole rock mounts. T9396 and T9397 were crushed prior to mounting because it appeared that grains would tend to pick out during grinding and polishing. T9398 bitumen impregnated sandstone was sufficiently coherent to mount without prior crushing.

T9396 proved to be a sandy siltstone with abundant organic matter and it grades to a shaly coal in some layers. Vitrinite is abundant together with inertinite. Liptinite is present but is much less abundant compared with the other two maceral groups. The vitrinite takes a good polish Plate III.3) but it was found that it reacted rapidly with the immersion oil and developed etch marks along previously invisible polishing scratches (Plate III.1). The time over which these developed appears to be about 1 minute, but it was sufficiently rapid to make estimation of the time very difficult. At the same time as the etch marks developed, the vitrinite reflectance decreased from initial values generally over 0.7% to under 0.6%. Although measurements were made as quickly as possible and on areas that had been immersed for as short a time as possible, it is considered that the mean obtained understates the initial vitrinite reflectance value. An estimate for the initial mean of about 0.75% appears reasonable. It is, however, possible that a mean free of interactions with the oil might be closer to 0.80%. In addition to reacting with the immersion oil, the vitrinite shows unusually strong fluorescence (Plates III.2, III.4 and III.6). Small amounts of oil inclusions are present and oil occurs within some voids in semifusinite (Plate III.6).

T9397 is a silty sandstone with minor amounts of dispersed organic matter (dom), but it was decided that the vitrinite reflectance values that would be obtained would not be as good as those from T9396 and vitrinite reflectance values were not measured. The sample also contains sparse but prominent oil inclusions within the sand grains and these are illustrated in Plates III.7 and III.8. The oil inclusions occur as small isolated inclusions and as elongate clusters of inclusions Most of the clusters are in fractures in the quartz. It is not clear that the fractures have healed with later overgrowths and it is more probable that the fractures remain open. A few of the oil inclusions may be within quartz overgrowths. Some of the larger inclusions contain gas bubbles, but the background fluorescence from beneath the gas bubbles prevents these being seen in the Plates.

T9398 is a sandstone that contains bitumens within some of the intergranular porosity as seen in Plates III.9 and III.10. The form shown in Plate III.9 is the most common and relatively few show the platy or bladed structures of Plate III.10.

The maturation level of the Permian section sampled is best estimated at 0.75% but may be as high as 0.8%. The bitumens assumed to be present within the carbonaceous shale and shaly coal impart strong fluorescence to the vitrinite. In this they appear to differ from the bitumens in both the sandstone and the bitumen found in the Comstock Mine. The silty sandstone contains abundant brightly fluorescing oil and this presumably was originally part of the same petroleum system as the bitumens. The presence of gas bubbles indicates that the gas to oil ratio of the oil part of the system was originally relatively high. It would, however, be consistent with the moderately high vitrinite reflectance found in the carbonaceous sample.

The bitumen within the sandstone has optical properties very similar to those of the bitumen in the Comstock Mine. It would be desirable to demonstrate chemical similarities, but the optical properties are so close that it would be contrary to the principle of least action to propose two different origins. The bitumen do not appear to represent surficial alteration as this type of bitumen usually shows strong fluorescence so it is more likely to represent a reservoir bitumen. It may be possible to distinguish between an origin from cracking and deasphalting by looking at the isotopic isotope characteristics.

The presence of such abundant evidence of oils and bitumens within the Permian sections of Australia is unusual. Light oils are produced in the Cooper Basin and oil seeps are known in some of the collieries in the Sydney Basin. However, none of these occurrences is known to be associated with bitumens. The author knows of no descriptions of bitumen deposits derived from the Permian section in basement below the Permian sections. Some bitumens are present in the basement rocks of the Cooper Basin (Keiraville Konsultants proprietary information) but these are pyrobitumens native to the Lower Palaeozoic and are not derived from the Permian section.

PLATES – SECTION III

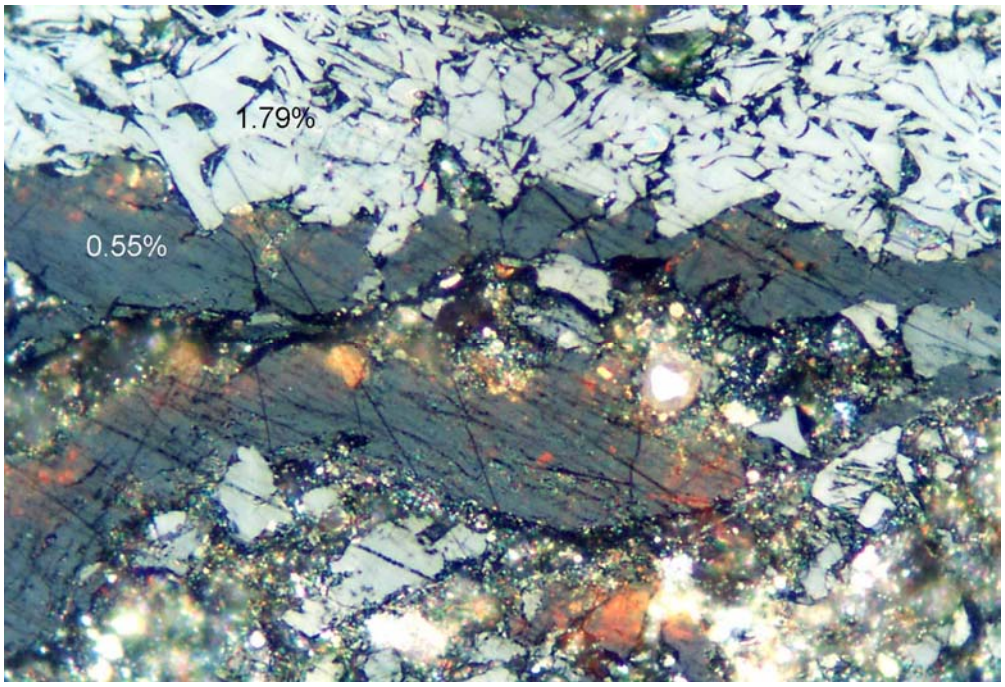

Plate III.1. T9396. Upper Permian shaly coal. Layers of vitrinite associated with semifusinite. This field has developed etch marks due to interaction with the immersion oil and the reflectance of 0.55% is lower than would have been obtained on initial immersion. $\overline{R}_v$max 0.67%. Reflected white light, field width 0.22 mm.

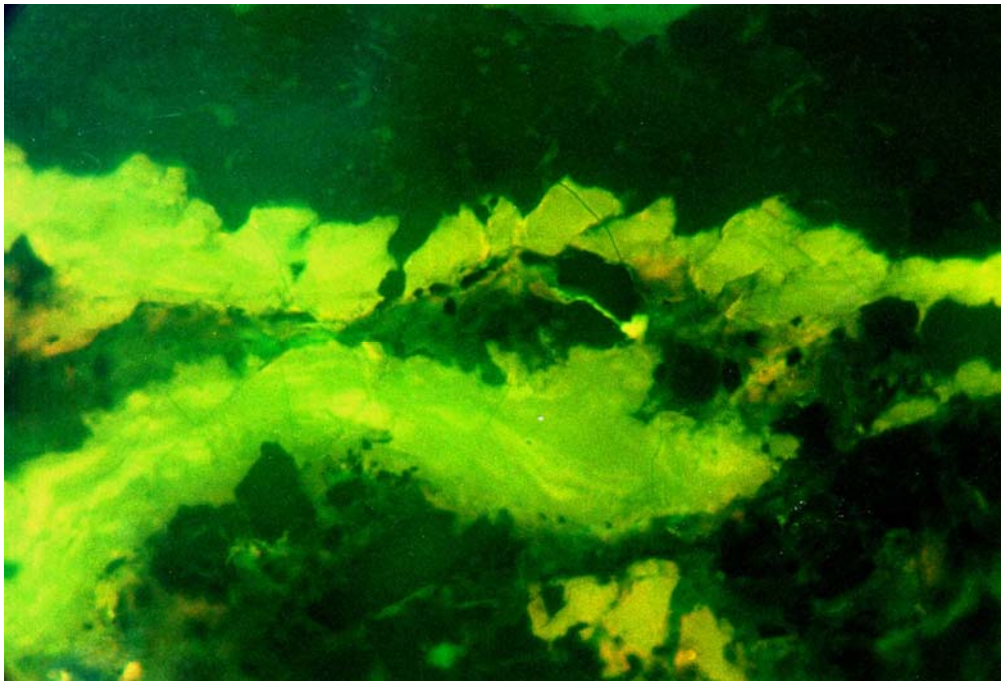

Plate III.2 T9396. Upper Permian shaly coal. As for Plate III.1 but in fluorescence-mode. The vitrinite shows unusually strong fluorescence that is assumed to be associated with the presence of bitumen impregnation. $\overline{R}_v$max 0.67%. Fluorescence-mode, field width 0.22 mm.

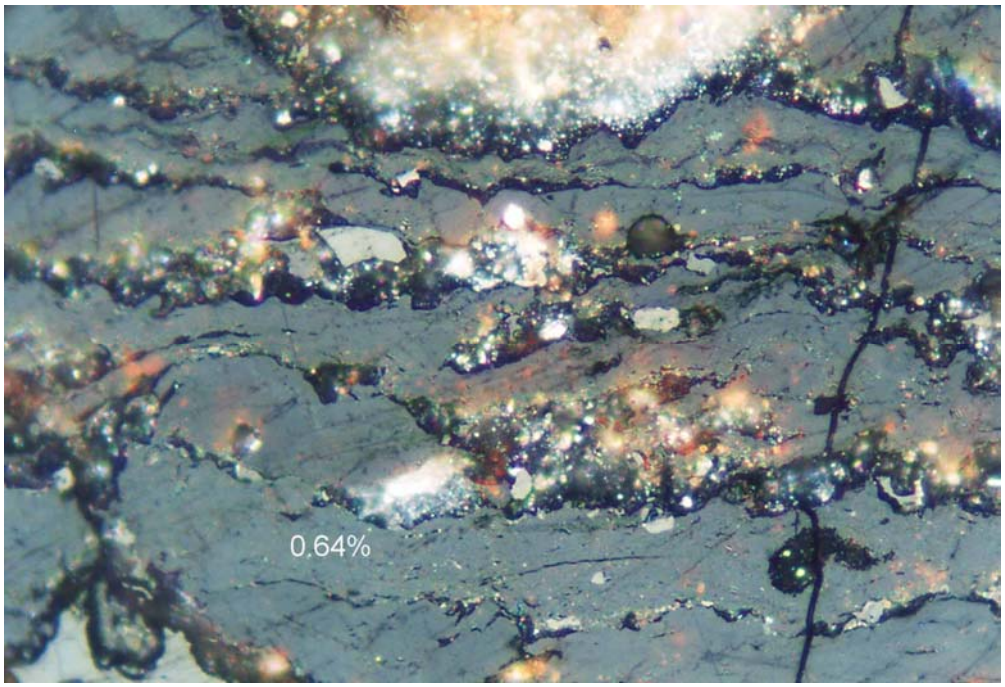

Plate III.3 T9396. Upper Permian shaly coal. Layers of vitrinite probably derived from leaves, photographed soon after immersion in oil. Note the absence of etching scratches and the higher reflectance value. $\overline{R}_v$max 0.67%. Reflected white light, field width

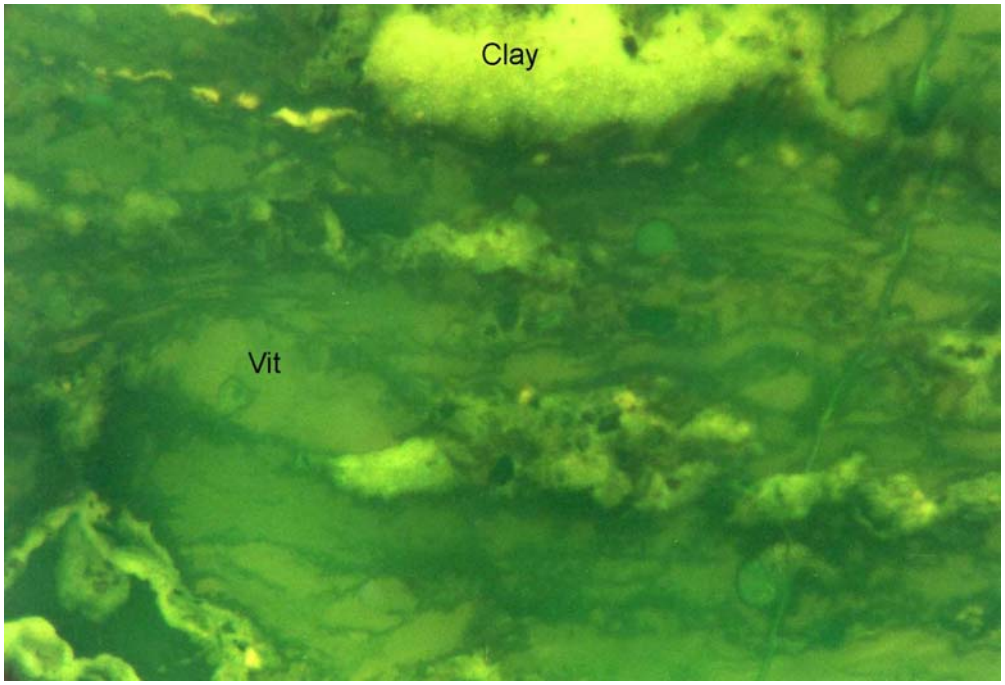

Plate III.4 T9396. Upper Permian shaly coal. As for Plate III.3 but in fluorescence-mode. The vitrinite shows unusually strong fluorescence and presumed botanical

structures are evident in this mode that appear to indicate bitumen uptake is controlled by tissue type. $\overline{R}_v$max 0.67%. Fluorescence-mode, field width 0.22 mm.

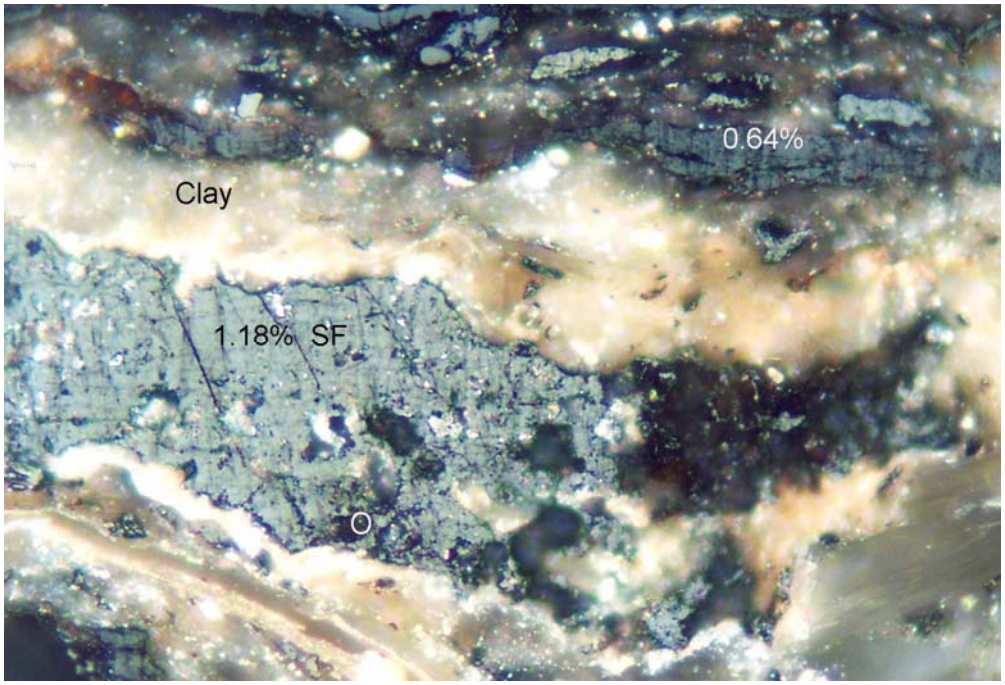

Plate III.5 T9396. Upper Permian carbonaceous shale. Lens of semifusinite with oil inclusion, and small lenses of detrovitrinite. $\overline{R}_v$max 0.67%. Reflected white light, field width 0.22 m.

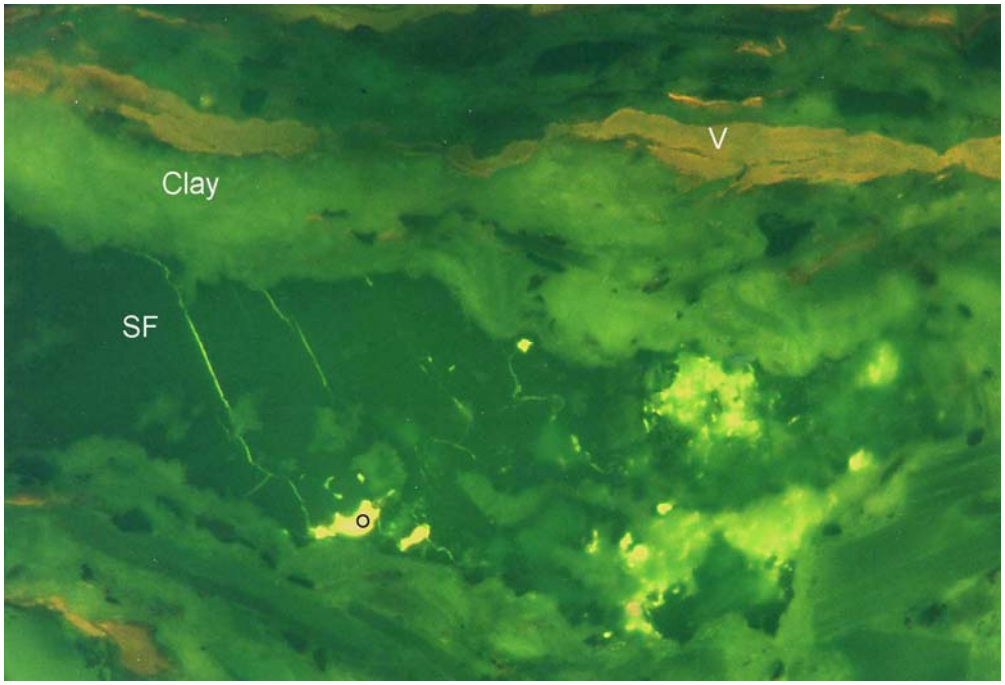

Plate III.6 T9396. Upper Permian carbonaceous shale. As for Plate III.5 but in fluorescence-mode. Bright yellow fluorescing oil inclusions in semifusinite and some smaller inclusions within clays to the right of the semifusinite lens. The vitrinite shows strong fluorescence. $\overline{R}_v$max 0.67%. Fluorescence-mode, field width 0.22 m

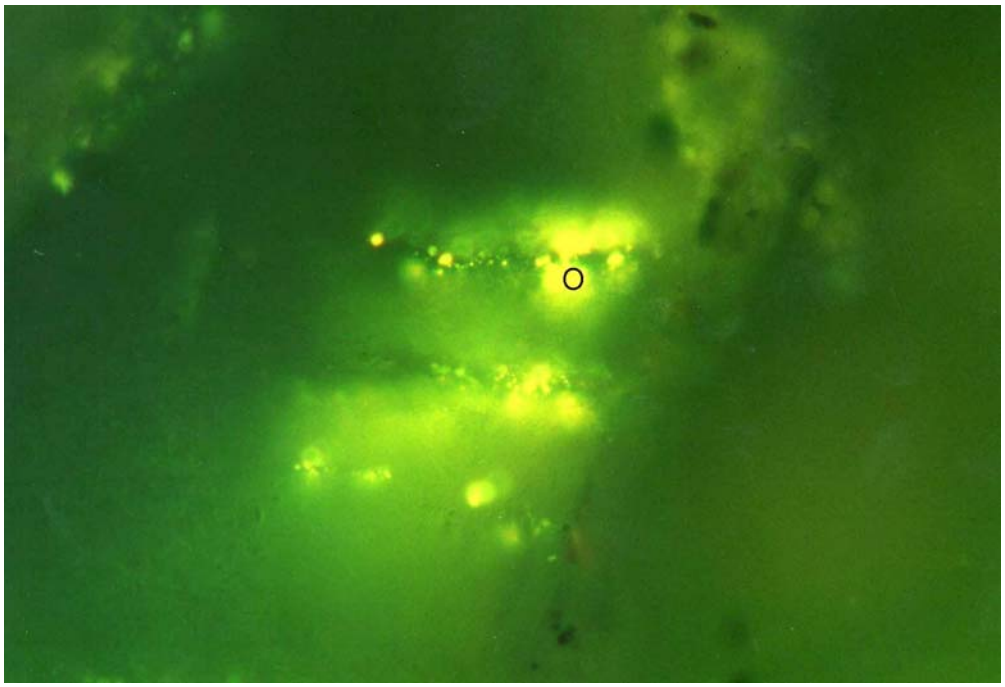

Plate III.7 T9397. Upper Permian silty sandstone. Bright yellow oil inclusions aligned along fractures within quartz grain. Fluorescence-mode, field width 0.22 mm.

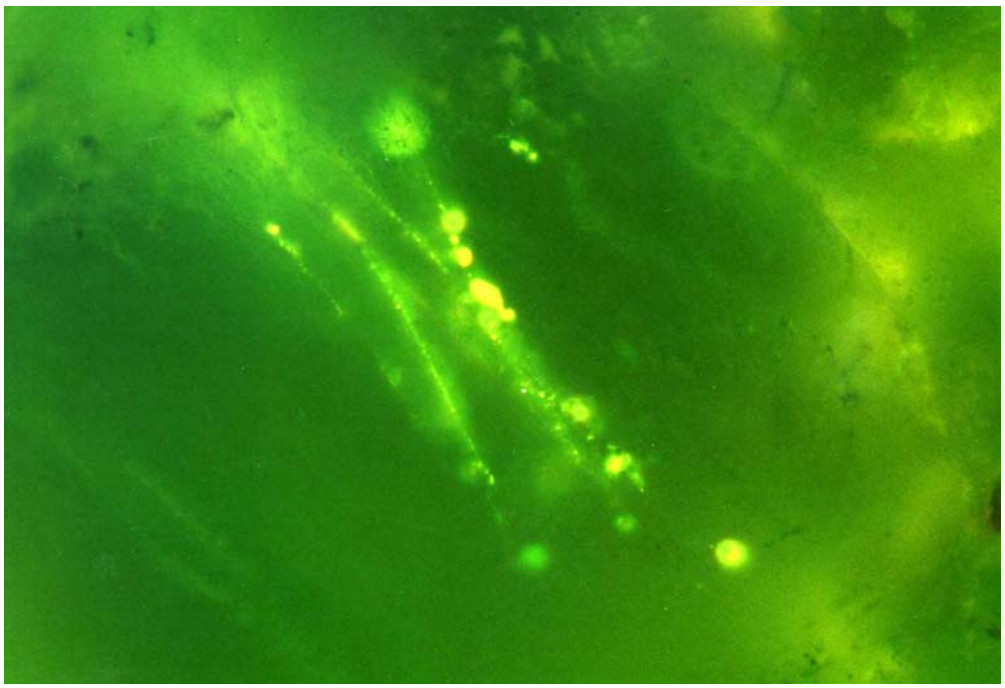

Plate III.8 T9397. Upper Permian silty sandstone. Bright yellow oil inclusions aligned along fractures within quartz grain. Fluorescence-mode, field width 0.22 mm.

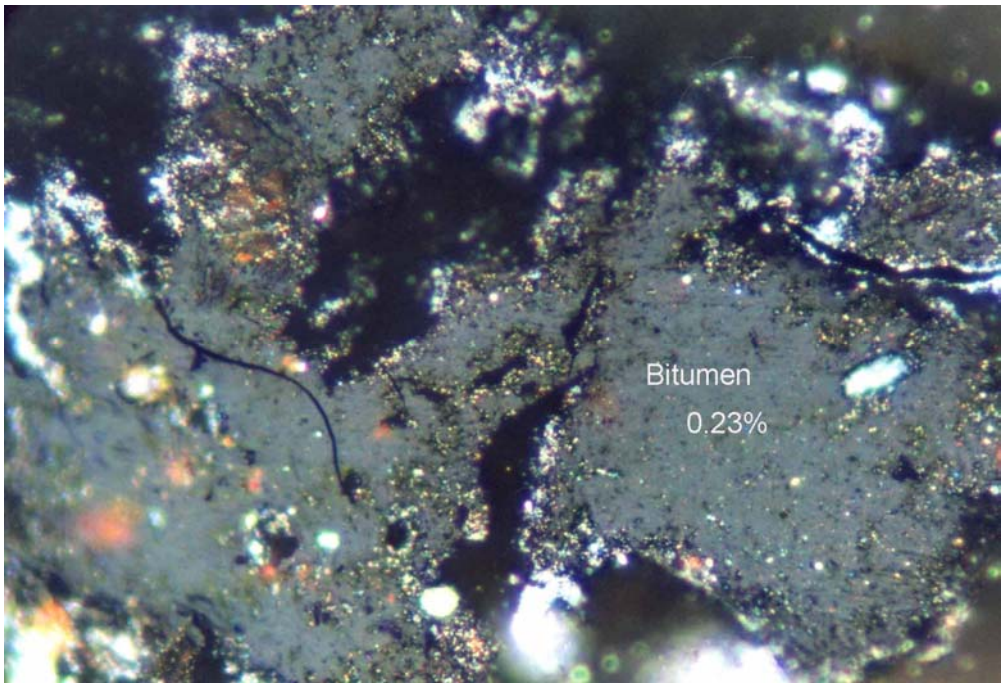

Plate III.9 T9398. Upper Permian, bitumen impregnated sandstone. Bitumen occurring within interstitial spaces between quartz grains. Reflected white light, field width 0.22 mm.

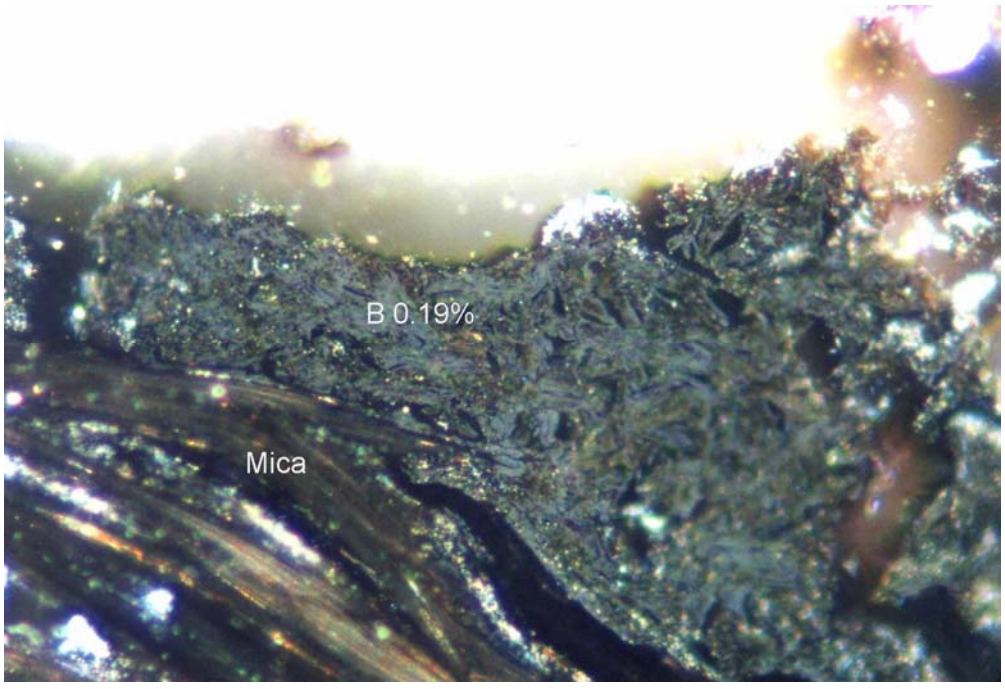

Plate III.10 T9398. Upper Permian, bitumen impregnated sandstone. Bitumen occurring within interstitial spaces between a quartz grain above showing strong

internal reflections and a mica grains below. The bitumen has a platy and radiating structure and appears to be associated with books of clays minerals. Reflected white light, field width 0.22 mm.

OUTCROPS NEAR COMSTOCK MINE, ZEEHAN TASMANIA

KK # Ref #.	Depth (m) /Type	$R_v$max Mean	Range	SD	N	Sample description including liptinite fluorescence, maceral abundances, mineral fluorescence
						SANDY SILTSTONE WITH PLANT REMAINS
T9396 Surface	O/C	0.67	0.58-0.86	0.068	25	Common cutinite orange to dull orange, sparse sporinite yellowish orange to orange. (Sandy siltstone tending to shaly coal with peat-like structures. Dom major, I>V>L. Inertinite and vitrinite major, liptinite common. The vitrinite shows moderate to strong orange fluorescence with I546 of about 0.25 to 0.33 whereas the sporinite shows I values of about 0.5*. The vitrinite rapidly develops enlarged scratches due to etching of the polished surface by the immersion oil. This is associated with a fall in reflectance and is presumed to be due to the presence of impregnating bitumens. The effect is so rapid that it was difficult to quantify. The reflectances reported were made by taking measurements as rapidly as possible after initial immersion. Approximately one to two minutes of immersion appears to causse a decrease from about 0.75% to 0.65%. A realistic figure for the mean on initial immersion is about 0.75%. The fluorescence of the sporinite suggests that the bitumens have not caused a major lowering of that value from the one that would be found for vitrinite not impregnated with bitumens. Rare bright yellow oil drops in lumens within semifusinite. Pyrite rare.)
						SANDY SILTSTONE WITH OIL INCLUSIONS
T9397 Surface	O/C	-	-	-	-	Fluorescing liptinite absent. (Sandy siltstone. Dom common, I> V>L. Inertinite and vitrinite sparse, liptinite rare. Reflectance values were not measured for the vitrinite because the surface quality was poor and similar alteration as found for T9396 was noted. The poor surface quality was due to the adhesion of polishing powder for reasons that are not clear. Sparse, but prominent oil drops, mostly within fractures in quartz grains. The larger inclusions show distinct gas bubbles. The oils show yellow fluorescence. More diffuse oil inclusions are associated with what appear to represent altered lithic fragments. Pyrite rare.)
						SANDSTONE WITH INTERSTITIAL BITUMENS
T9398 Surface	O/C Bitumen	- 0.21	- 0.17-0.24	- 0.022	- 16	Fluorescing liptinite absent. (Sandstone, moderately well sutured with lens shaped to ovoid interstices filled with low reflecting and non-fluorescing bitumens. Most of the bitumens are massive, and show weak structures within the bitumen that are generally concentric and run parallel with the walls of the interstices. Less common occurrences have the form of radiating booklets. This form is unusual and could be associated with emplacement in association with clay minerals or illite. Pyrite rare.)

The rank of the outcrop samples appears to be mid to late mature. The vitrinite in the coaly sample shows evidence of bitumen impregnation. The silty sample does not contain clear bitumens but rather unusually for an outcrop sample shows prominent oil inclusions. The more massive sandstone contains a bitumen phase that is very similar in terms of optical properties with the bitumen from the Comstock Mine.
*Measured relative to a uranyl glass standard.

ACC 19 November 2003

9. REFERENCES

Cook, A. C. and Kantsler. A. J. (Eds), 1980. *Oil Shale Petrology Workshop, Wollongong, 1980*. Keiraville Konsultants, 100p.

Standards Association of Australia, 2000. *Methods for Microscopical Determination of Reflectance of Coal Macerals.* AS 2486.

Taylor G. H, Teichmüller M, Davis, A, Diessel, C. F. K, Littke, R. and Robert, P., 1998. *Organic Petrology.* (Gebrüder Borntraeger, Berlin-Stuttgart) 704p.

APPENDIX G.

Organic petrology and maturation of three samples from Tasmania.

Report by Alan Cook.

ORGANIC PETROLOGY AND MATURATION OF THREE SAMPLES FROM TASMANIA

PREPARED FOR ALAN CHESTER

By

A.C.COOK

KEIRAVILLE KONSULTANTS
7 Dallas St
Keiraville, NSW, 2500
Australia

AUGUST 2004

ORGANIC PETROLOGY AND MATURATION OF THREE SAMPLES FROM TASMANIA

ALAN C COOK

CONTENTS

ORGANIC PETROLOGY AND MATURATION OF THREE SAMPLES FROM TASMANIA

Summary

Two coals from Mersey River equivalents and a carbonaceous shale from the Henty River in West Tasmania were received from Alan Chester. The samples were cut, impregnated with cold-setting resin and polished for petrographic examination. Vitrinite reflectances were measured on all three samples and maceral analyses were made using point count methods.

The coals are both rich in liptinite macerals. Both contain rare to sparse telalginite that is referable to *Reinschia* a genus similar to modern form *Botryococcus*. Telalginite was not, however, encountered during the point counts indicating the abundance is less than 0.2% (the percentage that corresponds with a single count in an analysis with 500 counts). Cutinite and sporinite are the most abundant liptinite macerals.

The general appearance of the coals is similar to that of the Greta coals from NSW. Similar to the Greta coals, pyrite is abundant and some marine influence has affected both coals.

The reflectance contrast between the vitrinite and both the liptinite and the inertinite is high. Fusinised resin bodies are present and form a small but characteristic part of the maceral assemblages.

In terms of maturation, the coals lie close to the boundary between low rank and medium in the new ISO coal classification system. In textural terms, however, they clearly have affinities with the medium rank coals.

The carbonaceous shale shows a higher level of maturation. Some lenses of telovitrinite are present and these appear to represent root tissues. Inertinite is the most abundant maceral group. Rare sporinite is present and shows dull orange fluorescence.

ORGANIC PETROLOGY AND MATURATION OF THREE SAMPLES FROM TASMANIA

ALAN C COOK

1. INTRODUCTION

Three samples were submitted by Alan Chester for determination of the level of maturation as assessed from vitrinite reflectance and to report on the presence or absence of alginite. Two of the samples are coals equivalent to the Mersey River coals and the third sample is a carbonaceous shale from the Henty River, West Tasmania. Details of the results for the individual samples are given in Appendix 2. Maceral abundances were determined using point counting analysis.

1.1 PREPARATION AND MOUNTING OF SAMPLES

The samples were slabbed, placed in silicone moulds and dried. The dried samples were mounted using cold-setting polyester resin. Polyester is preferred to the epoxy resins because it has a polishing hardness closer to that of coals. The blocks after mounting range up to 25 x 25 mm. The resin is mixed with MEKP (methyl ethyl ketone peroxide) and poured on to the samples and the resultant mixture stirred in with the grains to ensure mixing. The moulds were then placed in a vacuum oven and evacuated to about 750 mm Hg of vacuum. They were held at this vacuum level for approximately one minute to permit the escape of air and then returned to normal pressures. This procedure improves impregnation of the samples by the mounting resin.

1.2. GRINDING AND POLISHING

Samples were ground to expose the samples using 60 mesh paper and then finely ground using in succession 240, and 400 mesh wet and dry papers on rotating laps and then a 20 microns diamond lap. A final stage of grinding was done using 7-micron corundum powder on a velvet lap. This removes the fine scratches from the papers and reduces the polishing times that are required.

The coarse polishing stage used polishing grade chromium sesquioxide (GNM) on a velvet lap. Polishing speed for this stage was about 70 rpm. Chromium sesquioxide gives a rapid polish with only moderate relief. Any polishing powder that remains on the surface can easily be seen because of the distinctive green colour of chromium sesquioxide. This characteristic is useful during microscopic examination as remnant traces of polishing powder can be readily distinguished from mineral components. Samples were rotated during polishing to avoid a directional polish. Fine polishing was undertaken using gamma alumina on a velvet cloth lap with a variable speed lap. Normal polishing speed for this stage was about 50 r.p.m. This polishing agent and lap combination gives moderate polishing relief and controlled polishing relief is useful during identification of macerals.

The surfaces of the blocks were cleaned at each stage after polishing by rubbing on a clean velvet cloth. For all three samples, water was used as the carrying agent.

1.3. REFLECTANCE MEASUREMENTS

Reflectance measurements are made in accordance with AS 2486. A Leitz MPV 1.1. photometer mounted on a Leitz Orthoplan microscope, is used. Measurements are made using a 50x NPL oil immersion objective lens. The OPAK illuminator is set so that the Berek prism is in the light train and the polarizer is in the 45-degree position. A 10x ocular is used to project the image onto the field stop adjacent to the photometer. Total magnification from the system on to the photometer stop is 500x.

The field stop that is located in the mounting from the stabilized light source is set to illuminate about 30 microns square on the sample. For measurements, the stabilized quartz iodine lamp, photomultiplier tube (PMT) voltage combination is set to give a readout that is essentially a direct reading of reflectance, once the standards have been calibrated. The measuring stop in front of the photometer is set to an aperture giving a back projected image size on the sample of about 2 microns by 3 microns.

The standards used are the McCrone spinel (0.42%) yttrium aluminium garnet (0.90%) and the gallium gadolinium garnet (1.72%). Calibration runs are taken before and after each set of reflectance measurements or at any other time when there is evidence of drift. The main cause of rapid change is the presence of small air bubbles that rise into the oil from pores within the samples. Checking for air bubbles is done directly by introducing the Bertrand lens to the light path where a polarizing binocular tube is fitted. Temperature in the room with the photometer is kept within a range of 23°C $\pm$2°C.

Mean maximum reflectances are measured. To obtain these, after a vitrinite field had been acquired, the stage was rotated until a maximum is obtained. The stage is then rotated 180 degrees to obtain a second maximum. Provided the two values are within about 5% relative, they are accepted and averaged. Therefore the number of measurements taken is twice the number of fields reported as being measured. The overall mean, ranges and standard deviations are reported, together with descriptions of each sample, including estimated maceral abundances by volume. Variation of readings on rotation is usually associated with local tilt due to polishing relief or the development of desiccation cracks. A check on tilt can be made using the Bertrand lens. Although the effects of tilt cannot be eliminated, setting the stage at the location where N-S run out of the Bertrand image is at its lowest, will minimize them.

Even after careful centering of the lens, stage run-out is typically about 0.002 to 0.003 mm. This means that where pairs of readings are made, although these are almost on the same area of vitrinite, the exact areas for the two component readings for each measurement may be slightly different. Thus, the number of fields measured is effectively more than the number reported in the data listings. For this reason, means and histograms are more robust statistically than where single readings have been taken.

For samples with clearly defined vitrinite populations, the mean reflectance has stabilized after about 20 readings and the base number of fields measured (N) is 25 where sufficient fields can be found. Where multiple populations or other complications are present, the number of fields is increased provided sufficient fields are found. In the present case, the vitrinite populations are relatively simple and 25

fields would have been sufficient. However, for the coals, the number of fields measured was increased to just over 40 to provide more information on the distribution of individual vitrinite reflectance values.

Maceral and vitrinite reflectance accreditation certificate from ICCP numbered ICCP/FA/42.1/0136AB valid to 31/12/2004 (A C Cook)

1.4. MACERAL ANALYSES

The macerals recognized are listed in Appendix 1. The classification given here differs slightly from those used in ICCP 1994 and Taylor et al., (1998). The major differences relate to the combination of terms for lower rank vitrinite macerals (termed huminite in Taylor et al.) and to the macerals within alginite. The use of the term vitrinite over the full range of rank or maturation simplifies descriptions and does not result in the loss of any information.

The samples were point counted to try to determine the relative abundances of the liptinite macerals. For the coals, liptinite content ranges from 15 to 20%. The lower limit of detection with a 500-count analysis is 0.2%. In neither of the analyses on coals was a count recorded for telalginite although in many of the fields telalginite could be seen away from the cross hairs. The limit of detection for the point count is <0.2% as this corresponds to a single count. The number of points marginally exceeds 500 because the traverse where 500 is reached is counted to the end to avoid bias associated with the distribution of various lithologies.

For the descriptions abundance categories were used and these were recorded in the data given in Appendix 2. Examinations were made using the plane slip illuminator and fluorescence-mode was used for all fields in order to better detect fluorescing liptinite.

1.5. SEQUENCE DURING EXAMINATION OF SAMPLES

Samples are examined first using a low power air immersion lens in order to examine the overall textures. After immersion oil is placed on the sample, reflectance measurements are made as soon as possible. Experience shows that reflectance values can decrease following immersion in oil, usually after a period of some hours. Making reflectance measurements within an hour of initial immersion eliminates the possibility of this occurring. Some fluorescence examinations were undertaken concurrently with the measurement of reflectance, mostly for the lower vitrinite reflectance samples to check on the presence or absence of fluorescence from the vitrinite.

Following the measurement of vitrinite reflectance, the samples are examined in fluorescence and white light modes to obtain the maceral analyses. All the samples are examined using both white light and fluorescence-modes. Some photographs were taken during the measurement of vitrinite reflectance but most were taken after sample description had been completed.

Where abundance terms are used, these are defined as follows:

CATEGORY	PERCENTAGE (by volume)
ABSENT	0.0
RARE	<0.1
SPARSE	0.1<x<0.5
COMMON	0.5<x<2.0
ABUNDANT	2.0<x<10.0
MAJOR	10.0<x<50.0
DOMINANT	50.0-100

Coal and shaly coal are defined as:

COAL	ORGANIC MATTER >80%
SHALY COAL	40% < % ORGANIC MATTER <80%

2. ORGANIC FACIES PRESENT

The vitrinite reflectance data for the samples is summarised in Appendix 2 and the histograms are presented in Appendix 3.

The coals show vitrinite reflectance values of 0.46 and 0.47% respectively for Cat 1 and Cat 2. Small amounts of telalginite are present. The amounts are not sufficient to cause a major lowering of vitrinite reflectance similar to that reported by Hutton and Cook (1980) for torbanites. However, the vitrinite has probably been slightly influenced by the organic facies present and corrected values of between 0.50 and 0.55% are suggested for both samples allowing both for the abundance of pyrite and the presence of telalginite.

The coals are rich in liptinite with the main liptinite macerals being sporinite and cutinite (Plates 1, 2, 5, 6, 7, 8 and 11). Telalginite is rare to sparse (Plates 5, 6, 9, 10 and 11) but is visually prominent due to its strong fluorescence intensity. In illustrating the telalginite a compromise is required between losing botanical detail within the Reinschia colonies and rendering the sporinite and cutinite darker than desirable.

The coals are for the most part finely layered with Cat 1 being dominated by duroclarite and Cat 2 containing subequal amounts of duroclarite and clarodurite. Some thicker layers of vitrinite are present (Plates 1 and 9). These tend to show higher reflectances compared with the thinner layers that show more affinities to detrovitrinite. Some of the vitrinite-rich coal may be derived from leaf tissues.

Pyrite is widely distributed and is illustrated in Plate 5. The reflectance of the pyrite is close to 100 times that of vitrinite again making it difficult to illustrate detail of the two phases within the same illustration. The pyrite indicates some marine influence, but this may have been subsequent to the deposition of the coal rather than contemporaneous.

The inertinite population is characterised by the presence of some extremely high reflecting inertodetrinite as illustrated in Plate 1. The secretinite illustrated in Plates 3 and 4 is also very distinctive. It is derived from the fusination of special types of resin, commonly medullosan ferns, and is considered to be formed during fire episodes. The balance between high and lower reflecting inertinite is unusual for Gondwana coals, but is similar to that found in the Greta coals from NSW.

The finely layered nature of this type of coal has attracted some attention. The deposition of the peat is likely to have been hypautochtonous. The paucity of interbedded minerals precludes an allochthonous origin. The small size of most of the phyterals indicates a lack of large trees, but the presence of cutinite indicates forms with moderate to large sized leaves. Some of the inertinite may be attrital indicating some periods of higher water levels. The telalginite has probably entered the peat swamps at those times. Growth of the algae within the peat is less likely due to the low pH of most peat swamp settings.

3. MATURATION LEVELS

The ranges of vitrinite reflectance found for the coals are relatively small and the standard deviations are also low to moderately low. Thus the precision of the vitrinite reflectance means obtained is high. However, some variation may be present between plies and the means for other plies within seams could be slightly different. The coals lie at the top of the zone of oil generation.

The range for the carbonaceous shale is also relatively small. The mean value of 0.76% indicates that the section lies in the middle of the oil generation window.

4. HYDROCARBON POTENTIAL

The coals have excellent source potential. The presence of fluorescence from the vitrinite indicates that some generation has occurred within the coals. It is commonly argued that coals do not release liquid hydrocarbons although the abundance of oil in the Gippsland Basin and the ratio of organic matter present as coal to that as dispersed organic matter (dom) is a strong argument that the coals are effective source rocks. Although the telalaginite will have a high pyrolysis yield, the amounts present are too small to influence source potential. Additionally, the aliphatic molecules present in telalginite appear to be relatively refractory and during coalification, rather than generate liquids, they aromatise with the evolution of gaseous hydrocarbons.

The carbonaceous shale has poor source potential even though it has a relatively high TOC.

5. CONCLUSIONS

The coals are rich in liptinite and are similar in many respects to the Greta coals from NSW. The vitrinite reflectance data indicates that they lie close to the top of the oil window.

The carbonaceous shale lies in the middle of the oil generation window but has poor source potential for oil. At higher ranks, it would have some potential to generate gas.

6. REFERENCES

Hutton, A.C., and Cook, A.C., 1980. Influence of alginite on the reflectance of vitrinite from Joadja, N.S.W. and some other coals and oil shales containing alginite. Fuel, 59, pp. 711-714.

ICCP, 1995. Vitrinite Classification, ICCP System 1994. ICCP, Aachen, Germany, 1995, 24p.

Standards Association of Australia, 2000. Methods for microscopical determination of reflectance of coal macerals. AS 2486.

Standards Association of Australia, 1981. Determination of maceral group composition of bituminous coal and anthracite (hard) coal. AS 2515.

Standards Association of Australia, 1986. Coal maceral analysis. AS 2856, 22p.

Taylor, G.H., Teichmuller, M., Davis, A., Diessel, C.F.K., Littke, R., Robert, P., 1998. Organic Petrology. (Gebruder Borntraeger, Berlin-Stuttgart) 704p.

KEY TO PLATES

The plates were taken using 400 ASA negative film and the digital images produced from scanning 15 cm x 10 cm prints at 400 dpi and the macro photographs were made by scanning the polished surface at 1200 dpi.

Percentages indicate vitrinite reflectance at the location indicated.

Cut – cutinite

PLATES

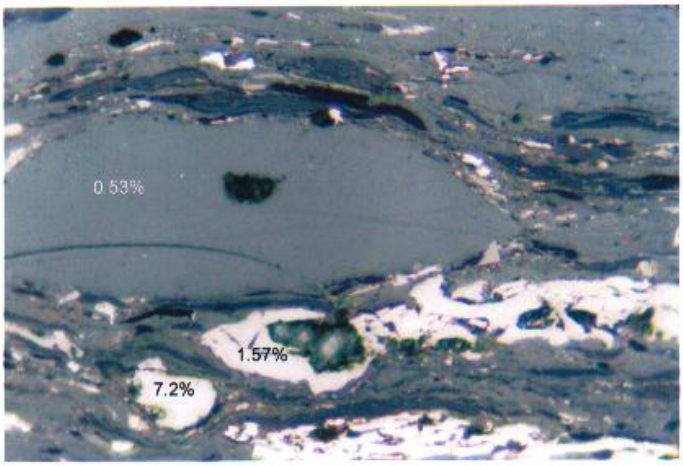

Plate 1 T9754. Cat 1. Clarite (upper part of the field) and duroclarite (lower part of the field). Liptinite shows very low reflectances and appears very dark. Some of the inertinite shows very high reflectances and some of the inertodetrinite in this field has a reflectance of 7.2%. Reflected white light mode, $\overline{R}_r$max 0.47%. Field width 0.22mm.

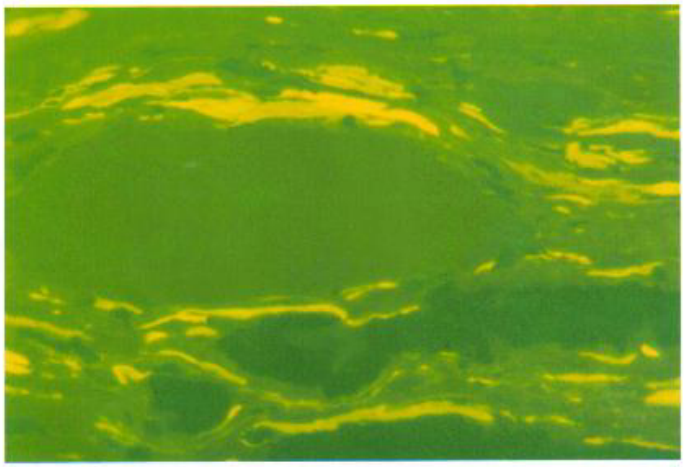

Plate 2. T9754. Cat 1. As for Plate 1, but in fluorescence-mode. Most of the liptinite is sporinite in this field. The vitrinite shows weak dull brown fluorescence. Fluorescence-mode, $\overline{R}_r$max 0.47%. Field width 0.22mm.

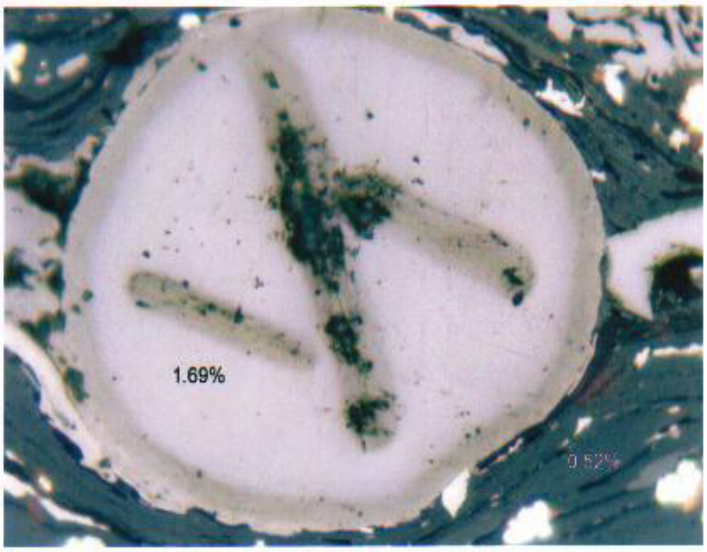

Plate 3. T9754. Cat 1. Large body of fusinised resin (secretinite). The rims and linear canals are commonly found in secretinite and appear to originate during the fusinisation process. Reflected white light mode, $\overline{R}_r$max 0.47%. Field width 0.22mm.

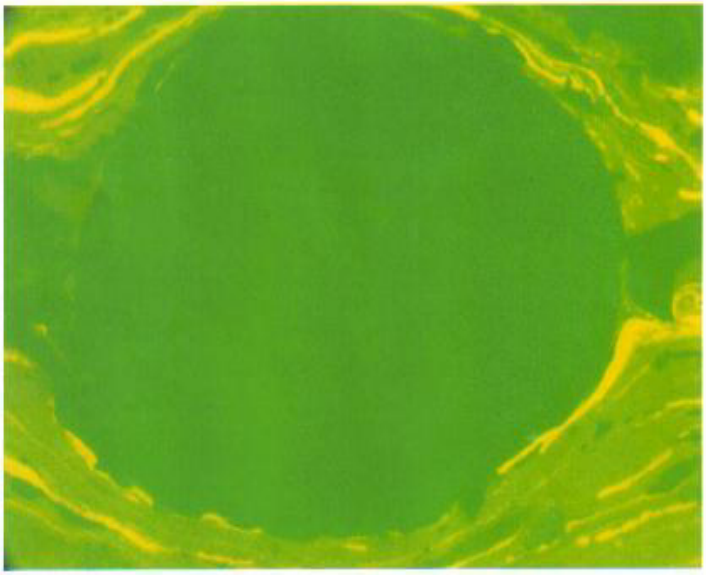

Plate 4 T9754. Cat 1. As for Plate 3, but in fluorescence-mode. Compaction structures are seen around the secretinite body. Fluorescence-mode, $\overline{R}_r$max 0.47%. Field width 0.22mm.

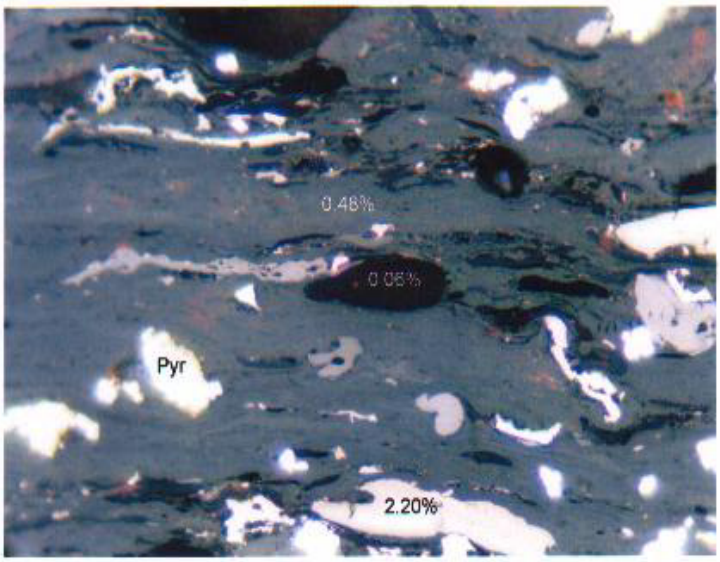

Plate 5. T9754. Cat 1. Duroclarite with abundant pyrite and small lens of telalginite. The pyrite indicates some marine influence, but the occurrence of pyrite and telalginite do not appear to be related. Reflected white light mode, $\overline{R}_v$max 0.47%. Field width 0.22mm.

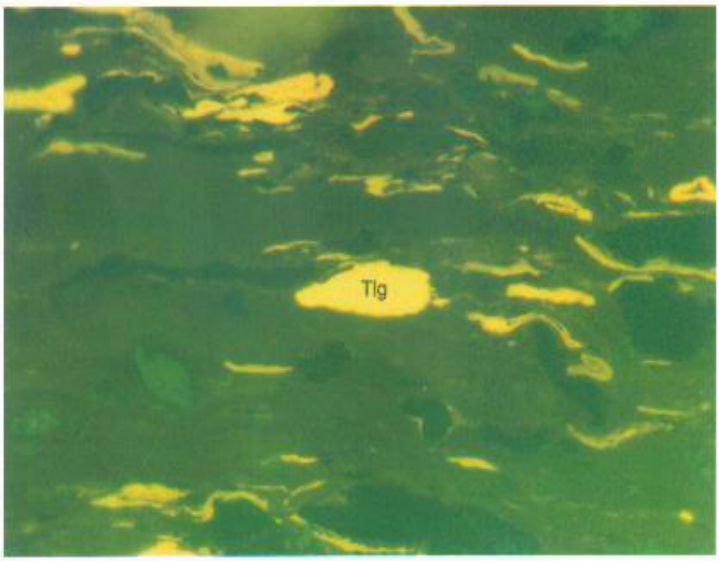

Plate 6 T9754. Cat 1. As for Plate 5, but in fluorescence-mode. The fluorescence intensity of the telalginite is markedly higher than that of the sporinite. Fluorescence-mode, $\overline{R}_v$max 0.47%. Field width 0.22mm.

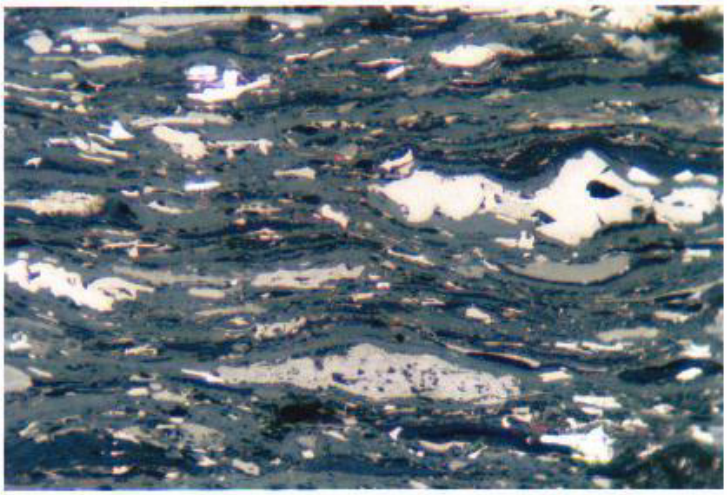

Plate 7. T9755. Cat 2. Coal transitional between duroclarite and clarodurite with abundant sporinite and cutinite associated with finely layered coal. Reflected white light mode. $\overline{R}_v$max 0.46%. Field width 0.22mm.

Plate 8 T9755. Cat 2. As for Plate 7 but in fluorescence-mode. Both the sporinite and the cutinite show strong orange fluorescence with some of the sporinite ranging to yellow. Fluorescence-mode. $\overline{R}_v$max 0.46%. Field width 0.22mm.

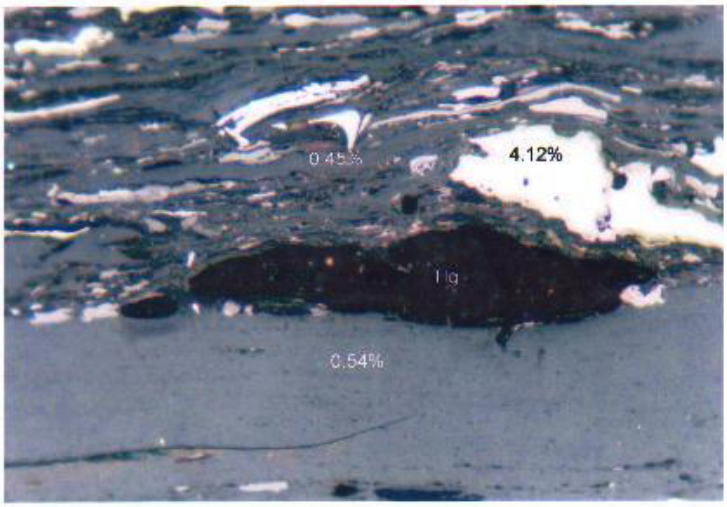

Plate 9. T9755. Cat 2. Telovitrinite overlain by a large lens of telalginite formed from *Reinschia sp* with spore-rich duroclarite in the upper part of the field. Reflected white light mode. $\overline{R}_v$max 0.46%. Field width 0.22mm.

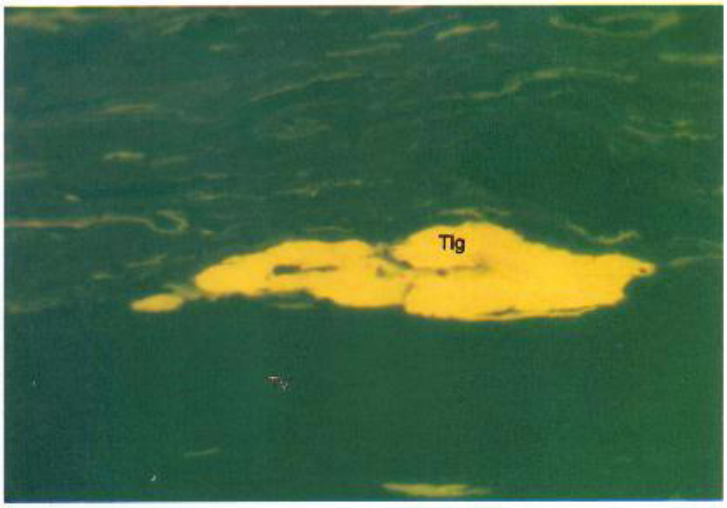

Plate 10 T9755. Cat 2. As for Plate 9 but in fluorescence-mode. Large compound lens of telalginite formed from *Reinschia sp*. The sporinite appears dark due to the contrast in fluorescence intensity between the telalginite and the sporinite. Fluorescence-mode. $\overline{R}_v$max 0.46%. Field width 0.22mm.

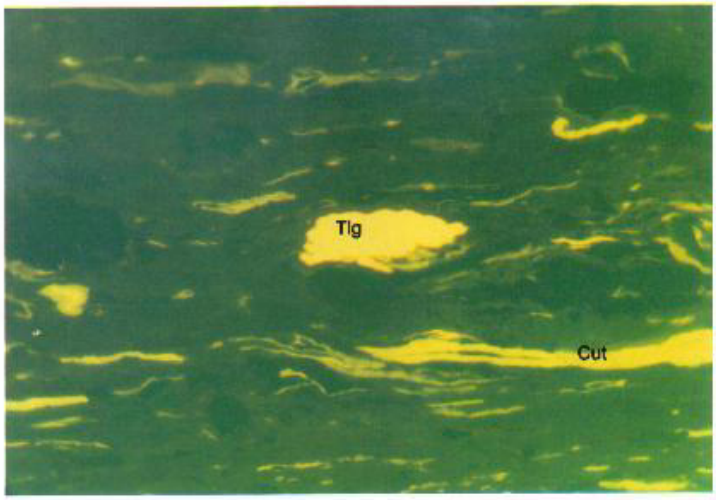

Plate 11. T9755. Cat 2. Coal rich in liptinite derived from cutinite and sporinite with a small lens of telalginite derived from *Botryococcus sp*. Fluorescence-mode. $\overline{R}_v$max 0.46%. Field width 0.22mm.

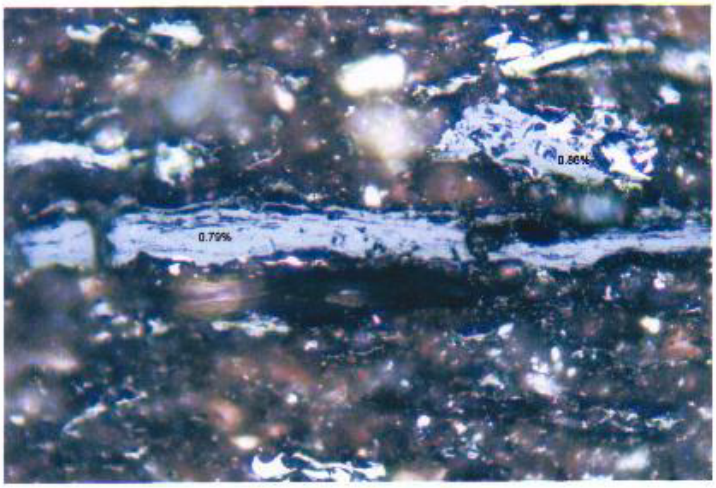

Plate 12. T9756. MQC. Carbonaceous shale with abundant inertinite and elongate lens of telovitrinite. The form of the telovitrinite is consistent with an origin from root tissues. Reflected white light mode. $\overline{R}_v$max 0.76%. Field width 0.22mm.

APPENDIX 1. MACERAL GROUPS, SUB-GROUPS, MACERALS AND SUB-MACERALS

MACERAL GROUP	MACERAL SUBGROUP	MACERAL	SUB-MACERAL
VITRINITE	TELOVITRINITE	TEXTINITE	TEXTINITE A&B
		TEXTO-ULMINITE	TELINITE
		EU-ULMINITE	
		TELOCOLLINITE	COLLOTELINITE
	DETROVITRINITE	ATTRINITE	
		DENSINITE	
		DESMOCOLLINITE	
	GELOVITRINITE	CORPOGELINITE	
		PORIGELINITE	
		EUGELINITE	
INERTINITE	TELO-INERTINITE	FUSINITE	
		SEMIFUSINITE	
		SCLEROTINITE	
	DETRO-INERTINITE	INERTODETRINITE	
		MICRINITE	
LIPTINITE		SPORINITE	
		CUTINITE	
		SUBERINITE	
		RESINITE	
		FLUORINITE	
		LIPTODETRINITE	
		ALGINITE	TELALGINITE
			LAMALGINITE
		BITUMINITE	
		EXSUDATINITE	

NOTE: ICCP uses the same divisions to the sub-group level (ICCP 1994 System). At the maceral level, ICCP terminology is now moving to use a single system for low and moderate to high levels of maturation.

* Exsudatinite is a primary bitumen and should be included with other bitumens but at present is included by ICCP within the maceral system.

APPENDIX 2. DETAILED RESULTS FOR THE JURASSIC SAMPLE SUITE.

Ref.	Depth (m)	Mean	$R_v$max Range	SD	N	Sample description including liptinite fluorescence, maceral abundances, mineral fluorescence
T9754 O/C	O/C	0.47	0.42-0.54	0.031	41	**CAT 1 – MERSEY R. EQUIV.** Abundant cutinite yellow to orange, common sporinite yellowish orange, rare cutinite orange, rare to sparse telalginite yellow to yellowish orange. (Finely layered coal, See maceral analysis for detailed composition of the coal. The telalginite is derived from very small colonies of *Botryococcus spp.* Pyrite abundant.)
T9755 O/C	O/C	0.46	0.38-0.54	0.045	42	**CAT 2 – MERSEY R. EQUIV.** Abundant sporinite yellow to orange, abundant cutinite yellowish orange to orange, rare to sparse telalginite yellow to yellowish orange. (Finely layered coal. See maceral analysis for detailed composition of the coal. The telalginite is derived from very small colonies of *Botryococcus spp.* Pyrite abundant.)
T9756 O/C	O/C	0.76	0.65-0.83	0.045	26	**MQC- 3 HENTY RIVER, WEST TASM.** Rare sporinite dull orange. (Carbonaceous siltstone. Dom abundant, I>V>L. Inertinite abundant, vitrinite sparse, liptinite rare. The vitrinite occurs as small and thin lenses of detrovitrinite with rare longer telovitrinite phytoclasts. The detrovitrinite is probably detrital, but some of the telovitrinite may represent small roots. The inertinite appears to be detrital. Mineral fluorescence moderate orange and weakly patchy with a possible weak green oil cut. Iron oxide grains sparse. Pyrite rare, possibly partially lost due to weathering.)

The sample from the upper seam has a higher content of vitrinite and liptinite is a major component of both coals. The blocks may not, however, be representative of the whole seam sections. Telalginite is present in small amounts within both seams but neither point count recorded an intersection with telalginite. The vitrinite reflectances are relatively low. The presence of the telalginite and the abundant pyrite indicate that a correction to the vitrinite reflectance is probably required but the correction needed is small. A best estimate for corrected vitrinite reflectance for both coals is about 0.50% to 0.55%.

The Henty River sample is much higher in rank compared with the coals. Inertinite is dominant in the siltstone. The telovitrinite that is present probably represents root tissues.

POINT COUNT RESULTS FOR SAMPLES

Sample number. T9754 Sample ID: Cat 1 Mersey R. Equivalent
Company: Alan Chester, U Tas Sample type: O/C

MACERAL GROUP %	MACERAL SUBGROUP %	MACERAL %		SUBMACERAL %
VITRINITE 66.7	**TELOVITRINITE** 52.12	TEXTINITE	0.00	TEXTINITE A & B
		TEXTO-ULMINITE	0.00	
		EU-ULMINITE	0.00	
		TELOCOLLINITE	52.12	COLLINITE
VIT (MF) 73.1	**DETROVITRINITE** 14.62	ATTRINITE	0.00	
		DENSINITE	0.00	
		DESMOCOLLINITE	14.62	
	GELOVITRINITE 0.00	CORPOGELINITE	0.00	
		PORIGELINITE	0.00	
		EUGELINITE	0.00	
INERTINITE 9.0	**TELO-INERTINITE** 5.38	FUSINITE	1.54	
		SEMIFUSINITE	3.65	
		MACRINITE	0.19	
		SCLEROTINITE	0.00	
INERT (MF) 9.9	**DETRO-INERTINITE** 3.65	INERTODETRINITE	3.46	
		MICRINITE	0.19	
LIPTINITE 15.6		SPORINITE	5.96	
		CUTINITE	8.85	
		SUBERINITE	0.00	
		RESINITE	0.77	
		FLUORINITE	0.00	
		LIPTODETRINITE	0.00	
LIPT (MF) 17.1		ALGINITE	0.00	TELALGINITE 0.00
				LAMALGINITE 0.00
		BITUMINITE	0.00	
NATURAL **COKE** 0.00		SEMICOKE	0.00	
		COKE	0.00	
		PYROLYTIC C	0.00	
MINERALS 8.7	QUARTZ 0.38	CLAY	2.12	GLAUCONITE 0.00
	CALCITE 0.00	SIDERITE	0.19	MARCASITE 0.00
	PYRITE 5.96	IRON OXIDES	0.00	OTHERS 0.00

NUMBER OF POINTS COUNTED:
REFLECTANCE: TELOVITRINITE 0.48 DETROVITRINITE 0.44 ALL VITRINITE 0.47

SD 0.031 NO. READINGS 41 SAMPLE TYPE O/C OPERATOR ACC

COMMENT: Sample is low rank and telovitrinite derived from leaf tissue and from wood are the main components. Although fusinite is not abundant overall, the ratio of fusinite to semifusinite is unusually high. Pyrite is abundant, occurring as small radiating masses.

POINT COUNT RESULTS FOR SAMPLES

Sample number. T9755 Sample ID: Cat 2 Mersey R. Equivalent
Company: Alan Chester, U Tas Sample type: O/C

MACERAL GROUP %	MACERAL SUBGROUP %	MACERAL %		SUBMACERAL %
VITRINITE 41.0	**TELOVITRINITE** 7.94	TEXTINITE	0.00	TEXTINITE A & B
		TEXTO-ULMINITE	0.00	
		EU-ULMINITE	0.00	
		TELOCOLLINITE	7.94	COLLINITE
VIT (MF) 44.3	**DETROVITRINITE** 33.11	ATTRINITE	0.00	
		DENSINITE	0.00	
		DESMOCOLLINITE	33.11	
	GELOVITRINITE 0.00	CORPOGELINITE	0.00	
		PORIGELINITE	0.00	
		EUGELINITE	0.00	
INERTINITE 31.9	**TELO-INERTINITE** 14.53	FUSINITE	6.25	
		SEMIFUSINITE	7.60	
		MACRINITE	0.68	
		SCLEROTINITE	0.00	
INERT (MF) 34.4	**DETRO-INERTINITE** 17.40	INERTODETRINITE	15.88	
		MICRINITE	1.52	
LIPTINITE 19.8		SPORINITE	13.85	
		CUTINITE	3.38	
		SUBERINITE	0.00	
		RESINITE	0.51	
		FLUORINITE	0.00	
		LIPTODETRINITE	2.03	
LIPT (MF) 21.3		ALGINITE	0.00	TELALGINITE 0.00
				LAMALGINITE 0.00
		BITUMINITE	0.00	
NATURAL **COKE** 0.0		SEMICOKE	0.00	
		COKE	0.00	
		PYROLYTIC C	0.00	
MINERALS 7.3	QUARTZ 0.68	CLAY	6.08	GLAUCONITE 0.00
	CALCITE 0.34	SIDERITE	0.00	MARCASITE 0.00
	PYRITE 0.17	IRON OXIDES	0.00	OTHERS 0.00

NUMBER OF POINTS COUNTED: 592
REFLECTANCE: TELOVITRINITE 0.47 DETROVITRINITE 0.42 ALL VITRINITE 0.46

SD 0.045 NO. READINGS 42 SAMPLE TYPE O/C OPERATOR ACC

COMMENT: Sample is dominated by finely laminated duroclarite with interbedded detrovitrinite, fragmental inertinite and sporinite and cutinite. Thicker lenses of telovitrinite, fusinite and semifusinite are present but subordinate. Pyrite is widely dispersed as small framboidal particles. A possible occurrence of pyrolytic carbon was noted.

POINT COUNT RESULTS FOR SAMPLES

Sample number. T9756 Sample ID: MQC 2

Company: Alan Chester, U Tas Sample type: O/C

MACERAL GROUP %	MACERAL SUBGROUP %	MACERAL %		SUBMACERAL %
VITRINITE 0.0	**TELOVITRINITE** 0.00	TEXTINITE	0.00	TEXTINITE A & B
		TEXTO-ULMINITE	0.00	
		EU-ULMINITE	0.00	
		TELOCOLLINITE	0.00	COLLINITE
VIT (MF) 0.0	**DETROVITRINITE** 0.00	ATTRINITE	0.00	
		DENSINITE	0.00	
		DESMOCOLLINITE	0.00	
	GELOVITRINITE 0.00	CORPOGELINITE	0.00	
		PORIGELINITE	0.00	
		EUGELINITE	0.00	
INERTINITE 8.4	**TELO-INERTINITE** 0.00	FUSINITE	0.00	
		SEMIFUSINITE	0.00	
		MACRINITE	0.00	
		SCLEROTINITE	0.00	
INERT (MF) 95.8	**DETRO-INERTINITE** 8.42	INERTODETRINITE	8.42	
		MICRINITE	0.00	
LIPTINITE 0.4		SPORINITE	0.37	
		CUTINITE	0.00	
		SUBERINITE	0.00	
		RESINITE	0.00	
		FLUORINITE	0.00	
		LIPTODETRINITE	0.00	
LIPT (MF) 4.2		ALGINITE	0.00	TELALGINITE 0.00
				LAMALGINITE 0.00
		BITUMINITE	0.00	
NATURAL **COKE** 0.0		SEMICOKE	0.00	
		COKE	0.00	
		PYROLYTIC C	0.00	
MINERALS 91.2	QUARTZ 12.45	CLAY	78.39	GLAUCONITE 0.00
	CALCITE 0.00	SIDERITE	0.00	MARCASITE 0.00
	PYRITE 0.37	IRON OXIDES	0.00	OTHERS 0.00

NUMBER OF POINTS COUNTED: 273
REFLECTANCE: TELOVITRINITE 0.78 DETROVITRINITE 0.76 ALL VITRINITE 0.76

SD 0.045 NO. READINGS 25 SAMPLE TYPE O/C OPERATOR ACC

COMMENT: Silty claystone. Organic matter is dominated by inertodetrinite, but vitrinite is present at a few rare horizons. Sporinite is rare.

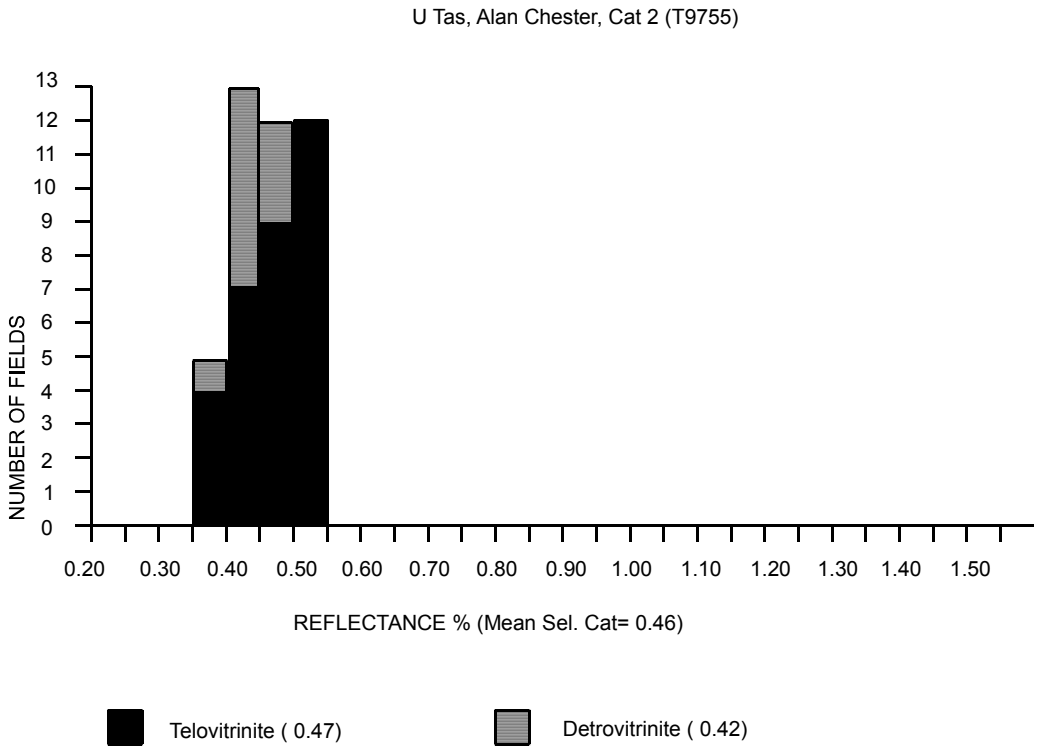

Category	No. of Readings	Mean	Standard Deviation
Telovitrinite	32	0.47	0.045
Detrovitrinite	10	0.42	0.024
Total:	42	0.46	0.045

Selected categories: Telovitrinite, Detrovitrinite.

No. of readings: 42

Mean of selected categories: 0.46

Standard deviation of selected categories: 0.045

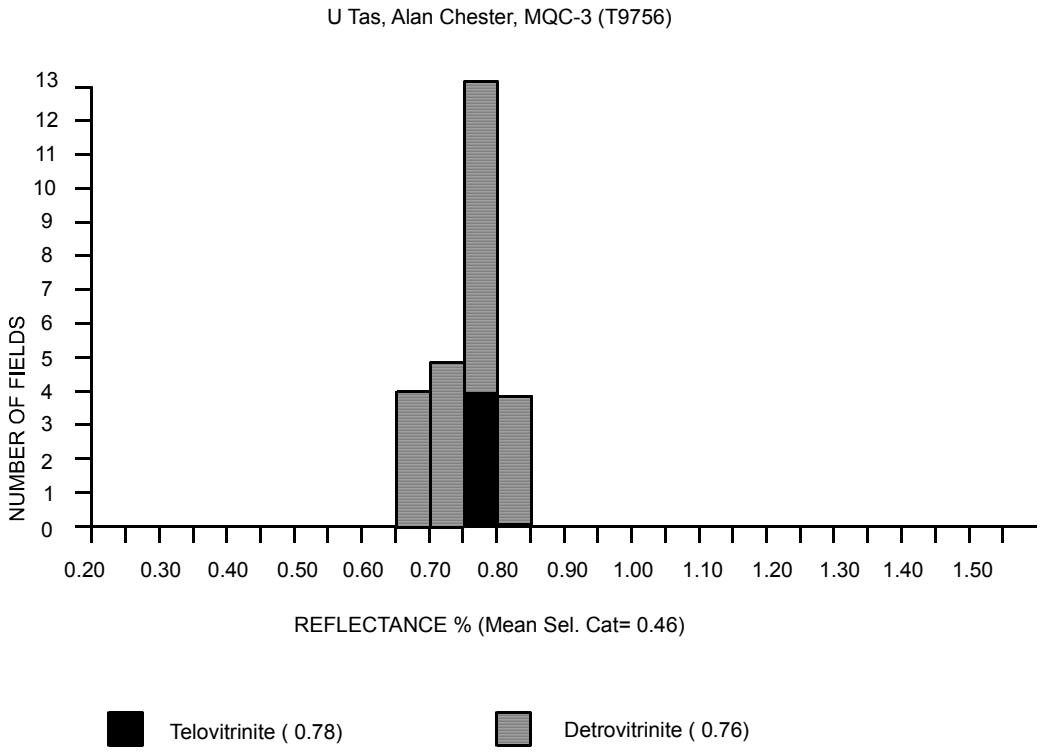

Category	No. of Readings	Mean	Standard Deviation
Telovitrinite	4	0.78	0.013
Detrovitrinite	22	0.76	0.048
Total:	26	0.76	0.045

Selected categories: Telovitrinite, Detrovitrinite

No. of readings: 26

Mean of selected categories: 0.76

Standard deviation of selected categories: 0.045

R	No Read	Pop Range	R	No Read	Pop Range	R	No Read	Pop Range	R	No Read	Pop Range	R	No Read	Pop Range	R	No Read	Pop Range	R	No Read	Pop Range	R	No Read	Pop Range	R
0.10			0.40			0.70			1.00			1.30			1.60			1.90			2.20			2.50
0.11			0.41			0.71			1.01			1.31			1.61			1.91			2.21			2.51
0.12			0.42	1		0.72			1.02			1.32			1.62			1.92			2.22			2.52
0.13			0.43	5	FGV	0.73			1.03			1.33			1.63			1.93			2.23			2.53
0.14			0.44			0.74			1.04			1.34			1.64			1.94			2.24			2.54
0.15			0.45	6		0.75			1.05			1.35			1.65			1.95			2.25			2.55
0.16			0.46	4		0.76			1.06			1.36			1.66			1.96			2.26			2.56
0.17			0.47	10		0.77			1.07			1.37			1.67			1.97			2.27			2.57
0.18			0.48	5		0.78			1.08			1.38			1.68			1.98			2.28			2.58
0.19			0.49	3		0.79			1.09			1.39			1.69			1.99			2.29			2.59
0.20			0.50			0.80			1.10			1.40			1.70			2.00			2.30			2.60
0.21			0.51	1		0.81			1.11			1.41			1.71			2.01			2.31			2.61
0.22			0.52	3		0.82			1.12			1.42			1.72			2.02			2.32			2.62
0.23			0.53		FGV	0.83			1.13			1.43			1.73			2.03			2.33			2.63
0.24			0.54	3		0.84			1.14			1.44			1.74			2.04			2.34			2.64
0.25			0.55			0.85			1.15			1.45			1.75			2.05			2.35			2.65
0.26			0.56			0.86			1.16			1.46			1.76			2.06			2.36			2.66
0.27			0.57			0.87			1.17			1.47			1.77			2.07			2.37			2.67
0.28			0.58			0.88			1.18			1.48			1.78			2.08			2.38			2.68
0.29			0.59			0.89			1.19			1.49			1.79			2.09			2.39			2.69
0.30			0.60			0.90			1.20			1.50			1.80			2.10			2.40			2.70
0.31			0.61			0.91			1.21			1.51			1.81			2.11			2.41			2.71
0.32			0.62			0.92			1.22			1.52			1.82			2.12			2.42			2.72
0.33			0.63			0.93			1.23			1.53			1.83			2.13			2.43			2.73
0.34			0.64			0.94			1.24			1.54			1.84			2.14			2.44			2.74
0.35			0.65			0.95			1.25			1.55			1.85			2.15			2.45			2.75
0.36			0.66			0.96			1.26			1.56			1.86			2.16			2.46			2.76
0.37			0.67			0.97			1.27			1.57			1.87			2.17			2.47			2.77
0.38			0.68			0.98			1.28			1.58			1.88			2.18			2.48			2.78
0.39			0.69			0.99			1.29			1.59			1.89			2.19			2.49			2.79

VITRINITE %	INERTINITE See Maceral Analysis Sheets	LIPTINITE See Maceral Analysis Sheets	OIL DROPS	BITUMEN

TV	DV	Sfus	Scler	Fus	Macr	ID	Micr	Spor	Cut	Sub	Res	Ltd	Bitumin	Telalgin	Lamalgin	Oil cut

Sample Number..T9754….Well Name…University of Tasmania, Alan Chester…Cat 1…..Depth……O/C……Sample Type…O/C…
Date..24/05/2004…Op..ACC….FGV –First Generation Vitrinite, RV –Reworked Vitrinite, BTT –Bituminite, B – Bitumen, Inert –Inertinite, Cav- Cavings,
DA – Drilling Mud Additives MICR D:\RWORK.ms6\UT04VRWB.doc

R	No Read	Pop Range	R	No Read	Pop Range	R	No Read	Pop Range	R	No Read	Pop Range	R	No Read	Pop Range	R	No Read	Pop Range	R	No Read	Pop Range	R	No Read	Pop Range	R	No Read	Pop Range
0.10			0.40	2		0.70			1.00			1.30			1.60			1.90			2.20			2.50		
0.11			0.41	2		0.71			1.01			1.31			1.61			1.91			2.21			2.51		
0.12			0.42	4		0.72			1.02			1.32			1.62			1.92			2.22			2.52		
0.13			0.43	2		0.73			1.03			1.33			1.63			1.93			2.23			2.53		
0.14			0.44	3		0.74			1.04			1.34			1.64			1.94			2.24			2.54		
0.15			0.45	3		0.75			1.05			1.35			1.65			1.95			2.25			2.55		

0.16			0.46	3		0.76			1.06			1.36			1.66			1.96			2.26			2.56		
0.17			0.47	1		0.77			1.07			1.37			1.67			1.97			2.27			2.57		
0.18			0.48	1		0.78			1.08			1.38			1.68			1.98			2.28			2.58		
0.19			0.49	4		0.79			1.09			1.39			1.69			1.99			2.29			2.59		
0.20			0.50	8		0.80			1.10			1.40			1.70			2.00			2.30			2.60		
0.21			0.51			0.81			1.11			1.41			1.71			2.01			2.31			2.61		
0.22			0.52	1		0.82			1.12			1.42			1.72			2.02			2.32			2.62		
0.23			0.53	2	FGV	0.83			1.13			1.43			1.73			2.03			2.33			2.63		
0.24			0.54	1	↓	0.84			1.14			1.44			1.74			2.04			2.34			2.64		
0.25			0.55			0.85			1.15			1.45			1.75			2.05			2.35			2.65		
0.26			0.56			0.86			1.16			1.46			1.76			2.06			2.36			2.66		
0.27			0.57			0.87			1.17			1.47			1.77			2.07			2.37			2.67		
0.28			0.58			0.88			1.18			1.48			1.78			2.08			2.38			2.68		
0.29			0.59			0.89			1.19			1.49			1.79			2.09			2.39			2.69		
0.30			0.60			0.90			1.20			1.50			1.80			2.10			2.40			2.70		
0.31			0.61			0.91			1.21			1.51			1.81			2.11			2.41			2.71		
0.32			0.62			0.92			1.22			1.52			1.82			2.12			2.42			2.72		
0.33			0.63			0.93			1.23			1.53			1.83			2.13			2.43			2.73		
0.34			0.64			0.94			1.24			1.54			1.84			2.14			2.44			2.74		
0.35			0.65			0.95			1.25			1.55			1.85			2.15			2.45			2.75		
0.36			0.66			0.96			1.26			1.56			1.86			2.16			2.46			2.76		
0.37			0.67			0.97			1.27			1.57			1.87			2.17			2.47			2.77		
0.38	2	↑	0.68			0.98			1.28			1.58			1.88			2.18			2.48			2.78		
0.39	3	FGV	0.69			0.99			1.29			1.59			1.89			2.19			2.49			2.79		

VITRINITE %	INERTINITE See Maceral Analysis Sheets	LIPTINITE See Maceral Analysis Sheets	OIL DROPS	BITUMEN

TV	DV	Sfus	Scler	Fus	Macr	ID	Micr	Spor	Cut	Sub	Res	Ltd	Bitumin	Telalgin	Lamalgin	Oil cut

Sample Number..T9755…Well Name..University of Tasmania, Alan Chester…….Cat 2……..Depth…….O/C…….Sample Type…O/C…
Date. ..24/05/2004.. Op..ACC…..FGV- First Generation Vitrinite, RV-Reworked Vitrinite, BTT – Bituminite, B – Bitumen, Inert – Inertinite, Cav – Cavings,
DA – Drilling Mud Additives MICR D:\RWORK.ms6\UT04VRWB.doc

R	No Read	Pop Range	R	No Read	Pop Range	R	No Read	Pop Range	R	No Read	Pop Range	R	No Read	Pop Range	R	No Read	Pop Range	R	No Read	Pop Range	R	No Read	Pop Range	R	No Read	Pop Range
0.10			0.40			0.70			1.00			1.30			1.60			1.90			2.20			2.50		
0.11			0.41			0.71			1.01			1.31			1.61			1.91			2.21			2.51		
0.12			0.42			0.72	2		1.02			1.32			1.62			1.92			2.22			2.52		

0.13			0.43			0.73			1.03			1.33			1.63			1.93			2.23			2.53		
0.14			0.44			0.74	4		1.04			1.34			1.64			1.94			2.24			2.54		
0.15			0.45			0.75			1.05			1.35			1.65			1.95			2.25			2.55		
0.16			0.46			0.76	2		1.06			1.36			1.66			1.96			2.26			2.56		
0.17			0.47			0.77	4		1.07			1.37			1.67			1.97			2.27			2.57		
0.18			0.48			0.78	4		1.08			1.38			1.68			1.98			2.28			2.58		
0.19			0.49			0.79	3		1.09			1.39			1.69			1.99			2.29			2.59		
0.20			0.50			0.80	1		1.10			1.40			1.70			2.00			2.30			2.60		
0.21			0.51			0.81	1		1.11			1.41			1.71			2.01			2.31			2.61		
0.22			0.52			0.82		FGV	1.12			1.42			1.72			2.02			2.32			2.62		
0.23			0.53			0.83	2	▼	1.13			1.43			1.73			2.03			2.33			2.63		
0.24			0.54			0.84			1.14			1.44			1.74			2.04			2.34			2.64		
0.25			0.55			0.85			1.15			1.45			1.75			2.05			2.35			2.65		
0.26			0.56			0.86			1.16			1.46			1.76			2.06			2.36			2.66		
0.27			0.57			0.87			1.17			1.47			1.77			2.07			2.37			2.67		
0.28			0.58			0.88			1.18			1.48			1.78			2.08			2.38			2.68		
0.29			0.59			0.89			1.19			1.49			1.79			2.09			2.39			2.69		
0.30			0.60			0.90			1.20			1.50			1.80			2.10			2.40			2.70		
0.31			0.61			0.91			1.21			1.51			1.81			2.11			2.41			2.71		
0.32			0.62			0.92			1.22			1.52			1.82			2.12			2.42			2.72		
0.33			0.63			0.93			1.23			1.53			1.83			2.13			2.43			2.73		
0.34			0.64			0.94			1.24			1.54			1.84			2.14			2.44			2.74		
0.35			0.65	1	▲	0.95			1.25			1.55			1.85			2.15			2.45			2.75		
0.36			0.66		FGV	0.96			1.26			1.56			1.86			2.16			2.46			2.76		
0.37			0.67		|	0.97			1.27			1.57			1.87			2.17			2.47			2.77		
0.38			0.68	2	|	0.98			1.28			1.58			1.88			2.18			2.48			2.78		
0.39			0.69	1	|	0.99			1.29			1.59			1.89			2.19			2.49			2.79		

VITRINITE %		INERTINITE See Maceral Analysis Sheets						LIPTINITE See Maceral Analysis Sheets								OIL DROPS	BITUMEN
TV	DV	Sfus	Scler	Fus	Macr	ID	Micr	Spor	Cut	Sub	Res	Ltd	Bitumin	Telalgin	Lamalgin	Oil cut	

Sample Number.. T9756…Well Name..University of Tasmania, Alan Chester……..MQC-3…….Depth……O/C……..Sample Type…O/C…..
Date. ..24/05/2004.. Op..ACC….FGV – First Generation Vitrinite, RV – Reworked Vitrinite, BTT – Bituminite, B – Bitumen, Inert – Inertinite, Cav – Cavings,
DA – Drilling Mud Additives

APPENDIX H.

Total organic carbon (TOC) values for Gordon Group and Precambrian dolomite from Hunterston DDH.

Upper Benjamin Limestone Samples.

Sample ID	TOC %	Location
UL01	0.34	Florentine Valley
UL02	0.20	Florentine Valley
UL03	0.08	Florentine Valley
UL04	0.08	Florentine Valley
UL05	0.10	Florentine Valley
UL06	0.08	Florentine Valley
UL07	0.18	Florentine Valley
UL08	0.04	Florentine Valley
UL09	0.10	Florentine Valley
UL10	0.10	Florentine Valley
UL11	0.12	Florentine Valley
UL12	0.04	Florentine Valley
UL13	0.06	Florentine Valley
UL14	0.14	Florentine Valley
UL15	0.08	Florentine Valley
UL16	0.28	Florentine Valley
UL17	0.16	Florentine Valley
UL18	0.10	Florentine Valley
UL19	0.06	Florentine Valley
UL20	0.12	Florentine Valley
UL21	0.18	Florentine Valley
UL22	0.12	Florentine Valley
UL23	0.18	Florentine Valley
UL24	0.10	Florentine Valley
UL25	0.78	Florentine Valley
UL26	0.26	Florentine Valley
UL27	0.06	Florentine Valley
UL28	0.10	Florentine Valley
UL29	0.24	Florentine Valley
UL30	0.24	Florentine Valley
UL31	0.12	Florentine Valley
UL32	0.14	Florentine Valley
UL33	0.08	Florentine Valley
UL34	0.12	Florentine Valley
UL35	0.16	Florentine Valley
UL36	0.10	Florentine Valley
UL37	0.14	Florentine Valley
UL38	0.16	Florentine Valley
UL39	0.12	Florentine Valley
UL40	0.20	Florentine Valley
CB13	0.46	Florentine Valley
CB14	1.16	Florentine Valley

CB16	0.58	Florentine Valley
CB17	0.37	Florentine Valley
CB18	0.27	Florentine Valley
CB19	0.09	Florentine Valley
CB20	0.19	Florentine Valley
CB25	0.07	Florentine Valley
CB26	0.70	Florentine Valley
CB27	0.07	Florentine Valley
CB29	0.10	Florentine Valley
CB30	0.43	Florentine Valley
CB31	0.16	Florentine Valley
CB32	0.64	Florentine Valley
SM1	0.40	Florentine Valley
11R1	1.37	Florentine Valley
WQR1	1.83	Florentine Valley
17/2	0.57	Florentine Valley
17/16	0.80	Florentine Valley
173	0.15	Florentine Valley
174	0.05	Florentine Valley
175	0.48	Florentine Valley
LR1	0.20	Lune River
LR2	0.70	Lune River

Lower Benjamin Limestone Samples.

Sample ID	**TOC %**	**Location**
CB2	0.10	Florentine Valley
CB3	0.16	Florentine Valley
CB4	0.16	Florentine Valley
CB6	0.06	Florentine Valley
CB11	0.10	Florentine Valley
CB12	0.10	Florentine Valley

Precambrian Dolomite Samples.

Sample ID	**TOC %**	**Location**
H984.8	<0.02	Hunterston DDH
H1041.9	<0.02	Hunterston DDH
H1098.6	<0.02	Hunterston DDH

All analyses by AMDEL.

APPENDIX J

Latitude and longitude of Tasmanian localities mentioned in thesis

Number	Locality	Lat	Long	
1	Acton	42 52S	147 29E	
2	Adventure Bay	43 20S	147 23E	
3	Alert Creek	41 05S	144 42E	
4	Anderson's Creek	41 04S	146 47E	
5	Andrew River	42 20S	145 45E	
6	Arthur River	41 05S	144 45E	
7	Badger River	42 00S	145 15E	
8	Bangor	41 13S	147 09E	
9	Beaconsfield	41 13S	146 47E	
10	Ben Lomond	41 32S	147 45E	
11	Bicheno	41 50S	148 20E	
12	Black Bluff	41 26S	145 58E	
13	Bluff Hill	41 01S	144 40E	
14	Bruny Island	43 20S	147 15E	
15	Bubs Hill	42 07S	145 47E	
16	Catagunya	42 27S	146 36E	
17	Claude Creek	41 30S	146 12E	
18	Coal River	42 40S	147 27E	
19	Colebrook	42 31S	147 25E	
20	Coles Bay	42 08S	148 18E	
21	Comstock	41 54S	145 08E	
22	Cotas Creek	41 31S	148 10E	
23	Couta Rocks	41 10S	144 40E	
24	Cradle Mountain	41 39S	145 58E	
25	Dazzler Range	41 13S	146 43E	
26	Denison Range	42 35S	146 16E	
27	Derwent River	42 30S	146 40E	
28	Dollie Creek	41 03S	144 12E	
29	Duck Creek	41 46S	145 00E	
30	Elderslie	42 36S	147 05E	
31	Eldon	42 30S	147 26E	
32	Eugenana	41 13S	146 18E	
33	Everlasting Hills	42 18S	146 01E	
34	Exit Cave	43 27S	146 51E	
35	Fingal	41 38S	148 01E	
36	Florentine Valley	42 35S	146 25E	
37	Flowery Gully	41 16S	146 49E	
38	Forest	40 51S	145 15E	
39	Geeveston	43 10S	146 58E	
40	Glenorchy	42 47S	147 22E	
41	Golden Valley	41 09S	146 43E	
42	Great Lake	41 50S	146 43E	
43	Grieves Siding	41 55S	145 20E	
44	Gunns Plains	41 16S	146 02E	
45	Hellyer Gorge	41 16S	145 36E	
46	Henty River	42 02S	145 15E	
47	Holder Plains	41 06S	145 10E	
48	Holder Quarry	41 08S	145 10E	
49	Hunterston	42 13S	146 57E	
50	Huntsmans Creek	41 30S	148 08E	
51	Huskisson Syncline	41 42S	145 28E	

52	Ida Bay	43 27S	146 54E	
53	Isle du Golfe	43 34S	146 31E	
54	Judds Cavern	43 14S	146 36E	
55	Kanannuh Bridge	41 07S	144 59E	
56	Kaoota	43 01S	147 10E	
57	King Island	39 50S	144 00E	
58	Lake Sydney	43 17S	146 37E	
59	Langloh	42 32S	146 49E	
60	Latrobe	41 14S	146 26E	
61	Leprena	43 32S	146 54E	
62	Liena	41 33S	146 14E	
63	Lonnavale	42 58S	146 49E	
64	Loongana	41 24S	146 00E	
65	Lune River	43 26S	146 54E	
66	Mallana	42 01S	145 16E	
67	Marion Bay	42 49S	147 51E	
68	Maydena	42 46S	146 38E	
69	McPartlan Pass	42 49S	146 23E	
70	Melrose	41 14S	146 16E	
71	Mersey Great Bend	41 17S	146 26E	
72	Mersey Valley	41 20S	146 25E	
73	Moina	41 29S	146 06E	
74	Mole Creek	41 34S	146 24E	
75	Mt Heemskirk	41 51S	145 10E	
76	Mt Housetop	41 19S	145 54E	
77	Mt La Perouse	43 30S	146 45E	
78	Mt Lloyd	43 34S	146 52E	
79	Mt Nicholas	41 33S	148 06E	
80	Mt Pelion	41 50S	146 00E	
81	Mt Vernon	42 29S	147 11E	
82	Mt Wylly	43 29S	146 40E	
83	New River Lagoon	43 30S	146 34E	
84	Oceana	41 56S	145 20E	
85	O'Connors Peak	41 52S	147 06E	
86	Olga Ridge	42 41S	145 48E	
87	Olga River	42 45S	145 45E	
88	Oonah	41 14S	145 38E	
89	Peggs Beach	40 51S	145 21E	
90	Pelham	42 34S	147 00E	
91	Picton River	43 12S	146 41E	
92	Point Cecil	43 33S	146 36E	
93	Point Hibbs	42 37S	145 16E	
94	Port Davey	43 20S	145 55E	
95	Precipitous Bluff	43 28S	146 36E	
96	Preolenna	41 05S	145 33E	
97	Que River	41 34S	145 40E	
98	Queenstown	42 05S	145 33E	
99	Railton	41 21S	146 26E	
100	Rapid River	41 10S	145 10E	
101	Relapse Creek	41 06S	145 31E	
102	Renison	41 48S	145 25E	
103	Rosebery	41 47S	145 33E	
104	Ross	42 02S	147 30E	
105	Salisbury River	43 23S	146 38E	
106	Salmon River	41 03S	144 50E	
107	Shoemaker Point	43 37S	146 40E	

108	Sisters Beach	40 55S	145 33E	
109	Sophia River	41 48S	145 42E	
110	Sorell Peninsula	42 20S	145 15E	
111	South Cape	43 38S	146 42E	
112	South Sumac	41 18S	145 02E	
113	St. Marys	41 32S	148 14E	
114	St. Valentines Peak	41 22S	145 46E	
115	Stanley	40 44S	145 18E	
116	Stonehenge	42 21S	147 40E	
117	Storey's Creek	41 38S	147 44E	
118	Storm Bay	43 12S	147 30E	
119	Strahan	42 12S	145 22E	
120	Strathblane	43 20S	146 38E	
121	Styx Valley	42 49S	146 40E	
122	Surprise Bay	43 36S	146 39E	
123	Temma	41 14S	144 45E	
124	The Quoin	42 09S	147 38E	
125	Tipunah Road	40 56S	145 14E	
126	Tunbridge	42 09S	147 28E	
127	Vale of Belvoir	41 32S	145 54E	
128	Vale of Rasselas	42 35S	146 20E	
129	Waratah Creek	41 18S	144 57E	
130	Wedge Plains	41 02S	145 15E	
131	Weld Valley	43 00S	146 40E	
132	Westfield Quarry	42 38S	146 30E	
133	Wetheron Tier	42 29S	147 02E	
134	Wherret's Lookout	42 43S	146 30E	
135	Wilmot Range	42 52S	145 58E	
136	Wilson River	41 40S	145 23E	
137	Woodbridge	43 10S	147 14E	
138	Woodbury	42 10S	147 24E	
139	York Plains	42 15S	147 27E	
140	Zeehan	41 52S	145 23E	

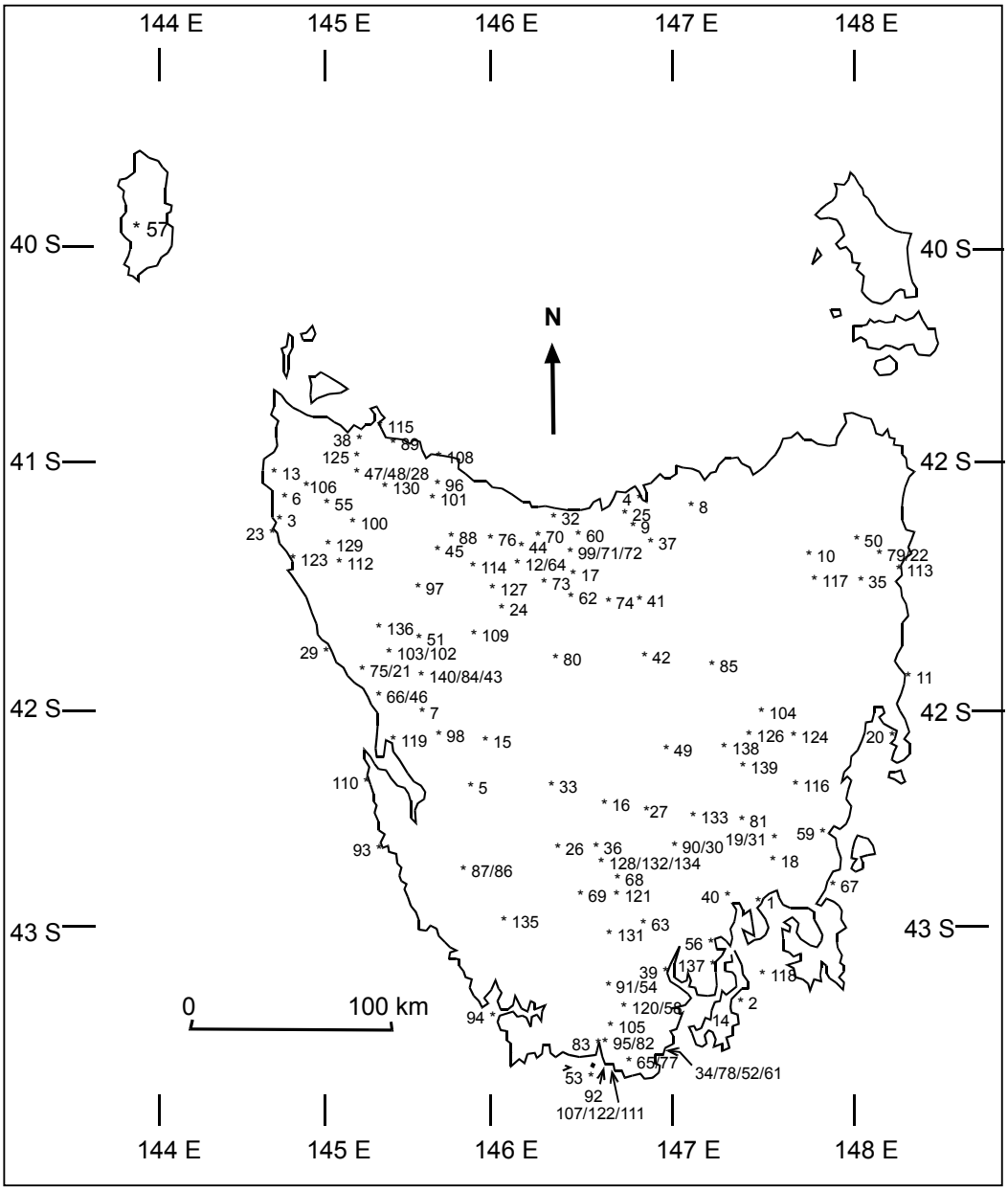

Figure J.1. Map showing positions of localities mentioned in thesis. Due to space limitations some localities are grouped and shown approximately. Numbered locations are detailed in table shown in Appendix J, along with latitude and longitude of each locality.

REFERENCES.

Akande, S. O., and B. D. Erdtmann, 1998, Burial metamorphism (thermal maturation) in Cretaceous sediments of the Southern Benue Trough and Anambra Basin, Nigeria: American Association of Petroleum Geologists Bulletin, v. 82, p. 1191-1206.

Akerman, T. E., 1998, Annual report RL8809, Oceana. 98_4225, Hobart, Mineral Resources Tasmania, unpublished, 10 p.

AMDEL, 2002a, Report LQ11777 to Alan Chester, Adelaide, unpublished, 4 p.

AMDEL, 2002b, Report LQ11847 to Alan Chester, Adelaide, unpublished, 4 p.

AMDEL, 2004a, Report PEAD0247 to Alan Chester, Adelaide, unpublished, 1 p.

AMDEL, 2004b, Report PEAD03103 to Alan Chester, Adelaide, unpublished, 4 p.

AMDEL, 2004c, Report PEAD04357 to Alan Chester, Adelaide, unpublished, 10 p.

AMDEL, 2004d, Report PEAD04440 to Alan Chester, Adelaide, unpublished, 6 p.

AMDEL, 2004e, Report PEAD04644 to Alan Chester, Adelaide, unpublished, 3 p.

Anderson, G. M., 1991, Organic maturation and ore precipitation in Southeast Missouri: Economic Geology, v. 86, p. 909-926.

Anderson, G. M., and R. W. Macqueen, 1982, Ore deposit models-6. Mississippi Valley lead-zinc deposits: Geoscience Canada, v. 9, p. 108-117.

Anon, 1967, Esso Bass-3 Tasmania well completion report. Esso Exploration Australia Inc. OR_0332, Hobart, Minerals Resources Tasmania, unpublished, 17 p.

Anon, 1981, Exploration Licence 37/39 Styx River, Tasmania. Report for the six months ending 1st November 1981, 81_1657, Hobart, Minerals Resources Tasmania, unpublished, 9 p.

Anon, 1982, Cape Sorell No.1. Geological Completion Report. OR_0358A, Hobart, Mineral Resources Tasmania, unpublished, 27 p.

Anon, 1984a, EL30/80 Report for the twelve months ended 15th April 1984. 84_2120, Hobart, Report to Minerals Resources Tasmania, unpublished, 14 p.

Anon, 1984b, Squid 1 and ST No1 well completion report. OR_0355B, Hobart, Mineral Resources Tasmania, unpublished, 30 p.

Anon, 1985, Tasmanian Devil 1 well completion report. OR_0356B, Hobart, Mineral Resources Tasmania, unpublished, 26 p.

Anon, 1997, Report on Shittim1 Well EL 1/88, Hobart, GSLM report to Minerals Resources Tasmania, unpublished, 6 p.

Anon, 1999, Final well report Barramundi 1. OR_0472, Hobart, Mineral Resources Tasmania, unpublished, 62 p.

Anon, 2005, Petroleum geoscience fact sheet, Canberra, Australian Government, Department of Industry, Tourism and Resources, 4 p.

Arkai, P., 1991, Chlorite crystallinity: an empirical approach and correlation with illite crystallinity, coal rank and mineral facies as exemplified by Palaeozoic and Mesozoic rocks of northeast Hungary: Journal of Metamorphic Geology, v. 9, p. 723-734.

Ashley, P. M., and R. A. Creelman, 1975, The Mount Black lead-zinc deposit, a probable Mississippi Valley-type sulphide occurrence at Coolemon Plains, southern New South Wales: Journal of the Geological Society of Australia, v. 22, p. 423-433.

Bacon, C. A., 1986, Coal in Tasmania: Advances in the study of the Sydney Basin, v. 20, p. 4-6.

Bacon, C. A., 1991, The coal resources of Tasmania: Geological Survey Bulletin 64, 166 p.
Bacon, C. A., and C. R. Calver, 1986, Petrography and paleoenvironments of some Permian coals, Nicholas Range, north east Tasmania. UR1986_34, Hobart, Minerals Resources Tasmania, unpublished, 9 p.
Bacon, C. A., C. R. Calver, C. J. Boreham, D. E. Leaman, K. C. Morrison, A. T. Revill, and J. K. Volkman, 2000, The petroleum potential of onshore Tasmania: a review: Geological Survey Bulletin 71, 93 p.
Bacon, C.A., and J. L. Everard, 1981, Pyroclastics in the Upper Parmeener Supergroup, near Bicheno, eastern Tasmania. Papers and Proceedings of the Royal Society of Tasmania, v.115, p. 29-36.
Baillie, P. W., 1989a, Jurassic-Cainozoic, *in* C. F. Burrett, and E. L. Martin, eds., Geology and mineral resources of Tasmania, v. Special publication 15: Brisbane, Geological Society of Australia, p. 333-340.
Baillie, P. W., 1989b, Silurian and Devonian sediments, *in* C. F. Burrett, and E. L. Martin, eds., Geology and mineral resources of Tasmania: Special Publications 15: Brisbane, Geological Society of Australia, p. 224.
Baillie, P. W., and C. M. Powell, 1989, Silurian-Devonian unit, *in* C. F. Burrett, and E. L. Martin, eds., Geology and mineral resources of Tasmania, v. Special Publication 15: Brisbane, Geological Society of Australia, p. 235-236.
Bajwah, Z. U., A. J. R. White, T. A. P. Kwak, and R. C. Price, 1995, The Renison granite, northwestern Tasmania: A petrological, geochemical and fluid inclusion study of hydrothermal alteration: Economic Geology, v. 90, p. 1663-1675.
Banks, M. R., 1989, Summary and structural development, *in* C. F. Burrett, and E. L. Martin, eds., The geology and mineral resources of Tasmania, v. Special publication 15: Brisbane, Geological Society of Australia, p. 293-294.
Banks, M. R., and P. W. Baillie, 1989, Late Cambrian to Devonian, *in* C. F. Burrett, and E. L. Martin, eds., Geology and mineral resources of Tasmania, v. Special Publication 15: Brisbane, Geological Society of Australia, p. 203.
Banks, M. R., and K. L. Burns, 1962, Eugenana Beds: Journal of the Geological Society of Australia, v. 9, p. 185-186.
Banks, M. R., and C. F. Burrett, 1979, A preliminary Ordovician biostratigraphy of Tasmania: Journal of the Geological Society of Australia, v. 26, p. 363-376.
Banks, M. R., and C. F. Burrett, 1989, Gordon Group, *in* C. F. Burrett, and E. L. Martin, eds., Geology and mineral resources of Tasmania: Special Publications 15: Brisbane, Geological Society of Australia, p. 201-212.
Banks, M. R., and C. R. Calver, 1989, Synthesis, *in* C. F. Burrett, and E. L. Martin, eds., Geology and mineral resources of Tasmania: Special Publication 15: Brisbane, Geological Society of Australia, p. 217-221.
Banks, M. R., and I. H. Naqvi, 1967, Some formations close to the Permo-Triassic boundary in Tasmania: Papers and Proceedings of the Royal Society of Tasmania, v. 101, p. 43-48.
Barton, T. J., 1999, Crustal structure of northern Tasmania based upon a deep seismic transect: Halls Gap SGTSG Conference Abstract Volume, p. 3-4.
Bathurst, R. G. C., 1971, Carbonate sediments and their diagenesis: Amsterdam, Elsevier Publishing Company, 620 p.
Bedi, J. C. S., 2003, Reservoir and source rock potential of the upper Parmeener Supergroup, Tasmania Basin, unpublished B.Sc. Honours Thesis, University of Tasmania, Hobart, 116 p.

Belfield, S., 2002, Volcanic hotspot wakes: Australasian Science, v. 23, p. 29-32.
Bendall, M. R., 1990, A history of petroleum occurrences and exploration in Tasmania, unpublished. 91_3236, Hobart, Report to Minerals Resources Tasmania, 9 p.
Bendall, M. R., C. F. Burrett, and H. J. Askin, 2000, Petroleum systems in Tasmania's frontier onshore basins: Australian Petroleum Exploration Association Journal, p. 26-38.
Bendall, M. R., J. K. Volkman, D. E. Leaman, and C. F. Burrett, 1991, Recent developments in exploration for oil in Tasmania: The Australian Petroleum Exploration Association Journal, p. 74-84.
Berner, R. A., 1970, Sedimentary pyrite formation: American Journal of Science, v. 268, p. 1-23.
Berry, R. F., 1993, Structure and mineralisation of western Tasmania. AMIRA Project P.291. Victoria Pass to Queenstown regional section, Hobart, CODES, University of Tasmania, p. 22-30.
Berry, R. F., O. H. Holm, and D. A. Steele, 2005, Chemical U-Th-Pb monazite dating and the Proterozoic history of King Island, southeast Australia: Australian Journal of Earth Sciences, v. 52, p. 461-471.
Bischoff, K., 1983, The geology of the Rocky Boat Inlet- Surprise Bay area. B.Sc. (Hons) Thesis, University of Tasmania, Hobart, unpublished, 229 p.
Black, L. P., C. R. Calver, D. B. Seymour, and A. R. Reed, 2004, SHRIMP U-Pb detrital zircon ages from Proterozoic and Early Palaeozoic sandstones and their bearing on the early geological evolution of Tasmania: Australian Journal of Earth Sciences, v. 51, p. 885-900.
Black, L. P., M. P. McClenaghan, R. J. Korsch, J. L. Everard, and C. Foudoulis, 2005, Significance of Devonian-Carboniferous igneous activity in Tasmania as derived from U-Pb SHRIMP dating of zircon: Australian Journal of Earth Sciences, v. 52, p. 807-829.
Blackburn, G., 2004, Summary seismic interpretation onshore Tasmania SEL 13/98, Report for Great South Land Minerals Limited, unpublished, 10 p.
Blenkinsop, T. G., 1988, Definition of low-grade metamorphic zones using illite crystallinity: Journal of Metamorphic Geology, v. 6, p. 623-636.
Blissett, A. H., 1962, Geological Survey Explanatory Report, One Mile Geological Map Series K55-5-50, Zeehan, 268 p.
Boger, S. D., and J. M. Miller, 2004, Terminal suturing of Gondwana and the onset of the Ross-Delamerian Orogeny: the cause and effect of Early Cambrian reconfiguration of plate motions: Earth and Planetary Science Letters, v. 219, p. 35-48.
Bois, C., P. Bouche, and R. Pelet, 1982, Global geologic history and distribution of hydrocarbon reserves: American Association of Petroleum Geologists Bulletin, v. 66, p. 1248-1270.
Bottrill, R. S., 1996, The Lonnavale oil seep: Tasmanian Geological Survey 1996/14.
Boulter, C. A., 1974, Structural sequence in the metamorphosed Precambrian rocks of the Frankland and Wilmot Ranges, southwestern Tasmania: Papers and Proceedings of the Royal Society of Tasmania, v. 107, p. 105-115.
Bradshaw, M., 1993, Australian petroleum systems: Petroleum Exploration Society of Australia Journal, v. July, p. 43-53.
Brill, B. A., 1988, Illite crystallinity, bo and Si content of K-white mica as indicators of metamorphic conditions in low-grade metamorphic rocks at Cobar, New South Wales: Australian Journal of Earth Sciences, v. 35, p. 295-302.

Bromfield, K., 2004, Jurassic palaeoenvironmental reconstruction using plants found at Lune River, south east Tasmania: Abstracts Geological Society of Australia, v. 75, p. 17.
Brown, A. V., 1985, Preliminary report on the Forest No.1 diamond-drill hole. UR1985_62, Hobart, Tasmania Department of Mines, unpublished, 2 p.
Brown, A. V., 1989, Crimson Creek Formation, *in* C. F. Burrett, and E. L. Martin, eds., Geology and Mineral Resources of Tasmania: Special publications, v. 15: Brisbane, Geological Society of Australia, p. 54-58.
Brown, A. V., 1989b, Eo-Cambrian-Cambrian, *in* C. F. Burrett, and E. L. Martin, eds., Geology and Mineral Resources of Tasmania: Special publications, v. 15: Brisbane, Geological Society of Australia, p. 47-83.
Brown, A. V., and A. H. Findlay, 1992, The 10th Legion Thrust, Zeehan district: Distribution, interpretation, regional and economic significance, Hobart, Mineral Resources Tasmania, UR1992_02, unpublished, 8 p.
Burrett, C. F., 1978, Stratigraphy and conodonts of the Ordovician Gordon Group, Tasmania, Ph.D. Thesis, University of Tasmania, Hobart, unpublished, 342 p.
Burrett, C. F., 1992, Conodont geothermometry in Palaeozoic carbonate rocks of Tasmania and its economic implications: Australian Journal of Earth Sciences, v. 39, p. 61-66.
Burrett, C. F., 1995, Ordovician Gordon Group carbonates, Zeehan region, Tasmania, Australia. Stratigraphy and palaeoenvironments. 97_3957A: Report to CRA, unpublished, 15 p.
Burrett, C. F., and R. H. Findlay, 1984, Cambrian and Ordovician conodonts from the Robertson Bay Group, Antarctica and their tectonic significance: Nature, v. 307, p. 723-726.
Burrett, C. F., J. R. Laurie, and B. Stait, 1981, Gordon Subgroup (Ordovician) carbonates at Precipitous Bluff and Point Cecil, Southern Tasmania: Papers and Proceedings of the Royal Society of Tasmania, v. 115, p. 93-99.
Burrett, C. F., and D. Tanner, 1997, Annual report 1997 EL's 1/88, 9/95, 21/95, Great South Land Minerals Proprietary Limited, Hobart, Mineral Resources Tasmania, unpublished, 40 p.
Calver, C. R., 1977, Palaeoecology of Lower Limestone Member, Florentine Valley. B.Sc. (Hons.) Thesis, University of Tasmania, Hobart, unpublished, 88 p.
Calver, C. R., 1984, Stratigraphy of a Late Palaeozoic borehole section at Douglas River, eastern Tasmania: A synthesis of marine macro-invertebrate and palynological data: Papers and Proceedings of the Royal Society of Tasmania, p. 137-162.
Calver, C. R., 1989, The Weld River Group: A major upper Precambrian dolomite sequence in Southern Tasmania: Papers and Proceedings of the Royal Society of Tasmania, v. 123, p. 43-53.
Calver, C. R., 1990, Lower Palaeozoic stratigraphy of the Florentine Valley: Hobart, Geological Society of Australia, Tasmania Division, 21 p.
Calver, C. R., 1992, Maydena DDH1 appraisal of the limestone resource at Risby's Basin. Report 1992/03: Department of Resources and Energy. Division of Mines and Mineral Resources, unpublished, 2 p.
Calver, C. R., 1998, Isotopic stratigraphy of the Neoproterozoic Togari Group, Tasmania: Australian Journal of Earth Sciences, v. 45, p. 865-874.
Calver, C. R., P. W. Baillie, J. L. Everard, D. B. Seymour, P. R. Williams, S. M. Forsyth, N. J. Turner, and E. Williams, 1987, Geological Atlas 1:50 000

Series, Sheet 8013N, Lyell: Tasmanian Geological Survey, Department of Mines.
Calver, C. R., N. J. Turner, M. P. McClenaghan, and J. McClenaghan, 1985, Geological Survey Explanatory Report. Sheet 80. Pedder: Hobart, Mineral Resources Tasmania, 103 p.
Calver, C. R., and M. R. Walter, 2000, The late Neoproterozoic Grassy Group of King Island, Tasmania: correlation and palaeogeographic significance: Precambrian Research, v. 100, p. 299-312.
Campbell, L., 1964, Moonie and oil search: Sydney, Edwards and Shaw, 151 p.
Cane, R. F., 1968, The nature of Tasmanian oil shale: Papers and Proceedings of the Royal Society of Tasmania, v. 102, p. 65-68.
Cane, R. F., and P. R. Albion, 1973, The organic geochemistry of torbanite precursors: Geochimica et Cosmochimica Acta, v. 37, p. 1543-1549.
Carey, S. P., and R. F. Berry, 1988, Thrust sheets at Point Hibbs, Tasmania: palaeontology, sedimentology and structure: Australian Journal of Earth Sciences, v. 35, p. 169-180.
Carey, S. W., 1960, Tasmania University Seismic Net, Hobart, University of Tasmania Publication 84, 15 p.
Cayley, R. A., D. H. Taylor, A. H. M. Vanden Berg, and D. H. Moore, 2002, Proterozoic-Early Palaeozoic rocks and the Tyennan Orogeny in central Victoria: the Selwyn Block and its tectonic implications: Australian Journal of Earth Sciences, v. 49, p. 225-254.
Clarke, A., 1995, Searching for palaeokarst at Ida Bay in southern Tasmania: Speleo Spiel, v. 287, p. 4-10.
Clarke, M. J., 1989, Lower Parmeener Supergroup, *in* C. F. Burrett, and E. L. Martin, eds., Geology and mineral resources of Tasmania, v. Special publication 15: Brisbane, Geological Society of Australia, p. 295-298.
Clarke, T. S., P. D. Burkholder, S. B. Smithson, and C. R. Bentley, 1997, Optimum seismic shooting and recording parameters and a preliminary crustal model for the Byrd Subglacial Basin: VII International Symposium on Antarctic Earth Sciences, p. 485-493.
Clota, G., 1981, Middle-Upper Ordovician sedimentology of the Chudleigh Limestone, Mayberry area, B.Sc. (Hons.) Thesis, University of Tasmania, unpublished, 111 p.
Collins, P. L. F., 1975, A radioactive anomaly in central northern Tasmania. TR18_28_31, Hobart, Report to Minerals Resources Tasmania, unpublished, 3 p.
Cook, A. C., 2004, Organic petrology and maturation of three samples from Tasmania, unpublished., Keiraville, Keiraville Konsultants, 13 p.
Cook, P. J., and J. M. Totterdell, 1991, Palaeogeographic atlas of Australia. Volume 2, Ordovician: Canberra, Bureau of Mineral Resources, 10 p.
Corbett, K. D., 1964, Geology of the Florentine Valley area. B.Sc. (Hons.) Thesis, University of Tasmania, Hobart, unpublished, 121 p.
Corbett, K. D., 1970, Sedimentology of an Upper Cambrian flysch-paralic sequence (Denison Group) on the Denison Range, south-west Tasmania, Ph.D. Thesis, University of Tasmania, Hobart, unpublished, 207 p.
Corbett, K. D., and M. R. Banks, 1974, Ordovician stratigraphy of the Florentine Synclinorium, southwest Tasmania: Papers and Proceedings of the Royal Society of Tasmania, v. 107, p. 207-238.

Cornell, C. D., G. A. Cowan, G. M. Kjellgren, J. G. Rankin, C. A. Wagner, R. J. Walla, and B. F. Wheeler, 1985, Yolla 1 final well report. OR_0310, Hobart, Mineral Resources Tasmania, unpublished, 95 p.

Correy, J. J., 1983, The geology of the rocks of the Gordon and Eldon Group correlates and the Parmeener Super-Group in the Mt. Bobs-the Boomerang area, Southwestern Tasmania, B.Sc. (Hons.) Thesis, University of Tasmania, unpublished, 170 p.

Cull, J. P., 1982, An appraisal of Australian heat-flow data: BMR Journal of Australian Geology and Geophysics, v. 7, p. 11-21.

Cull, J. P., 1991, Geothermal gradients in Australia, *in* B. Drummond, ed., The Australian lithosphere, v. 17, Geological Society of Australia, p. 147-156.

Cull, J. P., and D. Conley, 1983, Geothermal gradients and heat flow in Australian sedimentary basins: BMR Journal of Australian Geology and Geophysics, v. 8, p. 329-337.

Culp, B. L., 1970, Pelican 1 well completion report. OR_0351, Hobart, Mineral Resources Tasmania, unpublished, 100 p.

Curry, D. J., J. K. Emmett, and J. W. Hunt, 1994, Geochemistry of aliphatic-rich coals in the Cooper Basin, Australia and Taranaki Basin, New Zealand: implications for the occurrence of potentially oil-generative coals, *in* A. C. Scott, and A. J. Fleet, eds., Coal and coal-bearing strata as oil-prone source rocks: Geological Society special publication, v. 77: London, The Geological Society, p. 141-181.

Dalla Torre, M., C. De Capitani, M. Frey, M. B. Underwood, J. Mullis, and R. Cox, 1996, Very low-temperature metamorphism of shales from the Diablo Range, Franciscan Complex, California: new constraints on the exhumation path: Geological Society of America Bulletin, v. 108, p. 578-601.

De Graaf, L., 1983, Regional study of the Ben Lomond Granite. 83_2062, Hobart, Report to Minerals Resources Tasmania for the Shell Company of Australia, unpublished, 7 p.

De Lurio, J. L., and L. A. Frakes, 1999, Glendonites as a paleoenvironmental tool: Implications for early Cretaceous high latitude climates in Australia: Geochimica et Cosmochimica Acta, v. 63, p. 1039-1048.

Degeling, P. R., 1982, Wagga Wagga 1:250 000 Metallogenic map mine data sheets and metallogenic study: Geological Survey of NSW, p. 425-426.

Demaison, G. J., and B. J. Huizinga, 1991, Genetic classification of petroleum systems: American Association of Petroleum Geologists Bulletin, v. 75, p. 1626-1643.

Demaison, G. J., and G. T. Moore, 1980, Anoxic environments and oil source bed genesis: American Association of Petroleum Geologists Bulletin, v. 64, p. 1179-1209.

Denwer, K., 1981, Geology and geochemistry of the Tasmanite oil shale: B.Sc. Honours Thesis, University of Tasmania, unpublished, 84 p.

Derenne, S., C. Largeau, and F. Behar, 1994, Low polarity pyrolysis products of Permian to Recent Botryococcus-rich sediments: First evidence for the contribution of an isoprenoid algaenan to kerogen formation: Geochimica et Cosmochimica Acta, v. 58, p. 3703-3711.

Dickson, T. W., J. F. Lea, and T. G. Summons, 1984, Parattah EL18/82 Geology and coal resources estimate York Plains area, CRA Exploration Pty. Ltd. TCR 84_2294, Hobart, Mineral Resources Tasmania, unpublished, 35 p.

Diessel, C. F. K., 1992, Coal-bearing depositional systems: Berlin, Springer-Verlag, 721 p.
Dixon, G., and C. Sharples, 1986, Reconnaissance geological observations on Precambrian and Palaeozoic rocks of the New and Salisbury Rivers, southern Tasmania: Papers and Proceedings of the Royal Society of Tasmania, v. 120, p. 87-94.
Duba, D., and A. E. Williams-Jones, 1983, The application of illite crystallinity, organic matter reflectance and isotopic techniques to mineral exploration: a case study in southwestern Gaspe, Quebec: Economic Geology, v. 78, p. 1350-1363.
Eldridge, C. S., N. Williams, and J. L. Walshe, 1993, Sulphur isotope variability in sediment-hosted massive sulfide deposits as determined using the ion microprobe SHRIMP: A study of the H.Y.C. deposit at McArthur River, Northern Territory, Australia: Economic Geology, v. 88, p. 1-26.
Elliot, D. H., T. H. Fleming, P. R. Kyle, and K. A. Foland, 1999, Long-distance transport of magmas in the Jurassic Ferrar Large Igneous Province, Antarctica: Earth and Planetary Science Letters, v. 167, p. 89-104.
Elliot, D. H., and R. E. Hanson, 2001, Origin of widespread, exceptionally thick basaltic phreatomagmatic tuff breccia in the Middle Jurassic Prebble and Mawson Formations, Antarctica: Journal of volcanology and geothermal research, v. 111, p. 183-201.
Elliott, C. G., N. B. Woodward, and D. R. Gray, 1993, Complex regional fault history of the Badger Head region, northern Tasmania: Australian Journal of Earth Sciences, v. 40, p. 155-168.
Ellis, A. P., 1984, Mineralisation and palaeoenvironments in Gordon Group sediments, south of Zeehan, western Tasmania, B.Sc. (Hons.) Thesis, University of Tasmania, unpublished, 152 p.
Epstein, A. G., J. B. Epstein, and L. D. Harris, 1977, Conodont color alteration-an index to organic metamorphism: Geological Survey Professional Paper, v. 995, p. 1-27.
Etminan, H., and C. F. Hoffman, 1989, Biomarkers in fluid inclusions: A new tool in constraining source regimes and its implications for the genesis of Mississippi Valley-type deposits: Geology, v. 17, p. 19-22.
Everard, G. B., 1976, Appendix 3 Chapel Street bore hole, *in* D. E. Leaman, ed., Geological Atlas 1:50 000 series Sheet 82, Hobart. Explanatory Report: Hobart, Geological Survey of Tasmania, 7 p.
Everard, J. L., D. B. Seymour, A. R. Reed, M. P. McClenaghan, D. C. Green, C. R. Calver, and A. V. Brown, 2004, Regional geology of the southern Smithton Synclinorium. Explanatory report for the Roger, Sumac and Dempster 1:25 000 digital geological map sheets, northwestern Tasmania, Hobart, Minerals Resources Tasmania.
Fainstein, M., J. Harman, and A. Dickson, 2002, Australian gas supply and demand balance to 2019-20: ABARE report for the Commonwealth Department of Industry, Tourism and Resources, 37 p.
Ford, D., and P. Williams, 1989, Karst geomorphology and hydrology: London, Unwin Hyman, 601 p.
Foster, D. A., Gray, D. R., Spaggiari, C., 2005, Timing of subduction and exhumation along the Cambrian East Gondwanan margin, and the formation of Paleozoic backarc basins: Geological Society of America Bulletin, v. 117, p. 105-116.

Forsyth, S. M., 1989a, Geological Survey Explanatory Report, Geological Atlas 1:50 000 series, Sheet 61 (8313N) Interlaken, 75 p.
Forsyth, S. M., 1989b, Upper Parmeener Supergroup, *in* C. F. Burrett, and E. L. Martin, eds., The geology and mineral resources of Tasmania, v. Special Publication 15: Brisbane, Geological Society of Tasmania, p. 309-333.
Garven, G., S. W. Bull, and R. R. Large, 2001, Hydrothermal fluid flow models of stratiform ore genesis in the McArthur Basin, Northern Territory, Australia: Geofluids, v. 1, p. 289-311.
Gee, R. D., 1977, Geological Atlas 1 Mile Series, Zone 7, Sheet 28 (8015N), Burnie. Explanatory Report Geological Survey of Tasmania.
Gee, R. D., 1968, A revised stratigraphy for the Precambrian in north-west Tasmania: Papers and Proceedings of the Royal Society of Tasmania, v. 102, p. 7-10.
Glikson, M., T. Taylor, and D. Morris, 1992, Lower Palaeozoic and Precambrian petroleum source rocks and the coalification path of alginite: Organic Geochemistry, v. 18, p. 881-897.
Glover, D. C., 1996, The timing and style of Pb-Zn mineralisation at Grieves Siding, western Tasmania: Honours thesis, University of Tasmania, unpublished, 124 p.
Goede, A., 1976: Speleo Spiel, v. 119, p. 5-6.
Gottfried, D., L. P. Greenland, and E. Y. Campbell, 1968, Variation of Nb-Ta, Zr-Hf, Th-U, and K-Cs in two diabase-granophyre suites: Geochimica et Cosmochimica Acta, v. 32, p. 925-947.
Graves, C., C. Carnie, B. Turner, and M. Whitbread, 1998, Geological review of progress, observations and results of diamond drilling, Pasminco Rosebery Mine, unpublished, 27 p.
Green, D. C., 1989, Heat flow and heat production in Tasmania, *in* C. F. Burrett, and E. L. Martin, eds., Geology and mineral resources of Tasmania. Geological Society of Australia special publication 15: Brisbane, Geological Society of Australia, p. 461-463.
Green, G. R., 1983, The geological setting and formation of the Rosebery volcanic-hosted massive sulphide orebody, Tasmania, Ph.D. Thesis, University of Tasmania, Hobart, unpublished, 182 p.
Green, G. R., M. Solomon, and J. L. Walshe, 1981, The formation of the volcanic-hosted massive sulfide ore deposit at Rosebery, Tasmania: Economic Geology, v. 76, p. 304-338.
Groves, D. I., and M. Solomon, 1971, Report on exploration of SPL's 75, 76, 78 and EL 12/70, 71_0833, Hobart, Mineral Resources Tasmania, unpublished.
Gruber, A., 1999, ESRI User Group Conference Papers, San Diego, CA.
Gunn, P. J., T. E. Mackey, A. N. Yeates, R. G. Richardson, D. B. Seymour, M. P. McClenaghan, C. R. Calver, and M. J. Roach, 1997, The basement elements of Tasmania: Exploration Geophysics, v. 28, p. 225-231.
Guthrie, J. M., D. W. Houseknecht, and W. D. Johns, 1986, Relationships among vitrinite reflectance, illite crystallinity and organic geochemistry in organic strata, Ouachita Mountains, Oklahoma and Arkansas: American Association of Petroleum Geologists Bulletin, v. 70, p. 26-33.
Guthrie, J. M., and L. M. Pratt, 1995, Geochemical character and origin of oils in Ordovician reservoir rock, Illinois and Indiana, USA: American Association of Petroleum Geologists Bulletin, v. 79, p. 1631-1649.
Haenel, R., L. Rybach, and L. Stegena, 1988, Handbook of terrestrial heat-flow density determination; with guidelines and recommendations of the

International Heat Flow Commission: Dordrecht, Netherlands, Kluwer Academic Publishers, 486 p.
Haines, P. W., and T. Flottman, 1998, Delamerian Orogeny and potential foreland sedimentation: a review of age and stratigraphic constraints: Australian Journal of Earth Sciences, v. 45, p. 559-570.
Harris, A. G., 1979, Conodont color alteration, an organo-mineral metamorphic index, and its application to Appalachian Basin geology: Society of Economic Paleontologists and Mineralogists. Special publication, v. 26, p. 3-16.
Hassell, D. J., 1996, Appendix 1. Percussion drilling for dolomite at McRaes Hills, *in* W. L. Matthews, ed., Geological Atlas 1:50 000 series. Sheet 64 (8314S), Lake River. Explanatory Report: Hobart, Geological Survey of Tasmania, 8 p.
Heirer, K. S., and C. Brooks, 1966, Geochemistry and the genesis of the Heemskirk Granite, west Tasmania: Geochimica et Cosmochimica Acta, v. 30, p. 633-643.
Hergt, J. M., D. W. Peate, and C. J. Hawkesworth, 1991, The petrogenesis of Mesozoic Gondwana low-Ti flood basalts: Earth and Planetary Science Letters, v. 105, p. 134-148.
Heroux, Y., A. Chagnon, and R. Bertrand, 1979, Compilation and correlation of major thermal maturation indicators: American Association of Petroleum Geologists Bulletin, v. 63, p. 2128-2144.
Herrman, W., and J. D. H. Sumpton, 1982, Progress report EL1/77 Temma Area. 82_1721, Hobart, Mineral Resources Tasmania, unpublished, 97 p.
Hill, A. C., K. L. Cotter, and K. Grey, 2000, Mid-Neoproterozic biostratigraphy and isotope stratigraphy in Australia: Precambrian Research, v. 100, p. 281-298.
Hill, D., 1955, Ordovician corals from Ida Bay, Queenstown and Zeehan, Tasmania: Papers and Proceedings of the Royal Society of Tasmania, p. 237-254.
Hills, C. L., 1922, Tasmania's liquid oil possibilities, The Mercury, 12th April 1922, Hobart, 5 p.
Hinman, M. C., 1996, Constraints, timing and processes of stratiform base metal mineralisation at the HYC Ag-Pb-Zn deposit, McArthur River. New developments in metallogenic research: The McArthur River, Mount Isa, Cloncurry Minerals Province: James Cook University of North Queensland Economic Geology Research Unit, Extended Abstracts, Contributions, v. 56, p. 56-59.
Hoffman, C. F., C. B. Foster, T. G. Powell, and R. E. Summons, 1987, Hydrocarbon biomarkers from Ordovician sediments and the fossil alga, Gloeocapsomorpha prisca: Geochimica et Cosmochimica Acta, v. 51, p. 2681-2797.
Hoffman, C. F., R. W. Henley, N. C. Higgins, M. Solomon, and R. E. Summons, 1988, Biogenic hydrocarbons in fluid inclusions from the Aberfoyle tin-tungsten deposit, Tasmania, Australia: Chemical Geology, v. 70, p. 287-299.
Hoffman, P. F., A. J. Kaufman, G. P. Halverson, and D. P. Schrag, 1998, A Neoproterozoic snowball earth: Science, v. 281, p. 1342-1346.
Hofto, V., and K. C. Morrison, 1989, Economic geology of the Langloh coal deposit, EL27/79 Hamilton. 89_2956, Hobart, Minerals Resources Tasmania, unpublished, 10 p.
Holm, O. H., and R. F. Berry, 2002, Structural history of the Arthur Lineament, northwest Tasmania: an analysis of critical outcrops: Australian Journal of Earth Sciences, v. 49, p. 167-185.

Holm, O. H., A. J. Crawford, and R. F. Berry, 2003, Geochemical and tectonic settings of meta-igneous rocks in the Arthur Lineament and surrounding area, northwest Tasmania: Australian Journal of Earth Sciences, v. 50, p. 903-918.
Hughes, T. D., 1957, Limestones in Tasmania: Geological Survey Mineral Resources 10, Tasmanian Department of Mines, Hobart, 291 p.
Hughes, T. D., 1961, Uranium in Tasmania. UR1891_1961_241_243, Hobart, Report to Minerals Resources Tasmania, unpublished, 3 p.
Hunt, J. M., 1979, Petroleum geochemistry and geology: San Francisco, W.H. Freeman and Company, 617 p.
Hunt, J. M., 1995, Petroleum geochemistry and geology: New York, W.H.Freeman and Company, 743 p.
Hunter, M. A., T. R. Riley, and I. L. Millar, 2004, Middle Jurassic air-fall tuff in the sedimentary Latady Formation, eastern Ellsworth Land: Antarctic Science, v. 16, p. 185-190.
Hunziker, J. C., 1986, The evolution of illite to muscovite: an example of the behaviour of isotopes in low-grade metamorphic terrains: Chemical Geology, v. 57, p. 31-40.
Hutton, A. C., 1987, Joadja - Does anything change? Advances in the study of the Sydney Basin, v. 21, p. 49-56.
Jack, R. H., 1960, Report on the Oceana Mine, Zeehan, Hobart, Mineral Resources Tasmania, unpublished, 12 p.
Jaeger, J. C., and J. H. Sass, 1963, Lee's topographic correction in heat flow and the geothermal flux in Tasmania: Geofisica Pura E Applicata, v. 54, p. 53-63.
Jennings, J. N., 1982, Karst history: Helictite, v. 20, p. 37-52.
Johnson, D., 2004, The geology of Australia: Cambridge, Cambridge University Press, 276 p.
Jones, B. G., C. L. Fergusson, and P. F. Zambelli, 1993, Ordovician contourites in the Lachlan Fold Belt, eastern Australia: Sedimentary geology, v. 82, p. 253-270.
Jones, V.T., M.D. Matthews, and D.M. Richers, 1999, Geochemical remote sensing of the subsurface, *in* M.Hale, ed., Handbook of Exploration Geochemistry, v. 7, Elsevier Science.
Kawka, O. E., and B. R. T. Simoneit, 1994, Hydrothermal pyrolysis of organic matter in Guaymas Basin: Comparison of hydrocarbon distributions in subsurface sediments and seabed petroleums: Organic Geochemistry, v. 22, p. 947-978.
Kennedy, D. J., 1971, Geology of Flowery Gully (Northern Tasmania) and conodonts from the lowermost Gordon Limestone (Ordovician), B.Sc. (Hons.) Thesis, University of Tasmania, unpublished, 113 p.
Khwaja, A. A., 1981, Depositional and diagenetic environments of the Gordon Subgroup (Ordovician), Gunns Plains, N.W. Tasmania, Ph.D. Thesis, University of Tasmania, unpublished, 219 p.
Kiernan, K., 1989, Drainage evolution in a Tasmanian glaciokarst: Helictite, v. 27, p. 2-12.
Kiernan, K., 1993, The Exit Cave Quarry: tracing waterflows and resource policy evolution: Helictite, v. 31, p. 27-46.
Kiernan, K., 1995, An Atlas of Tasmanian Karst: Research report No.10. Tasmanian Forest Research Council Inc, v. 1, 351 p.
Kingma, J. T., 1974, The geological structure of New Zealand: New York, John Wiley and Sons, 407 p.
Kisch, H. J., 1980, Incipient metamorphism of Cambro-Silurian clastic rocks from the Jamtland Supergroup, Central Scandinavian Caledonides, Western Sweden:

illite crystallinity and 'vitrinite' reflectance: Journal of Geological Society of London, v. 137, p. 271-288.
Kisch, H. J., 1990, Calibration of the anchizone: a critical comparison of illite 'crystallinity' scales used for definition: Journal of Metamorphic Geology, v. 8, p. 31-46.
Klemme, H. D., and G. F. Ulmishek, 1991, Effective petroleum source rocks of the world: Stratigraphic distribution and controlling depositional factors: American Association of Petroleum Geologists Bulletin, v. 75, p. 1809-1851.
Kohn, B. P., A. J. W. Gleadow, R. W. Brown, K. Gallagher, P. B. O'Sullivan, and D. A. Foster, 2002, Shaping the Australian crust over the last 300 million years: insights from fission track thermotectonic imaging and denudation studies of key terranes: Australian Journal of Earth Sciences, v. 49, p. 697-717.
Kranck, E. H., and P. R. Eakins, 1965, Geology of granite: London, Interscience Publishers, 314 p.
Kubler, B., 1967, Anchimetamorphisme et schistosite: Centre de Recherches de Pau (Societe Nationale des Petroles d'Aquitaine) Bulletin, v. 1, p. 259-278.
Landais, P., A. Rochdi, C. Largeau, and S. Derenne, 1993, Chemical characterisation of torbanites by transmission micro-FTIR spectroscopy: Origin and extent of compositional heterogeneities: Geochimica et Cosmochimica Acta, v. 57, p. 2529-2539.
Lane, P., 2002, Seismic interpretation and basin analysis of the Longford Sub-Basin, B.Sc. (Hons.) Thesis, University of Tasmania, unpublished, Hobart, 94 p.
Lang, S. C., J. Kasson, L. C. Avenell, and N. Hall, 2000, Modern and ancient analogues for Permian cool-temperate peat forming fluvial lacustrine reservoir successions: American Association of Petroleum Geologists Bulletin, v. 84, p. 1452.
Laughrey, C. D., and F. J. Baldassare, 1998, Geochemistry and origin of some natural gases in the Plateau Province, Central Appalachian Basin, Pennsylvania and Ohio: American Association of Petroleum Geologists Bulletin, v. 82, p. 317-335.
Laurie, J. R., 1982, The taxonomy and biostratigraphy of the Ordovician and Early Silurian articulate brachiopods of Tasmania, Ph.D. Thesis, University of Tasmania, unpublished, 321 p.
Leaman, D. E., 1988a, Annual report for Conga Oil Proprietary Limited. 88_2816, Hobart, Report to Minerals Resources Tasmania, unpublished, 10 p.
Leaman, D. E., 1988b, Mt. Read Volcanics Project: Geophysical Report 8. Regional gravity field Tasmania, Hobart, Mineral Resources Tasmania, unpublished, 4 p.
Leaman, D. E., 1990, Inferences concerning the distribution and composition of pre-Carboniferous rocks in southeast Tasmania: Papers and Proceedings of the Royal Society of Tasmania, v. 124, p. 1-12.
Leaman, D. E., 1991, Progress report, interpretation of gravity and magnetic data EL1/88, central Tasmania for Conga Oil. 91_3235, Hobart, Minerals Resources Tasmania, unpublished, 10 p.
Leaman, D. E., 1993, Further evaluation of gravity and magnetic data RL 8809 Oceana, 93_3501A, Hobart, Mineral Resources Tasmania, unpublished, 13 p.
Leaman, D. E., 2001, Step into history in Tasmanian Reserves: Hobart, Leaman Geophysics, 416 p.

Leaman, D. E., and R. G. Richardson, 1992, A geophysical model of the major Tasmanian granitoids. UR1992_11, Hobart, Mineral Resources Tasmania, unpublished, 2 p.
Legge, J., 2001, Copper related alteration in the Smithton Synclinorium, north west Tasmania, B.Sc. (Hons.) Thesis, University of Tasmania, Hobart, unpublished, 120 p.
Li, Z. X., and C. M. Powell, 2001, An outline of the palaeogeographic evolution of the Australian region since the beginning of the Neoproterozoic: Earth-Science Reviews, v. 53, p. 237-277.
Logan, G. A., C. R. Calver, P. Gorian, R. E. Summons, J. M. Hayes, and M. R. Walter, 1999, Terminal Proterozoic mid-shelf benthic microbial mats in the Centralian Superbasin and their environmental significance: Geochimica et Cosmochimica Acta, v. 63, p. 1345-1358.
Longley, I. M., M. Bradshaw, and J. Hebberger, 2000, Australian petroleum provinces of the 21st century: Petroleum Exploration Society of Australia Journal, v. 28, p. 21-42.
Loucks, R. G., 1999, Paleocave carbonate reservoirs: Origins, burial, depth modifications, spatial complexity and reservoir implications: American Association of Petroleum Geologists Bulletin, v. 83, p. 1795-1834.
Lucarelli, L. J., 1965, Oil and gas exploration in southeastern Tasmania. Report to Mines Department Tasmania. 65_0408, Hobart, Minerals Resources Tasmania, unpublished, 13 p.
Lunt, C. K., 1969, Clam 1 well completion report. OR_0335, Hobart, Mineral Resources Tasmania, unpublished, 10 p.
Martini, I. P., and M. R. Banks, 1989, Sedimentology of the cold-climate, coal-bearing, Lower Permian, "Lower Freshwater sequence" of Tasmania: Sedimentary Geology, v. 64, p. 25-41.
Matthews, W. L., 1960, Geology of the Rapid River area. Technical Reports-Tasmania, Department of Mines. TR5_63_71, Hobart, Mineral Resources Tasmania, unpublished, 9 p.
Maynard, B., 1996, Reservoir characterisation of the Liffey/Faulkner Group. B.Sc. (Hons.) thesis, University of Tasmania, Hobart, unpublished, 79 p.
McClenaghan, M. P., and R. H. Findlay, 1989, Geological Atlas, 1:50 000 series, Sheet 64 (7913S), Macquarie Harbour: Hobart, Department of Mines, Tasmania.
McGilvray, C. T., 2003, Geology and mineralisation of the Oceana Zn-Pb-Ag deposit, Zeehan, western Tasmania. B.Sc. (Hons.) Thesis, University of Tasmania, Hobart, unpublished, 146 p.
McLaren, S., M. Sandiford, M. Hand, N. Neuman, L. Wyborn, and I. Bastrakova, 2003, The hot southern continent: heat flow and heat production in Australian Proterozoic terranes, *in* R. R. Hillis, and R. D. Muller, eds., Evolution and dynamics of the Australian Plate: Sydney, Geological Society of Australia Special Publication 22, p. 157-167.
McLoughlin, S., 1993, Plant fossil distributions in some Australian Permian non-marine sediments: Sedimentary geology, v. 85, p. 601-619.
McNeil, R. D., 1960, Geological reconnaissance of part of the Arthur River area. Technical Reports-Tasmania, Department of Mines. TR5_46_60, Hobart, Mineral Resources Tasmania, unpublished, 14 p.

Meffre, S., R. F. Berry, and M. Hall, 2000, Cambrian metamorphic complexes in Tasmania: tectonic implications: Australian Journal of Earth Sciences, v. 47, p. 971-985.
Mercer, P., 2002, A most dangerous occupation. Whaling, whalers and the Bayleys: Runnymede's maritime heritage: Hobart, National Trust of Australia (Tasmania), 81 p.
Merriman, R. J., and M. Frey, 1999, Patterns of very low-grade metamorphism in metapelitic rocks, *in* M. Frey and D. Robinson, eds., Low-grade Metamorphism, Oxford, Blackwell Science, p. 61-117.
Michael-Leiba, M. O., 1989, Macroseismic effects, locations and magnitudes of some early Tasmanian earthquakes: BMR Journal of Australian Geology and Geophysics, v. 11, p. 89-99.
Miller, S., and D. I. M. MacDonald, 2004, Metamorphic and thermal history of a fore-arc basin; the Fossil Bluff Group, Alexander Island, Antarctica: Journal of Petrology, v. 45, p. 1453-1465.
Moore, A. M. G., J. B. Willcox, N. F. Exon, and G. W. O'Brien, 1992, Continental shelf basins on the west Tasmania margin: The Australian Petroleum Exploration Association Journal, v. 32, p. 231-250.
Morris, D., and D. Taylor, 1995, Zinc mineralisation in the Gordon Limestone, pyrobitumen reflectance: Unpublished report to CRA, 18 p.
Mullis, J., M. Rahn, C. De Capitani, W. B. Stern, and M. Frey, 1995, How useful is illite crystallinity as a geothermometer? Terra Abstracts, v. 7 Supplement 1, p. 128-129.
Neuzil, C. E., 1995, Abnormal pressures as hydrodynamic phenomena: American Journal of Science, v. 295, p. 742-786.
Newstead, G., and A. Beck, 1953, Borehole temperature measuring equipment and the geothermal flux in Tasmania: Australian Journal of Physics, v. 6, p. 480-489.
Nicolaides, S., and M. W. Wallace, 1996, Stylolite formation in a Tertiary limestone (Clifton Formation) Australia: Annual Meeting Abstracts, American Association of Petroleum Geologists and Society of Economic Paleontologists and Mineralogists, v. 5, p. 105.
Nicoll, R. S., M. Owen, J. H. Shergold, J. R. Laurie, and J. D. Gorter, 1988, Ordovician event stratigraphy and the development of a Larapintine Seaway, central Australia: Bureau of Mineral Resources Record 1988/42, p. 72-77.
Offler, R., and D. J. Whitford, 1992, Wall-rock alteration and metamorphism of a volcanic-hosted massive sulfide deposit at Que River, Tasmania: petrology and mineralogy: Economic Geology, v. 87, p. 686-705.
O'Reilly, S. Y., and W. L. Griffin, 1985, A xenolith-derived geotherm for southeastern Australia and its geophysical implications: Tectonophysics, v. 111, p. 41-63.
O'Reilly, S. Y., and W. L. Griffin, 1987, Eastern Australia - 4000 kilometres of mantle samples, *in* P. H. Nixon, ed., Mantle xenoliths: Chichester, Wiley, p. 267-280.
Osborne, R. A. L., and L. Armstrong, 1996, Vadose weathering of sulphides and limestone cave development, evidence from eastern Australia: Helictite, v. 34, p. 5-16.
Osborne, R. A. L., and I. B. Cooper, 2001, Sulfide-bearing palaeokarst deposits in Lune River Quarry, Ida Bay, Tasmania: Australian Journal of Earth Sciences, v. 48, p. 409-416.

O'Sullivan, P. B., M. M. Mitchell, A. J. O'Sullivan, B. P. Kohn and A. J. W. Gleadow, 2000, Thermotectonic history of the Bassian Rise, Australia: implications for the breakup of eastern Gondwana along Australia's southeastern margins: Earth and Planetary Science Letters, v. 182, p. 31-47.

Page, M. G., 1978, Sedimentology and palaeoecology of the Upper Limestone Member, Benjamin Limestone: B.Sc. Honours thesis, University of Tasmania, unpublished, 167 p.

Patison, N. L., R. F. Berry, G. J. Davidson, B. P. Taylor, R. S. Bottrill, B. Manzi, J. Ryba, and R. E. Shepherd, 2001, Regional metamorphism of the Mathinna Group, northeast Tasmania: Australian Journal of Earth Sciences, v. 48, p. 281-292.

Patterson, D. J., H. H. Ohmoto and M. Solomon, 1981, Geological setting and genesis of cassiterite-sulfide mineralisation at Renison Bell, western Tasmania: Economic Geology, v. 76, p. 393-438.

Peters, K. E., 1986, Guidelines for evaluating petroleum source rock using programmed pyrolysis: American Association of Petroleum Geologists Bulletin, v. 70, p. 318-329.

Peters, K. E., C. C. Walters, and J. M. Moldowan, 2005, The Biomarker Guide, v. 2: Cambridge, Cambridge University Press, 1155 p.

Pisarevsky, S. A., Z. X. Li, K. Grey, and M. K. Stevens, 2001, A palaeomagnetic study of Empress 1A, a stratigraphic drillhole in the Officer Basin: evidence for low-latitude position of Australia in the Neoproterozoic: Precambrian Research, v. 110, p. 93-108.

Plint, A. G., N. Eyles, C. H. Eyles, and R. G. Walker, 1992, Control of sea level change, *in* R. G. Walker, and N. P. James, eds., Facies models: response to sea level change: Ontario, Geological Association of Canada, p. 15-25.

Pollack, H. N., S. J. Hurter, and J. R. Johnson, 1993, Heat flow from the earth's interior, analysis of the global data set: Reviews of Geophysics, v. 31, p. 267-280.

Powell, T. G., and C. J. Boreham, 1991, Petroleum generation and source rock assessment in terrigenous sequences: an update: Australian Petroleum Exploration Association Journal, v. 31, p. 297-311.

Powell, T. G., and C. J. Boreham, 1994, Terrestrially sourced oils: where do they exist and what are our limits of knowledge? - a geochemical perspective, *in* A. C. Scott, and A. J. Fleet, eds., Coal and coal-bearing strata as oil-prone source rocks, v. 77: London, The Geological Society, p. 213.

Preiss, W. V., 2000, The Adelaide Geosyncline of South Australia and its Neoproterozoic continental reconstruction: Precambrian Research, v. 100, p. 21-63.

Purvis, M. B. J., and J. P. Cull, 2001, Heat flow data in western Victoria: Australian Journal of Earth Sciences, v. 48, p. 1-4.

Raggatt, H. G., 1954, The search for oil in Australia and New Guinea: Supplement to Australian Institute of Mining and Metallurgy Bulletin, v. 172, 26 p.

Raheim, A, 1977, Petrology of the Strathgordon area, western Tasmania: Si4++ content of phengite micas as a monitor of metamorphic grade: Journal of the Geological Society of Australia, v. 24, p. 329-338.

Randall, C. J., 1997, Palynology and hydrocarbon potential of the Lower Parmeener Supergroup in Tasmania: B.Sc. Honours thesis, University of Tasmania, Hobart, unpublished, 83 p.

Reed, A. R., C. R. Calver, and R. S. Bottrill, 2002, Palaeozoic suturing of eastern and western Tasmania in the west Tamar region: implications for the tectonic evolution of southeast Australia: Australian Journal of Earth Sciences, v. 49, p. 809-830.
Reed, J. C., H. A. Illich, and B. Horsfield, 1986, Biochemical evolutionary significance of Ordovician oils and their sources: Organic Geochemistry, v. 10, p. 347-358.
Reid, A. M., 1923, Natural oil in the estate of Tasmania. UR1923_086_96, Hobart, Mineral Resources Tasmania, unpublished, 11 p.
Reid, A. M., 1929, North Bruny oil prospects, Hobart, Report to Tasmanian Mines Department, unpublished, p. 151-156.
Reid, C., 2002, The Tasmania Basin-Gondwanan Petroleum System Report, University of Tasmania, unpublished, 22 p.
Reid, C., 2003, Petroleum systems modelling onshore Tasmania, annual report, Hobart, University of Tasmania, unpublished, p. 29-48.
Reid, C., 2004, The Tasmania Basin-Gondwanan Petroleum System Final Report, Hobart, University of Tasmania, unpublished, 31 p.
Reid, C. M., and C. F. Burrett, 2004, The geology and hydrocarbon potential of the glaciomarine Lower Parmeener Supergroup, Tasmania Basin: Petroleum Exploration Society of Australia Special Publication, v. 2, p. 265-275.
Reid, C. M., A. D. Chester, A. R. Stacey, and C. F. Burrett, 2003, Stratigraphic results of diamond drilling of the Hunterston Dome, Tasmania: implications for palaeogeography and hydrocarbon potential: Papers and Proceedings of the Royal Society of Tasmania, v. 137, p. 87-94.
Reid, K., 1964, The geology of the Princess River Area: B.Sc. (Hons.) Thesis, University of Tasmania, unpublished, 73 p.
Rejebian, V. A., A. G. Harris, and J. S. Huebner, 1987, Conodont colour and textural alteration: an index to regional metamorphism, contact metamorphism and hydrothermal alteration: Geological Society of America Bulletin, v. 99, p. 471-479.
Revill, A. T., 1996, Hydrocarbons isolated from Lonnavale, seep, swab and bitumen samples, CSIRO Report, TDR-1: unpublished, 9 p.
Revill, A. T., and R. Esmay, 1999, Fingerprinting of two tars from Bruny Island, Tasmania, Hobart, CSIRO Marine Research, report to Tasmanian Department of Development and Resources, Rosny Park, unpublished.
Revill, A. T., J. K. Volkman, T. O'Leary, R. E. Summons, C. J. Boreham, M. R. Banks, and K. Denwer, 1994, Hydrocarbon biomarkers, thermal maturity, and depositional setting of tasmanite oil shales from Tasmania, Australia: Geochimica et Cosmochimica Acta, v. 58, p. 3803-3822.
Rhodes, D., E. A. Lantos, J. A. Lantos, R. J. Webb, and D. C. Owens, 1984, Pine Point orebodies and their relationship to stratigraphy, structures, dolomitization and karstification of the Middle Devonian barrier complex: Economic Geology, v. 79, p. 991-1055.
Richardson, R. G., 1980, Crustal seismology: Ph.D. Thesis, University of Tasmania, unpublished, 122 p.
Rigg, A. J., 1973, Durroon-1, Well completion report. OR_0336, Hobart, Mineral Resources Tasmania, unpublished, 27 p.
Rowling, J., 1995, Investigations of the Wyanbene Caves area: Helictite, v. 33, p. 29-34.

Rudd, E. A., 1951, Oil in Australia: Supplement to Australian Institute of Mining and Metallurgy Bulletin, 11 p.
Saito, Y., T. Tiba, and S. Matsubara, 1988, Precambrian and Cambrian cherts in northwestern Tasmania: Bulletin of the National Science Museum, Tokyo, v. 14, p. 59-70.
Sandiford, M., and S. McLaren, 2002, Tectonic feedback and the ordering of heat producing elements within the continental lithosphere: Earth and Planetary Science Letters, v. 204, p. 133-150.
Sass-Gustkiewicz, M., S. Dzulynski, and J. D. Ridge, 1982, The emplacement of zinc-lead sulfide ores in the Upper Silesian District- a contribution to the understanding of Mississippi Valley-type deposits: Economic Geology, v. 77, p. 392-412.
Saxon, M. S., 1994, Oceana, RL JV Annual report. 94_3637, Hobart, Mineral Resources Tasmania, unpublished, 22 p.
Scanlon, A. P., 1976, The Ordovician geology of the Eugenana Area, B.Sc. (Hons.) Thesis, University of Tasmania, Hobart, unpublished, 135 p.
Scott, B., 1957, Bubs Hill (Martin's Prospect), 57_0165, Hobart, Mineral Resources Tasmania, unpublished, 4 p.
Seymour, D. B., 1980, The Tabberabberan orogeny in northwest Tasmania, Ph.D. Thesis, University of Tasmania, Hobart, unpublished, 324 p.
Seymour, D. B., 1989, Sequential development of the structural trends, *in* C. F. Burrett, and E. L. Martin, eds., Geology and mineral resources of Tasmania: Special Publication 15: Brisbane, Geological Society of Australia, p. 241.
Seymour, D. B., and C. R. Calver, 1995a, Explanatory notes for the Time-Space Diagram and Stractotectonic Elements Map of Tasmania: Tasmanian Geological Survey Record 1995/01.
Seymour, D. B., and C. R. Calver, 1995b, Stratotectonics elements map: Tasmania Geological Survey, NGMA TASGO Project.
Sharples, C. E., 1979, Ordovician system, Ida Bay area, B.Sc. (Hons.) Thesis, University of Tasmania, unpublished, 175 p.
Shortt, C., 1884, Summary of observations on earthquake phenomena made in Tasmania during 1883 and 1884: Papers and Proceedings of the Royal Society of Tasmania, p. 263-270.
Shortt, C., 1885, Earthquake phenomena in Tasmania: Papers and Proceedings of the Royal Society of Tasmania, p. 400-402.
Snowdon, L. R., 1989, Organic matter properties and thermal evolution, *in* I. E. Hutcheon, ed., Short course in burial diagenesis, v. 15: Montreal, Mineralogical Association of Canada, p. 39-60.
Snowdon, L. R., 1995, Rock-Eval Tmax suppression: Documentation and amelioration: American Association of Petroleum Geologists Bulletin, v. 79, p. 1337-1348.
Spry, A., 1964, Precambrian rocks of Tasmania, PartVI. The Zeehan-Corinna Area: Papers and Proceedings of the Royal Society of Tasmania, v. 98, p. 23-48.
Stacey, A., 2004, Structural history of the Tasmania Basin derived from lineaments and palaeosurface analyses: 17th Australian Geological Convention. Abstracts 73 Dynamic Earth: Past, Present, Future, p. 123.
Stait, B., and J. Laurie, 1980, Lithostratigraphy and biostratigraphy of the Florentine Valley Formation in the Tim Shea Area, Southwest Tasmania: Papers and Proceedings of the Royal Society of Tasmania, v. 114, p. 201-207.

Stait, B. A., 1976, Palaeontology and biostratigraphy of the Florentine Valley Formation, B.Sc. (Hons.) Thesis, University of Tasmania, unpublished, 170 p.
Staplin, F. L., 1969, Sedimentary organic matter, organic metamorphism, and oil and gas occurrence: Bulletin of Canadian Petroleum Geology, v. 17, p. 47-66.
Steele, D. A., 1983, Report on the evaluation of eight geophysical anomalies in EL18/80 Arthur River, northwest Tasmania. 83_2001A, Hobart, Mineral Resources Tasmania, unpublished, 7 p.
Steenland, N. C., 1967, Aeromagnetic survey, offshore Tasmania. OR_0082, Hobart, Minerals Resources Tasmania, unpublished, 27 p.
Suggate, R. P., 1978, The geology of New Zealand, v. 1: Wellington, E.C. Keating Government Printer, 343 p.
Summons, T. G., 1981a, Preliminary report on petroleum potential onshore Tasmania. 81_1645B, Hobart, Mineral Resources Tasmania, unpublished, 30 p.
Summons, T. G., 1981b, Summary of limestone investigations in the Lune River area. UR1981_28, Hobart, Minerals Resources Tasmania, unpublished, 20 p.
Sutherland, F. L., 1976, Cainozoic volcanic rocks, *in* D. E. Leaman, ed., Geological Atlas, 1:50 000 series. Zone 7, sheet 82 (8312S), Hobart, Explanatory Report: Hobart, Geological Survey, Tasmania.
Sutherland, F. L., 1977, Cainozoic volcanic rocks, *in* D. E. Leaman, ed., Geological Atlas 1:50 000 series, sheet 75 (8312N), Brighton, Explanatory Report: Hobart, Geological Survey, Tasmania.
Sutherland, F. L., 1989, Tertiary Volcanism, *in* C. F. Burrett, and E. L. Martin, eds., Geology and mineral resources of Tasmania, v. Special Publication 15: Brisbane, Geological Society of Australia, p. 383-386.
Sutherland, F. L., and J. D. Hollis, 1982, Mantle-lower crust petrology from inclusions in basaltic rocks in eastern Australia: an outline: Journal of volcanology and geothermal research, v. 14, p. 1-29.
Sutherland, F. L., L. R. Raynor, and R. E. Pogson, 1994, Spinel to lherzolite transition in relation to high temperature palaeogeotherms, eastern Australia: Australian Journal of Earth Sciences, v. 41, p. 205-220.
Taheri, J., 1990, Petrographic, oxygen isotope and fluid inclusion studies and the clay mineralogy of core samples from DDH BC15 and sample BC F8, Weld River area, Hobart, Mines Consultancy Services report to Pegasus Gold Australia, unpublished, 5 p.
Taylor, S., 1983, Amoco-E.Z. exploration of the Gordon Limestone. 83_2071, Hobart, Mineral Resources Tasmania, unpublished, 9 p.
Taylor, S., 1989, Mineralisation, *in* C. F. Burrett, and E. L. Martin, eds., Geology and Mineral Resources of Tasmania, v. 15, Geological Society of Australia Special Publication, p. 221-223.
Taylor, S., and I. J. Mathison, 1990, Oceana, lead-zinc-silver deposit, *in* F. E. Hughes, ed., Geology of the mineral deposits of Australia and Papua New Guinea: Melbourne, The Australian Institute of Mining and Metallurgy, p. 1253-1256.
Tissot, B. P., and D. H. Welte, 1978, Petroleum formation and occurrence: Berlin, Springer-Verlag, 538 p.
Turner, N. J., 1989, Precambrian, *in* C. F. Burrett, and E. L. Martin, eds., Geology and Mineral Resources of Tasmania: Special publications, v. 15: Brisbane, Geological Society of Australia, p. 5-46.
Turner, N. J., 1990, Late Proterozoic of northwest Tasmania. Regional geology and mineral deposits, *in* F. E. Hughes, ed., Geology of the mineral deposits of

Australia and Papua New Guinea: Melbourne, The Australian Institute of Mining and Metallurgy, p. 1169-1174.
Turner, N. J., L. P. Black, and M. Kamperman, 1998, Dating of Neoproterozoic and Cambrian orogenies in Tasmania: Australian Journal of Earth Sciences, v. 45, p. 789-806.
Turner, N. J., and C. R. Calver, 1984, Geological Survey Explanatory Report, Geological Atlas 1:50 000 series, Sheet 49 (8415N), St Marys, Minerals Resources Tasmania, 159 p.
Twelvetrees, W. H., 1915, Reconnaissance of the country between Recherche Bay and New River, southern Tasmania, Hobart, Geological Survey Bulletin 24, 35 p.
Twelvetrees, W. H., 1917, The search for petroleum in Tasmania, Hobart, Mines Department Circular No.2, 18 p.
Veevers, J. J., and S. L. Eittreim, 1988, Reconstruction of Antarctica and Australia at breakup (95 $\pm$ 5 Ma) and rifting (160 Ma), Australian Journal of Earth Sciences, v. 35, p. 355-362.
Vincent, P. W., I. R. Mortimore, and D. M. McKirdey, 1985, Hydrocarbon generation, migration and entrapment in the Jackson-Nacowlah area, ATP 259P, southwestern Queensland: Australian Petroleum Exploration Association Journal, v. 25, p. 62-84.
Vitesnik, J., 1984, Crustal seismic survey. A traverse from Savage River to Fortescue Bay: B.Sc. (Hons.) Thesis, University of Tasmania, unpublished, 147 p.
Volkman, J. K., 1988, Hydrocarbons in Ordovician limestone from Queenstown and Lune River, Tasmania. 88_2816E, Hobart, CSIRO report to Conga Oil Proprietary Limited, unpublished, 40 p.
Volkman, J. K., 1999, Organic geochemistry of some Tasmanian rocks and hydrocarbon occurrences: Draft report to Great South Land Minerals, unpublished, 35 p.
Wade, A., 1915, Petroleum prospects on Bruny Island, Hobart, Report to Tasmanian Mines Department, OS_137_1, unpublished, 4 p.
Waples, D. W., 1985, Geochemistry in petroleum exploration: Boston, International Human Resources Development Corporation, 232 p.
Warr, L. N., and A. H. N. Rice, 1994, Interlaboratory standardization and calibration of clay mineral crystallinity and crystallite size data: Journal of Metamorphic Geology, v. 12, p. 141-152.
Webby, B. D., 1978, History of the Ordovician continental platform shelf margin of Australia: Journal of Geological Society of Australia, v. 25, p. 41-63.
Weldon, B. D., 1974, Ordovician Gordon Limestone Subgroup, Florentine Valley. B.Sc. (Hons.) Thesis, University of Tasmania, Hobart, unpublished, 172 p.
Wilkinson, R., 1991, Where God never trod: Balmain, David Ell Press, 482 p.
Williams, E., 1983, Appendix 1 Examination of core and two thin sections from sandstone/mudstone contact at 199.60 m, *in* M. J. Clarke, and N. Farmer, eds., A diamond drill hole at the Quoin, south-east Tasmania, Unpublished report of Department of Mines, Tasmania.
Williams, E., 1985, Thin section examination of rocks from the Woodbridge Bore. Appendix 1. UR1985_24, *in* N. Farmer, and M. J. Clarke, eds., A diamond drill hole at Peppermint Bay, Woodbridge, Unpublished report for Department of Mines Tasmania, 1 p.

Williams, S. J., 1976, Structure and metamorphism of the McPartlan Pass-Sentinels Area: Papers and Proceedings of the Royal Society of Tasmania, v. 110, p. 25-35.
Woods, T. J., 1995, Petroleum prospectivity of the Palaeozoic southeast Tasmania. B.Sc. (Hons.) Thesis, University of Tasmania, Hobart, unpublished, 81 p.
Woodward, N. B., D. R. Gray, and C. G. Elliott, 1993, Repeated Palaeozoic thrusting and allochthoneity of Precambrian basement, northern Tasmania: Australian Journal of Earth Sciences, v. 40, p. 297-311.
Wronski, E. B., 1977, Two heat flow values for Tasmania: Geophysical Journal of the Royal Astronomical Society, v. 48, p. 131-133.
Wythe, S., and M. Watson, 1996, Geochemical evaluation of an oil seep from Lonnavale, Tasmania, AMDEL Report, unpublished, 3 p.
Yeates, A. N., 1982, Tasmanian tin and tungsten granites: their radiometric characteristics, *in* J. S. Adkins, ed., Yearbook of the Bureau of Mineral Resources, Geology and Geophysics, v. 81: Canberra, Bureau of Mineral Resources, p. 19-20.